


Removal of manganese by adsorption onto newly synthesized TiO₂-based adsorbent during drinking water treatment

Katerina Fialova, Monika Motlochova, Lenka Cermakova, Katerina Novotna, Jana Bacova, Tomas Rousar, Jan Subrt & Martin Pivokonsky


To cite this article: Katerina Fialova, Monika Motlochova, Lenka Cermakova, Katerina Novotna, Jana Bacova, Tomas Rousar, Jan Subrt & Martin Pivokonsky (2023) Removal of manganese by adsorption onto newly synthesized TiO₂-based adsorbent during drinking water treatment, Environmental Technology, 44:9, 1322-1333, DOI: [10.1080/09593330.2021.2000042](https://doi.org/10.1080/09593330.2021.2000042)


To link to this article: <https://doi.org/10.1080/09593330.2021.2000042>

 View supplementary material [↗](#)


 Published online: 02 Dec 2021.

 Submit your article to this journal [↗](#)

 Article views: 170

 View related articles [↗](#)

 View Crossmark data [↗](#)

 Citing articles: 3 View citing articles [↗](#)



Removal of manganese by adsorption onto newly synthesized TiO₂-based adsorbent during drinking water treatment

Katerina Fialova^a, Monika Motlochova^b, Lenka Cermakova^a, Katerina Novotna^a, Jana Bacova^c, Tomas Rousar^c, Jan Subrt^b and Martin Pivokonsky^a

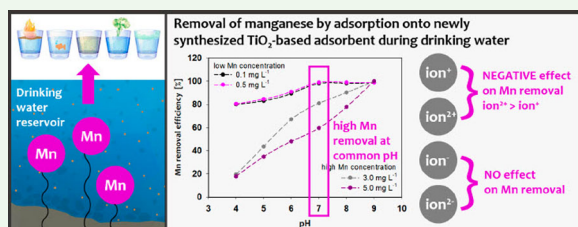
^aInstitute of Hydrodynamics of the Czech Academy of Sciences, Prague, Czech Republic; ^bInstitute of Inorganic Chemistry of the Czech Academy of Sciences, Husinec-Rez, Czech Republic; ^cDepartment of Biological and Biochemical Sciences, Faculty of Chemical Technology, University of Pardubice, Pardubice, Czech Republic

ABSTRACT

Manganese is naturally present in water, but its increased concentration in potable water is undesirable for multiple reasons. This study investigates an alternative method of demanganization by a newly synthesized TiO₂-based adsorbent prepared through the transformation of titanyl sulphate monohydrate to amorphous sodium titanate. Its adsorption capacity for Mn²⁺ was determined, while a range of influential factors, such as the effect of contact time, adsorbent dosage, pH value, and added ions was evaluated. The adsorbent appeared highly effective for Mn²⁺ removal owing to its unique characteristics. Besides adsorption via electrostatic interactions, ion-exchange was also involved in the Mn²⁺ removal. Although the Mn²⁺ removal occurred within the whole investigated pH range of 4–8, the maximum was achieved at pH 7, with $q_e = 73.83 \text{ mg g}^{-1}$. Equilibrium data revealed a good correlation with Langmuir isotherm in the absence of any ions or in the presence of monovalent co-existing ions, while the results in the presence of divalent co-existing ions showed a better fit to Freundlich isotherm. Additionally, the presence of monovalent cations (Na⁺, K⁺) only slightly decreased the Mn²⁺ removal efficiency as compared to divalent cations (Ca²⁺, Mg²⁺) that caused a greater decrease; however, the effect of anions (Cl⁻, SO₄²⁻) was insignificant. To provide insight into the adsorbent safety, the toxicity assessment was performed and showed no harmful effect on cell activity. Furthermore, the residual concentration of titanium after adsorption was always below the detection limit. The results imply that the synthesized TiO₂-based adsorbent is a safe promising alternative method for demanganization.

KEYWORDS

Adsorption; ion-exchange; manganese; titanium dioxide; drinking water treatment





Highlights

- The synthesis of amorphous TiO₂-based adsorbent was presented.
- The TiO₂-based adsorbent was found to be efficient for Mn²⁺ removal.
- The Mn²⁺ removal mechanisms were adsorption and ion-exchange.
- Increasing pH enhanced the efficiency of Mn²⁺ removal.

- Divalent cations decreased the Mn²⁺ removal efficiency more than monovalent cations.

1. Introduction

Manganese is a natural element commonly occurring in many water resources. The concentration of Mn in the surface water is on the order of hundredths or tenths of mg L⁻¹, while in groundwater, it can be by orders of magnitude higher and reach units of mg L⁻¹. However,

CONTACT Martin Pivokonsky  pivo@ih.cas.cz  Institute of Hydrodynamics of the Czech Academy of Sciences, Pod Patankou 30/5, 166 12 Prague 6, Czech Republic

Supplemental data for this article can be accessed <https://doi.org/10.1080/09593330.2021.2000042>

© 2021 Informa UK Limited, trading as Taylor & Francis Group

its presence in drinking water is undesirable and causes several operational and aesthetic problems and health risks. Concentrations of Mn^{2+} in water $> 0.1 \text{ mg L}^{-1}$ negatively affect its organoleptic properties, especially taste, odour, and colour [1]. Furthermore, Mn^{2+} ions are considered neurotoxic agents, and long-term environmental exposure is a supposed accelerator of the onset of Parkinson's disease [2]. Recent epidemiological studies concerning the consumption of water with Mn^{2+} concentrations on the order of $50\text{--}100 \mu\text{g L}^{-1}$ reported significant cognitive deficits among children [3]. From the operational point of view, Mn^{2+} causes incrustations in pipelines at concentrations $> 0.02 \text{ mg L}^{-1}$ [4] and is an undesirable nutrient substrate for the development of bacteria in water distribution networks [5]. From these findings, it is clear that maintaining acceptable concentrations of this element in drinking water is of great importance. The World Health Organization determined the maximum acceptable limit of Mn concentration in drinking water of 0.1 mg L^{-1} [6]; however, many countries follow the stricter limit according to the Environmental Protection Agency that recommends the maximum Mn concentration in drinking water of 0.05 mg L^{-1} [7].

Conventional methods used for demanganization are based on the conversion of soluble Mn^{2+} to insoluble removable precipitates. In theory, the oxidation of Mn^{2+} can be achieved by atmospheric oxygen via mechanical aeration of water, but the oxidation rate is very slow, and pH-dependent and alkalization is necessary to enhance the process [8]. When using oxidizing agents such as potassium permanganate or ozone, Mn^{2+} oxidation can be achieved even at pH of approximately neutral; however, these are associated with high operational costs. They may also be consumed for the oxidation of other compounds present in water, which increases oxidant demand [9]. Another possibility is so-called contact filtration, where Mn^{2+} is catalytically oxidized and trapped on the surface of a prepared filter cartridge coated with manganese dioxide [10]. There are disadvantages of this method, such as the higher amount of sludge and clogging of sand filters. For the above-described reasons, it would be advantageous to develop an alternative method of removing manganese that would be less dependent on pH value, more economical, and technologically easier [11].

Among other methods of Mn^{2+} removal are adsorption or cation-exchange. Many materials have been proposed for this purpose, such as activated carbon [12,13], oxidized multiwalled carbon nanotubes [14], biomatrixes prepared from various lignocellulosic wastes from agro-industry [15], zeolites [16] or

modified multivalent metal hydroxides [17,18]. These adsorbents are more or less efficient for Mn^{2+} removal from aqueous solution, but the required dose is mostly very high, which makes these methods expensive. In the case of adsorbents made of waste products, the costs could be reduced. On the other hand, their application in drinking water treatment can raise concerns, particularly if the adsorbent contains undesirable elements (e.g. NH_4^+) [19], which might be released into the treated water. Recently, more attention has been focused on adsorbents based on TiO_2 . The outstanding properties of TiO_2 -based adsorbents are, for instance, large surface area, high cation-exchange capacity, and high density of functional hydroxyl groups on the adsorbent surface [20,21]. Several variants of TiO_2 -based adsorbents have already been investigated for the removal of natural organic matter [22,23], humic acids [24,25], or synthetic organic matter [26]. Particular attention has then been paid to the use of TiO_2 -based adsorbent for the high-efficiency removal of metals [19,27] or radionuclides [28]. Nevertheless, to the best of our knowledge, the efficiency and usability of TiO_2 -based adsorbents for Mn^{2+} removal during drinking water treatment have not yet been studied.

Various sorbents prepared by hydrolysis of aqueous solutions of titanium salts [29] or titanium tetrachloride [19] lead to the formation of colloids of hydrated TiO_2 nanoparticles that are difficult to separate from the aqueous phase [30]. In addition, the corresponding synthetic procedures are difficult to control and result in products with variable properties, which complicates their practical use. In this study, the process for the synthesis of an amorphous alkaline titanate sorbent by reacting a solid titanyl sulphate monohydrate in an aqueous medium by reaction with an alkaline solution was developed. Under the reaction conditions, SO_4^{2-} anions were extracted from the solid phase, leaving the Ti–O framework intact to give solid amorphous titanate with excellent sorption capacity, e.g. for heavy metals or selected radionuclides [27,28,31]; therefore, it is expected to be effective for Mn^{2+} removal as well.

The main aims of this research were to (i) characterize the novel TiO_2 -based adsorbent; (ii) assess its efficiency for Mn^{2+} removal and describe the removal mechanisms; and (iii) investigate the effects of solution conditions such as pH and the presence of other cations and anions on Mn^{2+} removal. To the best of our knowledge, this work is the first to investigate the usability of a TiO_2 -based adsorbent for Mn^{2+} removal as an alternative method for demanganization during drinking water treatment.

2. Materials and methods

2.1. Synthesis of TiO₂-based adsorbent

Based on alkaline-controlled hydrolysis, sodium titanium oxide was prepared according to the following procedure [31]: 100 mL of cooled distilled water was mixed with ice and 0.14 mol NaOH in the form of a solution. After adding the solid titanyl sulphate (monohydrate, provided by local supplier PRECHEZA a. s.), the suspension had a temperature of 0 °C and pH of 10. While the mixture was magnetically stirred for 2 h, its temperature rose to room temperature. Then, the solid residue was decanted twice and filtered off. The solid product was dried at room temperature.

2.2. Characterization of TiO₂-based adsorbent

The total content of alkali metal in the prepared material was determined by dissolving 0.1 g of the sample in 50 mL of concentrated HNO₃ under heating. The solution was then analysed via atomic absorption spectroscopy (Varian AA240FS, LabX, Canada) in absorption mode at a wavelength of 589.0 nm and a slit width of 0.5 nm using a hollow cathode lamp in air/acetylene gas. The total content of the alkali metal cation was 133.8 mg L⁻¹.

Structural and morphology characterizations of the samples were observed by scanning electron microscopy (SEM). A JEOL JSM-6510 microscope (W-cathode, 20 nm resolution at 1 kV) was used for initial observation. Chemical analysis and mapping were performed using the attached energy-dispersive X-ray spectroscope (EDS) analyser from Oxford Instruments. Measurements were performed on native samples without coating. Semiquantitative EDS analyses were measured on compressed tablets.

Detailed phase analysis, including imaging and electron diffraction, was carried out on a JEOL JEM 3010 transmission electron microscope (TEM) operated at 300 kV (LaB₆, cathode, point resolution 1.7 Å). Images were recorded on a Gatan CCD camera with a resolution of 1024 × 1024 pixels using the Digital Micrograph software package. The powder samples were dispersed in ethanol, and the suspension was ultrasonicated for 2 min. A drop of the very dilute suspension was placed on a holey carbon-coated Cu grid and allowed to dry by evaporation at ambient temperature.

X-ray diffraction patterns were collected with a PANalytical X'Pert PRO diffractometer equipped with a conventional X-ray tube (CuK radiation, 40 kV, 30 mA,

point focus) and a multichannel detector X'Celerator with an anti-scatter shield. The sample was measured in transmission mode.

The surface area was determined by the BET method or V-t method using a Quantachrome Nova 4200e instrument. Nitrogen adsorption was carried out at -196 °C. Before analysis, the non-annealed samples were pre-treated at RT under vacuum for 35 h.

The dependence of zeta potential on pH was obtained using a Zetasizer Nano ZS (Malvern). Then, 0.1 g of the sample and 100 mL of water were prepared, and an adequate portion was dispersed by ultrasonication and injected into the electrophoretic cell. Zeta potential values were recorded in the pH range from 2 to 10. The pH adjustments were made with solutions of 0.25 and 0.025 M HCl and 0.25 M NaOH. The zeta potential was measured three times for each pH, and the average values are presented.

2.3. Preparation of Mn²⁺ aqueous solution

An aqueous solution of Mn²⁺ ions was prepared by dissolving the desired amount of Mn(NO₃)₂·4 H₂O in ultra-pure water (GW 65, Goldman Water, CZ) with the total alkalinity adjusted to 1.5 mmol L⁻¹ (a value common for natural raw water) by 0.125 M NaHCO₃. For purposes of investigating the pH effect on Mn²⁺ adsorption, the pH of model water was adjusted to pH 4–9 by using 0.1 M or 1 M NaOH and by 0.1 M or 1 M HCl, respectively. To investigate the effect of cations (Na⁺, K⁺, Ca²⁺, Mg²⁺) and anions (Cl⁻, SO₄²⁻) typically present in natural water, NaCl, KCl, K₂SO₄, CaCl₂·2 H₂O, MgCl₂, or MgSO₄·7 H₂O were added to Mn²⁺ solutions to attain amounts equal to 1 mmol L⁻¹. All chemicals were purchased from Sigma-Aldrich, USA.

2.4. Adsorption experiments and data evaluation

Equilibrium batch adsorption experiments were performed to evaluate the effectiveness of TiO₂-based adsorbent for Mn²⁺ removal and determine the effect of the solution pH value on this process. For this purpose, Mn²⁺ concentration range of 0.1–5 mg L⁻¹ was selected because these concentrations typically occur in natural waters. Solutions of 250 mL with known initial concentrations of Mn²⁺ were then adjusted to the desired pH of 4–9, and 40 mg L⁻¹ TiO₂-based material was added. The samples were placed in 250 mL borosilicate glass flasks and shaken on a magnetic stirrer (130 rpm) at room temperature (22 ± 0.5 °C) for 24 h. The applied time interval of 24 h sufficient to reach adsorption equilibrium was predetermined by the kinetic adsorption experiments performed for all

initial concentrations of Mn^{2+} with an adsorbent dosage of 40 mg L^{-1} and with predetermined optimal adsorbent dosage. After this time, the solutions were filtered through a $0.22 \mu\text{m}$ membrane filter (Millipore, USA) to remove TiO_2 -based adsorbent particles and analysed for residual Mn^{2+} concentration. The residual concentration of titanium was also measured. For each initial concentration of Mn^{2+} and pH value, control samples without the TiO_2 -based adsorbent were also processed to reveal potential adsorbate loss during the experiments. Similarly, experiments investigating the effect of coexisting ions on the adsorption of Mn^{2+} were conducted at pH 7 with samples prepared as described above. Each experiment was repeated three times.

The amount of Mn adsorbed per unit mass of adsorbent at equilibrium (q_e , mg g^{-1}) was calculated as follows (1):

$$q_e = (C_0 - C_e) \frac{V}{m} \quad (1)$$

where C_0 and C_e are the initial and equilibrium solution concentrations of Mn (mg L^{-1}), respectively, V is the solution volume (L), and m is the mass of the adsorbent (g).

The data obtained from the adsorption isotherm experiments were fitted to the Langmuir (2) and Freundlich (3) models given by the adapted equations as follows (2,3):

$$Q_e = \frac{a_m b C_e}{1 + b C_e} \quad (2)$$

and

$$q_e = K_f C_e^{1/n} \quad (3)$$

where q_e (mg g^{-1}) and C_e (mg L^{-1}) represent adsorbate uptake and solution concentration at equilibrium, respectively. Parameters a_m (mg g^{-1}) and K_f ((mg g^{-1})) ($\text{L mg}^{-1})^{1/n}$) are reflective of adsorption capacity; constants b (L mg^{-1}) and $1/n$ represent the surface affinity and the heterogeneity of surface site energy distribution, respectively.

The amount of Mn adsorbed at each time interval per unit mass of adsorbent, (q_t , mg g^{-1}), was calculated as follows (4):

$$q_t = C_0 - C_t \left(\frac{V}{m} \right) \quad (4)$$

where C_0 is the initial solution concentration of Mn (mg L^{-1}), C_t is the solution concentration of Mn at a specific time t (h), V is the volume of the solution (L) and m is the mass of the adsorbent (g).

2.5. Analytical methods

The concentrations of Mn^{2+} and coexisting cations (Na^+ , K^+ , Ca^{2+} , Mg^{2+}) were analysed before and after adsorption and were measured by inductively coupled plasma optical emission spectrometry (ICP OES, Optima 2000 DV, Perkin-Elmer, USA). The concentration of coexisting anions (Cl^- , SO_4^{2-}) was measured by the argentometric Mohr method with a standard solution of silver nitrate and potassium chromate as an indicator (analysis of Cl^-) and gravimetric analysis with barium chloride (analysis of SO_4^{2-}). Measurements of all samples were carried out in triplicate, and errors were less than 3%. Due to unclear effects and suspicion of titanium toxicity, its residual concentration in the solution was measured in all samples after adsorption by ICP OES as well.

3. Results and discussion

3.1. TiO_2 -based adsorbent characterization

The starting material titanyl sulphate monohydrate is formed by aggregates of isometric crystals with a broad size distribution, and according to EDS analysis, it contains Ti, S, and O in a ratio corresponding to the value expected from the chemical formula. The crystals of titanyl sulphate remained unchanged throughout the preparation process, and after immersion in an aqueous solution of sodium hydroxide, they provided material composed of aggregates of irregular planar crystals of size $1\text{--}2 \mu\text{m}$ (Figure 1(a–b)). The elemental composition of the final product involves (average of 3 measurements) 64.94 wt. % of oxygen, 6.77 wt. % of sodium, and 28.29 wt. % of titanium (Figure 1(c)). No impurities were found in the concentration detectable by the EDS method (approximately ≥ 0.01 wt. %), which is beneficial because the adsorbent application in drinking water treatment could raise concerns if it contained any undesirable elements (e.g. NH_4^+) [19]. Moreover, the toxicity assessment of the prepared adsorbent was conducted and confirmed its harmlessness – see details in **section S1**, Supplementary Data (SD); the results are depicted in Fig. S1, SD.

For a detailed investigation of the prepared sample, TEM was applied; individual crystals were observed (Figure 2(a)). In the selected area electron diffraction patterns, only wide indefinite rings were found (inset Figure 2(a)), implying that the prepared sample is amorphous. The powder XRD pattern shows the amorphous character of the adsorbent (Figure 2(b)). After subtracting the sample holder (Mylar foil) from the measured data, only very broad maxima can be seen centered at 30 , 45 , and $62^\circ 2\theta$ CuK α .

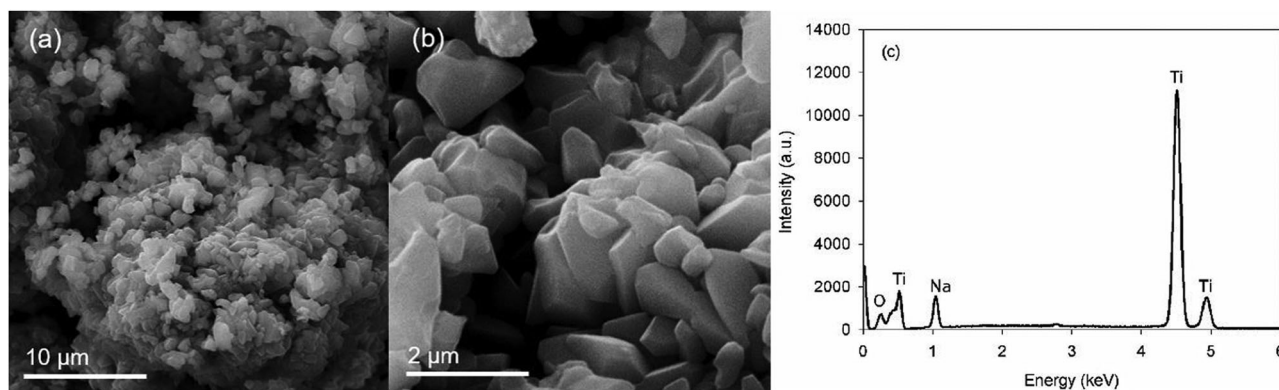


Figure 1 SEM (a, b) and SEM/EDS (c) of the prepared adsorbent.

The surface area and porosity measurements showed the purely mesoporous character of the prepared adsorbent with a BET surface area (S_{BET}) of $2.8 \text{ m}^2 \text{ g}^{-1}$, and the pore volume was $0.008 \text{ cm}^3 \text{ g}^{-1}$, which is in good agreement with data observed for similar adsorbents [31]. The average pore diameter in mesoporous parts was 3.5 nm.

The resulting product of the synthesis has the original morphological characteristics (of the starting titanyl sulphate) well preserved while maintaining the high surface area and porosity typical for nanoparticles. The TiO_2 -based adsorbent is mechanically highly resistant, it has no tendency to form colloids, and does not disintegrate in water even after a long time therefore it is easily separable from the aqueous environment.

Surfaces of metal oxides usually show a positive charge at low pH and a negative charge at high pH with a point of zero charge (PZC) in between [19]. This property is in keeping with the observations where the surface charge of the synthesized adsorbent was analysed in the pH range of 2–10 (Figure 3). The results showed that the zeta potential significantly changes with increasing pH from 2 to approximately 6 and then becomes stable at pH values in the rough pH interval 6–9. The zero zeta potential is at the value of $\text{pH}_{\text{PZC}} = 3.42$. This value is significantly lower than the pH_{PZC} of similar TiO_2 -based adsorbents in published papers [19, 23].

3.2. Adsorption experiments

Adsorption experiments were conducted at different pH values and in the presence of other cations and anions to investigate the effectiveness of TiO_2 -based adsorbent and to reveal the effects of the solution conditions on Mn^{2+} adsorption. The initial concentrations of Mn^{2+} (0.1 – 5 mg L^{-1}) were chosen based on their typical occurrence in natural waters. The equilibrium time of Mn^{2+} adsorption and optimal dosage of TiO_2 -based adsorbent

were evaluated by series of kinetics adsorption experiments.

3.2.1. Effect of contact time and adsorbent dosage

The effect of contact time was investigated for each initial concentration of Mn^{2+} (0.1 – 5 mg L^{-1}) with an adsorbent dosage of 40 mg L^{-1} at pH 7 by varying the adsorption time from 0 to 48 h. More information about kinetic adsorption experiments and modeling can be found in **section S2**, SD. The results of the kinetic experiments are depicted in Fig. S2, SD, the kinetic models fitting is shown in Fig. S3, SD, and the calculated kinetic parameters are shown in Table S1, SD, respectively. Kinetic adsorption experiments have shown fast initial uptake of Mn^{2+} from water, especially in the first 5 min, during which more than 20% of the initial Mn^{2+} concentration was removed. After 1 h more than 50% of Mn^{2+} was removed. The required time to attain the adsorption equilibrium was experimentally found to be approximately 8 h. Nevertheless, the time of 24 h was selected for the following experiments so as to assure that the adsorption equilibrium will be reached under all investigated conditions.

The effect of TiO_2 -based adsorbent dosage on the Mn^{2+} removal efficiency was investigated for each initial concentration of Mn^{2+} (0.1 – 5 mg L^{-1}) at pH 7. At the same time, detailed results on the dose optimization are depicted in Fig. S4, SD. It was experimentally found that the optimal adsorbent dosage for the initial Mn^{2+} concentration of 0.1, 0.5, 1.0, 1.5, 2.0, 2.5, 3.0 and 5.0 mg L^{-1} is 8, 12, 20, 40, 45, 50, 70, and 200 mg L^{-1} , respectively. Under the applied conditions (pH 7; alkalinity 1.5 mmol L^{-1} ; room temperature $22 \pm 0.5 \text{ }^\circ\text{C}$; concentration of Mn^{2+} 0.1 – 5 mg L^{-1} , optimal adsorbent dosage 8 – 200 mg L^{-1}), the adsorbent was able to remove a sufficient amount of Mn^{2+} to meet the strict hygienic limit of 0.05 mg L^{-1} within 8 h. The details are presented in Fig. S5, SD.

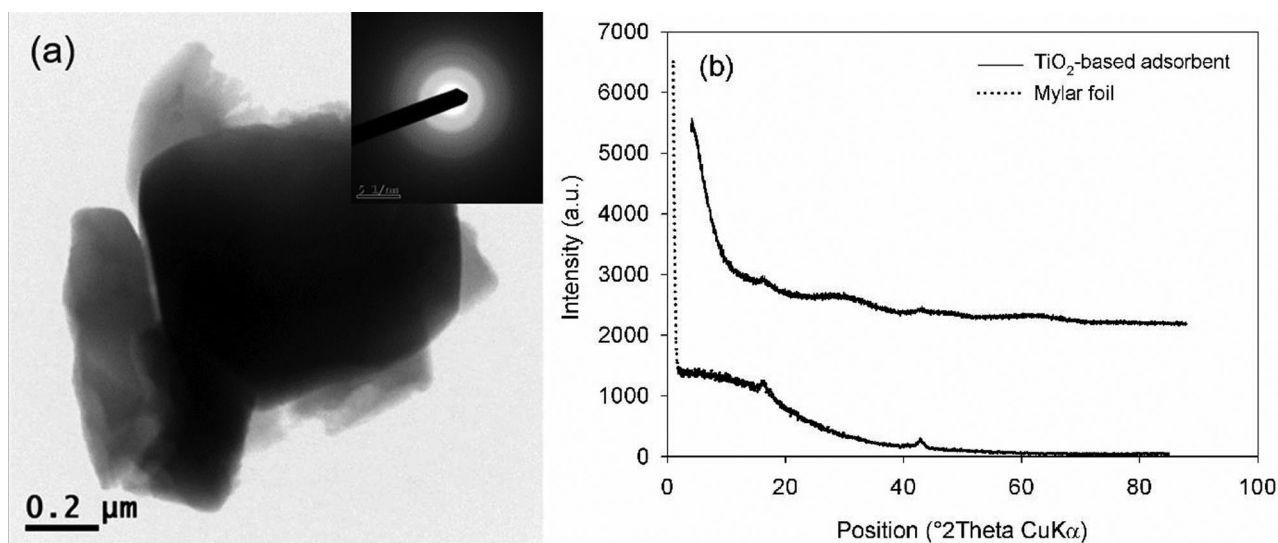


Figure 2 TEM/EDS (a) and powder XRD (b) of the prepared adsorbent.

3.2.2. The influence of pH value

The adsorption isotherms of Mn^{2+} adsorption onto TiO_2 -based adsorbent under different pH conditions (pH 4–7) are presented in Figure 4. The equilibrium data were analysed using Langmuir and Freundlich model. The Langmuir isotherm model was used to predict Mn^{2+} adsorption onto TiO_2 -based adsorbent under different pH based on the R^2 values higher obtained using this model compared to the Freundlich model. The calculated Langmuir and Freundlich model parameters are summarized in Table S2 Section A, SD.

The results of blank experiments performed without the adsorbent revealed that all the concentrations of

Mn^{2+} precipitated at pH 9, and the concentrations of Mn^{2+} above 1.5 mg L^{-1} also precipitated at pH 8, while these observations are in good agreement with the theoretical speciation of Mn according to hydrochemistry software Aqion 7.4.2. Due to this fact, adsorption experiments were not performed at these values. By contrast, under the experimental conditions at which the adsorption was investigated, Mn is anticipated to be present solely as Mn^{2+} , and the occurrence of higher oxidation states and/or Mn precipitation can be therefore neglected.

The results of batch adsorption experiments have shown that the adsorption efficiency of Mn^{2+} onto the

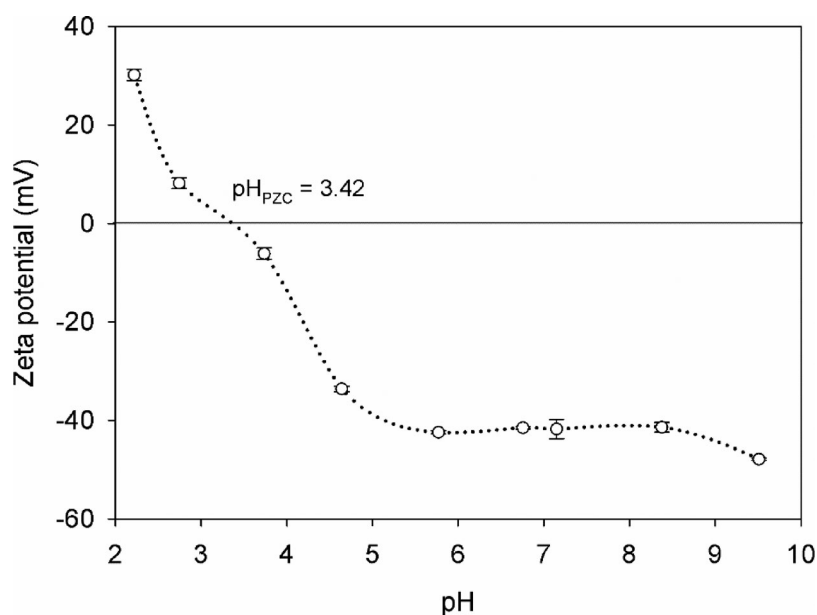


Figure 3 Dependence of zeta potential of TiO_2 -based adsorbent on pH value.

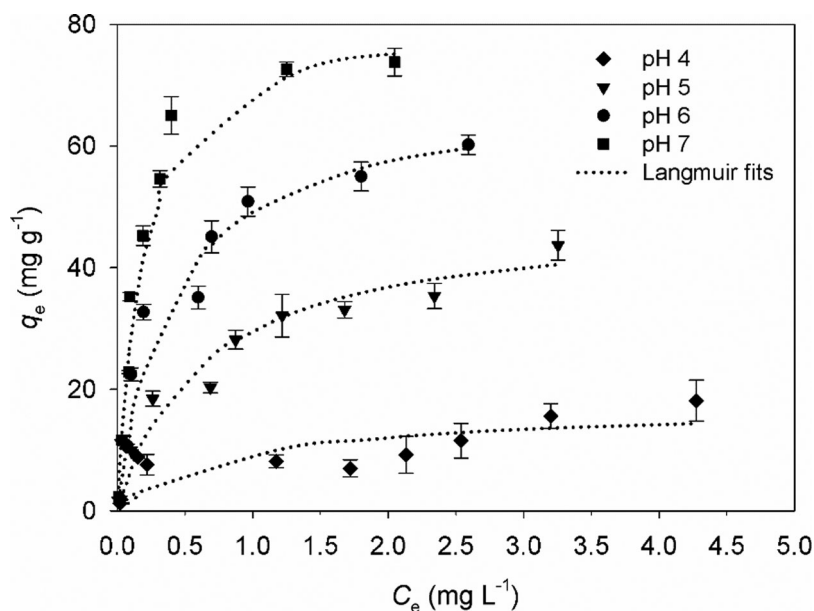


Figure 4 Adsorption isotherms of Mn^{2+} onto TiO_2 -based adsorbent under different pH conditions (the results for pH 8 are the same as for pH 7 and are not shown to maintain clarity).

TiO_2 -based adsorbent increases with increasing pH, which is associated with the charge properties of the adsorbent. The maximum removal efficiency was reached at pH 7, whereas the difference between pH 7 and 8 was completely negligible. The steepest increase in adsorption efficiency was observed from pH 4 to pH 6 because of the steep decrease in zeta potential; on the other hand, the insignificant difference in adsorption efficiency at pH 7 and 8 was probably caused by the almost constant value of zeta potential under these conditions (Figure 3). Similar to our study, Liu et al. [32] observed a steep increase in adsorption efficiency from pH 2 to pH 4 because of electrical inversion from positive to negative adsorbent surface charge.

Enhanced Mn^{2+} adsorption at higher pH values was also previously observed, e.g. when using carbon-based adsorbents [33]. Generally, an adsorbent in an aqueous solution carries a surface charge that is more or less pH-dependent. Cation adsorption is typically favoured at pH values above the adsorbent's pH_{PZC} owing to the attractive electrostatic interactions between the negatively charged adsorbent surface and the cations [33, 34]. In this study, the pH_{PZC} of the TiO_2 -based adsorbent was 3.42; thus, a negative charge of the adsorbent prevailed within the whole investigated pH range, enabling interactions with cations. However, as mentioned above, the zeta potential further varied with increasing pH value. With regard to TiO_2 -based adsorbents, Liu et al. [32] investigated the removal of metals (Cu^{2+} and Cd^{2+}) by titanate nanomaterials at pH 2–6 and confirmed higher removal

efficiency at higher pH values. A higher removal efficiency with increasing pH from 2–8 was also observed in the study by Motlochova et al. [27], where different alkali metals (Pb, Cu, and Cd) were removed using different types of TiO_2 -based adsorbents was investigated. A similar trend was observed by Sountharajah et al. [35], who focused on metal (Ni, Zn, Cd, Cu, and Pb) adsorption onto sodium titanate nanofibrous material. In addition to the increasing negative adsorbent surface charge, it was proposed that the formation of metal hydroxyl complexes that have a higher affinity for adsorption leads to an abrupt increase in metal removal [35]. The proceeding hydrolysis was also suggested to be involved in Mn^{2+} removal via adsorption [35].

In our study, the maximum Mn^{2+} adsorption was reached at pH 7 with $q_e = 73.83 \text{ mg g}^{-1}$. The q_e value was then lower by approximately 20%, 40%, and 75% at pH 6 ($q_e = 60.22 \text{ mg g}^{-1}$), pH 5 ($q_e = 43.66 \text{ mg g}^{-1}$), and pH 4 ($q_e = 18.16 \text{ mg g}^{-1}$), respectively. In the study by Kanna et al. [19], which compared the adsorption efficiency of hydrated amorphous TiO_2 and commercially available TiO_2 for Mn^{2+} removal at pH 7, the maximum adsorption efficiency ($q_e = 24.92 \text{ mg g}^{-1}$) was almost three times lower than that in our study, despite the higher value of $S_{\text{BET}} = 449 \text{ m}^2 \text{ g}^{-1}$. This could be explained by other factors, e.g. different surface charge (pH_{PZC}), etc.

On the other hand, higher removal efficiency in comparison with our study was reached in the study by Niksirat et al. [13], where activated carbon prepared from

tire residuals was used for Mn^{2+} removal. The higher adsorbed amount of Mn^{2+} ($q_e = 120 \text{ mg g}^{-1}$) at pH 7 was probably caused by the interplay of several adsorbent parameters (high $S_{\text{BET}} = 550 \text{ m}^2 \text{ g}^{-1}$, very low $\text{pH}_{\text{PZC}} = 2.7$, and high total pore volume $= 1.22 \text{ cm}^3 \text{ g}^{-1}$) [13].

As mentioned above, a significant disadvantage of some conventional oxidation-based demanganization methods is the need for an increased pH value [11]. By contrast, Mn^{2+} adsorption onto the TiO_2 -based adsorbent utilized in this study resulted in significant Mn^{2+} removal throughout the entire investigated pH range. Even at pH 4, the removal efficiency was up to 80% in the case of low initial Mn^{2+} concentrations ($0.1\text{--}0.5 \text{ mg L}^{-1}$). Additionally, the efficiency under pH values typical for natural waters (approximately 6.5–7.5) reached 90–99%. For high initial Mn^{2+} concentrations ($3\text{--}5 \text{ mg L}^{-1}$), the observed removal efficiency was much lower at the lowest pH values; however, neither such high initial Mn^{2+} concentrations nor such low pH values are expected in drinking water treatment. With higher pH ($\text{pH} > 6$) and at higher initial Mn^{2+} concentrations, the removal efficiency ranged between 50–80% at the applied adsorbent dose of only 40 mg L^{-1} . It should be emphasized that the used dose was optimized for Mn^{2+} concentrations of 1.5 mg L^{-1} . Thus, it can be assumed that the removal efficiency would increase with a higher adsorbent dosage (which was confirmed by kinetic adsorption experiments with the optimal adsorbent dosage at pH 7, see Table S3, SD). However, it is worth noting that for water treatment, the relevant concentration of Mn in raw water rarely occurs above 1 mg L^{-1} [36]. For initial Mn^{2+} concentrations in the range of $0.1\text{--}0.5 \text{ mg L}^{-1}$, the strict hygienic limit of Mn residual concentration in drinking water (0.05 mg L^{-1}) was reached even using the adsorbent dose of only 40 mg L^{-1} under all investigated pH values except pH 4.

3.2.3. Impact of coexisting ions on Mn^{2+} removal

The coexisting ions (cations: Na^+ , K^+ , Ca^{2+} , Mg^{2+} , and anions: Cl^- , SO_4^{2-}) were chosen based on their presence/importance in natural waters. Their effect on Mn^{2+} removal by adsorption onto TiO_2 -based adsorbent is presented in Figure 5. Similar to the data analysis of the influence of pH value, the equilibrium data related to the influence of coexisting ions were also analysed using the Langmuir and Freundlich model.

In the presence of monovalent ions, a better correlation between the experimental and model data (according to the higher R^2 values) was achieved by the Langmuir adsorption model; however, in the presence of divalent ions, the Freundlich adsorption model

displayed a better fit. The calculated Langmuir and Freundlich model parameters are summarized in Table S2 Section B, SD.

It was found that the presence of anions had no significant effect on the Mn^{2+} removal efficiency; on the other hand, the coexisting cations decreased the removal efficiency of Mn^{2+} . The amount of adsorbed Mn^{2+} decreased the most when divalent cations were added, while only a slight decrease in the adsorption of Mn^{2+} was observed when monovalent cations were present in the solution. To illustrate, when there were no additional ions, the removal of Mn^{2+} at the initial concentration of 0.5 mg L^{-1} was 99%. In the presence of Na^+ or K^+ , the efficiency decreased only slightly to 96%. By contrast, the addition of Ca^{2+} and Mg^{2+} ions resulted in Mn^{2+} removal decreases to 40% and 74%, respectively. The inhibiting effect of coexisting cations on Mn^{2+} removal decreased in the order $\text{Ca}^{2+} > \text{Mg}^{2+} > \text{K}^+ > \text{Na}^+$.

One possible explanation for the suppressed Mn^{2+} adsorption is the effect of ionic strength. When electrostatic interactions between the adsorbate and the adsorbent's surface are attractive, the adsorption efficiency decreases with increasing ionic strength. Conversely, when electrostatic interactions between adsorption participants are repulsive, the increase in ionic strength increases adsorption [37]. In this study, experiments were performed at pH 7, which enables strong, attractive electrostatic interactions between the adsorbent and the adsorbate; thus, the Mn^{2+} removal efficiency decreased with increasing concentrations of any cation. This effect was even more pronounced when divalent cations were present. The second possible explanation of the decrease in Mn^{2+} removal is divalent cations competing with Mn^{2+} for active sites of the adsorbent [38]. The occurrence of this phenomenon is highly probable in our study because the concentrations of added Ca^{2+} and Mg^{2+} in the solution decreased after adsorption (data not shown).

The difference between the impact of Na^+ and K^+ on Mn^{2+} removal was insignificant, as well as the difference between the impact of Cl^- and SO_4^{2-} . On the other hand, in comparison with Mg^{2+} , Ca^{2+} exhibited a higher inhibiting effect on Mn^{2+} removal efficiency. Based on the results of several studies [39, 40], the effect of coexisting ions is linearly related to the ionic radii of the competing ions.

By contrast, diverse results were reported by Rachel et al. [41], who investigated the impact of CaCl_2 on Mn^{2+} adsorption onto granular activated carbon and modified activated carbon. Based on the author's observations, the adsorption improved in accordance with the increasing concentration of CaCl_2 [41]. This could be

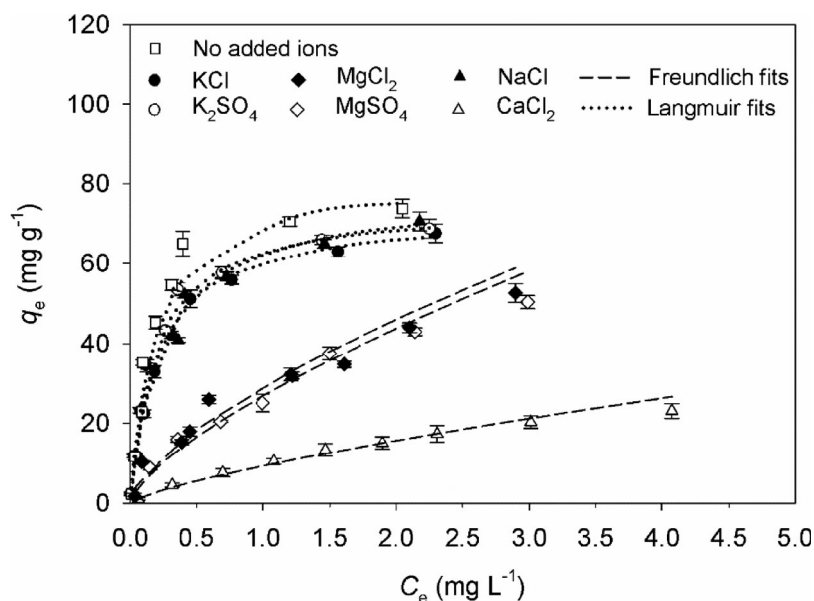


Figure 5 Effect of coexisting ions on Mn^{2+} removal.

ascribed to repulsive electrostatic forces between Mn^{2+} ions and the surface of the utilized adsorbent, which were suppressed by increasing ionic strength. Similarly, a positive effect of the presence of Ca^{2+} or Mg^{2+} ions was observed in studies where TiO_2 -based adsorbent was used for natural organic matter removal [23, 25, 42].

In the study by Motlochova et al. [27], which investigated the adsorption of Pb^{2+} , Cu^{2+} , and Cd^{2+} on different types of TiO_2 -based adsorbents, no significant impact of coexisting ions on the removal efficiency of the target compound was observed. This diverse trend can be explained by a very different concentration range of the adsorbed metals (hundreds of mg L^{-1} in the study by Motlochova et al. [27] vs tenths and units of mg L^{-1} in this study) and the concentration of coexisting ions.

3.2.4. Mn^{2+} removal mechanisms

The above-described results of the adsorption pH dependency indicate that electrostatic interactions between Mn^{2+} and negatively charged TiO_2 -based adsorbent surface are an important adsorption mechanism. However, the results of some studies investigating the removal of different metal ions (Pb^{2+} , Cu^{2+} , Cd^{2+}) by similar types of TiO_2 -based adsorbents [27, 32] also suggested the involvement of an ion-exchange mechanism. It was proposed that the amount of adsorbed metal ions was comparable to the desorbed amount of alkali metal originally incorporated in the adsorbent structure [27].

To investigate the contribution of ion-exchange in this study, the concentration of Na^+ was measured in

the samples before and after the adsorption experiment. It was found that the concentration of Na^+ slightly increased after adsorption; thus, ion-exchange apparently participated in Mn^{2+} removal. However, no direct correlation between the amount of desorbed Na^+ from the adsorbent surface and adsorbed Mn^{2+} was found. This was likely due to a very low initial concentration of Mn^{2+} ($0.1\text{--}5\text{ mg L}^{-1}$) in comparison to the concentration of Na^+ ($20\text{--}30\text{ mg L}^{-1}$) in the solution originating from NaHCO_3 used for alkalinity adjustment. In the studies by Motlochova et al. [27] and Liu et al. [32], much higher concentrations of adsorbates (10 mmol L^{-1} of Pb^{2+} , Cu^{2+} , and Cd^{2+} [27]; 50 mg L^{-1} Cu^{2+} and 100 mg L^{-1} Cd^{2+} [32]) were used. Nevertheless, it can be concluded that in our case, when environmentally relevant adsorbate concentrations were applied, the predominant adsorption mechanism was electrostatic interactions. Furthermore, Doula [43] investigated Mn^{2+} removal by adsorption onto Clinoptilolite and a modified Clinoptilolite-iron oxide system and found that the ion-exchange mechanism was predominant only if the initial Mn^{2+} concentration did not exceed 200 mg L^{-1} . Above this value, another adsorption mechanism occurred. Thus, the factors determining the interaction mechanism apparently also include the adsorbent-adsorbate ratio.

To conclude, under the conditions applied in this study, the dominant mechanism of Mn^{2+} adsorption onto TiO_2 -based adsorbent was most likely electrostatic interactions, accompanied by an ion-exchange mechanism. The advantage of Mn^{2+} removal driven by these mechanisms is that despite being pH-dependent,

certain removal was achieved throughout the entire investigated pH range.

4. Practical aspects

The main achievement of this work was the invention of an effective adsorptive material usable for Mn^{2+} removal in drinking water treatment in a wider pH range compared to conventional methods. The efficiency of the adsorbent was examined under different pH values and at various initial concentrations of Mn^{2+} , and the results suggest that under typical raw water pH (pH 6.5–7.5) and common initial Mn concentrations (up to 1.5 mg L^{-1}), this adsorbent with a dosage of only 40 mg L^{-1} is able to remove a sufficient amount of Mn^{2+} to comply with the strict hygienic limit for potable water of 0.05 mg L^{-1} Mn.

To provide an insight into the adsorbent safety, residual concentrations of titanium in the solution after adsorption were measured. The maximum allowed concentration of titanium in drinking water is not established [6], but the study by Dong et al. [44] suggested that the maximum allowable concentration of titanium in drinking water may be set at 0.1 mg L^{-1} . In our study, the measured titanium concentrations after the adsorption experiments were always below the detection limit (0.01 mg L^{-1}), which means that titanium is not released from the TiO_2 -based adsorbent and therefore does not pose any threat to drinking water. Moreover, it was verified that the adsorbent does not contain or release any other impurities (details in chapter 3.1). The toxicology assessment also confirmed the adsorbent safety (details in **S1**, SD).

5. Conclusion and future prospects

This study used a newly synthesized TiO_2 -based adsorbent prepared from titanyl sulphate monohydrate for Mn^{2+} removal, while the effects of different solution conditions (pH and coexisting ions) were investigated.

The results show that this adsorbent achieves high Mn^{2+} removal efficiency due to its unique features (such as amorphous structure and low pH_{PZC}). Based on our findings, there are two mechanisms involved in Mn^{2+} removal: (i) adsorption of Mn^{2+} onto TiO_2 -based adsorbent surface via electrostatic interactions and (ii) ion-exchange of Mn^{2+} for Na^+ . Mn^{2+} removal occurred throughout the whole range of tested pH values, but the efficiency was greater at higher pH due to the increase in negative charge on the adsorbent surface. When using the optimal adsorbent dosage at pH 7, the strict limit for manganese concentration (0.05 mg L^{-1}) was met for all investigated initial concentrations of

Mn. The influence of added anions was insignificant. On the other hand, added cations suppressed Mn^{2+} removal. A greater decrease in Mn^{2+} removal efficiency was observed in the presence of divalent cations, owing to a higher increase in the repulsive forces and competitive behaviour between Mn^{2+} and the additional cations; thus, the presence of divalent cations in raw water should be taken into account in future research focused on adsorbent utilization in practice. The equilibrium data were analysed using Langmuir and Freundlich model. The Langmuir isotherm model was used to predict Mn^{2+} adsorption onto TiO_2 -based adsorbent under different pH and in the presence of monovalent coexisting ions, whereas in the presence of divalent coexisting ions better correlation was achieved using the Freundlich isotherm model. In addition to the adsorption efficiency, an advantage of the adsorbent is that it contains no impurities and has no tendency to form colloids. Toxicity assessments showed that the sorbent did not cause any statistically significant damage to the cells. The residual concentration of Ti in every sample was below the detection limit. Additionally, synthesis of this adsorbent is economically feasible. The results suggest that this adsorbent might be a promising alternative to conventional methods for Mn^{2+} removal during drinking water treatment.

The results obtained in this study fulfil the basic knowledge of the functioning of Mn^{2+} removal by the newly synthesized TiO_2 -based adsorbent. Future research should focus on the real-life applications of this adsorbent for the drinking water treatment process. Preparation of the adsorbent in a granular form is currently being investigated, while this form would be usable in pressure filters, similar to granular activated carbon. Investigation of the regeneration process of the granular form of prepared adsorbent and its influence on the removal efficiency is also needed.

Acknowledgements

This work was supported by the institutional support of the Czech Academy of Sciences [RVO: 67985874] and [MSM200321901] and by the Research Infrastructure NanoEnviCz, supported by the Ministry of Education, Youth and Sports of the Czech Republic under Project No. LM2015073. The authors also thank to the Strategy AV21 of the Czech Academy of Sciences (VP20 – Water for life) for valuable support.

Disclosure statement

No potential conflict of interest was reported by the author(s).

Data availability statement

The data that support the findings of this study are available from the corresponding author, upon reasonable request.

References

- [1] Griffin AE. Significance and removal of manganese in water supplies. *J.-Am. Water Works Assoc.* **1960**;52(10):1326–1334.
- [2] Alias C, Benassi L, Bertazzi L, et al. Environmental exposure and health effects in a highly polluted area of northern Italy: a narrative review. *Environ. Sci. Pollut. Res.* **2019**;26:4555–4569.
- [3] Carriere A, Brouillon M, Sauve S, et al. Performance of point-of-use devices to remove manganese from drinking water. *J. Environ. Sci. Health Part A-Toxic/Hazard. Subst. Environ. Eng.* **2011**;46:601–607.
- [4] Bean EL. Potable water quality goals. *J.-Am. Water Works Assoc.* **1974**;66(4):221–230.
- [5] Casey TJ. (2009). Iron and manganese in water: Occurrence, drinking water standards, treatment options. Aquavarra Research Publications Water Engineering Papers Aquavarra Research Limited, 22a brook field avenue, Blackrock, County Dublin, Ireland.
- [6] World Health Organization. Guidelines for drinking water quality, fourth ed. Switzerland: WHO Press; **2011**.
- [7] U.S. Environmental Protection Agency. Edition of the drinking water standards and Health advisories. Washington, DC: Office of Water; **2018**.
- [8] Hem JD. Chemical equilibria and rates of manganese oxidation. United States department of the interior Stewart L. Udall, Geological Survey, Water-Supply Papers 1667A. Washington: US Government Printing Office; **1963**.
- [9] Kurtz S, Bilek F, Schlenstedt J, et al. (2009). Treating Mine Water contaminated with Iron, Manganese and high solid Carbon Loads under Tropical Conditions. Paper presented at Securing the Future and 8th ICARD, June 23–26, Skellefteå, Sweden.
- [10] Jez-Walkowiak J, Dymaczewski Z, Szuster-Janiaczyk A, et al. Efficiency of Mn removal of different filtration materials for groundwater treatment linking Chemical and physical properties. *Water (Basel)*. **2017**;9(498):1–12.
- [11] Tobiason JE, Bazilio A, Goodwill J, et al. Manganese removal from drinking water sources. *Curr. Pollution Rep.* **2016**;2:168–177.
- [12] Budinova T, Savova D, Tsyntsarski B, et al. Biomass waste-derived activated carbon for the removal of arsenic and manganese ions from aqueous solutions. *Appl. Surf. Sci.* **2009**;255:4650–4657.
- [13] Niksirat M, Sadeghi R, Esmaili J. Removal of Mn from aqueous solutions, by activated carbon obtained from tire residuals. *SN Appl. Sci.* **2019**;1:1–12.
- [14] Genesan P, Kamaraj R, Sozhan G, et al. Oxidized multi-walled carbon nanotubes as adsorbent for the removal of manganese from aqueous solution. *Environ. Sci. Pollut. Res.* **2013**;20:987–996.
- [15] Esfandiari N, Nasernejad B, Ebadi T. Removal of Mn(II) from groundwater by sugarcane bagasse and activated carbon (a comparative study): application of response surface methodology (RSM). *J. Ind. Eng. Chem.* **2014**;20:3726–3736.
- [16] Koshy N, Singh DN. Fly ash zeolites for water treatment applications. *J. Environ. Chem. Eng.* **2016**;4:1460–1472.
- [17] Khobragade MU, Nayak AK, Pal A. Application of response surface methodology to evaluate the removal efficiency of Mn(II), Ni(II), and Cu(II) by surfactant-modified alumina. *Clean Technol Environ Policy.* **2016**;18:1003–1020.
- [18] Khobragade MU, Pal A. Adsorptive removal of Mn(II) from water and wastewater by surfactant modified alumina. *Desalin. Water Treat.* **2016**;57:2775–2786.
- [19] Kanna M, Wongnawa S, Sherdshoopongse P, et al. Adsorption behavior of some metal ions on hydrated amorphous titanium dioxide surface. *Songklanakarin J. Sci. Technol.* **2005**;27(5):1017–1026.
- [20] Engates KE, Shipley HJ. Adsorption of Pb, Cd, Cu, Zn, and Ni to titanium dioxide nanoparticles: effect of particle size, solid concentration, and exhaustion. *Environ. Sci. Pollut. Res.* **2011**;18:386–395.
- [21] Santhosh C, Velmurugan V, Jacob G, et al. Role of nanomaterials in water treatment applications: A review. *Chem. Eng. J.* **2016**;306:1116–1137.
- [22] Mwaanga P, Carreway E, Schlautman MA. Preferential sorption of some natural organic matter fractions to titanium dioxide nanoparticles: influence of pH and ionic strength. *Environ. Monit. Assess.* **2014**;186:8833–8844.
- [23] Gora SL, Andrews SA. Adsorption of natural organic matter and disinfection byproduct precursors from surface water onto TiO₂ nanoparticles: pH effects, isotherm modeling, and implications for the use of TiO₂ for drinking water treatment. *Chemosphere.* **2017**;174:363–370.
- [24] Sun DD, Lee PF. TiO₂ microsphere for the removal of humic acid from water: complex surface adsorption mechanisms. *Sep. Purif. Technol.* **2012**;91:30–37.
- [25] Erhayem M, Sohn M. Effect of humic acid adsorption on titanium dioxide nanoparticles. *Sci. Total Environ.* **2014**;470–471:92–98.
- [26] Kim S-H, Shon H. Adsorption characterization for multi-component organic matters by titanium oxide (TiO₂) in wastewater. *Sep. Purif. Technol.* **2007**;45(8):1775–1792.
- [27] Motlochova M, Slovak V, Plizingrova E, et al. Highly-efficient removal of Pb(II), Cu(II) and Cd(II) from water by novel lithium, sodium and potassium titanate reusable microrods. *RSC Adv.* **2020**;10:3694–3704.
- [28] Klementova M, Motlochova M, Bohacek J, et al. Metatitanic acid pseudomorphs after titanate sulfates: nanostructured sorbents and precursors for crystalline Titania with desired particle size and shape. *Cryst. Growth Des.* **2017**;17:6762–6769.
- [29] Maslova MV, Gerasimova LG. Study of ion-exchange properties of hydrated titanium dioxide towards cesium and strontium cations. *Russ. J. Appl. Chem.* **2016**;89:1393–1401.
- [30] Hong TJ, Mao J, Tao FF, et al. Recyclable magnetic Titania nanocomposite from ilmenite with enhanced photocatalytic activity. *Molecules.* **2017**;22:1–16.
- [31] Motlochova M, Slovak V, Plizingrova E, et al. The influence of annealing temperature on properties of TiO₂ based materials as adsorbents of radionuclides. *Thermochim Acta.* **2019**;673:34–39.
- [32] Liu W, Sun W, Han Y, et al. Adsorption of Cu(II) and Cd(II) on titanate nanomaterials synthesized via hydrothermal

- method under different NaOH concentrations: Role of sodium content. *Coll. Surf., A*. 2014;452:13–147.
- [33] Savova D, Petrova N, Yardim MF, et al. The influence of the texture and surface properties of carbon adsorbents obtained from biomass products on the adsorption of manganese ions from aqueous solution. *Carbon N Y*. 2003;41(10):1897–1903.
- [34] Vassileva E, Proinova I, Hadjiivanov K. Solid-phase extraction of heavy metal ions on a high surface area titanium dioxide (anatase). *Analyst*. 1996;121:607–612.
- [35] Sountharajah DP, Loganathan P, Kandasamy J, et al. Adsorptive removal of heavy metals from water using sodium titanate nanofibres loaded onto GAC in fixed-bed columns. *J. Hazard. Mater*. 2015;287:306–316.
- [36] U.S. Environmental Protection Agency. (1976). *Quality Criteria for Water*, Office of Water and hazardous materials, Washington, DC.
- [37] López-Ramón V, Moreno-Castilla C, Rivera-Utrilla J, et al. Ionic strength effects in aqueous phase adsorption of metal ions on activated carbons. *Carbon N Y*. 2002;41:2009–2025.
- [38] Zhang H, Xu F, Xue J, et al. Enhanced removal of heavy metal ions from aqueous solution using manganese dioxide-loaded biochar: behavior and mechanism. *Sci Rep*. 2020;10(6067):1–13.
- [39] Vega FA, Covelo EF, Andrade ML. Competitive sorption and desorption of heavy metals in mine soils: influence of mine soil characteristics. *J. Colloid Interface Sci*. 2006;298:582–592.
- [40] Dong L, Liang J, Li Y, et al. Effect of coexisting ions on Cr (VI) adsorption onto surfactant modified auricularia auricula spent substrate in aqueous solution. *Ecotoxicol. Environ. Saf*. 2018;166:390–400.
- [41] Rachel NY, Nsami NJ, Placide BB, et al. Adsorption of manganese(II) ions from aqueous solutions onto granular activated carbon (GAC) and modified activated carbon (MAC). *Int. J. Innov. Sci. Eng. Technol*. 2015;2(8):606–614.
- [42] Gora SL, Andrews SA. Removal of natural organic matter and disinfection byproduct precursors from drinking water using photocatalytically regenerable nanoscale adsorbents. *Chemosphere*. 2019;218:52–63.
- [43] Doula MK. Removal of Mn²⁺ ions from drinking water by using Clinoptilolite and a Clinoptilolite-Fe oxide system. *Water Res*. 2006;40:3167–3176.
- [44] Dong SZ, Chen CZ, Li DM, et al. A study of hygienic standard for titanium in the source of drinking water. *Zhonghua Yu Fang Yi Xue Za Zhi*. 1993;27:26–28.

Supplementary Data for

Removal of manganese by adsorption onto newly synthesized TiO₂-based adsorbent during drinking water treatment

Katerina Fialova^a, Monika Motlochova^b, Lenka Cermakova^a, Katerina Novotna^a, Jana Bacova^c, Tomas Rousar^c, Jan Subrt^b, Martin Pivokonsky^{a,*}

^a*Institute of Hydrodynamics of the Czech Academy of Sciences, Pod Patankou 30/5, 166 12 Prague 6, Czech Republic*

^b*Institute of Inorganic Chemistry of the Czech Academy of Sciences, Husinec-Rez 1001, 250 68, Czech Republic*

^c*Department of Biological and Biochemical Sciences, Faculty of Chemical Technology, University of Pardubice, Studentska 573, 532 10 Pardubice, Czech Republic*

*Corresponding author:

Martin Pivokonsky

E-mail: pivo@ih.cas.cz; Tel: +420 233 109 068

This supplementary data contains the following sections, tables and figures:

S1. Toxicity assessment

Fig. S1 Effect of TiO₂-based adsorbent on dehydrogenase activity (a) and GSH levels (b) in A549 cells after 24 and 48 h of treatment. Multiwalled carbon nanotubes (MWCNTs; 100 µg mL⁻¹) were used as a positive control. Data are expressed as % of untreated cells (= control), means ± S.D. from three independent experiments, ***, p < 0.001, vs. control cells.

S2. Kinetic adsorption experiments

Fig. S2 Results of kinetic adsorption experiments for different initial concentrations of Mn²⁺ (0.1–5.0 mg L⁻¹) with the TiO₂-based adsorbent dosage of 40 mg L⁻¹ at pH 7.

Fig. S3 Kinetic modelling by (a) pseudo-first-order model and (b) pseudo-second-order model for different initial concentration of Mn²⁺ at pH 7 and TiO₂-based adsorbent dosage of 40 mg L⁻¹.

Table S1 Calculated pseudo-first-order and pseudo-second-order parameters for different initial concentration of Mn²⁺ at pH 7 and TiO₂-based adsorbent dosage of 40 mg L⁻¹.

Fig. S4 Optimization of the TiO₂-based adsorbent dosage for different initial concentrations of Mn²⁺ at pH 7; initial concentration of Mn (a) 0.1 mg L⁻¹, (b) 0.5 mg L⁻¹, (c) 1 mg L⁻¹, (d) 1.5 mg L⁻¹, (e) 2 mg L⁻¹, (f) 2.5 mg L⁻¹, (g) 3 mg L⁻¹, (h) 5 mg L⁻¹.

Fig. S5 Residual concentration of Mn after adsorption using the optimal adsorbent dosage, corresponding to 8, 12, 20, 40, 45, 50, 70 and 200 mg L⁻¹ TiO₂-based adsorbent for 0.1, 0.5, 1.0, 1.5, 2.0, 2.5, 3.0 and 5.0 mg L⁻¹ Mn, respectively; the experimental conditions were: pH 7; alkalinity 1.5 mmol L⁻¹; temperature 22 ± 0.5 °C.

Table S2 Freundlich and Langmuir model parameters for the adsorption of Mn²⁺ on the TiO₂-based adsorbent from aqueous solutions under different pH values in the absence of other ions (*Section A*) and at pH 7 with added ions (*Section B*).

Table S3 Comparison of Mn²⁺ removal efficiency in equilibrium time using TiO₂-based adsorbent dosage of 40 mg L⁻¹ and optimal TiO₂-based adsorbent dosage (for 2.0, 2.5, 3.0 and 5.0 it is 45, 50, 70 and 200 mg L⁻¹, respectively).

S1. Toxicity assessment

Due to the suspicion of titanium toxicity together with the consideration of TiO₂-based adsorbent applications in the drinking water industry, the potential harmfulness of the prepared adsorbent was tested by toxicological analysis on human cells.

S1.1 Methodology of cytotoxicity testing of TiO₂-based adsorbent

S1.1.1 Cell culture

The human lung carcinoma epithelial cell line A549 (ATCC CCL-185, Manassas, VA, USA) was used for cytotoxicity testing (Foster et al., 1998). A549 cells were cultured in Minimum Essential Medium (Invitrogen-Gibco, USA) supplemented with 10% fetal bovine serum (Invitrogen-Gibco, USA), 2 mmol L⁻¹ glutamine (Invitrogen-Gibco, USA), 1 mmol L⁻¹ pyruvate (Invitrogen-Gibco, USA), 10 mmol L⁻¹ zwitterionic sulfonic acid buffering agent HEPES (Invitrogen-Gibco, USA), and 50 μmol L⁻¹ penicillin-streptomycin solution (Invitrogen-Gibco, USA) and maintained at 37 °C and 5% CO₂. The cells were proven to be mycoplasma-free, and the origin of the cells was confirmed by short tandem repeat analysis.

S1.1.2 Treatment of cells with TiO₂-based adsorbent

A549 cells were seeded into 96-well plates at a density of 5·10³ cells per well. After 24 h of seeding, the cells were exposed to the TiO₂-based adsorbent. The adsorbent was suspended in culture medium to obtain final concentrations of 1, 10, and 100 μg mL⁻¹. Just before cell exposure, all sample solutions were vortexed and sonicated for 20 min. Untreated cells were used as a negative control. Multiwalled carbon nanotubes (MWCNTs, JRC Nanomaterials Repository, Ispra, Varese, Italy) at a concentration of 100 μg mL⁻¹ were established as a positive control.

All samples were tested for endotoxin contamination. Materials were suspended in endotoxin-free water at a concentration of 1 mg mL⁻¹. The samples were vortexed and sonicated for 15 min and then centrifuged at 15,000 g for 15 min. The endotoxin concentration was measured in the supernatant and assessed using the PyroGene™ Recombinant Factor C Assay (Lonza, Blackley, UK). According to the manufacturer's instructions, the endotoxin concentration was calculated using the standard curve, and the results were expressed as the endotoxin concentration in EU mL⁻¹.

The cells were incubated with the materials for 24 or 48 h, and the biological effect was tested using WST-1 and glutathione (GSH) assays. The WST-1 test (Sigma-Aldrich, USA) was used to detect the activity of mitochondrial dehydrogenases. After the treatment, WST-1 reagent was added to the A549 cells. The change in absorbance (0–1 h) was measured spectrophotometrically at a wavelength of 440 nm using a SPARK microplate reader (Tecan, Austria) and incubated at 37 °C. The dehydrogenase activity was expressed as the percentage of total cellular dehydrogenase activity relative to that in control cells (controls = 100%). The GSH levels were measured using an optimized bimane assay (Capek et al., 2017). After the treatment, 20 µL of the monochlorobimane solution at a final concentration of 40 µmol L⁻¹ was added to the cells, and the measurement was started. The fluorescence (*Ex/Em* = 394/490 nm) was measured kinetically for 20 min using a SPARK microplate reader (Tecan, Austria) at 37 °C. The fluorescence was expressed as the slope of a fluorescence change over time. The GSH levels were expressed as percentages relative to those in control cells (control = 100%). In both assays, the occurrence of material interference was evaluated. TiO₂-based adsorbent and MWCNTs were found to cause no interference in any of the tests when the background signal was always below 5% of that in the untreated controls.

All cellular experiments were repeated three times independently. The values were measured at least in quadruplets. The results are expressed as a mean ± S.D. Analysis of variance followed by Bonferroni posttest was used to perform the mean comparison at a significance level of $p = 0.05$ (*, $p < 0.05$, **, $p < 0.01$, ***, $p < 0.001$).

S1.2 Results of cell treatment with TiO₂-based adsorbent

Recently, few papers have been published that have shown the potential health hazards of TiO₂ nanoparticles (Borm et al., 2006; Jugan et al., 2012). Only nanoparticles of crystalline modifications of TiO₂, anatase and rutile have been studied in these publications, and no data on the health harmfulness of amorphous modifications are known. Due to the considered application in the water industry, their potential harmfulness was investigated.

According to the WST-1 test outcomes, no significant effect on dehydrogenase activity (**Fig. S1a**) was observed for any of the tested TiO₂-based adsorbent concentrations after 24 h of treatment. The concentration of 100 µg mL⁻¹ caused only a negligible decrease in dehydrogenases activity to 98 ± 5% ($p = 1.00$) vs. untreated cells. After 48 h of treatment, a significant decrease in dehydrogenases activity was apparent only in 100 µg mL⁻¹ TiO₂-based adsorbent treated cells where the dehydrogenase activity was reduced to 93 ± 6% ($p = 0.011$) vs. untreated cells. A large extent of cell damage was found in positive control cells after incubation with MWCNTs in both tested time periods.

Results on GSH levels in A459 cells treated with TiO₂-based adsorbent (**Fig. S1b**) confirmed the findings from the WST-1 test. A nonsignificant decrease of GSH concentrations to 98 ± 9% ($p = 1.00$) and 95 ± 3% ($p = 1.00$) compared to untreated cells was found in 100 µg mL⁻¹ TiO₂-based adsorbent treated cells after 24 and 48 h, respectively. Strong GSH depletion was only detectable in MWCNT-treated cells causing the depletion of GSH levels by 40–50% of those in controls. In conclusion, our results suggested that the TiO₂-based adsorbent does not cause significant cell toxicity.

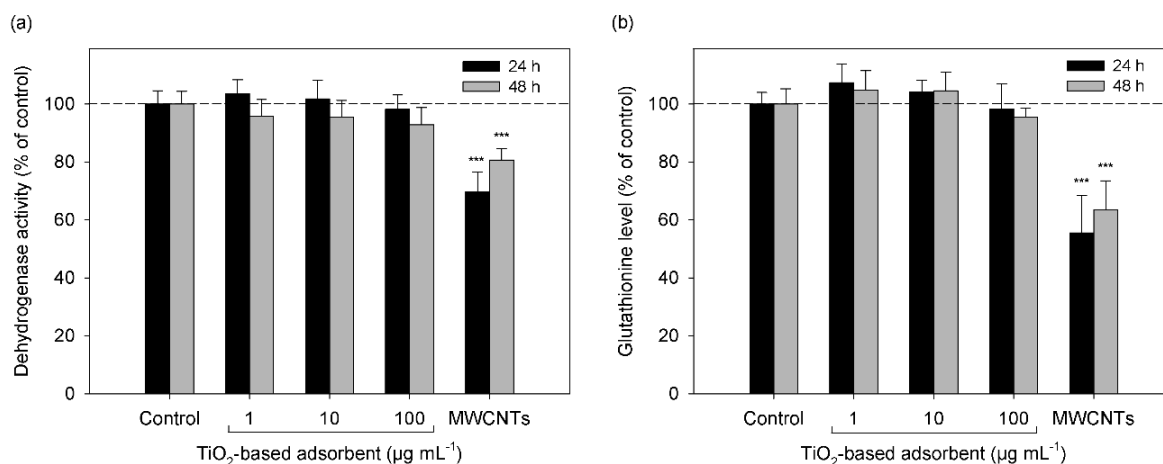


Fig. S1 Effect of TiO_2 -based adsorbent on dehydrogenase activity (a) and GSH levels (b) in A549 cells after 24 and 48 h of treatment. Multiwalled carbon nanotubes (MWCNTs; $100 \mu\text{g mL}^{-1}$) were used as a positive control. Data are expressed as % of untreated cells (= control), means \pm S.D. from three independent experiments, ***, $p < 0.001$, vs. control cells.

S2. Kinetic adsorption experiments

Kinetic adsorption experiments were performed to determine the equilibrium adsorption time. The amount of Mn adsorbed at each time interval per unit mass of adsorbent, (q_t , mg g^{-1}), was calculated as follows (1):

$$q_t = C_0 - C_t \left(\frac{V}{m} \right) \quad (1)$$

where C_0 is the initial solution concentration of Mn (mg L^{-1}), C_t is the solution concentration of Mn at a specific time t (h), V is the volume of the solution (L) and m is the mass of the adsorbent (g).

The results of adsorption kinetic experiments of Mn removal at each time interval per unit mass of adsorbent is depicted in **Fig. S2**.

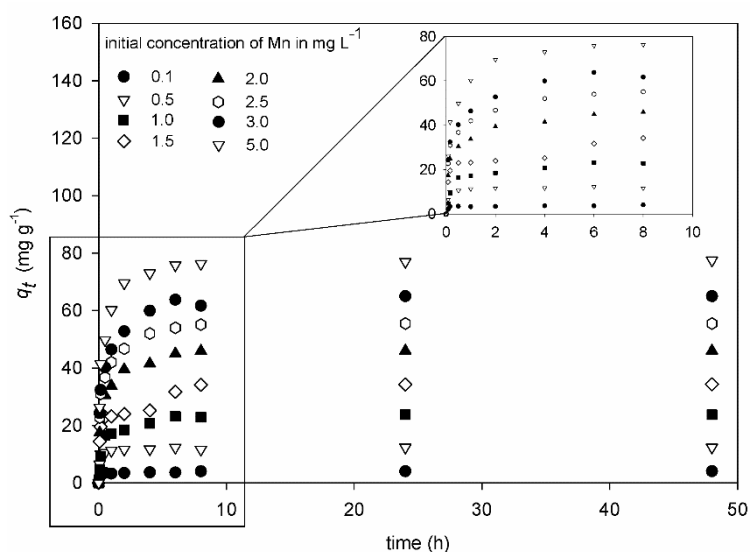


Fig. S2 Results of kinetic adsorption experiments for different initial concentrations of Mn^{2+} (0.1 – 5.0 mg L^{-1}) with the TiO_2 -based adsorbent dosage of 40 mg L^{-1} at pH 7.

The equilibrium capacities of 4.03, 11.63, 22.86, 34.18, 45.97, 55.10, 65.00, 76.28 mg L⁻¹ was reached within 8 h for initial Mn²⁺ concentration of 0.1, 0.5, 1.0, 1.5, 2.0, 3.0 and 5.0 mg L⁻¹, respectively.

In the vast majority of published works, the authors include modelling of kinetic data using different kinetic models to understand the dynamics of adsorption. Adsorption kinetics generally involves three steps, where one or a combination of more can be the rate-limiting step. Adsorption kinetics include (i) diffusion across the external boundary layer film surrounding the adsorbent particles, i.e., external diffusion or film diffusion; (ii) diffusion in the liquid contained in the pores and/or along the pore walls, i.e., internal diffusion or intra-particle diffusion; (iii) adsorption and desorption between the adsorbate and active sites, i.e., mass action. The last step, adsorption itself, is usually very rapid in comparison to the first and second steps. Therefore, the overall rate of adsorption is mostly controlled by the first or second step. Due to the sufficient speed of stirring in our study (130 rpm), the first step cannot be assumed to be the rate-limiting one.

The most commonly applied kinetic models are pseudo-first and pseudo-second-order models. The pseudo-first-order model (2) and pseudo-second-order model (3) are given by the following equations (2,3):

$$q_t = q_e(1 - \exp(-k_1 t)) \quad (2)$$

$$q_t = \frac{q_e^2 k_2 t}{1 + q_e k_2 t} \quad (3)$$

where q_t and q_e represent uptake of Mn (mg g⁻¹) at specific time t and at equilibrium, respectively, k_1 (h⁻¹), k_2 (g (mg h)⁻¹) are rate constants, and t is the specific time of sampling [h].

The applicability of the two kinetic models were examined by linear plot of $\ln(q_e - q_t)$ versus t , and (t/q_e) versus t , respectively. To quantify the applicability of each model, the correlation coefficient R^2 was calculated. The kinetic data were plotted using both the pseudo-first-order and pseudo-second-order models and are displayed along with the experimental data in **Fig. S3**. Calculated adsorption kinetics parameters for both applied kinetic models can be seen in the **Table S1**.

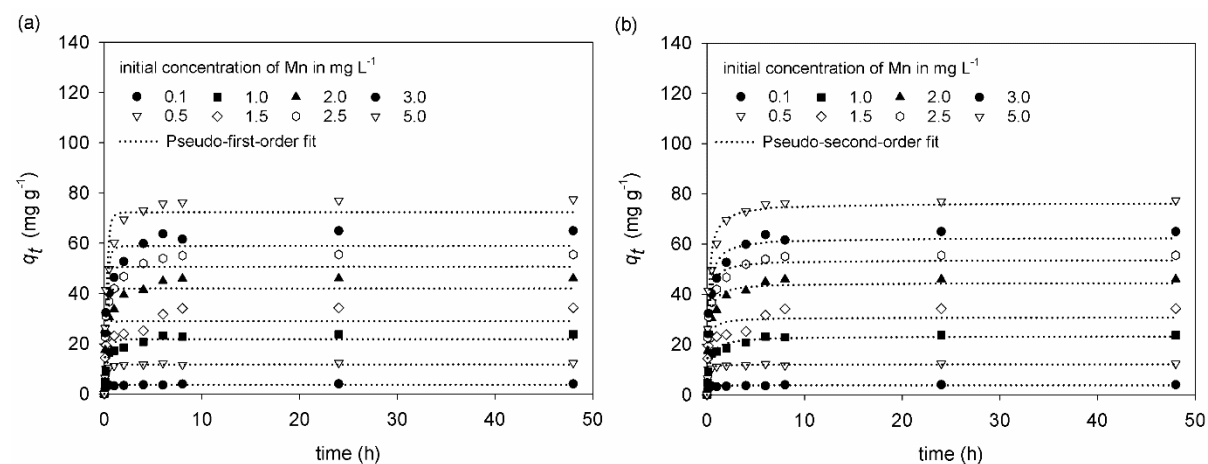


Fig. S3 Kinetic modelling by (a) pseudo-first-order model and (b) pseudo-second-order model for different initial concentration of Mn²⁺ at pH 7 and TiO₂-based adsorbent dosage of 40 mg L⁻¹.

Table S1 Calculated pseudo-first-order and pseudo-second-order parameters for each initial concentration of Mn^{2+} at pH 7 and TiO_2 -based adsorbent dosage of 40 mg L^{-1} .

Initial conc. of Mn (mg L^{-1})	$q_{e, \text{exp.}}$	Pseudo-first-order			Pseudo-second-order		
		$q_{e, \text{cal.}}$	k_1	R^2	$q_{e, \text{cal.}}$	k_2	R^2
0.1	4.06	3.71	11.365	0.9417	3.82	4.995	0.9449
0.5	12.38	11.76	10.410	0.9779	12.12	1.437	0.9838
1.0	23.75	21.82	2.692	0.9502	23.31	0.155	0.9838
1.5	34.34	28.98	6.973	0.8202	30.80	0.266	0.8882
2.0	46.00	42.01	4.704	0.9081	44.55	0.140	0.9713
2.5	55.50	50.67	5.241	0.9052	53.66	0.128	0.9702
3.0	65.00	58.93	3.783	0.8989	62.49	0.085	0.9661
5.0	77.44	72.36	3.831	0.9352	76.30	0.073	0.9842

Based on R^2 , the pseudo-second-order model explain the experimental data better. Nonetheless, it is known, that from statistical point of view, it is fundamentally wrong to compare the goodness of fit based only on R^2 . Therefore, a good fit of the kinetic model (according to R^2) does not necessarily mean that the data are following a particular kinetic model (Kumar and Gaur, 2011). The calculated value of an adsorbed amount of adsorbate per unit mass of adsorbent must be similar to the experimental value (El-Khaiary et al., 2010). The calculated q_t of pseudo-second-order model is closer to the experimental value than the pseudo-first calculated value which confirms that pseudo-second-order explains the experimental data better.

Our results are supported by the results of other studies. According to the study by Azizian et al. (2004) when the initial concentration of adsorbate is high (e.g. 500 mg L^{-1} of metal ions), the sorption kinetics fits better to the pseudo-first-order model, while for lower initial adsorbate concentration (e.g. 20 mg L^{-1} of metal ions), the sorption kinetics fits better to the pseudo-second-order model. In our study, the initial adsorbate concentration did not exceed 5 mg L^{-1} which can be considered as a low concentration of metal ions for adsorption. Furthermore, according to the other studies, pseudo-second-order model was successfully applied to the adsorption of metal ions (Nghah and Hanafiah, 2008; Debnath and Ghosh, 2008; Acharya et al., 2009; Kumar and Gaur, 2011; Maksin et al., 2012). In the study by Ho (2006) is reported that the pseudo-second-order model is used to describe the chemisorption involving valency forces through the sharing or exchange of electrons between the adsorbate and adsorbent as covalent forces, and ion-exchange. As we described in the manuscript, that ion-exchange is highly probably included in Mn^{2+} removal by our TiO_2 -based adsorbent, the pseudo-second-order model should be applied. Considering all these facts, the data obtained from the adsorption kinetic experiments are explained by pseudo-second-order model well.

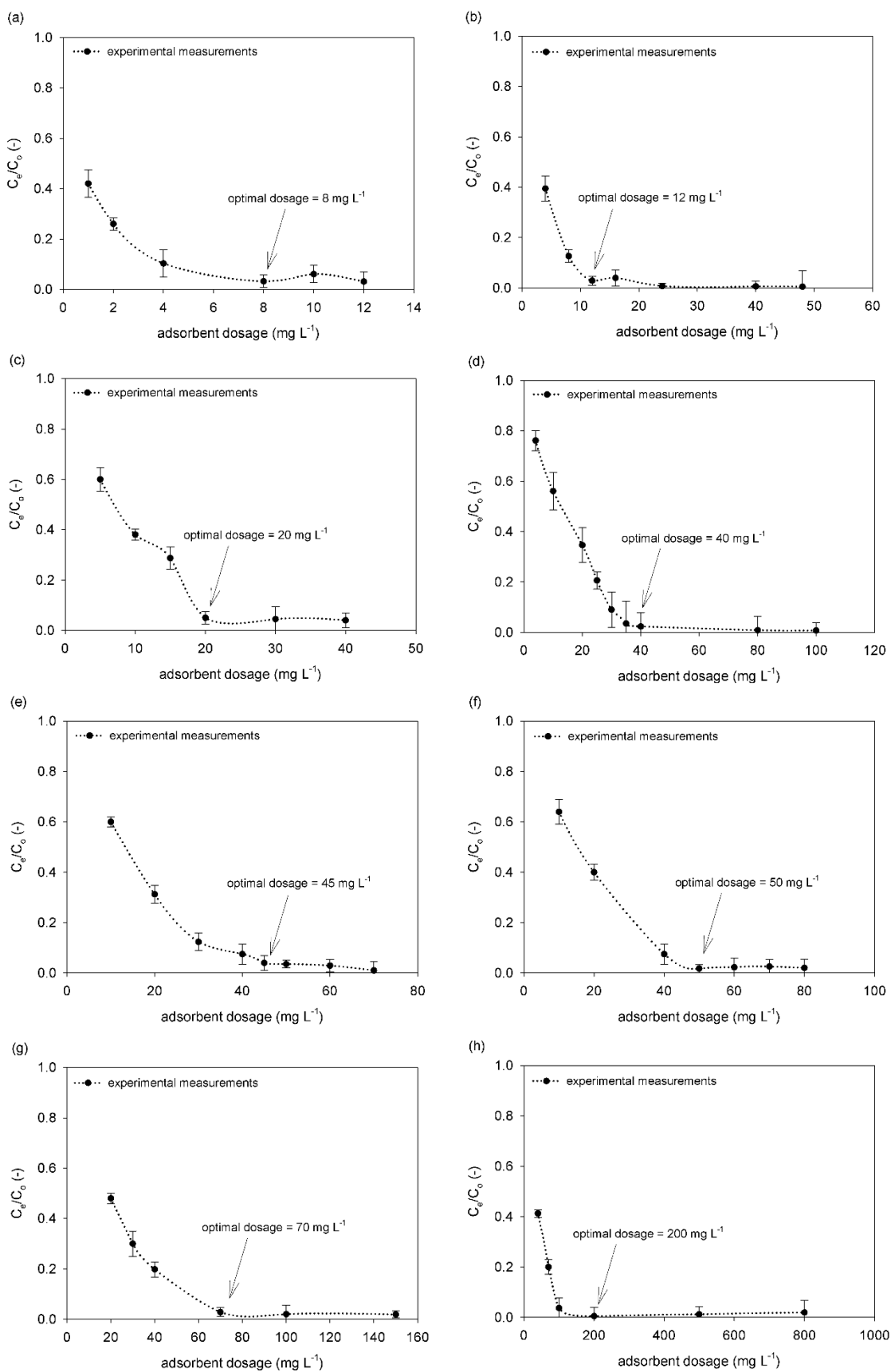


Fig. S4 Optimization of the TiO_2 -based adsorbent dosage for different initial concentrations of Mn^{2+} at pH 7; initial concentration of Mn: (a) 0.1 mg L^{-1} ; (b) 0.5 mg L^{-1} ; (c) 1 mg L^{-1} ; (d) 1.5 mg L^{-1} ; (e) 2 mg L^{-1} ; (f) 2.5 mg L^{-1} ; (g) 3 mg L^{-1} ; (h) 5 mg L^{-1} .

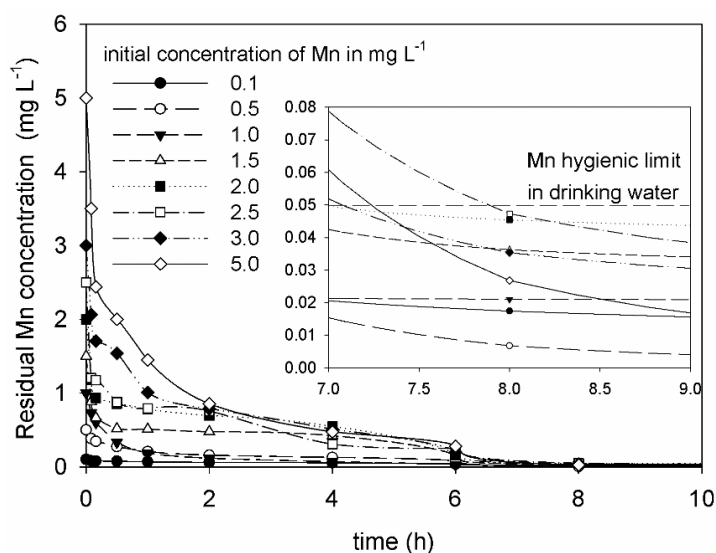


Fig. S5 Residual concentration of Mn after adsorption using the optimal adsorbent dosage, corresponding to 8, 12, 20, 40, 45, 50, 70 and 200 mg L⁻¹ TiO₂-based adsorbent for 0.1, 0.5, 1.0, 1.5, 2.0, 2.5, 3.0 and 5.0 mg L⁻¹ Mn, respectively; the experimental conditions were: pH 7; alkalinity 1.5 mmol L⁻¹; temperature 22 ± 0.5 °C.

Table S2 Freundlich and Langmuir model parameters for the adsorption of Mn²⁺ on the TiO₂-based adsorbent from aqueous solutions under different pH values in the absence of other ions (*Section A*) and at pH 7 with added ions (*Section B*).

Section A

pH	Freundlich			Langmuir		
	K_f	$1/n$	R^2	a_m	b	R^2
4	8.88	0.364	0.735	17.24	1.165	0.723
5	26.35	0.592	0.907	48.35	1.586	0.964
6	49.41	0.614	0.830	68.86	2.502	0.972
7	86.69	0.614	0.838	82.04	5.328	0.991

Section B

Added ions	Freundlich			Langmuir			
	K_f	$1/n$	R^2	a_m	b	R^2	
No added ions	86.69	0.614	0.838	82.04	5.328	0.991	
mono-valent cations	NaCl	68.28	0.585	0.855	77.52	4.115	0.991
	KCl	63.58	0.550	0.932	72.87	4.786	0.999
	K ₂ SO ₄	71.02	0.569	0.831	74.95	5.159	0.993
di-valent cations	MgSO ₄	26.91	0.702	0.980	68.79	0.773	0.941
	MgCl ₂	28.98	0.667	0.915	67.00	0.913	0.910
	CaCl ₂	9.31	0.750	0.991	36.12	0.411	0.980

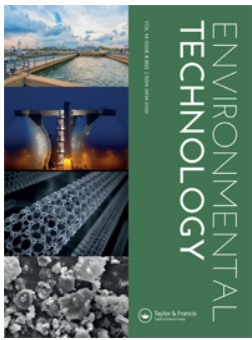
*Units: K_f [(mg g⁻¹) (L mg⁻¹)^{1/n}], n (-), a_m (mg g⁻¹), b (L mg⁻¹), R^2 (-).

Table S3 Comparison of Mn²⁺ removal efficiency in equilibrium time using TiO₂-based adsorbent dosage of 40 mg L⁻¹ and optimal TiO₂-based adsorbent dosage (for 2.0, 2.5, 3.0 and 5.0 it is 45, 50, 70 and 200 mg L⁻¹, respectively).

Initial concentration of Mn ²⁺ (mg g ⁻¹)	Removal efficiency in equilibrium (%)	
	adsorbent dosage of 40 mg L ⁻¹	optimal adsorbent dosage
2.0	92.0	98.1
2.5	88.8	98.3
3.0	86.7	98.9
5.0	66.6	99.5

References

- Acharya, J., Sahu, J.N., Sahoo, B.K., Mohanty, C.R., Meikap, B.C., 2009. Removal of chromium(VI) from wastewater by activated carbon developed from *Tamarind wood* activated with zinc chloride. *Chemical Engineering Journal* 150, 25–39.
- Azizian, S., 2004. Kinetic models of sorption: a theoretical analysis. *Journal of Colloid and Interface Science* 276, 47–52.
- Borm, J.A., Robbins, D., Haubold, S., Kuhlbusch, T., Fissan, H., Donaldson, K., Schins, R., Stone, V., Kreyling, W., Lademann, J., Krutmann, J., Warheit, D., Oberdorster, E., 2006. The potential risks of nanomaterials: a review carried out for ECETOC, *Particle and Fibre Toxicology* 3, 35.
- Capek, J., Hauschke, M., Bruckova, L., Rousar, T., 2017. Comparison of glutathione levels measured using optimized monochlorobimane assay with those from ortho-phthalaldehyde assay in intact cells, *Journal of Pharmacological and Toxicological Methods* 88, 40–45.
- Debnath, S., Ghosh, U.Ch., 2008. Kinetics, isotherm and thermodynamics for Cr(III) and Cr(IV) adsorption from aqueous solutions by crystalline hydrous titanium oxide. *Journal of Chemical Thermodynamics* 40, 67–77.
- El-Khaiary, M., Malash, G.F., Ho, Y-S., 2010. On the use of linearized pseudo-second-order kinetic equations for modeling adsorption systems. *Desalination* 257, 93–101.
- Foster, K.A., Oster, C.G., Mayer, M. M., Avery, M. L., Audus, K. L., 1998. Characterization of the A549 cell line as a type II pulmonary epithelial cell model for drug metabolism, *Experimental Cell Research* 243, 359–366.
- Ho, Y-S., 2006. Review of second-order models for adsorption systems. *Journal of Hazardous Materials* B136, 681–689.
- Jugan, M.L., Barillet, S., Simon-Deckers, A., Herlin-Boime, N., Sauvaigo, S., Douki, T. Carriere, M., 2012. Titanium dioxide nanoparticles exhibit genotoxicity and impair DNA repair activity in A549 cells, *Nanotoxicology* 6, 501–513.
- Kumar, D., Gaur, J.P., 2011. Chemical reaction- and particle diffusion-based kinetic modeling of metal biosorption by a *Phormidium* sp.-dominated cyanobacterial mat. *Bioresources Technology* 102, 633–640.
- Maksin, D.D., Klkakević, S.O., Đolić, M.B., Marković, J.P., Ekmešćić, B.M., Onjia, A.E., Nastasović, A.B., 2012. Kinetic modeling of heavy metal sorption by vinyl pyridinebased copolymer. *Hemijska industrija* 66 (6), 795–804.
- Ngah, W.S.W., Hanafiah, M.A.K.M., 2008. Biosorption of copper ions from dilute aqueous solutions on base treated rubber (*Hevea brasiliensis*) leaves powder: kinetics isotherm, and biosorption mechanisms. *Journal of Environmental Sciences* 20, 1168–1176.




Investigating adsorption of model low-MW AOM components onto different types of activated carbon – influence of temperature and pH value

Lenka Cermakova, Katerina Fialova, Ivana Kopecka, Magdalena Baresova & Martin Pivokonsky


To cite this article: Lenka Cermakova, Katerina Fialova, Ivana Kopecka, Magdalena Baresova & Martin Pivokonsky (2022) Investigating adsorption of model low-MW AOM components onto different types of activated carbon – influence of temperature and pH value, Environmental Technology, 43:8, 1152-1162, DOI: [10.1080/09593330.2020.1820082](https://doi.org/10.1080/09593330.2020.1820082)

To link to this article: <https://doi.org/10.1080/09593330.2020.1820082>

 View supplementary material [↗](#)


 Published online: 17 Sep 2020.

 Submit your article to this journal [↗](#)

 Article views: 159

 View related articles [↗](#)

 View Crossmark data [↗](#)

 Citing articles: 2 View citing articles [↗](#)



Investigating adsorption of model low-MW AOM components onto different types of activated carbon – influence of temperature and pH value

Lenka Cermakova ^{a,b}, Katerina Fialova ^a, Ivana Kopecka ^a, Magdalena Baresova ^a and Martin Pivokonsky ^a

^aInstitute of Hydrodynamics of the Czech Academy of Sciences, Prague 6, Czech Republic; ^bInstitute for Environmental Studies, Faculty of Science, Charles University, Prague 2, Czech Republic

ABSTRACT

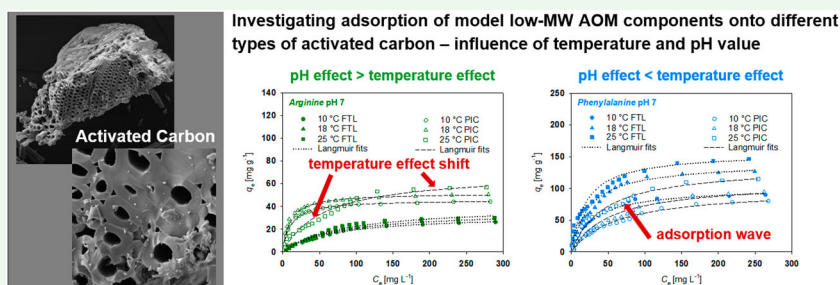
Low molecular weight algal organic matter (AOM), as a frequent water contaminant with poor coagulation efficiency, adversely affects the quality of produced water and serves as a source of potentially carcinogenic disinfection by-products. AOM removal from water is inevitable to eliminate the negative health and environmental impacts. This research evaluates the removal of arginine, phenylalanine and aspartic acid, which are amino acids abundant in AOM. Adsorption experiments were performed at 10, 18 and 25 °C and pH 5, 7 and 9 using two different activated carbons (FTL, PIC). Amino acids showed endothermic adsorption behaviour, with a higher removal at higher temperature. Higher temperature increased the diffusion of amino acid molecules, reduced the solution viscosity, or enhanced the hydrophobic interactions contributing to adsorption. The effect of temperature manifested differently during experiments depending on the chemical nature of the amino acids, the pH value and the surface properties of the carbon. Phenylalanine isotherms showed specific waves (Langmuir type 4). pH had a greater effect on arginine adsorption than did temperature. Aspartic acid isotherms exhibited a decrease in adsorption at higher pH values and higher temperatures. The principal mechanisms involved in amino acid adsorption were hydrophobic interactions, electrostatic interactions or hydrogen bonds.

ARTICLE HISTORY

Received 2 June 2020
Accepted 31 August 2020

KEYWORDS

Adsorption; algal organic matter; amino acid; temperature; water treatment





Highlights

- Amino acids were adsorbed on different carbons at temperatures of 10, 18 and 25 °C.
- Amino acids adsorption was an endothermic process under the given conditions.
- Temperature affects the adsorption of amino acids depending on their concentration.
- The effect of temperature depends on the dominant mechanism involved in adsorption.
- Phenylalanine may exhibit Langmuir type 4 adsorption isotherms.

1. Introduction

The problems associated with the presence of low-molecular-weight algal organic matter (AOM) in waters treated for drinking purposes have become increasingly important over the last few years. This organic material, produced by cyanobacteria and green algae as extracellular organic matter (EOM) or originating from the lysis of their cells as cellular organic matter (COM), has been reported to be more difficult to remove by coagulation processes than are algal products with high molecular weights (MW > 10 kDa) [1]. Both EOM and COM

CONTACT Martin Pivokonsky  pivo@ih.cas.cz  Institute of Hydrodynamics of the Czech Academy of Sciences, Pod Patankou 30/5, Prague 6 166 12, Czech Republic

 Supplemental data for this article can be accessed <https://doi.org/10.1080/09593330.2020.1820082>.

© 2020 Informa UK Limited, trading as Taylor & Francis Group

contain a variety of peptides and free and combined amino acids (AAs), which together represent the dominant part of the low-MW fraction ($MW < 10$ kDa) [2]. These compounds adversely affect the quality of produced water, the consumption of the coagulation agent or the disinfection efficiency [3,4]. Free AAs have been reported to be among the most reactive nitrogenous organic compounds; these compounds can interfere with aqueous chlorine and are associated with the formation of harmful disinfection by-products, such as trihalomethanes and haloacetic acids [5]. AAs cause taste and odour problems [6], and they may also serve as a potential source of biodegradable organic carbon for microorganisms in the water distribution network [7,8].

Many studies have revealed the importance of algal removal in drinking water treatment plants [4,9,10]. However, as far as we know, there is only one study aimed at eliminating cyanobacterial AAs concerning potable water production [11]. Most studies have been performed in the fields of biochemistry, medicine, geochemistry or the food industry [12]. It is clear from the available research that the removal efficiency of conventional water treatment approaches based on destabilization and aggregation is negligible for low-MW compounds such as AAs [1] and other treatment methods should be used for their elimination. Adsorption onto activated carbon (AC) represents a possibility for addressing this challenge because AC adsorbents are commonly used by water utilities to control other natural or anthropogenic pollutants, such as humic substances, cyanotoxins and pesticides [10,13]. AC adsorbents are often part of a treatment line, and minimal additional costs are required. If the AC and specific treatment conditions are appropriately selected, low-MW organic substances of various origins and chemical properties (e.g. with different functional groups, such as $-OH$, $-SH$, $-COOH$, $=NH_2^+$, and $-NH_3^+$) will be effectively removed [14–16]. Our previous study revealed that the adsorption efficiency of cyanobacterial AAs fundamentally depends on the pH and ionic strength of the solution. Electrostatic interactions, hydrophobic interactions and/or hydrogen bonds were identified as the dominant mechanisms of *Arg*, *Asp* and *Phe* adsorption on AC [11]. However, there is little information in the literature concerning the influence of water temperature on the removal of AAs by AC, although temperature is one of the main factors influencing the adsorption process [17].

The temperature of raw water varies from 4 to 20 °C depending on the season, which affects the entire water treatment process, from coagulation through adsorption to disinfection [18]. Temperature affects not only the adsorption equilibrium but also the adsorption

kinetics [19]. It has been proven that the solution viscosity, the solubility of organic compounds [20], the Brownian and diffusion motion of molecules [21], the kinetic energy of molecules [22] and adsorbent chemistry are temperature-dependent variables. A detailed analysis of adsorption thermodynamics can provide insight into intermolecular interactions between the adsorbate and adsorbent at the phase interface [23].

Adsorption is generally considered to be a spontaneous process with an exothermic nature, and an increased uptake of organic molecules is expected when the adsorption temperature decreases [17]. Sebben and Pendleton [23] observed an exothermic response for AAs adsorbed onto mineral silica with an oxide surface. Glycine and lysine experienced a greater negative effect with increased temperature than did glutamic acid. An increase in uptake with reduced temperature was also described by Titus et al. [24] for phenylalanine, alanine, tyrosine and tryptophan on highly hydrophobic NaZSM-5 zeolite. The isotherms were essentially independent of pH, but they varied significantly with temperature. The same adsorption pattern was confirmed by the study of Clark et al. [25]. The performance of an agricultural residue-based AC was evaluated with respect to the removal of phenylalanine from aqueous solutions, and the results showed that the higher the temperature was, the lower the adsorbed amount. However, some studies have reported that the amount of organic compounds adsorbed on AC increases with increasing temperature; hence, the process is endothermic [26,27]. Liu et al. [28] observed that the adsorption of arginine from diluted aqueous solution onto spherical cellulose is also an endothermic process. The adsorbed amount of arginine increased with temperature from 20 to 50 °C. One possible explanation for the endothermic nature of the adsorption process is related to hydration. For a compound to adsorb to the adsorbent surface, it must first lose part of its hydration coating, which occurs at the same time as energy consumption [29]. The increase in adsorption efficiency due to higher temperature can also be explained by the fact that with increasing temperature, molecules interact more easily with each other. This behaviour results in the formation of larger associates that are able to bind to the active centres on the AC surface [26]. It is even possible that a change from monolayer adsorption to multilayer adsorption may occur at higher concentrations of a given substance due to higher temperature [30].

A number of studies have compared the effect of different temperatures on adsorption and then concluded whether the process is exothermic or endothermic. However, these studies often do not explain the

possible reasons for the thermodynamic behaviour of the investigated substances. The results are sometimes inconsistent, and more detailed research on this issue is needed.

The purpose of this study was twofold. First, we investigated the effect of different solution temperatures (10, 18 and 25 °C) on the adsorption behaviour of arginine (*Arg*), phenylalanine (*Phe*) and aspartic acid (*Asp*) on AC. These amino acids are the major amino acids in AOM; they are commonly identified in natural waters and in treated water after coagulation/flocculation. Second, we focused on complementing the findings of AA adsorption from our previous study [11], which may help elucidate the removal of low-MW AOM in water treatment. Since the adsorption of AAs is highly pH dependent, thermodynamic experiments were performed at three different pH values of 5, 7 and 9. Two types of granular activated carbon (GAC) with different chemical properties (Filtrisorb TL830 and Picabiol 12 × 40) were used. Both adsorbents are designed for water treatment technologies.

2. Materials and methods

All experimental solutions were prepared from analytical reagent-grade chemicals and demineralized water (GW 65, Goldman Water, CZ) with a total alkalinity of 1.5 mmol L⁻¹ adjusted with 0.125 M NaHCO₃ to approximate the typical alkalinity of raw surface water.

2.1. Adsorbates and their analysis

Adsorption experiments were performed with three AAs with different chemical and structural properties (Table 1): *L*-arginine (*Arg*), *L*-phenylalanine (*Phe*) and *L*-aspartic acid (*Asp*) (Sigma-Aldrich, U.S.A.). The adsorbates were selected based on the results of our previous study, where we evaluated the concentrations of AAs in AOM and summarized the effects of solution pH and ionic strength on the removal of cyanobacterial AAs by GAC [11]. Significant concentrations of free AAs have been detected in AOM produced by *Microcystis aeruginosa*, a cyanobacterium responsible for serious problems in water reservoirs in many countries, including the Czech Republic [5]. *Arg*, *Phe* and *Asp* have been identified as the most abundant AAs in the cellular portion of AOM [11]. Cyanobacterial cells are generally rich in *Arg* and *Asp* because these AAs together form cyanophycin, a co-polymer that serves as a nitrogen reservoir [31].

The side chain of *Phe* is formed by an aromatic ring that gives the amino acid a non-polar character and allows it to participate in hydrophobic interactions.

Table 1. General characteristics of the amino acids and granular activated carbons.

Characteristics of adsorbate	<i>L</i> -arginine (<i>Arg</i>)	<i>L</i> -phenylalanine (<i>Phe</i>)	<i>L</i> -aspartic acid (<i>Asp</i>)
MW (Da)	174.20	165.19	133.10
pI	10.76	5.48	2.98
Solubility (mg 100 mL ⁻¹)	14.87	2.69	0.45
Functional groups	α-COOH (pK _a = 2.17) α-NH ₂ (pK _a = 9.04) guanidyl group (pK _a = 12.48)	α-COOH (pK _a = 1.83) α-NH ₂ (pK _a = 9.13)	α-COOH (pK _a = 2.09) α-NH ₂ (pK _a = 9.82) β-COOH (pK _a = 3.86)
Characteristics of adsorbent	Filtrisorb TL830 (FTL)	Picabiol 12 × 40 (PIC)	
Precursor	Bituminous coal	Vegetal material	
Activation agent	Water steam	Phosphoric acid	
S _{BET} (m ² g ⁻¹)	1036	1692	
S _{mezo} (m ² g ⁻¹)	419	765	
V _{total} (cm ³ g ⁻¹)	0.61	1.21	
V _{micro} (cm ³ g ⁻¹)	0.29	0.47	
(V _{micro} /V _{total})·100 (%)	47	39	
pH _{pzc}	7.75	4.45	
Acidity (mmol g ⁻¹)	0.295	2.045	
Basicity (mmol g ⁻¹)	0.255	0.112	

Note: Surface characteristics of FTL and PIC samples are slightly different in the present study and the former study of Cermakova et al. [11] (mainly in pH_{pzc} values), even if the GACs was of the same type. This may be because the manufacturer provided for both studies identical types of GACs but different series of them. However, there was no change in the fact that the charge of PIC was negative throughout the whole experimental pH 5–9 and that it changed from positive to negative in the case of FTL when the experimental pH exceeded its pH_{pzc} in both studies.

Arg is classified as a basic amino acid with amino and guanidyl groups in the side chain. It carries a predominantly positive charge in the experimental pH range of 5–9 due to the protonation of amino groups. *Asp* is a hydrophilic amino acid with acidic character due to the presence of carboxylic groups. It is negatively charged in the experimental pH range of 5–9. The pH-dependent forms of all three AAs are shown in Figure 1.

Amino acid quantification was accomplished based on dissolved organic carbon (DOC) analysis before and after the adsorption experiments. DOC was calculated as the difference between total carbon (TC) and inorganic carbon (IC). All samples were first filtered through a 0.22 μm membrane filter (Millipore, U.S.A.). A total organic carbon analyser (TOC-V_{CPH}) with an autosampler (ASI-V, Shimadzu Corporation, Japan) was used for the measurements. Calibration was performed using potassium hydrogen phthalate as a TC standard and sodium bicarbonate and sodium carbonate as IC standards. Each sample was analysed in triplicate, and the relative error was < 2%. The calibration curve for amino acid

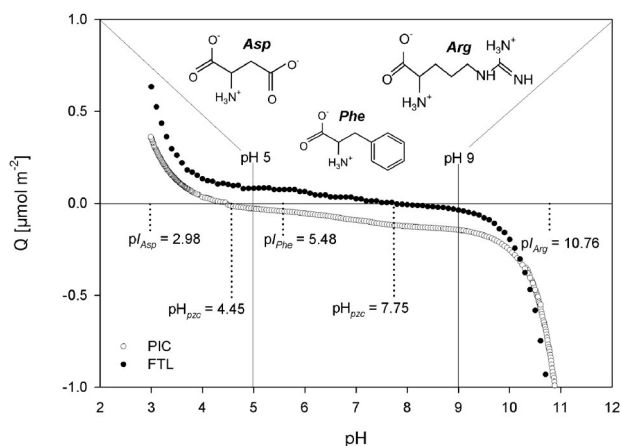


Figure 1. Schematic representation of the charge conditions for the adsorption of the amino acids *Phe*, *Asp* and *Arg* from water solution on the granular activated carbons FTL and PIC (pI – isoelectric point of the amino acid, pH_{pzc} – point of zero charge of the activated carbon, Q – surface charge of the activated carbon in $\mu\text{mol m}^{-2}$).

concentrations (C_{AA}), expressed as DOC in mg L^{-1} , is given in our previous study [11-Supplementary data].

2.2. Adsorbents and their characterization

The granular activated carbons Filtrasorb TL830 (FTL) (Chemviron Carbon, U.S.A.) and Picabiol 12×40 (PIC) (Jacobi Carbons, Japan), manufactured for the treatment of water samples containing AOM, taste and odour compounds, cyanobacterial toxins or AAs, were applied in adsorption experiments. The textural properties of the GACs were characterized in terms of the specific surface area (S_{BET}), total pore volume (V_{total}) or volume of micropores (V_{micro}). The point of zero charge (pH_{pzc}), indicating the surface charge of an adsorbent at different pH values, was also determined for both GACs according to the methodology of Álvarez-Merino et al. [32]. A negative charge predominates on the surface of the adsorbent at a pH lower than pH_{pzc} . If the experimental pH is higher than pH_{pzc} , the total charge on the adsorbent surface is considered to be positive. The details of the performed characterization methods, as well as more reasons for choosing these types of adsorbents, are explained in our previous paper [16]. All other characteristics of the GACs including for example the amount of acidic and basic functional groups, are summarized in Table 1. Overview of the charge conditions in the adsorption system under the experimental pH values can be seen in Figure 1. Based on the characteristics given in Table 1, it is evident that adsorption of target amino acids will occur in the micropore region due to their very

low molecular weight. The representation of this pore category is significant in both GAC samples (about 40% and more). Moreover, based on the information provided by the manufacturers, both types of GAC are suitable for the adsorption of target pollutants even in the presence of high molecular weight organics. Competition for sites or pore blocking is not expected.

2.3. Adsorption experiments and data evaluation

Adsorption isotherms of *Arg*, *Phe* and *Asp* were obtained by batch experiments performed by shaking samples (250 mL) of each of the AAs ($5\text{--}300 \text{ mg L}^{-1}$ DOC) for 48 h with 400 mg L^{-1} of adsorbent (FTL or PIC) at pH 5, 7 and 9. Each experiment was performed in triplicate, and the data were reported as the average value \pm standard deviation (SD). Standard deviations of equilibrium surface concentrations (q_e) are summarized in Table S1 in Supplementary Material. The time interval required to establish adsorption equilibrium was predetermined by kinetic tests. An example of this kinetic test is presented in Figure S1 in Supplementary Material. The effect of solution temperature on the removal of AAs was simulated by performing the tests at different temperatures of 10, 18 and $25 \text{ }^\circ\text{C}$. Full details of sample preparation and treatment methods are given in our previous work [11]. The amount of AAs adsorbed per unit mass of adsorbent at equilibrium (q_e , mg g^{-1}) was calculated as follows:

$$q_e = (C_0 - C_e) \frac{V}{m} \quad (1)$$

where C_0 and C_e are the initial and equilibrium solution concentrations of AAs (mg L^{-1}), respectively, V is the solution volume (L), and m is the mass of the adsorbent (g).

The correlation of the experimental adsorption data with the Langmuir (2) and Freundlich (3) isotherm models was undertaken to gain an understanding of the adsorption behaviour. The isotherm models are given by the following equations:

$$q_e = \frac{a_m b C_e}{1 + b C_e} \quad (2)$$

and

$$q_e = K_f C_e^{1/n} \quad (3)$$

where q_e (mg g^{-1}) and C_e (mg L^{-1}) represent the adsorbate uptake and solution concentration at equilibrium, respectively. The parameters a_m (mg g^{-1}) and K_f [$(\text{mg g}^{-1})(\text{L mg}^{-1})^{1/n}$] reflect the adsorption capacity; the constants b and $1/n$ represent the surface affinity and the

heterogeneity of surface site energy distribution, respectively.

3. Results and discussion

3.1. Adsorption of amino acids at different temperatures

The effect of solution temperature on *Arg*, *Phe* and *Asp* adsorption was investigated by a series of batch equilibrium tests at three different temperatures of 10, 18 and 25 °C and at pH 5, 7 and 9. The experimental data were fitted to the Freundlich and Langmuir adsorption isotherm models. The parameters of both models are summarized in Table S2 in the Supplementary Material. The Freundlich parameter K_f reflects the adsorption capacity, and the constant $1/n$ describes the heterogeneity of the surface site energy distribution. The Langmuir parameter a_m represents the maximum adsorbate uptake at monolayer coverage, and the parameter b reflects the surface affinity and the rate of change in uptake. The values of the coefficients of determination (R^2) were higher for the Langmuir model, which more accurately represented the experimental data and was therefore included in the figures predicting amino acid adsorption.

3.2. Equilibrium adsorption of arginine

Figure 2 shows the experimental and model data for the adsorption of *Arg* on the GACs (FTL and PIC). The equilibrium data are displayed as a function of solution temperature at individual pH values. The Langmuir isotherm model was used to predict adsorption data based on the higher R^2 values obtained using this model than the Freundlich model (Table S2). *Arg* was the only investigated AA that was more efficiently adsorbed on PIC than on FTL. The highest efficiency was achieved at pH 9 and at 25 °C ($q_e = 76.8 \pm 2.64 \text{ mg g}^{-1}$); on the other hand, the lowest efficiency was measured at pH 5 and 10 °C ($q_e = 31.5 \pm 2.71 \text{ mg g}^{-1}$). The functional groups on the PIC surface were negatively charged because the experimental pH values were higher than the PIC pH_{pZC} of 4.45 (see Table 1). The overall negative charge of the adsorbent continued to increase with increasing pH from 5 to 9 (Figure 1). *Arg* had a predominantly positive charge under all experimental conditions, and thus, attractive electrostatic interactions between the PIC surface and *Arg* occurred. The manifestation of these interactions was also supported by the high amount of acidic functional groups on PIC (Table 1) [11]. As the pH of the solution decreased, the PIC negative charge also decreased, and the adsorption

efficiency gradually declined. The effect of pH on *Arg* adsorption on PIC was much greater than the dependency on solution temperature [12]. The effect of temperature was clearly observable only at pH 9, when the

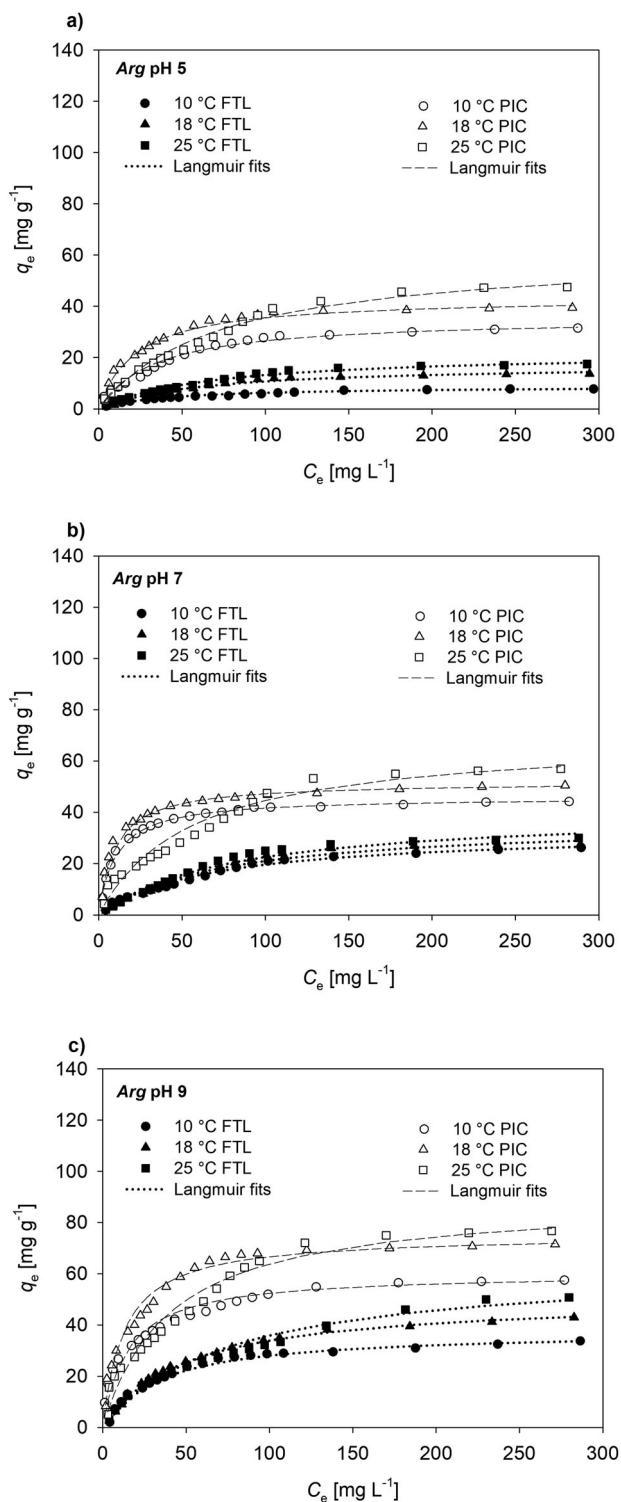


Figure 2. Isotherms and fits to the Langmuir model for the adsorption of *Arg* on FTL and PIC at different temperatures (10, 18 and 25 °C) and at (a) pH 5, (b) pH 7 and (c) pH 9.

electrostatic interactions between PIC and *Arg* were the strongest. The difference in *Arg* uptake at 10 and 25 °C was $\sim 20 \text{ mg g}^{-1}$ at pH 9, while only half this difference was observed at pH 7. The temperature trend was inconsistent at pH 5 and pH 7. A higher adsorption efficiency was achieved at 18 °C than at 25 °C at lower concentrations of *Arg*; however, at higher concentrations ($C_e \geq 120 \text{ mg L}^{-1}$), the adsorption efficiency measured at 25 °C was greater, and the overall process showed signs of endothermic adsorption (i.e. q_e at 10 °C $<$ q_e at 18 °C $<$ q_e at 25 °C). The link between the effect of temperature and the concentration of adsorbate in the solution was also confirmed by the study of Liu et al. [28]. A detailed view of the isotherms measured at 25 °C showed that these isotherms were initially more linear at lower *Arg* concentrations than isotherms measured at 10 or 18 °C. The initial slope of an isotherm depends on the rate of change of site availability with an increasing amount of solute adsorbed. Linearity of an isotherm usually means that the availability of adsorption sites remains constant at certain concentrations. Similar isotherm characteristics have been observed for the adsorption of certain amino acids and peptides in water on silica. The mechanism under such conditions is rather obscure, and it probably involves a contribution from the hydrogen bonding of amino groups with silica [33].

Similar trends were obtained for *Arg* adsorption on FTL. The effect of pH on *Arg* adsorption on FTL was significant, and *Arg* removal decreased in the order of pH 9 > pH 7 > pH 5. This result corresponded well with the trends in data and parameters predicted by both isotherm models in Table S1. However, the adsorption efficiency on FTL was lower than that of PIC (pH 9 and 25 °C: $q_e = 50.8 \pm 2.55 \text{ mg g}^{-1}$; pH 5 and 10 °C: $q_e = 7.8 \pm 2.36 \text{ mg g}^{-1}$). The dominant adsorption mechanism on FTL was electrostatic interactions, as in the case of PIC. These interactions were weaker due to the less negative charge of FTL caused by less amount of acidic functional groups, and thus, the overall adsorption efficiency was lower. Similar results and the dominant influence of electrostatic interactions were confirmed in a study by O' Connor et al. [34]. Hydrogen bonds formed between *Arg* and FTL functional groups probably also contributed to adsorption, especially at pH 5 and pH 7, at which values electrostatic interactions were less dominant [11].

The adsorption efficiency increased with an increase in temperature from 10 to 25 °C at all pH values, and the adsorption process could be considered endothermic. A hydrating coating can be formed around water-soluble substances to stabilize them. A higher temperature probably provides the energy needed to break the

bonds with water and thereby allows the adsorption of *Arg* [29,35]. A higher solution temperature may also increase the diffusion rate of molecules, which can then more easily penetrate into the inner structure of the adsorbent and bind there [36]. However, the effect of temperature on *Arg* adsorption was generally less pronounced than the effect of pH. This effect can clearly be seen from the *Arg* isotherms measured at pH 7 (Figure 2). A small effect of temperature was also described by Sebben and Pendleton [23] in the case of lysine adsorption.

3.3. Equilibrium adsorption of phenylalanine

Figure 3 shows experimental and model data for the adsorption of *Phe* on FTL and PIC. The equilibrium data are displayed as a function of solution temperature at individual pH values. The results of equilibrium adsorption tests with *Phe* differ significantly from those with *Arg* (Figure 2). *Phe* adsorbed on FTL better than on PIC and this can be related to the manifestation of hydrophobic interactions. According acid-base characterization of GACs based on Boehm titration (Table 1), FTL is generally less charged than PIC, thus hydrophobic bonds could be more pronounced. The highest adsorption efficiency was achieved at 25 °C, with almost no difference between individual pH values (pH 5: $q_e = 148.8 \pm 3.20 \text{ mg g}^{-1}$, pH 7: $q_e = 146.5 \pm 3.10 \text{ mg g}^{-1}$, pH 9: $q_e = 145.5 \pm 3.15 \text{ mg g}^{-1}$). This behaviour was also reflected in the small differences between the a_m parameters of the Langmuir model (Table S2). Temperature had a greater effect on *Phe* adsorption than did pH. The equilibrium surface concentration of *Phe* increased with increasing temperature on both GACs in the order 10 °C < 18 °C < 25 °C, so the adsorption process can be characterized as endothermic under all experimental pH values (see Figure 3). A higher temperature imparted more kinetic energy to the *Phe* molecules, which led to an increase in their diffusion [26], and the molecules could penetrate more rapidly into the internal porous structure of the GACs [37]. The properties of *Phe* are influenced by the aromatic nucleus in its side chain, which makes this amino acid strongly hydrophobic in nature. *Phe* prefers to minimize contact with water at all pH values by changing its conformation or by adsorption from solution [38]. *Phe* molecules can be oriented parallel to the adsorbent surface due to the aromatic nucleus. This position is more energy efficient than other positions [39,40]. Hydrophobic interactions between *Phe* molecules are enhanced at higher temperatures, and the molecules cluster into larger associates that can be adsorbed as a complex. Thus, more *Phe* molecules are adsorbed to GAC than expected due to the

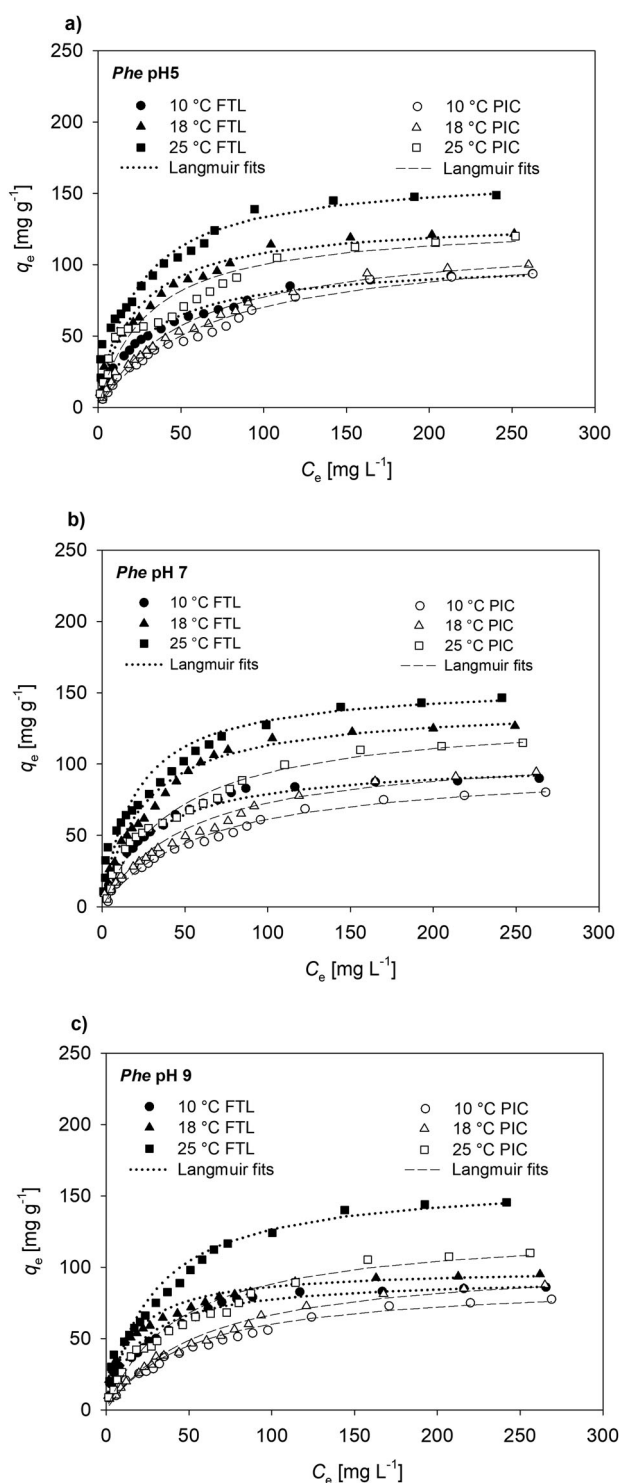


Figure 3. Isotherms and fits to the Langmuir model for the adsorption of *Phe* on FTL and PIC at different temperatures (10, 18 and 25 °C) and at (a) pH 5, (b) pH 7 and (c) pH 9.

number of action centres [26]. *Phe* molecules need to interact through hydrophobic bonds, not only with themselves but also directly with the surface of GAC [11]. According to Alves et al. [40], adsorbed *Phe* molecules can further react with *Phe* molecules that are

still dissolved in solution by means of hydrogen bonds, which contributes to a further increase in adsorption. These interactions are supported by higher temperatures.

The adsorption of AAs including *Phe* to a silicate adsorbent at 20–60 °C was studied by Basiuk et al. [41], and the results showed the exothermic nature of the adsorption of all investigated AAs. Silvério et al. [42] also evaluated *Phe* adsorption on layered hydroxides and found that the process was exothermic at experimental temperatures of 25–37 °C. The differences in the results of these individual studies are probably related to the different characteristics of the adsorbents and different experimental conditions applied.

The adsorption efficiency of *Phe* on PIC was lower than that on FTL due to the different surface charges of the two GACs (see Figure 1). In addition to hydrophobic interactions, which are considered to be the dominant forces controlling the adsorption of *Phe* on GAC, electrostatic interactions are present in the case of PIC. Because of the high acidity of PIC, the repulsive interactions between the dissociated carboxyl group of *Phe* and the negatively charged PIC surface groups reduce adsorption [more details in 11].

A detailed examination of Figure 3 reveals a wave in the *Phe* isotherms for both GACs. The wave occurs at all pH values and temperatures but is particularly evident at pH 5 and 25 °C (see Figure S2 in the Supplementary Material). Moreover, the wave is probably influenced by the initial concentration of adsorbate, since it can always be observed at approximately $C_e \sim 50 \text{ mg L}^{-1}$. According to Giles et al. [33], the isotherms were classified as sub-group 4 of the Langmuir type (L4). The isotherms were also included in the same classification group in the study by El Shafei et al. [38] examining the amino acid histidine, which is very similar to *Phe* in properties. The study of Scheufele et al. [30] explains this wave phenomenon by the change in adsorption mechanism from monolayer to multilayer at a higher initial adsorbate concentration ($C_e > 100 \text{ mg L}^{-1}$). Waves in adsorption isotherms can also be found in other studies [14,43], but these studies do not provide a further explanation.

3.4. Equilibrium adsorption of aspartic acid

Figure 4 shows experimental and model data for the adsorption of *Asp* on FTL and PIC. The equilibrium data are displayed as a function of solution temperature at individual pH values. The Langmuir isotherm model was used to predict adsorption data based on the higher R^2 values obtained for this model than the Freundlich model (Table S2). *Asp*, a hydrophilic

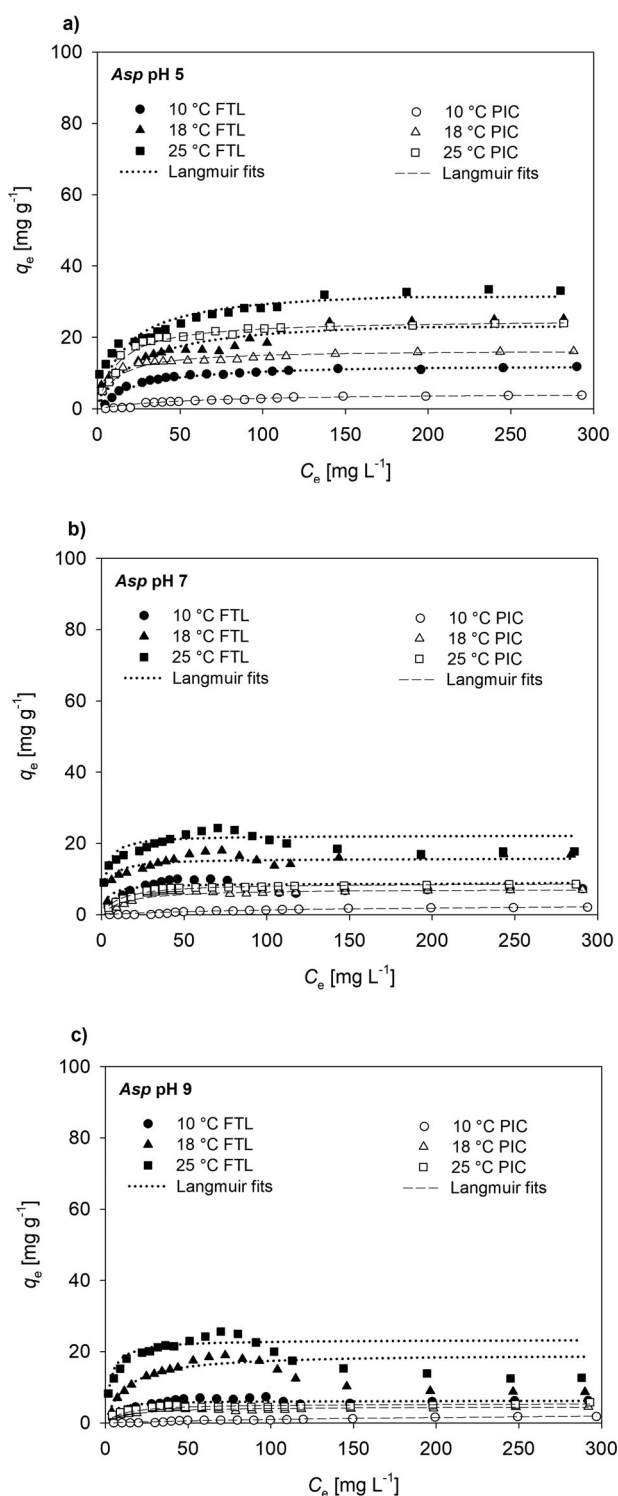


Figure 4. Isotherms and fits to the Langmuir model for the adsorption of *Asp* on FTL and PIC at different temperatures (10, 18 and 25 °C) and at (a) pH 5, (b) pH 7 and (c) pH 9.

compound, differs significantly from the other examined AAs because it prefers interactions with water molecules over adsorption on GAC [11]. This behaviour was particularly evident during adsorption on PIC when the repulsive electrostatic interactions between the

dissociated *Asp* carboxylic groups and negative PIC surface with a high amount of acidic functional groups (see Figure 1 and Table 1) resulted in a reduction in adsorption at all experimental pH values [11]. The amount of *Asp* adsorbed onto PIC decreased as the pH increased in the order of pH 9 > pH 7 > pH 5. This trend was also confirmed by the study of Greiner et al. [44] on the adsorption of aspartic and glutamic acid on an Al₂O₃ mineral surface. *Asp* adsorption was endothermic in nature, and q_e decreased with decreasing temperature. Because of the negligible q_e values at pH 7 and pH 9, the effect of temperature was clearly noticeable only at pH 5. At this pH and at 25 °C, the overall highest adsorption efficiency of *Asp* on PIC was achieved (25 °C: $q_e = 24.0 \pm 3.90 \text{ mg g}^{-1}$; 18 °C: $q_e = 16.0 \pm 3.87 \text{ mg g}^{-1}$; 10 °C: $q_e = 3.8 \pm 2.53 \text{ mg g}^{-1}$). Due to the hydrophilicity of *Asp* and the predominant repulsive electrostatic forces, hydrogen bonds appeared to be the dominant adsorption mechanism [11]. The importance of this type of interaction in glutamic acid adsorption was also demonstrated by the study of Sebben and Pendleton [23] on nonporous silica. However, *Asp* adsorption on PIC under other experimental conditions was negligible compared to that of the other examined AAs.

Asp adsorption on FTL was more efficient than adsorption on PIC. One possible explanation is the different acid–base character of FTL and PIC, when the less amount of negative charged acidic functional groups on FTL probably led to the decrease of repulsive electrostatics interactions. The higher adsorption efficiency for FTL was also reflected by the differences in adsorption model parameters (see Table S1). The solution temperature had a greater effect on *Asp* adsorption than did pH, as shown in Figure 4. Adsorption increased with increasing temperature from 10 to 25 °C at all experimental pH values and was considered to be endothermic. The highest adsorption efficiency on FTL was achieved at pH 5, when the FTL net surface charge was positive, while the *Asp* charge was negative at all experimental pH values. Attractive electrostatic interactions between opposite charges in the adsorption system increased the adsorption efficiency under these experimental conditions [11]. The *Asp* isotherms had a shape corresponding to the L4 group in the classification system by Gilles et al. [33], as was observed in the case of *Phe*. The typical wave was evident mainly at pH 7 and pH 9, when the positive effect of attractive electrostatic interactions was weaker. The *Asp* isotherms also showed a decrease in the adsorbed amount at higher pH values and higher temperatures. This phenomenon appears to be related to the concentration of *Asp* in solution. At

lower concentrations, *Asp* was adsorbed mainly due to hydrogen bonds, but at higher concentrations ($C_e > 80 \text{ mg L}^{-1}$), *Asp* molecules strongly manifested their hydrophilic character and formed something like a hydration layer, which stabilized them in solution and prevented their adsorption. There could even be desorption. However, we are currently unable to confirm these assumptions, and further research is needed. Neither the Langmuir nor Freundlich model considers the desorption of molecules in its assumptions, which was also evident from the low R^2 values in Table S1. In particular, the Freundlich model was not practically applicable to describe *Asp* adsorption on either adsorbent. A better correlation between the experimental and model data was achieved by the Langmuir adsorption model, as observed in the study of He et al. [43].

4. Conclusions

The study provided insight into the GAC adsorption of arginine (*Arg*), phenylalanine (*Phe*) and aspartic acid (*Asp*). The effect of temperature on the removal of these amino acids from water solution was investigated through laboratory equilibrium experiments at 10, 18 and 25 °C with the activated carbons FTL and PIC at pH 5, 7 and 9.

It was found that the solution temperature had an effect on the adsorption efficiency of *Arg*, *Phe* and *Asp* and that this effect was different depending mainly on the chemical nature of the amino acids, the pH value and the surface properties of the GAC. *Phe* and *Asp* were removed more efficiently on FTL, while *Arg* was adsorbed better on PIC. The overall greatest adsorption efficiency was achieved for *Phe*.

The adsorption efficiency increased with increasing temperature from 10 to 25 °C for all three investigated amino acids, and thus, the adsorption was considered to be endothermic. This nature applies to both GACs used. Higher temperature probably increased the diffusion of amino acid molecules, reduced the solution viscosity, and/or enhanced the hydrophobic interactions that contribute to adsorption.

If the dominant adsorption mechanism is based on interactions controlled by the solution pH, then the effect of solution temperature on adsorption will not be very apparent. This behaviour was confirmed in the case of *Arg*, which was adsorbed mainly due to electrostatic interactions that are strongly dependent on the solution pH. The temperature had the least effect on the studied amino acids in this case. On the other hand, the effect of temperature was the most noticeable during the adsorption of *Phe*. The dominant mechanism in *Phe* adsorption was due to hydrophobic interactions,

which are minimally affected by pH. The hydrophobic interactions between *Phe* molecules were enhanced at higher temperatures, and the molecules clustered into larger associates that could be adsorbed as a complex.

Asp adsorption was mainly influenced by the hydrophilic nature of this amino acid, which hinders adsorption. The adsorption isotherms even showed a decrease in the adsorbed amount at higher concentrations. The effect of temperature differed according to the applied GAC. In the case of adsorption on PIC, where strong repulsive electrostatic interactions were involved, temperature showed little effect. In the case of FTL, however, effects of both temperature and pH were observed, and the adsorption of *Asp* on this GAC was up to twice that of PIC.

5. Practical aspects

The results of the study indicate that the temperature of the solution (water) affects the adsorption efficiency, and this effect is more pronounced when hydrophobic interactions are the main adsorption mechanism. However, it is obvious that in real operation under applied conditions at the water treatment plant, solution temperature is not a decisive influencing adsorption factor. The pH value of the solution (water) is a more important parameter in relation to water treatment than the temperature. It is due to that pH value determines the protonation/deprotonation of the functional groups on the surface of the GACs and in the adsorbate structure, and thus controls the manifestation and extent of involved interactions and significantly affects the adsorption efficiency. Therefore, we should focus primarily on the pH value in optimization of water treatment. An important finding is also that adsorption of low molecular weight AOM such as amino acids seems to be endothermic. This is advantageous due to the fact that the development of algal bloom is associated with the warm season of the year.

Acknowledgements

This work was supported by the institutional support of the Czech Academy of Sciences [RVO: 67985874].

Disclosure statement

No potential conflict of interest was reported by the author(s).

Funding

This work was supported by Czech Academy of Sciences [grant number RVO: 67985874].

ORCID

Lenka Cermakova  <http://orcid.org/0000-0002-2035-2172>
 Ivana Kopecka  <http://orcid.org/0000-0002-1997-9736>
 Magdalena Baresova  <http://orcid.org/0000-0002-1380-6666>
 Martin Pivokonsky  <http://orcid.org/0000-0003-2067-2632>

References

- [1] Pivokonsky M, Safarikova J, Bubakova P, et al. Coagulation of peptides and proteins produced by *Microcystis aeruginosa*: interaction mechanisms and the effect of Fe-peptide/protein complexes formation. *Water Res.* **2012**;46:5583–5590.
- [2] Pivokonsky M, Safarikova J, Baresova M, et al. A comparison of the character of algal extracellular versus cellular organic matter produced by cyanobacterium, diatom and green alga. *Water Res.* **2014**;51:37–46.
- [3] Li L, Gao N, Deng Y, et al. Characterization of intracellular & extracellular algae organic matters (AOM) of *Microcystis aeruginosa* and formation of AOM-associated disinfection byproducts and odor & taste compounds. *Water Res.* **2012**;46:1233–1240.
- [4] Ma M, Liu R, Liu H, et al. Effects and mechanisms of pre-chlorination on *Microcystis aeruginosa* removal by alum coagulation: significance of the released intracellular organic matter. *Sep Purif Technol.* **2012**;86:19–25.
- [5] Fang J, Yang X, Ma J, et al. Characterization of algal organic matter and formation of DBPs from chlor(am)ination. *Water Res.* **2010**;44:5897–5906.
- [6] Freuze I, Brosillon S, Laplanche A, et al. Effect of chlorination on the formation of odorous disinfection byproducts. *Water Res.* **2005**;39:2636–2642.
- [7] Gagnon GA, Slawson RM, Huck PM. Effect of easily biodegradable organic compounds on bacterial growth in a bench-scale drinking water distribution system. *Can J Civ Eng.* **2000**;27:412–420.
- [8] Hong HC, Wong MH, Liang Y. Amino acids as precursors of trihalomethane and haloacetic acid formation during chlorination. *Arch Environ Contam Toxicol.* **2009**;56:638–645.
- [9] Her N, Amy G, Park H-R, et al. Characterizing algogenic organic matter (AOM) and evaluating associated NF membrane fouling. *Water Res.* **2004**;38:1427–1438.
- [10] Dixon MB, Richard Y, Ho L, et al. A coagulation–powdered activated carbon–ultrafiltration – multiple barrier approach for removing toxins from two Australian cyanobacterial blooms. *J Hazard Mater.* **2011**;186(2011):1553–1559.
- [11] Cermakova L, Kopecka I, Pivokonsky M, et al. Removal of cyanobacterial amino acids in water treatment by activated carbon adsorption. *Sep Purif Technol.* **2017**;173:330–338.
- [12] Gao Q, Xu W, Xu Y, et al. Amino acid adsorption on mesoporous materials: influence of types of aminoacids, modification of mesoporous materials, and solution conditions. *J Phys Chem B.* **2008**;112:2261–2267.
- [13] Qiu H, Lv L, Pan B-C, et al. Critical review in adsorption kinetic models. *J Zhejiang Univ Sci A.* **2009**;10:716–724.
- [14] Huang W-J, Cheng B-L, Cheng Y-L. Adsorption of microcystin-LR by three types of activated carbon. *J Hazard Mater.* **2007**;141:115–122.
- [15] Ho L, Lambling P, Bustamante H, et al. Application of powdered activated carbon for the adsorption of cylindrospermopsin and microcystin toxins from drinking water supplies. *Water Res.* **2011**;45:2954–2964.
- [16] Kopecka I, Pivokonsky M, Pivokonska L, et al. Adsorption of peptides produced by cyanobacterium *Microcystis aeruginosa* onto granular activated carbon. *Carbon.* **2014**;69:595–608.
- [17] Moreno-Castilla C. Adsorption of organic molecules from aqueous solutions on carbon materials. *Carbon.* **2004**;42:83–94.
- [18] Marois-Fiset JT, Carabin A, Lavoie A, et al. Effects of temperature and pH on reduction of bacteria in a point-of-use drinking water treatment product for emergency relief. *Appl Environ Microbiol.* **2013**;79:2107–2109.
- [19] Rabe M, Verdes D, Seeger S. Understanding protein adsorption phenomena at solid surfaces. *Adv Colloid Interface Sci.* **2011**;162:87–106.
- [20] Amend JP, Helgeson HC. Solubilities of the common L- α -amino acids as a function of temperature and solution pH. *Pure Appl Chem.* **1997**;69:935–942.
- [21] Liu FF, Fan JL, Wang SG, et al. Adsorption of natural organic matter analogues by multi-walled carbon nanotubes: comparison with powdered activated carbon. *Chem Eng J.* **2013**;219:450–458.
- [22] Terzyk AP, Rychlicki G, Biniak S, et al. New correlations between the composition of the surface layer of carbon and its physicochemical properties exposed while paracetamol is adsorbed at different temperatures and pH. *J Colloid Interface Sci.* **2003**;257:13–30.
- [23] Sebben D, Pendleton P. (Amino acid + silica) adsorption thermodynamics: effects of temperature. *J Chem Thermodyn.* **2015**;87:96–102.
- [24] Titus E, Kalkar AK, Gaikar VG. Equilibrium studies of adsorption of amino acids on NaZSM-5 zeolite. *Colloids Surf A Physicochem Eng Asp.* **2003**;223:55–61.
- [25] Clark HM, Alves CCC, Franca AS, et al. Evaluation of the performance of an agricultural residue-based activated carbon aiming at removal of phenylalanine from aqueous solutions. *LWT Food Sci Technol.* **2012**;49:155–161.
- [26] Schreiber B, Brinkmann T, Schamlz V, et al. Adsorption of dissolved organic matter onto activated carbon – the influence of temperature, absorption wavelength, and molecular size. *Water Res.* **2005**;39:3449–3456.
- [27] Tan IAW, Ahmad AL, Hameed BH. Adsorption isotherms, kinetics, thermodynamics and desorption studies of 2,4,6-trichlorophenol on oil palm empty fruit bunch-based activated carbon. *J Hazard Mater.* **2009**;164:473–482.
- [28] Liu M, Huang J, Deng Y. Adsorption behaviors of L-arginine from aqueous solutions on a spherical cellulose adsorbent containing the sulfonic group. *Bioresour Technol.* **2007**;98:1144–1148.
- [29] Anastopoulos I, Kyzas GZ. Are the thermodynamic parameters correctly estimated in liquid-phase adsorption phenomena? *J Mol Liq.* **2016**;218:174–185.
- [30] Scheufler FB, Módenes AN, Borba CE, et al. Monolayer – multilayer adsorption phenomenological model: kinetics, equilibrium and thermodynamics. *Chem Eng J.* **2016**;284:1328–1341.
- [31] Flores E, Arévalo S, Burnat M. Cyanophycin and arginine metabolism in cyanobacteria. *Algal Res.* **2019**;42:1–10.

- [32] Álvarez-Merino MA, Fontecha-Cámara MA, López-Ramón MV, et al. Temperature dependence of the point of zero charge of oxidized and non-oxidized activated carbons. *Carbon*. 2008;46:778–787.
- [33] Giles CH, MacEwan TH, Nakhwa SN, et al. Studies in adsorption. Part XI. A system of classification of solution adsorption isotherms, and its use in diagnosis of adsorption mechanisms and in measurement of specific surface areas of solids. *J Soc Dye Colour*. 1960;786:3973–3993.
- [34] O' Connor AJ, Hokura A, Kisler JM, et al. Amino acid adsorption onto mesoporous silica molecular sieves. *Sep Purif Technol*. 2006;48:197–201.
- [35] Yang S, Zhao D, Zhang H, et al. Impact of environmental conditions on the sorption behavior of Pb(II) in Na-bentonite suspensions. *J Hazard Mater*. 2010;183:632–640.
- [36] Al-Degs YS, El-Barghouthi MI, El-Sheikh AH, et al. Effect of solution pH, ionic strength, and temperature on adsorption behavior of reactive dyes on activated carbon. *Dyes Pigm*. 2008;77:16–23.
- [37] Jiao F, Fu Z, Shuai L, et al. Removal of phenylalanine from water with calcined CuZnAl-CO₃ layered double hydroxides. *Nonferrous Metal Soc*. 2012;22:476–482.
- [38] El Shafei GMS, Moussa NA. Adsorption of some essential amino acids on hydroxyapatite. *J Colloid Interface Sci*. 2001;238:160–166.
- [39] Rajesh C, Majumder C, Mizuseki H, et al. A theoretical study on the interaction of aromatic amino acids with graphene and single walled carbon nanotube. *J Chem Phys*. 2009;130:124911.
- [40] Alves CCO, Franca AS, Oliveira LS. Removal of phenylalanine from aqueous solutions with thermo-chemically modified corn cobs as adsorbents. *LWT Food Sci Technol*. 2013;51:1–8.
- [41] Basiuk VA, Gromovoy TY. Comparative study of amino acid adsorption on bare and octadecyl silica from water using high-performance liquid chromatography. *Colloids Surf A Physicochem Eng Asp*. 1996;118:127–140.
- [42] Silvério F, dos Reis MJ, Tronto J, et al. Adsorption of phenylalanine on layered double hydroxides: effect of temperature and ionic strength. *J Mater Sci*. 2007;43:434–439.
- [43] He J, Lin R, Long H, et al. Adsorption characteristics of amino acids on to calcium oxalate. *J Colloid Interface Sci*. 2015;454:144–151.
- [44] Greiner E, Kumar K, Sumit M, et al. Adsorption of L-glutamic acid and L-aspartic acid to γ -Al₂O₃. *Geochim Cosmochim Acta*. 2014;133:142–155.

Supplementary Material for

Investigating adsorption of model low-MW AOM components onto different types of activated carbon – influence of temperature and pH value

Lenka Cermakova^{a,b}, Katerina Fialova^a, Ivana Kopecka^a, Magdalena Baresova^a, Martin Pivokonsky^{a,*}

^aInstitute of Hydrodynamics of the Czech Academy of Sciences, Pod Patankou 30/5, 166 12 Prague 6, Czech Republic

^bInstitute for Environmental Studies, Faculty of Science, Charles University, Benatska 2, 128 01 Prague 2, Czech Republic

*Corresponding author:

E-mail: pivo@ih.cas.cz (Martin Pivokonsky)

Tel: +420 233 109 068

This Supplementary Material contains the following tables and figures:

Table S1. Standard deviations (SD) of equilibrium surface concentrations (q_e) measured in adsorption of amino acids on FTL and PIC at different pH values and solution temperature.

Figure S1. An example of the kinetic test for *Phe* adsorption on GAC FTL and PIC at pH 7 and 10, 18 and 25 °C.

Table S2. Parameters of the Langmuir and Freundlich isotherm models for the adsorption of AAs on FTL and PIC at different solution pH values and temperatures.

Figure S2. Detailed view of the waves in *Phe* adsorption isotherms on a) FTL and b) PIC at pH 5 and 10, 18 and 25 °C.

Table S1. Standard deviations (SD) of equilibrium surface concentrations (q_e) measured in adsorption of amino acids on FTL and PIC at different pH values and solution temperature.

AA	Conditions	SD* GAC FTL [mg g ⁻¹]	SD* GAC PIC [mg g ⁻¹]	
<i>Arg</i>	pH5	25 °C	0.19-3.20	0.22-3.14
		18 °C	0.20-3.09	0.24-3.29
		10 °C	0.23-3.15	0.21-3.21
	pH7	25 °C	0.18-3.21	0.19-3.23
		18 °C	0.21-3.14	0.22-3.18
		10 °C	0.22-3.23	0.21-3.22
	pH9	25 °C	0.22-3.15	0.22-3.24
		18 °C	0.21-2.98	0.22-3.19
		10 °C	0.18-3.11	0.24-3.20
<i>Phe</i>	pH5	25 °C	0.20-3.60	0.23-3.52
		18 °C	0.24-3.45	0.25-3.49
		10 °C	0.26-3.51	0.21-3.48
	pH7	25 °C	0.19-3.20	0.24-3.49
		18 °C	0.21-3.23	0.23-3.50
		10 °C	0.22-3.52	0.20-3.43
	pH9	25 °C	0.22-3.19	0.25-3.42
		18 °C	0.20-3.49	0.20-3.61
		10 °C	0.23-3.50	0.22-3.41
<i>Asp</i>	pH5	25 °C	0.26-4.11	0.30-4.30
		18 °C	0.24-3.92	0.29-4.13
		10 °C	0.28-3.90	0.31-3.89
	pH7	25 °C	0.24-3.85	0.32-3.62
		18 °C	0.21-4.24	0.29-3.83
		10 °C	0.30-3.72	0.28-3.78
	pH9	25 °C	0.29-3.93	0.33-3.99
		18 °C	0.31-3.89	0.32-4.03
		10 °C	0.32-4.01	0.33-3.65

*SD is given in the range of experimental concentrations 5 – 300 mg L⁻¹ DOC

Table S2. Parameters of the Langmuir and Freundlich isotherm models for the adsorption of AAs on FTL and PIC at different solution pH values and temperatures.

AA	Conditions		FTL						PIC					
			Langmuir			Freundlich			Langmuir			Freundlich		
			a_m	b	R^2	K_f	$1/n$	R^2	a_m	b	R^2	K_f	$1/n$	R^2
<i>Arg</i>	pH5	25 °C	22.22	0.015	0.988	0.76	0.61	0.947	61.35	0.014	0.984	2.11	0.602	0.978
		18 °C	17.33	0.016	0.982	0.58	0.627	0.925	43.48	0.045	0.991	4.30	0.462	0.788
		10 °C	8.84	0.024	0.991	0.80	0.433	0.950	35.59	0.029	0.994	3.13	0.454	0.951
	pH7	25 °C	40.49	0.013	0.974	0.96	0.68	0.949	69.44	0.018	0.973	3.69	0.527	0.947
		18 °C	36.23	0.014	0.972	1.21	0.607	0.965	51.81	0.103	0.999	11.75	0.307	0.769
		10 °C	32.68	0.031	0.987	1.24	0.587	0.951	45.87	0.099	0.999	9.65	0.321	0.793
	pH9	25 °C	63.29	0.016	0.977	2.16	0.597	0.966	89.29	0.025	0.984	6.17	0.500	0.904
		18 °C	50.76	0.02	0.994	2.20	0.591	0.900	75.19	0.078	0.999	12.58	0.367	0.878
		10 °C	37.74	0.029	0.985	2.48	0.527	0.821	60.24	0.067	0.997	12.27	0.310	0.952
<i>Phe</i>	pH5	25 °C	163.93	0.044	0.963	18.61	0.431	0.727	129.87	0.034	0.979	12.51	0.445	0.938
		18 °C	131.58	0.046	0.995	14.55	0.437	0.955	120.48	0.018	0.984	5.48	0.565	0.972
		10 °C	103.09	0.034	0.995	8.89	0.472	0.948	117.65	0.015	0.981	4.07	0.610	0.970
	pH7	25 °C	156.25	0.051	0.991	19.46	0.413	0.938	135.14	0.023	0.985	6.61	0.579	0.894
		18 °C	140.85	0.041	0.994	13.05	0.471	0.958	111.11	0.019	0.970	6.84	0.496	0.990
		10 °C	102.04	0.034	0.967	7.17	0.533	0.788	99.01	0.016	0.978	3.63	0.609	0.915
	pH9	25 °C	161.29	0.036	0.989	14.23	0.474	0.923	126.58	0.023	0.979	8.19	0.505	0.977
		18 °C	99.01	0.068	0.997	16.48	0.362	0.912	105.26	0.017	0.979	5.12	0.543	0.978
		10 °C	92.59	0.051	0.996	11.69	0.411	0.923	90.09	0.02	0.977	5.90	0.487	0.974
<i>Asp</i>	pH5	25 °C	34.01	0.061	0.985	8.95	0.250	0.986	25.00	0.085	0.999	5.27	0.314	0.804
		18 °C	25.64	0.043	0.956	5.03	0.300	0.971	16.5	0.097	0.998	5.52	0.213	0.823
		10 °C	12.71	0.044	0.985	1.13	0.498	0.806	4.53	0.018	0.993	0.47	0.384	0.959
	pH7	25 °C	22.27	0.435	0.984	9.81	0.194	0.881	8.87	0.091	0.999	2.10	0.289	0.770
		18 °C	16.47	0.204	0.983	5.08	0.262	0.635	7.27	0.071	0.992	1.18	0.371	0.665
		10 °C	8.77	0.318	0.911	1.79	0.402	0.716	3.13	0.007	0.967	0.13	0.496	0.939
	pH9	25 °C	23.36	0.362	0.973	10.26	0.176	0.515	5.43	0.093	0.991	2.29	0.161	0.741
		18 °C	16.47	0.197	0.910	4.57	0.267	0.419	4.62	0.071	0.984	1.64	0.191	0.723
		10 °C	6.22	0.262	0.959	1.23	0.375	0.625	3.41	0.004	0.738	0.01	0.973	0.700

Units: K_f [(mg g⁻¹) (L mg⁻¹)^{1/n}], n [-], R [-], a_m [mg g⁻¹], b [L mg⁻¹]

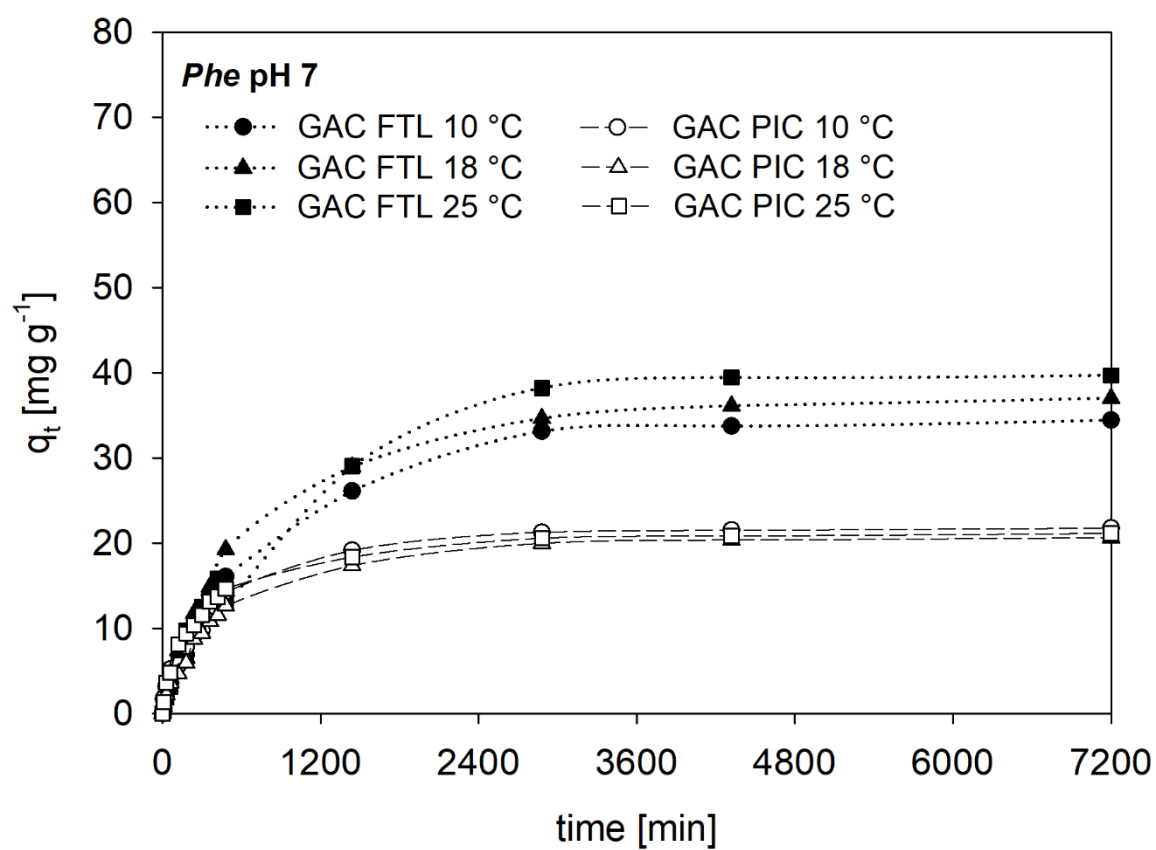


Figure S1. An example of the kinetic test for *Phe* adsorption on GAC FTL and PIC at pH 7 and 10, 18 and 25 °C.

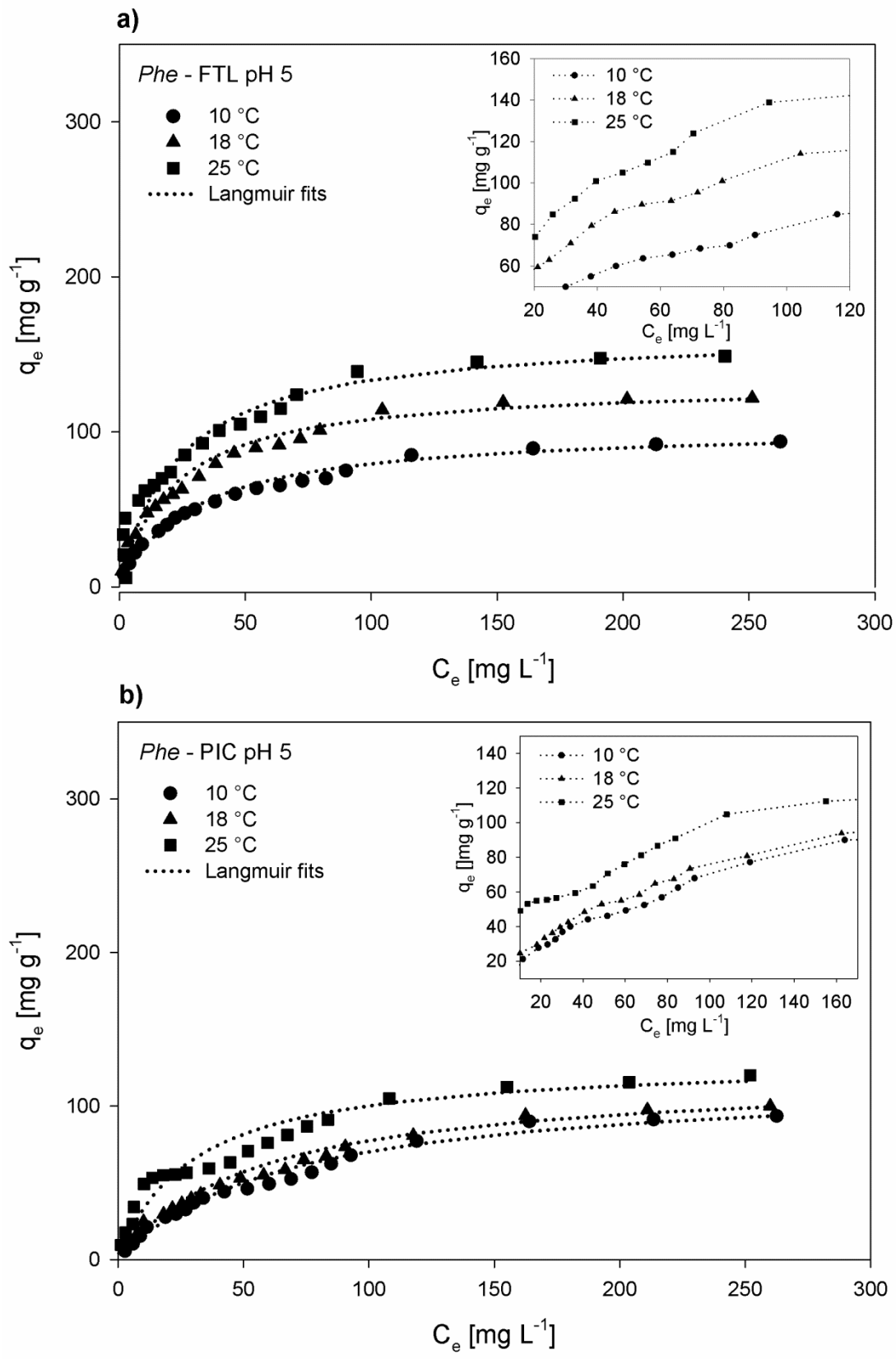


Figure S2. Detailed view of the waves in *Phe* adsorption isotherms on a) FTL and b) PIC at pH 5 and 10, 18 and 25 °C.



Review

Current knowledge in the field of algal organic matter adsorption onto activated carbon in drinking water treatment



Martin Pivokonsky^{a,*}, Ivana Kopecka^a, Lenka Cermakova^a, Katerina Fialova^a, Katerina Novotna^a, Tomas Cajthaml^b, Rita K. Henderson^c, Lenka Pivokonska^a

^a Institute of Hydrodynamics of the Czech Academy of Sciences, Pod Patankou 30/5, 166 12 Prague 6, Czech Republic

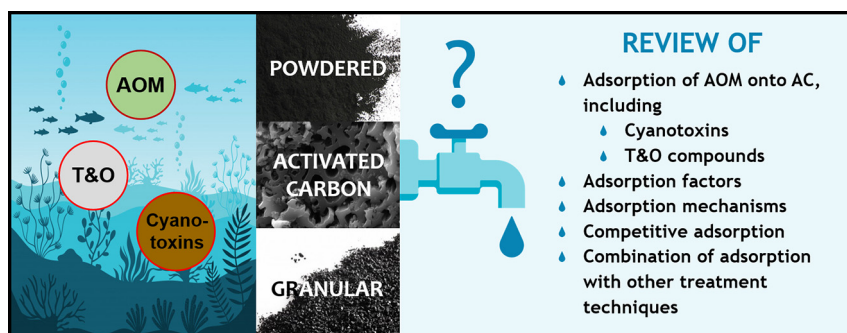
^b Institute of Microbiology of the Czech Academy of Sciences, Videnska 1083, 142 20 Prague 4, Czech Republic

^c School of Chemical Engineering, The University of New South Wales, Sydney 2052, Australia

HIGHLIGHTS

- The adsorption of AOM, toxins and T&O compounds onto GAC/PAC was reviewed.
- The combination of adsorption with other water treatment processes was evaluated.
- The properties of AOM, AC and solution as main adsorption factors were analysed.
- The adsorption mechanisms and the competitive adsorption of AOM were described.
- The application of laboratory results in practice was proposed as a future interest.

GRAPHICAL ABSTRACT



ARTICLE INFO

Article history:

Received 28 June 2021

Received in revised form 30 July 2021

Accepted 31 July 2021

Available online 2 August 2021

Editor: Dimitra A. Lambropoulou

Keywords:

Algal organic matter

Adsorption

Activated carbon

Drinking water treatment

Micropollutants

ABSTRACT

The increasing occurrence of algal and cyanobacterial blooms and the related formation of algal organic matter (AOM) is a worldwide issue that endangers the quality of freshwater sources and affects water treatment processes. The associated problems involve the production of toxins or taste and odor compounds, increasing coagulant demand, inhibition of removal of other polluting compounds, and in many cases, AOM acts as a precursor of disinfection by-products. Previous research has shown that for sufficient AOM removal, the conventional drinking water treatment based on coagulation/flocculation must be often accompanied by additional polishing technologies such as adsorption onto activated carbon (AC). This state-of-the-art review is intended to serve as a summary of the most current research on the adsorption of AOM onto AC concerning drinking water treatment. It summarizes emerging trends in this field with an emphasis on the type of AOM compounds removed and on the adsorption mechanisms and influencing factors involved. Additionally, also the principles of competitive adsorption of AOM and other organic pollutants are elaborated. Further, this paper also synthesizes previous knowledge on combining AC adsorption with other treatment techniques for enhanced AOM removal in order to provide a practical resource for researchers, water treatment plant operators and engineers. Finally, research gaps regarding the AOM adsorption onto AC are identified, including, e.g., adsorption of AOM residuals recalcitrant to coagulation/flocculation, suitability of pre-oxidation of AOM prior to the AC adsorption, relationships

* Corresponding author.

E-mail address: pivo@ih.cas.cz (M. Pivokonsky).

between the solution properties and AOM adsorption behaviour, or AOM as a cause of competitive adsorption. Also, focus should be laid on continuous flow column experiments using water with multi-component composition, because these would greatly contribute to transferring the theoretical knowledge to practice.

© 2021 Elsevier B.V. All rights reserved.

Contents

1.	Introduction	2
2.	Adsorption of algal organic matter onto activated carbon	3
2.1.	Cyanotoxins and their adsorption onto activated carbon.	5
2.2.	Taste and odor compounds and their adsorption onto activated carbon	5
2.3.	Combination of activated carbon adsorption with other treatment techniques.	10
2.3.1.	Pre-oxidation + AC	10
2.3.2.	AC + membrane filtration	10
2.3.3.	Combined treatments	10
3.	Factors influencing algal organic matter adsorption onto activated carbon	10
3.1.	The characteristics of activated carbon.	11
3.2.	The characteristics of adsorbate.	11
3.3.	The characteristics of the solution.	11
4.	Mechanisms of algal organic matter adsorption onto activated carbon.	12
5.	Competitive adsorption.	14
6.	Conclusion and future outlook.	15
	CRediT authorship contribution statement.	15
	Declaration of competing interest.	15
	Acknowledgements	15
	References	16

1. Introduction

Currently, climate change and increasing eutrophication are manifested in the proliferation of algal and cyanobacterial blooms (Heisler et al., 2008; Paerl and Huisman, 2008). These blooms not only comprise cells but also associated algal organic matter (AOM), which is released into water either as metabolic by-products (extracellular organic matter – EOM) or due to cell lysis (cellular organic matter – COM) during stationary and decline growth phases. AOM is therefore becoming increasingly important in drinking water treatment plants (DWTP) where it affects the quality of water and all treatment processes (Henderson et al., 2008a; Pivokonsky et al., 2016).

In general, AOM is classified as an autochthonous part of natural organic matter (NOM), which is present in all surface and underground waters (Leenheer and Croué, 2003; Pivokonsky et al., 2006; Henderson et al., 2008a, 2008b; Matilainen et al., 2011). The allochthonous part of NOM consists of well-researched humic substances of terrestrial origin such as fulvic and humic acids (Collins et al., 1986; Frimmel, 1998; Nissinen et al., 2001; Leenheer and Croué, 2003; Marhaba et al., 2003; Matilainen et al., 2011). These two groups of NOM differ from each other not only in origin, but also in size, chemical composition or charge. They also affect DWTP processes differently as was summarized earlier (Pivokonsky et al., 2006, 2015). AOM (both EOM and COM) has variable composition that depends on many intrinsic and external factors, including the species and strain, the growth phase, and environmental conditions, such as temperature, light and nutrient availability. In general, AOM comprises a heterogeneous mixture of proteins, peptides, amino acids, mono-, di-, oligo- and polysaccharides, lipids, fatty acids, nucleic acids and lipopolysaccharides, etc., in diverse proportions (Hoyer et al., 1985; Pivokonsky et al., 2006, 2014; Henderson et al., 2008b; Huang et al., 2012; Leloup et al., 2013). Such variability leads to differences in characteristics such as the hydrophobicity, charge properties, and molecular weight (MW) distribution, all of which are important with regard to DWTP performance (Pivokonsky et al., 2006, 2009b, 2014, 2016; Henderson et al., 2008a; Baresova et al., 2017).

Although several studies have demonstrated that a proportion of AOM, particularly its hydrophobic and/or high-MW fraction, is treatable by conventional water treatment based on coagulation/flocculation if it is adequately optimized (Pivokonsky et al., 2009a, 2009b; Henderson et al., 2010; Matsui et al., 2012), some AOM fractions are not removed by coagulation/flocculation and form undesirable residual organic content in treated water (Takaara et al., 2007; Pivokonsky et al., 2006, 2009a, 2009b, 2012; Safarikova et al., 2013). Additionally, the presence of AOM often deteriorates the organoleptic properties of water owing to the occurrence of taste and odor (T&O) compounds (Huang et al., 2007a; Zhang et al., 2011a), and leads to significant human health concerns due to the potential for the presence of harmful toxins (Gheraout et al., 2010; Shi et al., 2012) and its ability to serve as a precursor for the formation of hazardous disinfection by-products (DBPs) (Kilduff et al., 1998a, 1998b; Newcombe, 2006; Huang et al., 2009; Zhou et al., 2014).

Adsorption onto activated carbon (AC) is a process commonly used in DWTP for the removal of residual organic pollutants of anthropogenic origin (Zietzschmann et al., 2016; Oba et al., 2021; Shahrokhi-Shahraki et al., 2021; Wang et al., 2021), as well as impurities arising from natural processes, such as ammonia (Wongcharee et al., 2020) and humic and fulvic NOM (Matilainen et al., 2002, 2006; Velten et al., 2011; Newcombe, 2006; Shimizu et al., 2018). Growing problems with an excess of algal blooms have also shown that AC adsorption is a promising solution for enhancing the removal of recalcitrant AOM, including trace organics within AOM such as toxins or T&O compounds (Hnatukova et al., 2011; Kopecka et al., 2014; Zhu et al., 2016; Cermakova et al., 2017, 2020; Wang et al., 2020). AC can be used in DWTPs in the form of a powder (powdered activated carbon – PAC) or granules (granular activated carbon – GAC). PAC is usually applied seasonally as required, e.g., to treat a rapid influx of T&O compounds or cyanobacterial toxins (Srinivasan and Sorial, 2011; Ho et al., 2011). PAC addition most often occurs during dosing of coagulant prior to coagulation/flocculation, or during sedimentation before sand filtration (Fig. 1a). PAC is then removed as a waste product. In contrast, GAC is placed in filters for continual application as a penultimate treatment stage before water disinfection (Fig. 1b), as a final barrier to anthropogenic micropollutants

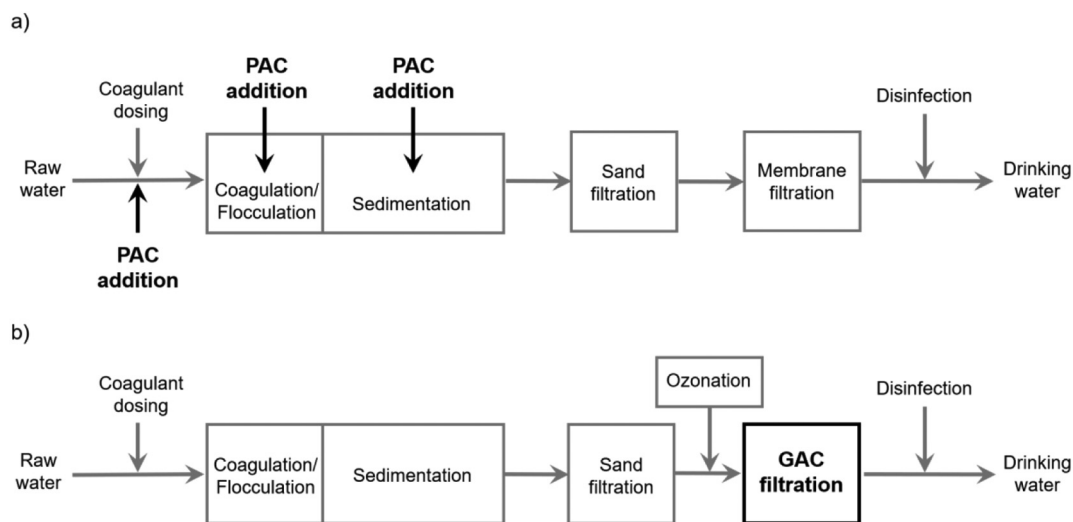


Fig. 1. An example of common PAC (a) and GAC (b) application in a water treatment plant.

(Tang et al., 2020) or residual organic compounds (Faruqi et al., 2018). Unlike PAC, GAC can be reused after regeneration by heat or water vapour (Newcombe, 2006).

Although AC adsorption alone or AC adsorption in combination with other treatment techniques (e.g., ozonation or membrane filtration) may successfully reduce the concentration of residual AOM compounds below the threshold concentration (Zoschke et al., 2011; Zhang et al., 2016; Lin et al., 2021), it can bring about several difficulties. For example, AOM has been reported to interfere with the adsorption of other key pollutants (Matsushita et al., 2008; Hnatukova et al., 2011; Campinas et al., 2013; Kopecka et al., 2014). However, the studies devoted to this theme often substantially differ in experimental conditions, such as type of AC and adsorbate, experimental pH, ionic strength (IS), and temperature, that are highly influential for the adsorption process, thus the results are not easily comparable. Consequently, the mechanisms by which AOM adsorbs onto AC and the specific conditions that dictate when AC could be used to treat recalcitrant AOM without it being viewed as interferential are unknown. A basic overview of AC applications with regard to AOM was published as a part of the review on the impact of AOM on drinking water treatment processes as a whole (Pivokonsky et al., 2016). However, a more detailed review that assesses these unknowns in connection with individual AOM components is missing, although it may help to face the increasingly frequent occurrence of algal products, to react faster during their treatment and thus to make the whole treatment process more efficient and potentially cheaper. This state-of-the-art review is intended to fulfil the literature gap with a specific focus on the following:

- i. The identification of AOM fractions removable by adsorption onto AC and description of the removal of AOM or its specific components (toxins, T&O compounds) by AC adsorption;
- ii. The elucidation of the main influencing factors that affect AOM adsorption, including the crucial characteristics of adsorbed compounds, AC and external conditions;
- iii. The description of the mechanisms and interactions involved in the adsorption of AOM onto AC and elaboration of the competitive adsorption between AOM and other compounds;
- iv. A discussion of AOM removal using AC adsorption in combination with other treatments (coagulation, membrane filtration, and pre-oxidation);
- v. The recognition of knowledge gaps and description of the need for future research.

2. Adsorption of algal organic matter onto activated carbon

Studies on the adsorption of AOM are not abundant, with the exception of studies exclusively focused on the adsorption of toxins and T&O compounds, to which separate chapters are devoted (see Sections 2.1 and 2.2). The overview of the main studies devoted to the adsorption of AOM as a whole, or AOM components other than toxins and T&O compounds, is provided in Table 1. The inclusion of the adsorption step in the water treatment process greatly increases the total removal efficiency of AOM. In particular, adsorption is suitable for eliminating various low-MW AOM, which in addition to T&O compounds and toxins includes also peptides, amino acids or amides.

In studies of COM peptides of *Microcystis aeruginosa* with an MW < 10 kDa adsorption efficiency increased when pH was decreasing. For example, a four-fold increase in adsorption efficiency from pH 8 to 5 were observed when using an initial concentration of 150 mg L⁻¹ as dissolved organic carbon (DOC) (Kopecka et al., 2014) while a two-fold increase was observed in another study (Hnatukova et al., 2011), with differences attributed to GAC type leading to different surface charge interactions. In addition, the adsorption was also affected by the ionic strength of the solution. Overall, the highest removal efficiency of the low-MW COM peptides was achieved when using GAC Picabiol 12 × 40 (PIC) compared to other studied types of carbon at pH 5 and high IS of the solution (0.3 M NaCl), which was due to a high portion of mesopores in the structure of GAC PIC and electrostatic attractions between functional groups of GAC PIC and COM peptides which were enabled by the presence of salt ions. The influence of varied adsorption factors and the action of individual adsorption mechanisms are described in detail in Sections 3 and 4.

Free and combined amino acids (AAs) are other important low-MW components of AOM. Although the content of AAs in water is usually several times lower than that of peptides, the concentration of free AAs reaching up to 1 mg L⁻¹ has been reported (Thurman, 1985). So far, only two studies have investigated the removal of AAs by AC related to drinking water treatment (Cermakova et al., 2017, 2020). The adsorption efficiency of selected AAs at 22 ± 0.5 °C was found to be dependent on the nature of the functional groups of their side chain, GAC type, ionic strength and, more significantly, on solution pH, which determines the surface charge of both AAs and GAC. To illustrate, phenylalanine (*Phe*) better adsorbed to GAC Filtrasorb TL830 (FTL) than GAC PIC, due to FTL's more balanced ratio of acidic and basic surface groups, while arginine (*Arg*) was preferably adsorbed on negatively charged GAC PIC. The highest amount of *Arg* under given experimental conditions was

Table 1
An overview of selected AOM adsorption studies.

Adsorbate	Adsorbent	Treatment process/experiment	Main results	Reference
EOM and COM from <i>Chlorella</i> sp.	unspecified AC	laboratory-scale column experiments with/without ozone, subsequent chlorination	<ul style="list-style-type: none"> DBPs precursors formed thanks to ozonation were further removed by AC treatment AC treatment significantly decreased trihalo-methane (THM) precursor concentration 	Lin et al. (2021)
arginine, phenylalanine, aspartic acid	GAC Filtrasorb TL 830 (Chemviron Carbon, USA), GAC Picabiol 12 × 40 (Jacobi Carbons, Japan)	laboratory-scale batch adsorption experiments	<ul style="list-style-type: none"> Adsorption of amino acids was an endothermic process under the given conditions Temperature affects the adsorption of amino acids depending on their concentration and the dominant adsorption mechanism involved 	Cermakova et al. (2020)
<i>p</i> -nitrophenol and amides (as model substances for low MW AOM)	PAC Norit SA 2 (Cabot Norit Nederland B. V)	laboratory-scale batch adsorption experiments	<ul style="list-style-type: none"> Amides inhibited the adsorption efficiency of <i>p</i>-nitrophenol by concentrating at the solid/liquid interface 	Jovic et al. (2020)
EOM from <i>M. aeruginosa</i>	wood based PAC (Kangxin, China)	laboratory-scale batch adsorption experiments with immersed polyvinyl chloride ultrafiltration (UF) membrane	<ul style="list-style-type: none"> PAC addition improved the removal of EOM Pre-deposited PAC caused a steady increase in membrane fouling, while conventionally-dosed PAC impeded the development of membrane fouling 	Zhang et al. (2019a)
NOM from water containing algal blooms of <i>Anabaena</i> , <i>Aphanizomenon</i> , <i>Microcystis</i> , <i>Oscillatoria</i>	unspecified PAC (Calgon Carbon Company WPH-M, USA)	laboratory-scale batch adsorption experiments	<ul style="list-style-type: none"> PAC preferentially removed substances with MW 0.02–1.1 kDa (PAC dose 30 mg L⁻¹) substances with MW 1.1–10 kDa were removed only at the high PAC dose (100–200 mg L⁻¹) 	Park et al. (2019)
EOM in algal-rich surface water, <i>Microcystis</i> toxins, THMs	PAC (Aladdin Chemical, China)	Laboratory pretreatment of PAC, UV/PAC and UV/Cl/PAC for UF membrane filtration	<ul style="list-style-type: none"> UV/PAC and UV/Cl/PAC improved the removal of algal toxins UV/Cl/PAC was effective in reducing THM formation potential 	Xing et al. (2019)
arginine, phenylalanine, aspartic acid	GAC Filtrasorb TL 830 (Chemviron Carbon, USA), GAC Picabiol 12 × 40 (Jacobi Carbons, Japan)	laboratory-scale batch adsorption experiments	<ul style="list-style-type: none"> GAC is an effective adsorbent for amino acids included in AOM, but the adsorption may be impaired by hydrophilicity of the adsorbate Adsorption of amino acids onto GAC occurred by electrostatic interactions, hydrophobic interactions and hydrogen bonding and/or by a combination of them Adsorption efficiency for individual amino acids fundamentally depends on solution pH; the removal of amino acids was reduced in the presence of NaCl background electrolyte 	Cermakova et al. (2017)
COM peptides <10 kDa of <i>M. aeruginosa</i>	GAC Filtrasorb TL830 (Chemviron Carbon, Belgium), Picabiol 12 × 40 (Pica Carbon, France)	laboratory batch and kinetic adsorption experiments	<ul style="list-style-type: none"> Decreasing pH value and increasing ionic strength enhanced adsorption of COM peptides COM peptides with MW of 1.0–4.5 kDa were adsorbed preferentially Electrostatic interactions and hydrogen bonds were dominant mechanisms of COM peptides adsorption 	Kopecka et al. (2014)
Cells, EOM and COM from <i>M. aeruginosa</i> in stationary phase	unspecified PAC (China)	laboratory-scale experiments with a hollow-fibre polyvinyl chloride UF membrane and PAC	<ul style="list-style-type: none"> UF removed all <i>M. aeruginosa</i> cells but not EOM The addition of 4 g L⁻¹ PAC to the immersed UF reactor enhanced the DOC removal by 10.9 ± 1.7% and microcystin (MC) removal by 40.8 ± 4.2% 	Zhang et al. (2011b)
COM peptides <10 kDa of <i>M. aeruginosa</i> and herbicides alachlor and terbuthylazine	GAC Norit 1240 (Cabot Norit Americas Inc., USA), Filtrasorb 400 (Chemviron Carbon, Belgium)	laboratory batch and kinetic adsorption experiments	<ul style="list-style-type: none"> Electrostatic interactions and hydrogen bonding seemed to be dominant adsorption mechanisms of COM peptides Low MW COM peptides with MW of 0.7, 0.9, 1.3 and 1.7 kDa competed with herbicides the most 	Hnatukova et al. (2011)
Cells, EOM and COM from <i>M. aeruginosa</i> in exponential phase and humic acids and tannic acid (TA) as NOM surrogate	PAC Norit SA-UF (Cabot Norit Americas Inc., USA)	laboratory-scale constant flow experiments with hollow-fibre cellulose acetate UF membrane and PAC	<ul style="list-style-type: none"> UF and PAC/UF removed all <i>M. aeruginosa</i> cells but not the extracellular microcystins With no background NOM, PAC/UF achieved 93–98% MC removal Required PAC dose was affected by NOM type, concentration, and initial microcystin concentration 	Campinas and Rosa (2010a)

removed at pH 9 compared to pH 5 and 7, because PIC carried the highest negative charge at this pH value. This was evident from the determined pH of the point of zero charge (pH_{PZC}) of GAC PIC (3.5) and the associated pH-dependent surface charge profile (Cermakova et al., 2017). Details on the meaning of pH_{PZC} are given below in Sections 3.1. and 3.3., because they are closely related to the chemical properties of the AC surface and solution characteristics. Conversely, there was insignificant adsorption of aspartic acid (*Asp*) on either GAC type owing to *Asp* strong hydrophilicity, which has been described as the cause of weak adsorption on other adsorbents as well (Ikhsan et al., 2004; Gao et al., 2008; Greiner et al., 2014). In contrast to observations with COM peptides, the adsorption of AAs decreased as the ionic strength

increased by adding NaCl to the solution (Cermakova et al., 2017). This might be because peptides form a heterogeneous mixture of several substances, whereas AAs were used individually as a homogeneous solution in the experiments; however, the lack of research on the effect of ionic strength on AOM adsorption means detailed conclusions cannot be drawn.

Other studies have focused on removing AOM or NOM from water containing algal blooms by adsorption onto PAC (Zhang et al., 2011b; Park et al., 2019; Zhang et al., 2019a). The authors found that adsorption onto PAC was effective especially for low-MW NOM and proteinaceous low-aromaticity substances. At PAC dose of 200 mg L⁻¹, the removal rate of DOC with the initial concentration of 10 mg L⁻¹ was nearly 47%

compared with 8% with no PAC addition. Moreover, PAC addition showed consistent reduction in the formation potential of DBPs, namely, trihalomethanes, haloacetic acids and haloacetonitriles, indicative of its effectiveness in removing DBP precursors (Park et al., 2019). The conventional PAC addition also improved the removal of EOM produced by *M. aeruginosa* and, moreover, it impeded the development of ultrafiltration (UF) membrane fouling. EOM adsorption efficiency rose as the PAC dose increased from 0 to 2000 mg L⁻¹, reaching a maximum of 22.3% removal of DOC. Because the removal rate of UV₂₅₄ absorbance was consistently higher than that of DOC (maximum of 31.9% vs 22.3%) at the same PAC dose, it is likely that PAC has poor adsorption capacity for polysaccharides and proteins that are not detectable by UV absorbance at the corresponding wavelength (Zhang et al., 2019a). The same observation was described in Zhang et al. (2011b), where they evaluated the effect of PAC addition on the treatment of algal-rich water by UF. The study found that while the addition of 4000 mg L⁻¹ PAC enhanced removal of UV₂₅₄ by 27.1 ± 1.7%, the DOC removal was improved only by 10.9 ± 1.7%, which was ascribed to the small effect of PAC on the rejection of hydrophilic high-MW AOM, such as carbohydrates and proteins.

2.1. Cyanotoxins and their adsorption onto activated carbon

The studies concerning the adsorption of AOM components on AC are mainly focused on the removal of toxins originating from cyanobacteria (Table 2). Cyanotoxins, which are produced as the secondary metabolites, especially during the exponential and stationary growth phase, are normally stored within the cyanobacterial cells. However, cyanotoxins are released into surrounding water by natural cell lysis after the cells die (Pietsch et al., 2002; Sun et al., 2018) or during certain water treatment processes that result in cell damage (Pietsch et al., 2002), which causes an increase in the toxin concentration and endangers water quality (Quian et al., 2014). As the conventional water treatment is incapable of effectively removing cyanotoxins because of their low MW, advanced technologies, including membrane processes (e.g., ultrafiltration), biologically active filtration, advanced oxidation (e.g., chlorination or ozonation) or adsorption onto GAC and PAC as a part of a multi-barrier approach are then required (Rositano et al., 2001; Bandala et al., 2004; Rodríguez et al., 2007; Campinas and Rosa, 2010b; Sun et al., 2018; Sengül et al., 2018; Xing et al., 2019).

An overview of the most commonly produced toxins is given in Table 3. Four main classes of cyanotoxins are recognized according to their structure, namely, cyclic peptides, alkaloids, polyketides, and amino acids. One group of the most toxic cyclic peptides occurring in water are microcystins (MCs) (Sun et al., 2018), which are a widespread and abundant class of cyanotoxins that are produced by numerous cyanobacteria, e.g., *Microcystis*, *Anabaena*, *Planktothrix* (*Oscillatoria*), *Nostoc*, *Hapalosiphon*, and *Anabaenopsis*. More than 100 congeners of MCs that vary over physical and chemical properties have been recognized (He et al., 2016; Ilieva et al., 2019). The MW of MC congeners ranges from 985 to 1024 Da. Because of the presence of 2 carboxylic groups and 1 amino group in their molecules, MCs carry a net negative charge at pH range 3–12 (Campinas and Rosa, 2006). MCs are considered to be potential tumor promoters (Nishiwaki-Matsushima et al., 1992). Consumption of water containing these toxins can lead to diarrhoea, nausea, vomiting and even death (Ho et al., 2011; He et al., 2016; Ilieva et al., 2019). One of the most toxic congeners of MCs is MC-LR, for which World Health Organization (WHO) has determined a guideline limit of 1 µg L⁻¹ in drinking water (WHO, 2011).

A general conclusion about the adsorption of toxins on AC is not easy to draw, because their adsorption behaviour has been described contradictorily in the literature. Some authors reported differences in the adsorption of MC variants, which were observed to adsorb with an efficiency decreasing in the order MC-RR > MC-YR > MC-LR > MC-LA, attributable to their increasing hydrophobicity (Cook and Newcombe, 2002, 2008; Ho et al., 2011), while another study observed no

significant difference between adsorption rates of MC-LR, MC-LY, MC-LW, and MC-LF onto different PACs (Campinas and Rosa, 2006). Additionally, similar adsorption behaviour was observed between MC-RR and alkaloid structured cyanotoxin cylindrospermopsin, probably because of similar neutral net charge properties at experimental pH conditions (pH 6.0–8.5) and the hydrophilic nature of both toxins (Frosco et al., 2009; Ho et al., 2011).

The MW of MCs is approximately 1000 Da, leading to their adsorption in AC mesopores (diameter 2–50 nm) (Donati et al., 1994; Campinas and Rosa, 2006; Huang et al., 2007b; Ho et al., 2011). More precisely, the most suitable pore size diameter for MC adsorption ranges from 8.5 to 14 nm (Park et al., 2017). Hence, wood-based ACs have been found to adsorb MCs more effectively than ACs derived from other starting materials because these ACs possess a high mesopore volume (Donati et al., 1994; Pendleton et al., 2001; Huang et al., 2007b; Ho et al., 2011; Zhang et al., 2011c; Zhu et al., 2016; Sengül et al., 2018). Anatoxin-a (MW of 165 Da), which is considered the smallest cyanotoxin (He et al., 2016), and saxitoxin (STX) (MW of 299 Da) are capable of being adsorbed in narrower pores than MCs, i.e. in micropores (diameter < 2 nm) (Molica et al., 2005; Yu et al., 2007; Shi et al., 2012).

The effect of the solution properties, such as pH or ionic strength, on the efficiency of cyanotoxins adsorption was also investigated. The results showed that the effect of ionic strength varies with adsorbate surface concentration (the amount of adsorbate adsorbed per 1 g of AC), molecular size or valence of the added cation (mono- or divalent). As an example, potassium did not affect the adsorption kinetics or capacity of MC-LR onto PAC, while calcium enhanced it (Campinas and Rosa, 2006), attributed to MC-LR configuration changes that were more pronounced when Ca²⁺ was added. Ca²⁺ supplementary effects may also lie in the diminishing intra- and intermolecular repulsions or the creation of new adsorption sites (Kilduff et al., 1996; Andelkovic et al., 2004; Campinas and Rosa, 2006). The effect of different anions on the adsorption of toxins was also investigated. Zhu et al. (2016) found that all investigated anions (Cl⁻, NO₃⁻, SO₄²⁻, and CO₃²⁻) reduced the adsorption efficiency of MC-LR with the most significant hindering effect caused by NO₃⁻.

Investigation of STX removal, an alkaloid structured cyanotoxin, confirmed strong pH dependency of adsorption onto charged adsorbent such as AC (Shi et al., 2012). Adsorption efficiency of STX increased with increasing pH because of the electrostatic interactions between functional groups of STX and PAC surface. An appropriate adjustment of pH value changed the ionization of PAC surface groups that led to the diminishing of repulsive electrostatic interactions between the positively charged STX and the adsorbent. In contrast, MC adsorption was enhanced with decreasing pH because MC is predominantly negatively charged at pH range 3–12 (Pendleton et al., 2001; Zhang et al., 2011c; Zhu et al., 2016).

The adsorption of cyanotoxins was proposed to be affected by the solution temperature and favoured at its lower values (Pendleton et al., 2001; Park et al., 2017). Zhu et al. (2016) reported the negative adsorption enthalpy changes for MCs indicating the adsorption process is exothermic in nature. The decreased randomness of MC molecular adsorption onto the surface of PAC was attributed to some structural changes in the adsorbate and adsorbent. Therefore, it was concluded that the MC adsorption capacities increased as the temperature decreased.

2.2. Taste and odor compounds and their adsorption onto activated carbon

T&O compounds are metabolites of certain benthic and planktonic cyanobacteria and filamentous bacteria (Jüttner, 1995; Ridal et al., 2001). They are non-toxic for human health or aquatic biota (Watson, 2013; Burgos et al., 2014) but they reduce the quality of water by causing an earthy, musty or fishy odor or taste and unpleasant colour, arousing the suspicions of consumers even at trace concentrations (Young

Table 2
An overview of selected cyanotoxin adsorption studies.

Adsorbate	Adsorbent	Treatment process/experiment	Main results	Reference
MC-LR	Mesoporous AC (St Louis, MO, USA; MA, USA) Mesoporous silica (St Louis, MO, USA; MA, USA)	laboratory-scale batch adsorption experiments	<ul style="list-style-type: none"> – MC-LR adsorption on mesoporous materials was driven by mesopore diffusion and hydrophobic interactions – MC-LR adsorption was more efficient on mesoporous AC than on mesoporous silica (mesoporous AC had wider pore size distribution than mesoporous silica) 	Park et al. (2020)
MC-LR from <i>M. aeruginosa</i> in stationary phase, atrazine and p-chloronitrobenzene	Unspecified PAC (Aladdin Chemical, Shanghai, China)	laboratory-scale experiments with UV/PAC, UV/Cl, UV/Cl/PAC and UF	<ul style="list-style-type: none"> – UF without pre-treatment removed less than 13% of MC regardless of its initial concentration – UV/Cl/PAC enhanced removal efficiency of MC-LR and micropollutants to 42–46% – UV/PAC and UV/Cl/PAC significantly alleviated UF membrane fouling 	Xing et al. (2019)
MCs from <i>M. aeruginosa</i> laboratory-grown culture (Algae Culture Collection of Istanbul University, Faculty of Fisheries, Department of Freshwater Biology, Istanbul, Turkey)	Unspecified PAC (Sigma Aldrich)	laboratory-scale experiments with conventional (coagulation/flocculation/sedimentation) and advanced (adsorption, membrane filtration) treatment processes	<ul style="list-style-type: none"> – The conventional treatment process was insufficient for MC removal. MC removal by PAC adsorption achieved 84% efficiency – 94% MC removal was achieved when conventional treatment process with PAC were combined with UF membrane – PAC starting material, pore size distribution, dose and contact time, and initial MCs concentration affected removal efficiency of MCs 	Sengül et al. (2018)
MC-LR in natural water containing NOM	Mesoporous ACs (Sigma Aldrich, USA)	laboratory-scale batch and kinetic experiments	<ul style="list-style-type: none"> – MC-LR adsorption onto applied AC was effective and rapid due to its mesoporous distribution of pores – The most suitable pore size for MC-LR adsorption ranged from 8.5 to 14 nm – The adsorption of MC-LR was independent of pH and background NOM concentration 	Park et al. (2017)
MCs produced and extracted from <i>M. aeruginosa</i> laboratory-grown culture (Pasteur Culture Collection) and TA as NOM surrogate	PAC Norit SA-UF (Cabot Norit Americas Inc., USA)	laboratory-scale batch and kinetic experiments	<ul style="list-style-type: none"> – MC-LR and TA were strong competitors because of similar molecular size – Competition mechanisms seemed to be dependent more on the competitor/contaminant molar ratio than on the initial concentrations 	Campinas et al. (2013)
Saxitoxins (STXs) from the Institute for Marine Biosciences (National Research Council of Canada, Ottawa, Ontario, Canada)	PAC WPH, HydroDarco B, Aqua Nuchar	laboratory-scale batch and kinetic adsorption experiments	<ul style="list-style-type: none"> – Background NOM caused reduction in STX adsorption at neutral pH, the effect was smaller at higher pH – Adsorption of STX was strongly pH dependant – Adsorption efficiency of STX onto coal-based PAC was enhanced with increasing pH – pH value, PAC type and dose, contact time, and NOM concentration are major influencing factors of STX adsorption 	Shi et al. (2012)
MC-LR in synthetic and natural water containing NOM	Low-cost syntactic adsorbent from bamboo charcoal modified with chitosan	batch adsorption experiments	<ul style="list-style-type: none"> – A new adsorbent from bamboo charcoal modified with chitosan was developed for MC removal from water – Adsorption efficiency of MC-LR onto synthesized adsorbent was strongly pH dependent and was enhanced at low pH – Background NOM caused reduction in MC-LR adsorption 	Zhang et al. (2011c)

Table 2 (continued)

Adsorbate	Adsorbent	Treatment process/experiment	Main results	Reference
CYN, MC variants (MC-LR, MC-LY, MC-LW, MC-LF)	PAC A (Waikerie WTP), B (Sydney WTP)	laboratory-scale batch adsorption experiments	<ul style="list-style-type: none"> – PAC with smaller particle diameter (10 µm) seemed to be more effective to remove CYN and MCs from water than PAC with larger ones (20–25 µm) – The variants of MC were adsorbed in the order: MC-RR > MC-YR > MC-LR > MC-LA. CYN was adsorbed similarly as MC-RR 	Ho et al. (2011)
MC-LR extracted from <i>M. aeruginosa</i> laboratory-grown culture (Pasteur Culture Collection, PCC 7820)	PAC Norit SA-UF (Cabot Norit Americas Inc., USA)	constant flow experiments with a hydrophilic UF hollow-fibre membrane and mesoporous fine-PAC	<ul style="list-style-type: none"> – Required PAC dose was influenced by NOM type and concentration, and by initial MC concentration – PAC/UF achieved 93–98% MC removal in the absence of background NOM – MC concentration 5 µg L⁻¹ was effectively removed by 10 mg L⁻¹ PAC in the presence of 2.5 mg L⁻¹ NOM surrogate 	Campinas and Rosa (2010b)
MCs extracted from <i>M. aeruginosa</i> from a lake – Gippsland, Victoria, Australia	GAC A6 (PICA Carbons, Australia)	laboratory column experiments	<ul style="list-style-type: none"> – MC can be removed by biodegradation in GAC and sand columns – Biodegradation was dependent on temperature and initial bacteria density – Bacteria capable of degrading MC were probably inactivated at 40 °C 	Wang et al. (2007)
MC variants (MC-LR, MC-LY, MC-LW, MC-LF) produced and extracted from <i>M. aeruginosa</i> laboratory-grown culture (Pasteur Culture Collection, PCC 7820), and salicylic acid, TA, humic acid as NOM surrogates	PAC Norit SA-UF (Cabot Norit Americas Inc., USA)	laboratory-scale batch and kinetic adsorption experiments	<ul style="list-style-type: none"> – While Ca²⁺ enhanced MC-LR kinetics and adsorption capacity, K⁺ had no effect – The influence of K⁺ and Ca²⁺ on NOM surrogates depended on the adsorbate MW 	Campinas and Rosa (2006)
MC-LR	PAC synthesized from tree <i>Moringa oleifera</i>	laboratory-scale batch adsorption experiments	<ul style="list-style-type: none"> – A dose of 10 mg low cost AC from <i>M. oleifera</i> seed husk L⁻¹ reduced the initial MC-LR concentration of 20 mg L⁻¹ by 93–98% 	Warhurst et al. (1997)
MC-LR in synthetic and natural water containing NOM	GAC Haycarb, Norit 0,8 Surpa, Filtrasorb F-100	laboratory-scale batch and kinetic adsorption experiments	<ul style="list-style-type: none"> – MC-LR removal efficiency was more than 80% by conventional treatment process combined with AC – background NOM caused reduction in MC adsorption – A low-level residuals concentration (0.1–0.5 µg L⁻¹) of MC-LR can be found in the water after conventional treatment process with PAC or GAC adsorption 	Lambert et al. (1996)
MC-LR in natural water containing NOM	PAC Cecarbon PAC 200 (Atochem, USA), Picatif PCO normal (Pica, France), Picazine (Pica, France), Calgon type WPL (Calgon, Belgium), OHO ASTM M325 (Haycarb, Sri Lanka), Norit W20 (Norit, Holland), Nuchar SA (Westvaco, USA), Prototype PAC (Australia)	laboratory-scale batch adsorption experiments	<ul style="list-style-type: none"> – Background NOM caused reduction in MC-LR adsorption – The most effective for adsorption of MC-LR was the wood-based PAC with large mesopore volume, followed by coal-based ones – The adsorption efficiency was related to the volume of mesopores which was dependent on the starting material – AC quality parameters such surface area, iodine and phenol numbers were found to be insignificant in correlation with the adsorption capacities for MC-LR 	Donati et al. (1994)

Note: MC-LR, -LY, -LW, -LF, -RR, -LA, etc. are different variants of the microcystin (MC).

Table 3
An overview of the cyanotoxins.

Structure	Cyanotoxin	MW (Da)	Toxicity	Cyanobacteria genera
Cyclic peptides	^a Microcystins	985–1024	hepatotoxicity	<i>Microcystis</i> , <i>Anabaena</i> , <i>Planktothrix</i> (<i>Oscillatoria</i>), <i>Nostoc</i> , <i>Hapalosiphon</i> , <i>Anabaenopsis</i>
	Nodularin	825	hepatotoxicity	<i>Nodularia</i>
Alkaloids	^a Cylindrospermopsin	415	hepatotoxicity	<i>Cylindrospermopsis</i> , <i>Aphanizomenon</i> , <i>Umezakia</i>
	^a Anatoxin-a	165	neurotoxicity	<i>Anabaena</i> , <i>Planktothrix</i> (<i>Oscillatoria</i>), <i>Aphanizomenon</i>
	Anatoxin-a(S)	252	neurotoxicity	<i>Anabaena</i>
	Saxitoxin	299	neurotoxicity	<i>Anabaena</i> , <i>Aphanizomenon</i> , <i>Lyngbya</i> , <i>Cylindrospermopsis</i>
	Lyngbyatoxin-a	437	dermatotoxicity, gastroenteral toxicity	<i>Lyngbya</i>
Polyketides	Lipopolysaccharides		potential irritant; affects any exposed tissue	All - component of the outer membrane of cyanobacteria
	Aplysiatoxin	671	dermatotoxicity	<i>Lyngbya</i> , <i>Schizothrix</i> , <i>Planktothrix</i> (<i>Oscillatoria</i>)
Amino acid	β -Methylamino-L-alanine (BMAA)	118	neurotoxicity	All

^a The most abundant cyanotoxins.

et al., 1995). The most significant and frequently reported T&O compounds are geosmin (trans-1,10-dimethyl-trans-9-decalol), 2-methylisoborneol (usually abbreviated as MIB), dimethyl trisulfide, and β -cyclocitral. These compounds belong to the AOM substances that are not removed sufficiently by conventional treatment processes (Bruce et al., 2002), by oxidation processes (Lalezary et al., 1986; Li et al., 2019), or by membrane filtration (Bruchet and Laine, 2005), mainly because of their very low MW and low concentrations present in water (the concentration of T&O compounds ranges in ng L⁻¹ while the concentration of NOM ranges in mg L⁻¹) (Newcombe et al., 2002a). The most common approach to removing T&O compounds is adsorption onto AC (Chen et al., 1997; Pendleton et al., 1997; Graham et al., 2000; Cook et al., 2001; Ridal et al., 2001; Hepplewhite et al., 2004; Zhang et al., 2011c; Zoschke et al., 2011; Summers et al., 2013; Ma et al., 2019; Wang et al., 2020). T&O compounds, such as geosmin (182.3 Da) and MIB (168.3 Da) are preferentially adsorbed in micropores (diameter 0.8–2 nm) (Yu et al., 2007; Campinas et al., 2013) in comparison to other AOM with approximately MW > 300 Da that preferentially occupy different categories of pores, namely mesopores (diameter 2–50 nm). An overview of the main T&O adsorption studies is given in Table 4.

The most likely mechanism of geosmin and MIB adsorption is through hydrophobic attraction to the carbon surface because both compounds prefer contact with another hydrophobic surface rather than contact with water (Newcombe et al., 1997; Matsui et al., 2015). MIB must displace any water that covers the adsorbent surface before adsorption from aqueous solution; thus, the adsorption can be enhanced by the application of more hydrophobic AC (e.g., coconut-based) because the surface coverage on such carbon by bound water is smaller than that on the more hydrophilic carbons (e.g., wood-based) and MIB adsorption is, therefore, easier (Newcombe et al., 1997; Matsui et al., 2015). Poor adsorption efficiency determined for wood-based or lignite ACs can be explained also by less micropore volume or high carbon-oxygen content, which is typical for hydrophilic AC (Chen et al., 1997; Pendleton et al., 1997; Considine et al., 2001; Matsui et al., 2015). However, there are also studies that evaluated carbon-oxygen content to be insignificant for adsorption efficiency as well as other carbon quality parameters, such as iodine, tannin and methylene blue number, meso-, and total pore volume, or specific surface area (Chen et al., 1997; Yu et al., 2007).

The studies comparing the adsorption efficiency of geosmin and MIB found that geosmin is adsorbed better onto AC than MIB (Lalezary et al., 1986; Cook et al., 2001; Yu et al., 2007; Zoschke et al., 2011; Summers et al., 2013; Kim et al., 2014) due to the lower solubility, flatter structure and slightly higher hydrophobicity of geosmin compared to MIB. For example, Ridal et al. (2001) reported 75–84% removal efficiency of geosmin by GAC filtration added to conventional gravity filters compared to 52–78% efficiency for MIB. Investigation of geosmin and MIB adsorption also showed that adsorption capacities for these compounds

significantly vary with the particle size of the adsorbent. The application of PAC with smaller particle diameter enhanced the overall removal of T&O compounds because smaller particle diameter yields greater surface area (Matsui et al., 2013, 2015), thus particle size can be another parameter indicator for the selection of AC with the highest removal efficiency for those compounds (Yu et al., 2007). While the adsorption of MIB and geosmin has been widely studied, there are only a few studies concerning the removal of other T&O compounds by AC adsorption (Peter et al., 2009; Zhang et al., 2011a). Dimethyl trisulfide and β -cyclocitral are also hydrophobic compounds with similar MW to MIB and geosmin (the MW of dimethyl trisulfide is 126 Da and that of β -cyclocitral is 152 Da). Thus, it can be expected that the adsorption behaviour of all the mentioned T&O compounds will be similar but ongoing research should be supplemented in the future for a clear conclusion.

While pH, ionic strength and temperature have been shown to play an important role in adsorption for toxins or AOM (as discussed in the previous sections), no significant pH effect was observed for geosmin and MIB adsorption (Sugiura et al., 1997; Graham et al., 2000) as well as for β -cyclocitral adsorption at the pH range of 2–13. Dimethyl trisulfide adsorption was only slightly enhanced at pH > 10 compared to lower pH values (Zhang et al., 2011a). The independence of adsorption on the pH value was explained by the existence of these micropollutants in a neutral form in acidic, neutral or alkaline solutions (Zhang et al., 2011a) which contrasts with previously discussed AOM and toxins which are typically negatively charged at relevant pH values. No studies investigating the effect of ionic strength on the adsorption of T&O compounds could be found and research concerning thermodynamics of adsorption are also lacking. Although the adsorption is generally considered as an exothermic process, Ma et al. (2019) revealed that the observed adsorption of geosmin and MIB is endothermic and spontaneous based on the obtained thermodynamic parameters (changes in the heat of adsorption, entropy, and Gibbs free energy). Adsorption kinetics of T&O compounds onto different types of ACs have been well studied and geosmin has been found to have a higher adsorption rate than MIB (Cook et al., 2001; Kim et al., 2014). Based on several models, Ma et al. (2019) described the kinetics of algal odorant adsorption as a process mainly governed by one-site occupancy surface adsorption with weak sorbate-sorbate interactions and indicated that the adsorption is related to the activation energy.

Many studies reported that the presence of NOM greatly reduced the adsorption of T&O compounds, due to competitive adsorption (Chen et al., 1997; Newcombe et al., 2002a, 2002b; Hepplewhite et al., 2004; Zoschke et al., 2011; Zhang et al., 2011a; Matsui et al., 2012, 2013; Summers et al., 2013; Kim et al., 2014). The low-MW NOM fraction is adsorbed in the same category of pores and competes with geosmin and MIB directly for active sites, while the high-MW NOM cause pore blockage (Newcombe et al., 1997, 2002c). Some findings even showed that MIB adsorption was more sensitive to NOM characteristics and

Table 4
An overview of selected T&O compound adsorption studies.

Adsorbate	Adsorbent	Treatment process/experiment	Main results	Reference
MIB in natural water containing NOM	PAC SAE Super (Norit, Netherlands)	ozonation and laboratory-scale batch adsorption experiments	<ul style="list-style-type: none"> Ozone reduced NOM aromaticity and increased amount of low MW NOM by destroying the high MW ones Reduced NOM competition with MIB was observed with increasing ozone consumption in three natural waters 	Wang et al. (2020)
MIB and geosmin (main adsorbates) and dimethametryn, propylamide, fenitrothion, acibenzolar-S-methyl, m-cresol (3-methylphenol), benzothiazole, and phenol (supplementary adsorbates)	PAC A (SP23, Pica), B (F-100D, Calgon Carbon Japak KK), C (SHW Norit), D (Taiko W, Futamura Chemical Co.), E (6WD, Calgon Carbon, Japan KK), F (Taiko W, Futamura Chemical Co.), G (MP23, Pica), H (Taiko W, Futamura Chemical Co.), I (6D, Calgon Carbon Japan KK)	laboratory-scale batch adsorption experiments	<ul style="list-style-type: none"> With decreasing AC particle diameter, the adsorption capacity for geosmin and MIB increased A negative correlation was found in adsorption capacity and carbon-oxygen content Adsorption onto AC with low hydrophilicity and high microporosity enhanced removal of hydrophobic micropollutants such as geosmin Reducing the particle size of AC did not lead to a change in adsorption capacity of hydrophilic compounds 	Matsui et al. (2015)
MIB and geosmin in natural water containing NOM	PAC Taikou-W (Futamura Chemical Industries Co., Gifu, Japan) superfine powdered activated carbon (SPAC) was prepared by pulverizing PAC in a wet bead mill (Metawater Co., Tokyo, Japan)	laboratory-scale batch and kinetic adsorption experiments	<ul style="list-style-type: none"> Background NOM caused reduction in adsorption of MIB and geosmin SPAC with lower particle size adsorbed MIB and geosmin more effectively than PAC Adsorption kinetics of SPAC was completely different from PAC Adsorption kinetics of geosmin was slower than kinetics of MIB 	Matsui et al. (2013)
MIB in natural water containing NOM	PAC was pulverized into SPAC Taikou-W, (Futamura Chemical Industries Co., Gifu, Japan)	laboratory-scale batch adsorption experiments	<ul style="list-style-type: none"> MW of competing NOM was similar to MIB, thus both compounds adsorbed in the same type of pores Adsorption of MIB onto PAC decreased due to competing NOM Adsorption capacity of SPAC for MIB was not affected by increasing NOM uptake due to carbon size reduction 	Matsui et al. (2012)
dimethyl trisulfide and β -cyclocitral in natural water to simulate T&O products of <i>M. aeruginosa</i>	Unspecified GAC	laboratory-scale batch adsorption experiments	<ul style="list-style-type: none"> Dimethyl trisulfide adsorption was enhanced with increasing pH value, whereas β-cyclocitral adsorption was not significantly influenced by pH value Low MW NOM inhibited the adsorption of both odorant compounds The greatest inhibiting effect was found for NOM with MW < 1000 Da, and it decreased with the increase of the NOM MW 	Zhang et al. (2011a)
MIB and geosmin in natural water containing NOM	PAC SA Super (Cabot Norit Americas Inc., USA)	laboratory-scale batch adsorption experiments	<ul style="list-style-type: none"> Geosmin adsorbed better onto PAC than MIB Adsorption of geosmin was independent of its initial concentration Adsorption of geosmin and MIB decreased with increasing concentration of NOM Mainly low MW NOM competed with the target compounds 	Zoschke et al. (2011)
MIB and geosmin	PAC B1 (Tangshan Huaneng Carbon Corporation, China), B2 and B3 (Ningxia Taixi Carbon Corporation, China), F (Tangshan Huaneng Carbon Corporation, China), W (Shanxi Xinhua Carbon Corporation, China)	laboratory-scale batch adsorption experiments	<ul style="list-style-type: none"> AC quality parameters such as iodine number, methylene blue number, meso- and total pore volumes, surface area, oxygen and carbon-oxygen contents were found to be insignificant in correlation with the adsorption capacities for MIB and geosmin A linear relationship between the micropore volumes and the adsorption capacities for MIB and geosmin was found 	Yu et al. (2007)
MIB in natural water containing NOM	PAC PCO and HP (PICA Activated Carbon, Australia)	laboratory-scale batch and kinetic adsorption experiments	<ul style="list-style-type: none"> The low MW NOM competed with MIB the most by direct competition for active sites The pore blockage was observed in case of microporous ACs by low MW NOM, and in mesoporous ACs by higher MW NOM 	Hepplewhite et al. (2004)
MIB in natural water containing NOM	GAC F400 (Chemviron Carbon, Belgium), Ca10 (Carbochem, USA), Sa30 (Pica Carbon, France), P1100 (Pica Carbon, France), PCO (Pica Carbon, France), HP (Pica Carbon, France)	laboratory-scale batch and kinetic adsorption experiments	<ul style="list-style-type: none"> Background NOM caused reduction in MIB adsorption The low MW NOM competed with MIB by direct competition for active sites The high MW NOM caused pore blockage 	Newcombe et al. (2002a, 2002b)
MIB in natural water containing NOM	unspecified GACs (Calgon Carbon Corp., Pittsburgh)		<ul style="list-style-type: none"> AC quality parameters such as iodine and tannin numbers were found to be insignificant in measuring the adsorption capacity for MIB Bituminous AC resulted in the highest adsorption capacity for MIB Background NOM caused reduction in MIB adsorption due to competitive effects 	Chen et al. (1997)

concentration than geosmin (Sugiura et al., 1997; Cook et al., 2001; Kim et al., 2014). Competition has also been described for other T&O compounds, dimethyl trisulfide and β -cyclocitral, where as in previous cases, low MW NOM has the greatest reduction potential in adsorption (Zhang et al., 2011a). More general details on competition and a description of its basic mechanisms in AOM adsorption are provided below in Section 5.

2.3. Combination of activated carbon adsorption with other treatment techniques

In general, any treatment involving PAC or GAC adsorption is expected to be more efficient when preceded by conventional water treatment based on coagulation/flocculation conducted as a separate technological step (Kweon et al., 2009; Papageorgiou et al., 2014). Nevertheless, the following chapter is rather focused on direct conjunction of AC with other treatment techniques, including pre-oxidation, membrane filtration, or their combinations.

2.3.1. Pre-oxidation + AC

Pre-oxidation can significantly affect properties of organic substances, e.g., reduce their hydrophobicity and aromaticity, cut down the MW by breaking larger constituents into smaller molecules, alter polarity, increase the amount of carboxylic functional groups, etc., and thus impacts the adsorption behaviour of organic matter (Lamsal et al., 2011; Huang et al., 2017; Wang et al., 2020); suitable pre-oxidation may be therefore applied to modulate AC adsorption (Chien et al., 2018; Xing et al., 2019). For example, pre-ozonation followed by GAC adsorption is a promising technology for the removal of low-MW organic compounds (Seredynska-Sobecka et al., 2006; Klymenko et al., 2010). However, the effect of pre-ozonation is strongly dependent on the source water characteristics, such as pH, DOC, temperature and alkalinity, and on the ozone dose (Chang et al., 2002; Beniwal et al., 2018). When GAC is used in conjunction with ozone, it is sometimes denoted as biological activated carbon (BAC) in the literature, owing to the formation of a biological film in the filter (Newcombe, 2006); thus, this term is utilized when referring to the corresponding studies.

To date, little attention was paid specifically to pre-oxidation and subsequent AC adsorption of AOM, but in general, the application of pre-oxidants appears beneficial (Chien et al., 2018; Xing et al., 2019). In the study by Chien et al. (2018) where algae-laden water was treated, pre-ozonation improved DOC removal by BAC adsorption from 41% (BAC alone) to 51%. Also, other pre-oxidants than ozone may be utilized. The AOM removal using UV or UV/Cl oxidation-enhanced PAC adsorption was studied in Xing et al. (2019). Both pre-oxidation methods improved AOM adsorption onto PAC (PAC alone 5–7.2%; UV-PAC 7.2–11%; and UV/Cl-PAC 9.4–17%) as well as MC-LR removal (PAC alone 25–27%; UV-PAC 36–43%; and UV/Cl-PAC 42–46%).

Additionally, the changes in the character of organic matter caused by pre-oxidation may also affect the course of competitive adsorption. For example, Wang et al. (2020) observed that the change of NOM properties caused by pre-ozonation (decrease in aromaticity and hydrophobicity) eliminated competitive adsorption between the NOM and MIB, and thus enhanced MIB adsorption onto PAC. However, in case that pre-oxidation results in increased NOM adsorption rate, it can rather cause a reduction in the adsorption efficiency of target compounds (Newcombe et al., 2002c; Lerman et al., 2013; Wang et al., 2020).

2.3.2. AC + membrane filtration

PAC is applicable prior to membrane filtration so as to improve its performance for the removal of target impurities, including, e.g., micropollutants and T&O compounds (Kim et al., 2014) or DBPs precursors (Jacangelo et al., 1995), or to reduce undesirable membrane fouling (Oh et al., 2006; Kweon et al., 2009). However, there are only few studies dealing with the use of PAC combined with membrane

filtration particularly for AOM removal (Campinas and Rosa, 2010b; Zhang et al., 2011b; Zhang et al., 2019a, 2019b). In general, the PAC addition resulted in improved AOM removal. For example, in Zhang et al. (2011b), PAC increased the removal of *M. aeruginosa* AOM by $10.9 \pm 1.7\%$ in terms of DOC when compared to UF alone, and additionally, the elimination of MCs was significantly enhanced (by $40.8 \pm 4.2\%$). Even higher increase in *M. aeruginosa* AOM removal by UF as a result of PAC addition, i.e., from 35 to 55%, was observed by Campinas and Rosa (2010b). Furthermore, the use of PAC reduced the membrane fouling caused by AOM and therefore significantly prolonged the filtration cycle. Nevertheless, in the same study, PAC was found not able to adsorb highly hydrophilic EOM compounds. Further, the impact of PAC dosing method – pre-deposition on the membrane surface versus conventional pre-mixing – on UF performance and AOM removal has also been assessed (Zhang et al., 2019a, 2019b). The latter means was considered more suitable as it not only improved the AOM removal but also decreased the membrane fouling, whereas it was aggravated in case of pre-deposition of GAC.

2.3.3. Combined treatments

A combination of ozone and PAC simultaneously with UF for the treatment of algal-rich water was studied by Huang et al. (2017). Residual DOC concentration decreased with increasing ozone and PAC doses with a maximum DOC removal of 42%, while a reduction of membrane fouling was achieved. Removal of AOM and MC-LR using UV and UV/Cl oxidation-enhanced PAC adsorption and UF was studied in Xing et al. (2019). Both pre-oxidation methods improved AOM adsorption onto PAC as well as MC-LR removal and decreased the membrane fouling (UF alone 81 kPa; UV-PAC 67 kPa; and UV/Cl-PAC 56 kPa).

The performance of advanced treatment consisting of coagulation/flocculation with PAC addition and subsequent UF for the removal of MCs was investigated by Sengül et al. (2018), while the efficiency was as high as 94 or 96%, depending on the type of utilized UF membrane. This was significantly more than for any of the treatments standing alone; for example, the two investigated membranes removed max 69 and 75% of MCs, respectively, without the pre-treatment. However, the contribution of PAC in the combined process was not sufficiently elucidated. Similar treatment (coagulation/flocculation with PAC and UF) was applied in the study by Dixon et al. (2011) for the removal of AOM produced by two cyanobacterial species (*Anabaena circinalis* and *Microcystis flos-aquae*) together with their cells. In the case of *A. circinalis*, the AOM removal efficiency was 35% when UF alone was used, while the coagulation/flocculation pre-treatment resulted in a shift to 69% removal, and it further increased with PAC addition up to 71%. For *M. flos-aquae*, the AOM removal efficiency reached 65% by UF alone, and it increased only slightly (to 66%) after the coagulation/flocculation-PAC pre-treatment. However, the application of PAC significantly improved the removal of intracellular MCs (UF alone 70%; coagulation/flocculation-UF 49%; coagulation/flocculation/PAC-UF 92%). The variations between the two cyanobacterial species were most likely caused by a different number of cells and diverse composition of their AOM.

3. Factors influencing algal organic matter adsorption onto activated carbon

Many studies have shown that the adsorption of organic matter onto AC is influenced by numerous physical and chemical factors (Bjelopavlic et al., 1999; Pelekani and Snoeyink, 1999; Velten et al., 2011; Hnatukova et al., 2011; Cermakova et al., 2017). In addition to the form of applied AC and the characteristics of target adsorbate, in particular, the solution properties and composition play an essential role in the adsorption process (Moreno-Castilla, 2004; Campinas and Rosa, 2006; Newcombe, 2006). The following subchapters discuss the main adsorption factors related to AOM on specific examples.

3.1. The characteristics of activated carbon

The adsorption efficiency of AC for an individual organic compound is determined not only by the AC dose, but particularly by its specific surface area, pore size distribution (PSD), or surface chemistry (Bjelopavlic et al., 1999; Pelekani and Snoeyink, 1999; Ebie et al., 2001; Dastgheib et al., 2004; Newcombe, 2006; Li et al., 2012). The first factor mentioned has been determined to govern the adsorption efficiency, especially in the case of anthropogenic pollutants (e.g., pesticides) and low-MW humic substances (Newcombe, 2006). In the case of AOM, adsorbents with a specific surface area of approximately $670 \text{ m}^2 \text{ g}^{-1}$ and higher appear to be the most effective (Yu et al., 2007; Jovic et al., 2020). However, the efficiency of AOM adsorption is given by the PSD of the AC, i.e., representation of different pore size categories in AC structure, rather than by the absolute surface area value (Li et al., 2012). AOM molecules preferentially become trapped in the pores that correspond to their size because there are plenty of contact points available between the AOM molecules and the AC surface (i.e., active sites) (Li et al., 2003a, 2003b; Moreno-Castilla, 2004). For example, AOM peptides with an MW of several units of kDa (Pivokonsky et al., 2012, 2014) are adsorbed primarily in micropores (diameter $< 2 \text{ nm}$) and mesopores (diameter $2\text{--}50 \text{ nm}$) (Kopecka et al., 2014). A similar finding for the adsorption of natural dissolved organic matter (DOM) with average sizes between 0.5 and 5 nm was reported, and it was confirmed that ACs with surface area mostly distributed in secondary micropores (diameter $0.8\text{--}2 \text{ nm}$) and the smallest mesopores should be used for enhanced adsorption of organic molecules of this size from water (Dastgheib et al., 2004; Newcombe, 2006). Moreover, Park et al. (2019) demonstrated that AOM with an MW of $0.02\text{--}1.1 \text{ kDa}$ was removed preferentially at a low PAC dose (30 mg L^{-1}), while a higher PAC dose (100 mg L^{-1}) was favoured for removal of AOM with MW of between 1.1 and 10 kDa . A more detailed analysis determined that the MW of $0.8\text{--}1.2 \text{ kDa}$ exclusively corresponded to protein-related compounds produced by examined algae and cyanobacteria.

Ensuring that the PSD of the AC is appropriate for the size of the target pollutants is important especially when they are present as a mixture of substances of different molecular weights. If the AC comprises sufficiently wide PSD then both low and high-MW AOM can be adsorbed with adsorption efficiency depending on direct competition for adsorption sites (Pelekani and Snoeyink, 1999; Ebie et al., 2001). However, if the pores are only suitable for the adsorption of low-MW AOM, high-MW AOM might be completely excluded from adsorption or it may adsorb in transport pores (macro- and mesopores) and at the micropore entrances and blocks them for smaller molecules and thus limit the adsorption of these compounds (Hnatukova et al., 2011; Kopecka et al., 2014). The degree of pore blockage (indirect competition) is then given by the AC dose and the ratio of low- and high-MW substances (Pelekani and Snoeyink, 1999; Ebie et al., 2001). The mechanism of this is further discussed in Section 5.

The chemical properties of AC surface including the type and number of functional groups on the AC surface have a significant influence on the adsorption efficiency as well. The AC surface can display acidic character due to the presence of functional groups including carboxyls, phenols, lactones and acid anhydrides (Barton et al., 1997; Bjelopavlic et al., 1999; Moreno-Castilla, 2004), which dissociate to produce a negative surface charge (Álvarez-Merino et al., 2008). As well, the surface of AC poses a basic character attributed to delocalized π -electrons of the basal planes, nitrogen functionalities and surface oxygen-containing groups, such as pyrones, chromenes, diketones and quinones, which accept protons from the solution and are responsible for the positive surface charge (Barton et al., 1997; Benaddi et al., 2000; Montes-Morán et al., 2004). The pH, where the negative charge of AC surface is equal to the positive charge, corresponds to the point of zero charge (pH_{PZC}). Because the charge state of functional groups is fundamentally influenced by the solution pH, this topic and its practical impact are discussed in Sections 3.3. and 4, respectively.

3.2. The characteristics of adsorbate

In terms of adsorbate properties, its MW, the degree of hydrophobicity, the nature and the number of functional groups fundamentally influence the adsorption efficiency, and the pH affects the form of the adsorbate (Newcombe et al., 1997; Ebie et al., 2001; Kilduff and Karanfil, 2002; Kim and Yu, 2005; Dixon et al., 2011; Zhang et al., 2011a, 2011b).

Adsorption efficiency generally increases with decreasing MW of the adsorbed organic compounds (Newcombe et al., 1997; Kim and Yu, 2005; Hnatukova et al., 2011; Zhang et al., 2011a, 2011b; Kopecka et al., 2014). For example, the removal efficiency of low-MW MCs (MW of approximately 1 kDa) in AOM of *M. aeruginosa* increased in the presence of PAC while the concentration of the associated high-MW proteins and polysaccharides remained stable (Zhang et al., 2011b). Dixon et al. (2011) reported that EOM of cyanobacteria *A. circinalis* in the range between 1.5 and 3 kDa was preferentially removed prior to higher MW compounds. This is consistent also with the studies of Hnatukova et al. (2011) and Kopecka et al. (2014), where COM peptides with an MW of $0.7\text{--}4.5 \text{ kDa}$ were adsorbed with higher efficiency than peptides with an MW of 8.3 and 9.5 kDa .

The conformation of the adsorbed molecules (i.e., their spatial arrangement), as well as the supramolecular structure identified for some types of NOM (clustering of small organic molecules by strong and weak hydrogen bonds) (Piccolo, 2001; Wells and Stretz, 2019) must also be considered in relation to the adsorption efficiency. The conformation is affected by the experimental conditions (in particular by the pH value and/or the solution ionic strength), which determine the overall charge of the molecule. If the amount of negative and positive charge in the molecule is balanced, there are no significant intramolecular repulsive forces, and the molecules tend to take a more compact shape allowing them easier entry into the internal pore structure of AC (Huang et al., 2007a; Goscianska et al., 2013, 2014; Kopecka et al., 2014). The total molecule charge is determined by the type and number of functional groups involved. For example, AOM peptides/proteins with a low MW below 10 kDa , which are the most resistant to coagulation and at the same time their concentrations in water can be lowered by using AC, have amphoteric characteristic because of the functional groups, such as $-\text{OH}$, $-\text{COOH}$, $-\text{SH}$, $-\text{NH}_3^+$, and $=\text{NH}_2^+$. These groups can release or accept protons depending on the pH conditions (Creighton, 1993). The presence of both positively and negatively charged functional groups in AOM peptides/proteins within a relatively wide pH range, allows them to interact electrostatically with both positively and negatively charged particles in water or on the AC surface (see Section 3.1) (Hnatukova et al., 2011; Kopecka et al., 2014; Pivokonsky et al., 2016). As the charge of these groups is directly influenced by the pH value of the solution, the effect of interactions between AOM and AC functionalities and its effect on adsorption will be discussed in more detail in the next sections, which are devoted to the solution properties and interactions (Sections 3.3. and 4, respectively).

3.3. The characteristics of the solution

The pH value, ionic strength, temperature, and chemistry are the main solution properties that play an important role in the AOM adsorption process (Newcombe and Drikas, 1997; Bjelopavlic et al., 1999; Moreno-Castilla, 2004; Campinas and Rosa, 2006; Knappe, 2006; Hnatukova et al., 2011; Kopecka et al., 2014). Depending on the pH, positively or negatively charged functional groups predominate in AOM molecules (Safarikova et al., 2013). As previously discussed, pH will also affect the characteristics (protonation/deprotonation) of functional groups on the AC surface. If the pH of the solution is lower than the pH_{PZC} , the total charge of AC is positive and vice-versa (Moreno-Castilla, 2004; Knappe, 2006). Protonated and deprotonated AOM and AC functional groups participate in various types of interactions (electrostatic, hydrophobic, and hydrogen bonding) during adsorption, thus

substantially affect the efficiency of the whole process (Moreno-Castilla, 2004; Hnatukova et al., 2011; Abouleish and Wells, 2015). AOM adsorption efficiency has been observed to increase with decreasing pH of the solution. The adsorption of COM peptides of *M. aeruginosa* (expressed as DOC removal) on two GACs with pH_{PZC} of 5.5 and 6.7, respectively, was approximately twice as high at pH 5 than at pH 8.5 (Hnatukova et al., 2011). The pH 5 was lower than the determined pI (isoelectric point) values of COM peptides (5.25–8.05), thus there were strong attractive electrostatic forces between positively charged groups of peptides (e.g., $=NH_2^+$, $\alpha-NH_3^+$, $\epsilon-NH_3^+$) and negatively charged groups on the AC surface (e.g., $-COO^-$). Increasing pH caused the dissociation of acidic oxygen functional groups on the GAC to give a negative charge, while the negative charge increased in the peptides due to dissociation of functional groups, such as $-COO^-$ and $-S^-$, leading to strong repulsive electrostatic interactions (Hnatukova et al., 2011). Thus, the extent of electrostatic repulsion during adsorption can be predicted based on the determination of peptides pI and of AC net surface charge (Kopecka et al., 2014). The rate and nature of adsorption interactions between AC and adsorbate is also affected by the solution ionic strength (Fig. 2). Ionic strength mainly influences electrostatic interactions and its effect varies depending on the type of AC and solution pH. Generally, as the solution ionic strength increases, repulsive electrostatic interactions are suppressed and thereby enable non-electrostatic forces to prevail, leading to an increase in adsorption efficiency (Newcombe and Drikas, 1997; Bjelopavlic et al., 1999; Moreno-Castilla, 2004; Campinas and Rosa, 2006). The effect of ionic strength on adsorption also depends on the adsorbate concentration: if the concentration of adsorbed compounds on the AC surface is low and attractive forces predominate, the adsorption efficiency decreases with increase in ionic strength. The salt ions weaken the attraction forces, thereby reducing the adsorption rate. However, if repulsive interactions predominate at low levels of adsorbed compounds on the surface of the AC, the added salts may partially screen these interactions and increase the adsorption rate. If the concentration of adsorbed compounds on the AC surface is high, molecules of the same charge get too close, and repulsive forces will be applied between them (Silvério et al., 2008; Kopecka et al., 2014; Sebben and Pendleton, 2015a; Cermakova et al., 2017). Because of the predominantly negatively charged AOM, when the AC with low pH_{PZC} is used, the increase in ionic strength leads to an increase in adsorption efficiency because of its shielding of repulsive forces between the equally charged AC and AOM functional groups over almost the entire pH

range. Conversely, when AC with the high value of pH_{PZC} is applied, the effect of increasing solution ionic strength at different pH values may manifest differently depending on the charge ratios throughout the system (Kopecka et al., 2014).

Solution temperature may also have a significant effect on the adsorption of organic compounds (Moreno-Castilla, 2004; Schreiber et al., 2005) because it affects the kinetic energy, the Brownian motion of the adsorbed particles, the viscosity of the solution and the solubility of the adsorbed compound. Changes in the temperature may have both positive and negative effect on the adsorption efficiency, depending mainly on the type of adsorbate and the experimental setup (Amend and Helgeson, 1997; Terzyk et al., 2003; Rabe et al., 2011; Liu et al., 2013). Adsorption is inherently assumed as an exothermic process; hence, the efficiency of the process increases with decreasing temperature (Moreno-Castilla, 2004; Sebben and Pendleton, 2015b). However, some studies proved increasing rates of adsorption efficiency of organic compounds with increasing solution temperature (Schreiber et al., 2005; Liu et al., 2007; Zhang et al., 2011a; Kim et al., 2014). This may be related to the role of the solvent (water) in this process, where some organic compounds must, at first, break their bonds with other molecules of the adsorbate before adsorption onto AC. This breaking of the bonds between the solvent and the adsorbate may require energy supplied, for example, in the form of an increase in the temperature of the solution (Liu et al., 2007; Anastopoulos and Kyzas, 2016). Although it can be concluded that the solution temperature affects adsorption efficiency of AC for natural organic compounds, there is only one study addressing this issue in direct linkage to AOM. In the study by Cermakova et al. (2020) the effect of temperature on the adsorption of AAs abundant in AOM (*Arg*, *Phe*, *Asp*) was examined at the temperatures of 10, 18 and 25 °C on two GACs. From laboratory batch experiments, it was concluded that the effect of temperature is dependent mainly on the chemical nature of the AAs, the pH value, and the surface properties of the GAC. All tests proved that the adsorption of AAs shows signs of endothermic reaction. Compared to the experiments under lower temperatures of 18 and 10 °C, the highest adsorption efficiency was achieved at 25 °C for all examined AAs. However, differences between AAs were found. In the case of *Arg* adsorption, the effect of temperature was smaller than the effect of pH. In contrast, the adsorption of *Phe* was strongly dependent on the solution temperature and almost independent of the pH, which was explained by the action of different adsorption mechanisms. While the predominant mechanism of *Arg* adsorption was based on the attractive electrostatic interactions that are directly influenced by the solution pH, *Phe* was primarily adsorbed by hydrophobic interactions (Cermakova et al., 2017). Interestingly, higher temperature also led to a slight increase in the adsorption efficiency of *Phe* due to the creation of large associates of adsorbate molecules that adsorbed onto AC as a complex. The same effect has so far been described by Schreiber et al. (2005) only for DOM. Thus, more detailed studies need to be done in the future to confirm and accurately and comprehensively assess the effect of temperature on the adsorption efficiency of substances that come from cyanobacteria and algae and not from the terrestrial environment.

4. Mechanisms of algal organic matter adsorption onto activated carbon

Most organic molecules interact with AC surfaces through non-specific dispersion forces (Bjelopavlic et al., 1999; Moreno-Castilla, 2004; Newcombe, 2006). These interactions are very numerous and important as they act between all kinds of particles. Limited in number but strong interactions may take place through electrostatic forces and hydrogen bonding between polar or polarizable molecules of adsorbate and mostly oxygen-containing groups located within the AC pore structure or on the edges of the carbon graphene layers (Andreu et al., 2007). These interactions are linked to the particular sites in both the adsorbent and adsorbate structures; thus, they are so-called specific.

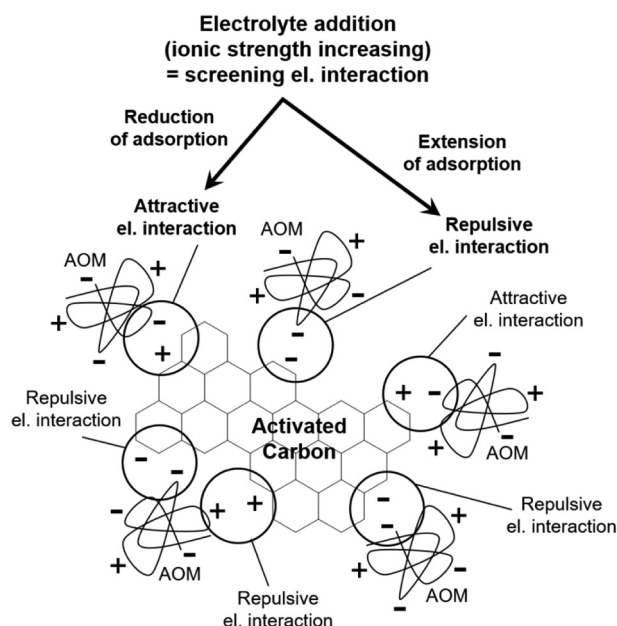


Fig. 2. A scheme of the influence of solution ionic strength on AOM adsorption efficiency.

Hydrophobic interactions and π - π interactions have been identified as another mechanism by which the adsorption of AOM molecules on AC occurs (Hnatukova et al., 2011; Kopecka et al., 2014; Cermakova et al., 2017, 2020). The first ones lie in the tendency of the molecules to adsorb on a carbon surface rather than to stay dissolved in water (Newcombe and Drikas, 1997). Attractive π - π interactions are formed between delocalized π electrons of polyaromatic basal planes of the AC and π -electrons of aromatic structures in AOM or other organic molecules (Newcombe and Drikas, 1997; Moreno-Castilla, 2004; Hnatukova et al., 2011; Cermakova et al., 2017). A scheme of the different types of interactions and mechanisms identified in the adsorption of AOM onto AC is shown in Fig. 3.

The interactions of COM peptides (< 10 kDa) isolated from cyanobacterium *M. aeruginosa* and AC surface were first described by Hnatukova et al. (2011) who investigated the removal of these low-MW AOM components during laboratory-scale experiments with two commercial GACs at different pH values. Increased adsorption onto both carbons at acidic pH 5 was explained by the formation of hydrogen bonds between protonated functional groups of COM peptides and protonated surface groups of the carbons. A similar concept of protein-surface interactions was described in several studies for adsorbents with surface properties similar to AC (Yoon et al., 1999; Zhou et al., 2007; Katiyar et al., 2010). Additionally, some peptide molecules might become unfolded because of the high amount of negatively charged functionalities at higher pH values and the whole peptide mixture was thus less compact and more elongated, which could also contribute to the poor adsorption at alkaline pH (Gorham et al., 2007).

The published data indicate that electrostatic interactions and hydrogen bonding are also dominant in the adsorption of other cyanobacterial components with very low MW, such as AAs, amides and cyanotoxins (Campinas and Rosa, 2006; He et al., 2016; Liu et al., 2019; Park et al., 2019; Jovic et al., 2020). Hydrogen bonds are usually formed between protonated functional groups of adsorption participants, as it was reported for N heteroatoms of guanidyl group in arginine molecules and hydroxyl or carboxyl groups of AC (Sebben and Pendleton, 2015a; Cermakova et al., 2017). Attractive electrostatic forces were found to be beneficial for the adsorption of several AAs, such as histidine (Vinu et al., 2006), lysine (O'Connor et al., 2006), arginine (Gao et al., 2008) or phenylalanine (Clark et al., 2012) on different types of adsorbents. In contrast, strong repulsive interactions preventing aspartic and glutamic acid from the adsorption on porous and mineral surfaces have been reported (Tentorio and Canova, 1989; Ikhsan et al., 2004; Gao et al., 2008; Greiner et al., 2014).

Hydrophobic interactions are involved in the adsorption of AOM onto AC if the adsorbate (or its part) is hydrophobic in nature. The adsorbate then seeks to limit contact with water molecules by binding to the hydrophobic surface of AC (Moreno-Castilla, 2004). These interactions dominate, for example, in the adsorption of small AAs with a non-polar chain (Titus et al., 2003; Vinu et al., 2006; Clark et al., 2012), especially under experimental conditions that do not allow the development of electrostatic interactions (Clark et al., 2012). In addition to the direct hydrophobic interactions with AC surface, Cermakova et al. (2017) reported that the removal of cyanobacterial AA *Phe* was enhanced by intermolecular hydrophobic interactions leading to the formation of associates consisting of several *Phe* molecules arranged together by hydrophobic parts, which were then adsorbed as a unit for example by electrostatic interactions (Vinu et al., 2006; Clark et al., 2012). It should be noted that the extent to which hydrophobic interactions contribute to AC adsorption is still a subject of discussion, as there are studies that have also demonstrated the hydrophilic character of the AC surface (Schrader, 1975; Ashraf et al., 2013).

Solution ionic strength is another key factor that strongly influences AOM adsorption mechanism, especially through the added salt that shields the surface charge of adsorption participants (Moreno-Castilla, 2004; Campinas and Rosa, 2006). Thus, electrostatic interactions (attractive and repulsive) between AC surface and AOM are affected. At certain conditions, several modes of increased ionic strength effect have been described for the adsorption of AOM or similar organic molecules (see details in Section 3.3.) (Newcombe and Drikas, 1997; Bjelopavlic et al., 1999; Moreno-Castilla, 2004; Newcombe, 2006). If repulsive electrostatic interactions predominate among the adsorption participants, the repulsion may be shielded by the added salt, thus the adsorption efficiency increases (Bjelopavlic et al., 1999). Some studies have also confirmed that higher ionic strength led to a higher adsorption efficiency of organic substances because of the changes in their chemical and structural properties. Particularly at higher adsorbed amounts, when molecules of adsorbate are nearby, the intra- and intermolecular repulsions between functional groups of adsorbates can be reduced by an addition of electrolyte. The molecules then shrink spatially, and their removal is facilitated as has been described in the literature (Newcombe and Drikas, 1997; Campinas and Rosa, 2006). If the adsorbent and adsorbate are reverse-charged and electrostatic attraction occurs between them, the addition of the electrolyte attenuates these forces and the adsorption efficiency decreases, especially when high ionic strength is applied (Bjelopavlic et al., 1999; Hnatukova et al., 2011; Kopecka et al., 2014). For example, an increase in ionic

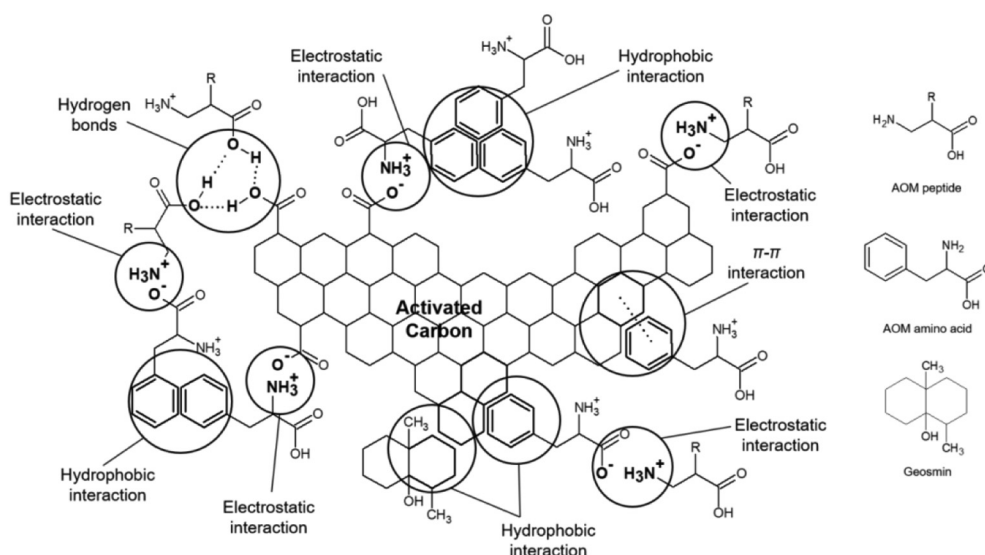


Fig. 3. A scheme of the different types of interactions and mechanisms identified in the adsorption of AOM onto AC.

strength from 2.5 mM KCl to 10 mM KCl caused a decrease in the level of the adsorption of tannic acid (TA) (a model compound for low-MW NOM) onto PAC because of a weakening of attractive electrostatic forces as was reported in the study of Campinas and Rosa (2006). Goscianska et al. (2013, 2014) showed that the removal of AAs may decrease because of high ionic strength when the adsorption occurs at a pH close to *pI* of the adsorbed substance. A balanced amount of positive and negative charge in the adsorbate structure is assumed under these conditions. The molecules are in compact form because of strong intramolecular forces and better penetrate to the internal structure of AC. However, the addition of electrolyte will result in changes in the charge ratio inside the AA molecule and thus weaken these forces and decrease the adsorption efficiency.

5. Competitive adsorption

As previously mentioned, AC is used particularly for the removal of specific natural and anthropogenic micropollutants, such as pesticides, toxins and T&O compounds, which occur in water in very low concentrations of nano- or micrograms per litre. However, raw water contains naturally occurring backgrounds of readily adsorbed NOM in concentrations up to 100,000 times higher compared to the micropollutants (Newcombe et al., 1997, 2002a), leading to competition between NOM and the micropollutants during AC treatment, which may decrease the adsorption efficiency of the target micropollutants (Newcombe et al., 1997, 2002a, 2002b; Kilduff et al., 1998b; Pelekani and Snoeyink, 1999, 2000, 2001; Li et al., 2003a, 2003b; Matsui et al., 2003, 2012; Huang et al., 2007b; Zoschke et al., 2011; Zhang et al., 2011b; Campinas et al., 2013). NOM adversely affects both the adsorption equilibrium and kinetics of organic micropollutants through two basic mechanisms: (1) direct competition for AC active sites and (2) AC pore blockage (indirect competition) (Fig. 4) (Newcombe et al., 1997, 2002a, 2002b; Kilduff et al., 1998a; Pelekani and Snoeyink, 1999, 2000, 2001; Li et al., 2003a, 2003b; Matsui et al., 2003; Huang et al., 2007b; Campinas et al., 2013). Whether competition occurs and which of the mechanisms prevails is determined particularly by the relationship between the adsorbate size and the PSD of AC and is also dependent on the adsorbate initial concentration, or rather on the

competitor/contaminant ratio (Pelekani and Snoeyink, 1999, 2000, 2001; Zhang et al., 2011b; Zoschke et al., 2011; Campinas et al., 2013). In addition to competition during the simultaneous adsorption of NOM and micropollutants, NOM presence may cause another significant phenomenon – “carbon fouling” in fixed bed GAC columns by both of the aforementioned competition mechanisms. NOM usually permeates through the column faster than micropollutants because of their slower kinetics. Thus, the GAC in filters is preloaded with NOM before it comes in contact with micropollutants due to differences in size and in the exploration of the different pore sizes. Moreover, as GAC filters are operated continuously and micropollutants can occur less often than NOM, background NOM preloading on AC in the filters can cause decreased removal capacity for micropollutants (Li et al., 2003b). AOM behaves similarly – residual concentrations of AOM after conventional treatment may cause carbon fouling or obstruct the removal of other organic compounds during simultaneous adsorption. On the other hand, very small AOM substances, such as T&O compounds or toxins, may suffer from the competitive adsorption of higher-MW organics, either AOM or another NOM, as evidenced below.

To the best of our knowledge, only one study dealt strictly with AOM as the causer of competitive adsorption (Hnatukova et al., 2011). The authors investigated the effect of COM peptides (MW < 10 kDa) produced by cyanobacterium *M. aeruginosa* on adsorption efficiency of herbicides alachlor and terbuthylazine and found that the high affinity of COM peptides for the AC surface caused a significant decrease in the herbicides' adsorption efficiency. This observation was more pronounced at pH 5 than at pH 8.5, which corresponds to the high adsorption efficiency of the COM peptides alone at pH 5. COM peptides with MW of 0.7–1.7 kDa were found to be the major contributors to the reduction of AC capacity for the herbicides by direct site competition. On the other hand, peptides with MW above 2.3 kDa that were unable to occupy the same pores as pesticides caused pore blockage (Hnatukova et al., 2011). Results of this study agree with the observation of Pelekani and Snoeyink (1999) that investigated the competition mechanism between NOM and the herbicide atrazine. They stated that NOM capable of access a fraction of pores where atrazine adsorption took place, caused direct site competition. However, when NOM blocked access but did not penetrate into these pores, indirect site competition (pore blockage) occurred.

Other studies on the competitive adsorption dealt with the impact of NOM background on the adsorption efficiency of T&O compounds (mostly MIB and geosmin) and cyanobacterial toxins (mainly microcystins and saxitoxin) (Newcombe et al., 1997, 2002a, 2002b; Zoschke et al., 2011; Matsui et al., 2012; Campinas et al., 2013; Kim et al., 2014). According to many studies, the adsorption efficiency for these small target compounds is affected by the NOM fractions of similarly low MW through direct competition for the adsorption sites (Newcombe et al., 1997, 2002a, 2002b; Zoschke et al., 2011; Matsui et al., 2012, 2013; Campinas et al., 2013). Larger NOM molecules rather adsorb in larger pores or onto the external surface of AC and do not compete for the same sites (Newcombe et al., 1997; Matsui et al., 2013). Campinas et al. (2013) evaluated the competition mechanisms in microcystin and TA simultaneous adsorption and found that both compounds are strong competitors because of their similar molecular size. Thus, water with a high concentration of TA may strongly affect MC residuals in the treated water. A similar finding was achieved in the study by Newcombe et al. (2002c) investigating the adsorption of MIB in the presence of NOM. The direct competition for active sites was reported as a major competitive mechanism when the MWs of NOM and MIB were similar. However, other studies suggest that only a small fraction of NOM has sufficiently low MW that enables direct competition with T&O compounds for the active sites in AC micropores (Zoschke et al., 2011; Matsui et al., 2012, 2013). According to Matsui et al. (2012, 2013), less than 2% of the entire NOM represents the direct competitors for the adsorption of geosmin and MIB. In the case of MCs that have higher MW of approximately 1 kDa and preferentially adsorb in AC

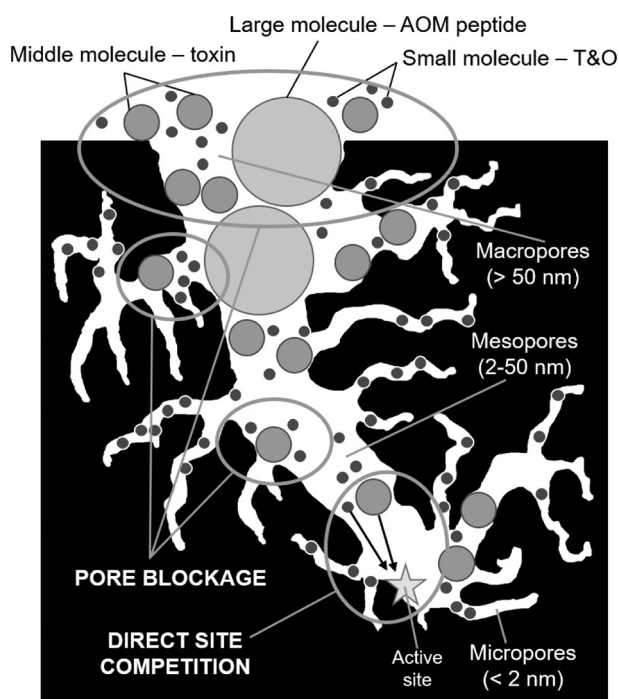


Fig. 4. A scheme of two basic mechanisms of competitive adsorption.

mesopores, the directly competing NOM fraction is greater (Huang et al., 2007b; Campinas et al., 2013).

Pore blockage significantly contributes to the decrease in adsorption efficiency of both AOM toxins and T&O compounds as well (Pelekani and Snoeyink, 1999, 2001; Ebie et al., 2001; Li et al., 2003a; Campinas et al., 2013). According to Pelekani and Snoeyink (1999, 2000), pore blockage by NOM is the dominant competition mechanism, particularly in the case of AC with a high proportion of primary micropores (diameter < 0.8 nm). In the case of AC with a prevalence of secondary micropores (diameter 0.8–2 nm) and mesopores (diameter 2–50 nm), the dominant competitive mechanism of NOM is direct competition for adsorption sites. This phenomenon was also confirmed in the study by Li et al. (2003b), where compared to PAC with higher content of large micropores and mesopores, PAC with a small fraction of large pores suffered from pore blockage much more. Pore blockage was assumed to be the dominant competitive mechanism also in the study by Jovic et al. (2020) investigating the adsorption of p-nitrophenol onto PAC in the presence of amides as model substances of low-MW AOM. The results were based on the average pore size of the PAC (2 nm) used and the mean MW of amide molecules that presumably concentrated at the interface of AC and therefore prevented p-nitrophenol from adsorption. In addition, pore blockage plays a very important role in the abovementioned “preloading” phenomenon of GAC filters (Li et al., 2003b).

Determining whether the direct competition or the pore blockage is the main competitive mechanism is often very difficult. Because of the high heterogeneity of NOM, both mechanisms of competitive adsorption can appear simultaneously as controlled by the adsorption conditions (Newcombe et al., 1997, 2002a, 2002b; Pelekani and Snoeyink, 1999, 2001; Li et al., 2003a, 2003b; Campinas et al., 2013). Nevertheless, it can be generally concluded that while low-MW NOM reduces adsorption capacity of AOM through direct competition for active sites, NOM of higher MW hinders adsorption kinetics of AOM by pore blockage (Li et al., 2003a).

6. Conclusion and future outlook

DWTP operation is becoming increasingly challenging because of the growing frequency and extent of AOM occurrence in raw water, while the conventional treatment process based on coagulation/flocculation is not sufficient for the removal of all AOM fractions. Especially, low-MW AOM requires further treatment; otherwise, it causes deterioration in the quality of produced water. Adsorption onto AC seems to be a suitable method for eliminating residual low-MW AOM, including cyanobacterial toxins and T&O compounds; however, it is a very complicated process influenced by various factors. This review summarizes the current knowledge of AOM adsorption onto AC with regard to drinking water treatment. The following conclusions and proposals for future research have been identified:

- While much is known about the adsorption of specific algal metabolites, such as toxins (mainly MCs) and T&O compounds (geosmin or MIB), considerably less information is available on the adsorption of AOM as a mixture, or on its two basic fractions, EOM and COM. Both EOM and COM have different properties than MCs and T&O compounds (MW, chemical composition, charge); thus, more attention should be paid particularly to the removal of AOM mixture and its residual concentrations after coagulation/flocculation treatment by additional methods such as adsorption onto AC.
- Adsorption onto AC is often used in combination with other treatment techniques, especially with membrane filtration, where AC improves the removal efficiency of target compounds and may prevent membrane fouling. To improve further the overall treatment process of AOM, the use of pre-oxidation methods associated with AC adsorption can also be appropriate, as these methods lead to improved DOC and toxin removal and decreased membrane fouling.
- Adsorption is a complex process influenced by many factors related to

the adsorbate, adsorbent and solution properties. In terms of adsorbate, MW, molecule structure and content of functional groups are essential in the adsorption process. In terms of AC, PSD and surface charge play an important role in adsorption efficiency. Finally, pH and ionic strength are the main solution properties that control adsorption performance. Temperature is another solution factor that generally affects adsorption as a physical process, but in the case of AOM adsorption on AC, there are not enough studies to clearly demonstrate how temperature affects, for example, the arrangement of adsorbed molecules or their kinetics in solution and adsorbent's pores.

- Electrostatic interactions, hydrogen bonds, hydrophobic effect, and π - π interactions have been identified as mechanisms involved in the adsorption of AOM. The combination and extent of these interactions are strongly dependent on pH and ionic strength of the solution.
- Competitive adsorption between AOM and other pollutants and AC fouling are the two very important phenomena that occur during AC adsorption in water treatment. In the context of these issues, AOM can be the originator of competition during the adsorption process on the one hand, but in other cases it may be adversely affected by competition itself. While studies focusing on deteriorating the removal of microcystins and T&O compounds because of the competitive adsorption are common, there is only one study investigating and describing AOM as an originator of competitive adsorption. Since adsorption onto AC is often used to eliminate anthropogenic micropollutants and specific low-MW AOM that may coexist in a water source, it is necessary to expand research in this area to minimize the negative effect on water treatment efficiency.
- Many studies investigating the adsorption of AOM onto AC are performed under laboratory conditions by equilibrium experiments with isolated AOM compounds or model substances to identify and to describe adsorption patterns and mechanisms perfectly, which is undoubtedly essential. However, this research also needs to be transferred to the field for more practical applications that use continuous flow column experiments with real raw water with multi-component composition.

It can also be expected, that unexplored types of anthropogenic micropollutants (e.g., pesticides metabolites, by-products, drugs) (McMahen et al., 2016; Pietrzak et al., 2020; Melin et al., 2020; Chen et al., 2021) with the potential to interact and/or compete with AOM during adsorption, or new types of microorganisms producing AOM (Gin et al., 2021), will be identified as problematic in water. It should also be considered that the supramolecular structure of NOM has also been identified (Wells and Stretz, 2019), but has not yet received sufficient attention despite it may affect the treatability of these substances in drinking water production. Thus, the research should focus on the ways how to help the water treatment plants to respond to these issues appropriately.

CRedit authorship contribution statement

Martin Pivokonsky: Conceptualization, Supervision, Project administration, Writing – review & editing, Funding acquisition. **Ivana Kopecka:** Conceptualization, Writing – original draft, Investigation. **Lenka Cermakova:** Conceptualization, Writing – original draft, Visualization, Project administration. **Katerina Fialova:** Writing – original draft, Visualization. **Katerina Novotna:** Writing – review & editing, Visualization. **Tomas Cajthaml:** Writing – review & editing. **Rita K. Henderson:** Writing – review & editing. **Lenka Pivokonska:** Conceptualization, Writing – review & editing.

Declaration of competing interest

The authors declare that they have no known competing financial interests or personal relationships that could have appeared to influence the work reported in this paper.

Acknowledgements

This work was supported by the institutional support of the Czech Academy of Sciences [RVO: 67985874]. The authors also thank to the Strategy AV21 of the Czech Academy of Sciences (VP20 – Water for life) for valuable support.

References

- Abouleish, M.Y.Z., Wells, M.J.M., 2015. Trihalomethane formation potential of aquatic and terrestrial fulvic and humic acids: sorption on activated carbon. *Sci. Total Environ.* 521–522, 293–304.
- Álvarez-Merino, M.A., Fontecha-Cámara, M.A., López-Ramón, M.V., Moreno-Castilla, C., 2008. Temperature dependence of the point of zero charge of oxidized and non-oxidized activated carbons. *Carbon* 46 (5), 778–787.
- Amend, J.P., Helgeson, H.C., 1997. Solubilities of the common L- α -amino acids as a function of temperature and solution pH. *Pure Appl. Chem.* 69 (5), 935–942.
- Anastopoulos, I., Kyzas, G.Z., 2016. Are the thermodynamic parameters correctly estimated in liquid-phase adsorption phenomena? *J. Mol. Liq.* 218, 174–185.
- Andelkovic, T., Perovic, J.M., Purenovic, M.M., Andelkovic, D., 2004. Destabilization and aggregation of aqueous humic acids solution by metal ions. *Facta Univ. Ser. Phys. Chem. Technol.* 3 (1), 79–85.
- Andreu, A., Stoeckli, H.F., Bradley, R.H., 2007. Specific and non-specific interactions on non-porous carbon black surfaces. *Carbon* 45, 1854–1864.
- Ashraf, A., Dastgheib, S.A., Mensing, G., Shannon, M.A., 2013. Surface characteristics of selected carbon materials exposed to supercritical water. *J. Supercrit. Fluids* 66, 32–40.
- Bandala, E., Martínez, R.D., Martínez, E., Dionysou, D.D., 2004. Degradation of microcystin-LR toxin by Fenton and PhotoFenton processes. *Toxicol* 43 (7), 829–832.
- Baresova, M., Pivokonsky, M., Novotna, K., Naceradská, J., Branyik, T., 2017. An application of cellular organic matter to coagulation of cyanobacterial cells (*Merismopedia tenuissima*). *Water Res.* 122, 70–77.
- Barton, S.S., Evans, M.J.B., Halliop, E., MacDonald, J.A.T., 1997. Acidic and basic sites on the surface of porous carbon. *Carbon* 35 (9), 1361–1366.
- Benaddi, H., Bandosz, T.J., Jagiello, J., Schwartz, J.A., Rouzaud, J.N., Legras, D., Béguin, F., 2000. Surface functionality and porosity of activated carbons obtained from chemical activation of wood. *Carbon* 38, 2085–2100.
- Benival, D., Taylor-Edmonds, L., Armour, J., Andrews, R., 2018. Ozone/peroxide advanced oxidation in combination with biofiltration for taste and odour control and organics removal. *Chemosphere* 212, 272–281.
- Bjelopavlic, M., Newcombe, G., Hayes, R., 1999. Adsorption of NOM onto activated carbon: effect of surface charge, ionic strength, and pore volume distribution. *J. Colloid Interface Sci.* 210 (2), 271–280.
- Bruce, D., Westerhoff, P., Brawley-Chesworth, A., 2002. Removal of 2-methylisoborneol and geosmin in surface water treatment plants in Arizona. *J. Water Supply* 51, 183–197.
- Bruchet, A., Laine, J.M., 2005. Efficiency of membrane process for taste and odor removal. *Water Sci. Technol.* 51 (6–7), 257–265.
- Burgos, L., Lehmann, M., Sim on Rodrigues de Andrade, S., 2014. Agents of earthy-musty taste and odor in water: evaluation of cytotoxicity, genotoxicity and toxicogenomics. *Sci. Total Environ.* 490, 679–685.
- Campinas, M., Rosa, M.J., 2006. The ionic strength effect on microcystin and natural organic matter surrogate adsorption onto PAC. *J. Colloid Interface Sci.* 299 (2), 520–529.
- Campinas, M., Rosa, M.J., 2010a. Assessing PAC contribution to the NOM fouling control in PAC/UF systems. *Water Res.* 44 (5), 1636–1644.
- Campinas, M., Rosa, M.J., 2010b. Removal of microcystins by PAC/UF. *Sep. Purif. Technol.* 71, 114–120.
- Campinas, M., Viegas, R.M.C., Rosa, M.J., 2013. Modelling and understanding the competitive adsorption of microcystins and tannic acid. *Water Res.* 47, 5690–5699.
- Cermakova, L., Kopecka, I., Pivokonsky, M., Pivokonska, J., Janda, V., 2017. Removal of cyanobacterial amino acids in water treatment by activated carbon adsorption. *Sep. Purif. Technol.* 173, 330–338.
- Cermakova, L., Fialova, K., Kopecka, I., Baresova, M., Pivokonsky, M., 2020. Investigating adsorption of model low-MW AOM components onto different types of activated carbon – influence of temperature and pH value. *Environ. Technol.* <https://doi.org/10.1080/09593330.2020.1820082>.
- Chang, E.E., Liang, C.H., Ko, Y.W., Chiang, P.C., 2002. Effect of ozone dosage for removal of model compounds by ozone/GAC treatment. *Ozone Sci. Eng.* 24, 357–367.
- Chen, G., Dussert, B.W., Suffet, I.H., 1997. Evaluation of granular activated carbons for removal of methylisoborneol to below odor threshold concentration in drinking water. *Water Res.* 31 (5), 1155–1163.
- Chen, X., Zhou, Q., Liu, F., Peng, Q., Bian, Y., 2021. Performance and kinetic of pesticide residues removal by microporous starch immobilized laccase in a combined adsorption and biotransformation process. *Environ. Technol. Innov.* 21, 101235.
- Chien, Ch., Wu, S.-P., Ke, H.-C., Lo, S.-L., Tung, H.-H., 2018. Comparing ozonation and biofiltration treatment of source water with high cyanobacterial-derived organic matter: the case of a water treatment plant followed by a small-scale water distribution system. *Int. J. Environ. Res. Public Health* 15 (12), 2633.
- Clark, H.M., Alves, C.C.C., Franca, A.S., Oliveira, L.S., 2012. Evaluation of the performance of an agricultural residue-based activated carbon aiming at removal of phenylalanine from aqueous solution. *LWT-Food Sci. Technol.* 49, 155–161.
- Collins, M.R., Amy, G.L., Steelink, C., 1986. Molecular weight distribution, carboxylic acidity, and humic substances content of aquatic organic matter: implications for removal during water treatment. *Environ. Sci. Technol.* 20 (10), 1028–1032.
- Considine, R., Denoyel, R., Pendleton, P., Schumann, R., Wong, S.-H., 2001. The influence of surface chemistry on activated carbon adsorption of 2-methylisoborneol from aqueous solution. *Colloids Surf. A Physicochem. Eng. Asp.* 179 (2–3), 271–280.
- Cook, D., Newcombe, G., 2002. Removal of microcystin variants with powdered activated carbon. *Water Sci. Technol. Water Supply* 2 (5), 201–207.
- Cook, D., Newcombe, G., 2008. Comparison and modeling of the adsorption of two microcystin analogues onto powdered activated carbon. *Environ. Technol.* 29 (5), 525–534.
- Cook, D., Newcombe, G., Sztajnbock, P., 2001. The application of powdered activated carbon for MIB and geosmin removal: predicting PAC doses in four raw waters. *Water Res.* 35 (5), 1325–1333.
- Creighton, T.E., 1993. *Proteins: Structures and Molecular Properties*. second ed. W.H. Freeman and Company, New York 507 pp.
- Dastgheib, S.A., Karanfil, T., Cheng, W., 2004. Tailoring activated carbons enhanced removal of natural organic matter from natural waters. *Carbon* 42 (3), 547–557.
- Dixon, M.B., Richard, Y., Ho, L., Chow, C.W.K., O'Neill, B.K., Newcombe, G., 2011. A coagulation-powdered activated carbon-ultrafiltration-multiple barrier approach for removing toxins from two Australian cyanobacterial blooms. *J. Hazard. Mater.* 186 (2–3), 1553–1559.
- Donati, C., Drikas, M., Hayes, R., Newcombe, G., 1994. Microcystin-LR adsorption by powdered activated carbon. *Water Res.* 28 (8), 1735–1742.
- Ebie, K., Li, F., Azuma, Y., Yuasa, A., Hagashita, T., 2001. Pore distribution effect of activated carbon in adsorbing organic micropollutants from natural water. *Water Res.* 35 (1), 167–179.
- Faruqi, A., Henderson, M., Henderson, R.K., Stuetz, R., Gladman, B., McDowall, B., Zamyadi, A., 2018. Removal of algal taste and odour compounds by granular and biological activated carbon in full-scale water treatment plants. *Water Sci. Technol. Water Supply* 18 (5), 1531–1544.
- Frimmel, F.H., 1998. Characterization of natural organic matter as major constituents in aquatic systems. *J. Contam. Hydrol.* 35 (1–3), 201–216.
- Froschio, S.M., Cannon, E., Lau, H.M., Humpage, A.R., 2009. Limited uptake of the cyanobacterial toxin cylindrospermopsin by vero cells. *Toxicol* 54, 862–868.
- Gao, Q., Xu, W., Xu, Y., Wu, D., Sun, Y., Deng, F., Shen, W., 2008. Amino acid adsorption on mesoporous materials: influence of types of amino acids, modification of mesoporous materials, and solution conditions. *J. Phys. Chem. B* 112 (7), 2261–2267.
- Ghermaout, B., Ghermaout, D., Saiba, A., 2010. Algae and cyanotoxins removal by coagulation/flocculation: a review. *Desalin. Water Treat.* 20, 133–143.
- Gin, K.Y.-H., Sim, Z.-Y., Goh, K.C., Kok, J.W.K., Te, S.H., Tran, N.H., Li, W., He, Y., 2021. Novel cyanotoxin-producing *Synechococcus* in tropical lakes. *Water Res.* 192, 116828.
- Gorham, J.M., Wnuk, J.D., Shin, M., Fairbrother, H., 2007. Adsorption of natural organic matter onto carbonaceous surfaces: atomic force microscopy study. *Environ. Sci. Technol.* 41 (4), 1238–1244.
- Goscianska, J., Olejnik, A., Pietrzak, R., 2013. Adsorption of L-phenylalanine onto mesoporous silica. *Mater. Chem. Phys.* 142, 586–593.
- Goscianska, J., Pietrzak, R., Olejnik, A., 2014. Adsorption of L-phenylalanine onto ordered mesoporous carbons prepared by hard template method. *J. Taiwan Inst. Chem. Eng.* 45, 347–353.
- Graham, M.R., Summers, R.S., Simpson, M.R., Macleod, B.W., 2000. Modeling equilibrium adsorption of 2-methylisoborneol and geosmin in natural waters. *Water Res.* 34 (8), 2291–2300.
- Greiner, E., Kumar, K., Sumit, M., Giuffrè, A., Zhao, W., Pedersen, J., Sahai, N., 2014. Adsorption of L-glutamic acid and L-aspartic acid to ?-Al₂O₃. *Geochim. Cosmochim. Acta* 133, 142–155.
- He, X., Liu, Y.-L., Conklin, A., Westrick, J., Weavers, L.K., Dionysiou, D.D., Lenhart, J.J., Mouser, P.J., Szlag, D., Walker, H.W., 2016. Toxic cyanobacteria and drinking water: impacts, detection, and treatment. *Harmful Algae* 54, 174–193.
- Heisler, J., Gilbert, P.M., Burkholder, J.M., Anderson, D.M., Cochlan, W., Dennison, W.C., Dortch, Q., Gobler, C.J., Heil, C.A., Humphries, E., Lewitus, A., Magnien, R., Marshall, H.G., Sellner, K., Stockwell, D.A., Stoecker, D.K., Suddleson, M., 2008. Eutrophication and harmful algal blooms: a scientific consensus. *Harmful Algae* 8, 3–13.
- Henderson, R., Parsons, S.A., Jefferson, B., 2008a. The impact of algal properties and pre-oxidation on solid-liquid separation of algae. *Water Res.* 42, 1827–1845.
- Henderson, R.K., Baker, A., Parsons, S.A., Jefferson, B., 2008b. Characterisation of algogenic organic matter extracted from cyanobacteria, green algae and diatoms. *Water Res.* 42 (13), 3435–3445.
- Henderson, R.K., Parsons, S.A., Jefferson, B., 2010. The impact of differing cell and algogenic organic matter (AOM) characteristics on the coagulation and flotation of algae. *Water Res.* 44 (12), 3617–3624.
- Hepplewhite, C., Newcombe, G., Knappe, D.R.U., 2004. NOM and MIB, who wins in the competition for activated carbon adsorption sites? *Water Sci. Technol.* 49 (9), 257–265.
- Hnatukova, P., Kopecka, I., Pivokonsky, M., 2011. Adsorption of cellular peptides of *Microcystis aeruginosa* and two herbicides onto activated carbon: effect of surface charge and interactions. *Water Res.* 45 (11), 3359–3368.
- Ho, L., Lambling, P., Bustamante, H., Duker, P., Newcombe, G., 2011. Application of powdered activated carbon for the adsorption of cylindrospermopsin and microcystin toxins from drinking water supplies. *Water Res.* 45 (9), 2954–2964.
- Hoyer, O., Lüsse, B., Bernhardt, H., 1985. Isolation and characterization of extracellular organic matter (EOM) from algae. *Z. Wasser Abwasserforschung* 18 (2), 76–90.
- Huang, W.J., Lai, C.H., Cheng, Y.L., 2007a. Evaluation of extracellular products and mutagenicity in cyanobacteria cultures separated from a eutrophic reservoir. *Sci. Total Environ.* 377 (2–3), 214–223.
- Huang, W.J., Cheng, B.L., Cheng, Y.L., 2007b. Adsorption of microcystin-LR by three types of activated carbon. *J. Hazard. Mater.* 141 (1), 115–122.

- Huang, J., Graham, N., Templeton, M.R., Zhang, Y., Collins, C., Nieuwenhuijsen, M., 2009. A comparison of the role of two blue-green algae in THM and HAA formation. *Water Res.* 43, 3009–3018.
- Huang, W., Chu, H., Dong, B., 2012. Characteristics of algogenic organic matter generated under different nutrient conditions and subsequent impact on microfiltration membrane fouling. *Desalination* 293, 104–111.
- Huang, W., Wang, L., Zhou, W., Lv, W., Hu, M., Chu, H., Dong, B., 2017. Effect of combined ozone and PAC pretreatment on ultrafiltration membrane fouling control and mechanisms. *J. Membr. Sci.* 533, 378–389.
- Ikhshan, J., Johnson, B.B., Wells, J.D., Angove, M.J., 2004. Adsorption of aspartic acid onto kaolinite. *J. Colloid Interface Sci.* 273, 1–5.
- Ilieva, V., Kondeva-Burdina, M., Georgieva, T., Pavlova, V., 2019. Toxicity of cyanobacteria. organotropy of cyanotoxins and toxicodynamics of cyanotoxins by species. *Pharmacia* 66 (3), 91–97.
- Jacangelo, J.G., Lañé, J.-M., Cummings, E.W., Adham, S.S., 1995. UF with pretreatment for removing DBP precursors. *J. Am. Water Works Assoc.* 87, 100–112.
- Jovic, B., Kordic, B., Miskov, V., Trickovic, J., Kovacevic, M., Petrovic, S., 2020. Amides as a model system of low molar mass algal organic matter. influence on the adsorption of p-nitrophenol on activated carbon. *Arab. J. Chem.* 13, 59–66.
- Jüttner, F., 1995. Physiology and biochemistry of odorous compounds from freshwater cyanobacteria and algae. *Water Sci. Technol.* 31 (11), 69–78.
- Katiyar, A., Thiel, S.W., Gulians, V.V., Pinto, N.G., 2010. Investigation of the mechanism of protein adsorption on ordered mesoporous silica using flow microcalorimetry. *J. Chromatogr. A* 1217, 1593–1588.
- Kilduff, J.E., Karanfil, T., 2002. Trichlorethylene adsorption by activated carbon preloaded with humic substances: effects of solution chemistry. *Water Res.* 36 (7), 1685–1698.
- Kilduff, J.E., Karafantil, T., Chin, Y.-P., Weber Jr., W.J., 1996. Adsorption of natural organic polyelectrolytes by activated carbon: a size-exclusion chromatography study. *Environ. Sci. Technol.* 30 (4), 1336–1343.
- Kilduff, J.E., Karafantil, T., Weber Jr., W.J., 1998a. Competitive effects of displaceable organic compounds on trichlorethylene uptake by activated carbon. II. Model verification and applicability to natural organic matter. *J. Colloid Interface Sci.* 205 (2), 280–289.
- Kilduff, J.E., Karafantil, T., Weber Jr., W.J., 1998b. Competitive effects of nondisplaceable organic compounds on trichlorethylene uptake by activated carbon. I. Thermodynamic predictions and model sensitivity analyses. *J. Colloid Interface Sci.* 205, 271–279.
- Kim, H.C., Yu, M.J., 2005. Characterization of natural organic matter in conventional water treatment processes for selection of treatment processes focused on DBPs control. *Water Res.* 39 (19), 4779–4789.
- Kim, C., Lee, S.I., Hwang, S., Cho, M., Kim, H.-S., Noh, S.H., 2014. Removal of geosmin and 2-methylisoborneol (2-MIB) by membrane system combined with powdered activated carbon (PAC) for drinking water treatment. *J. Water Process Eng.* 4, 91–98.
- Klymenko, N.A., Kozyatnyk, I., Savchyna, L., 2010. Removing of fulvic acids by ozonation and biological active carbon filtration. *Water Res.* 44, 5316–5322.
- D.R.U. Knappe 2006. Surface chemistry effects in activated carbon adsorption of industrial pollutants. *Interface Science in Drinking Water Treatment. Theory and Applications. Interface Science and Technology – vol. 10.* Newcombe, G., a Dixon, D. (edit), Elsevier Ltd., 155–177.
- Kopecka, I., Pivokonsky, M., Pivokonska, L., Hnatukova, P., Safarikova, J., 2014. Adsorption of peptides produced by cyanobacterium *Microcystis aeruginosa* onto granular activated carbon. *Carbon* 69, 595–608.
- Kweon, J.H., Hur, H.-W., Seo, G.-T., Jang, T.-R., Park, J.-H., Choi, K.Y., Kim, H.S., 2009. Evaluation of coagulation and PAC adsorption pretreatments on membrane filtration for surface water in Korea: a pilot study. *Desalination* 249, 212–216.
- Lalezary, S., Pirbazari, M., McGuire, M.J., 1986. Evaluating activated carbons for removing low concentrations of taste- and odor-producing organics. *J. Am. Water Works Assoc.* 78 (11), 76–82.
- Lambert, T.W., Holmes, Ch.F.B., Hrudsey, S.E., 1996. Adsorption of microcystin-LR by activated carbon and removal in full scale water treatment. *Water Res.* 30 (6), 1411–1422.
- Lamsal, R., Margaret, Walsh, M.E. G.A., Gagnon, 2011. Comparison of advanced oxidation process for the removal of natural organic matter. *Water Res.* 45, 3263–3269.
- Leenheer, J.A., Croué, J.P., 2003. Characterizing aquatic dissolved organic matter. *Environ. Sci. Technol.* 37 (1), 18A–26A.
- Leloup, M., Nicolau, R., Pallier, V., Yéprémian, C., Feuillade-Cathalifaud, G., 2013. Organic matter produced by algae and cyanobacteria: quantitative and qualitative characterization. *J. Environ. Sci.* 25 (6), 1089–1097.
- Lerman, I., Chen, Y., Xing, B., Chefetz, B., 2013. Adsorption of carbamazepine by carbon nanotubes: effect of DOM introduction and competition with phenanthrene and bisphenol A. *Environ. Pollut.* 182, 169–176.
- Li, Q., Snoeyink, B.J., Campos, C., 2003a. Elucidating competitive adsorption mechanisms of atrazine and NOM using model compounds. *Water Res.* 37, 773–784.
- Li, Q., Snoeyink, B.J., Campos, C., 2003b. Pore blockage effect of NOM on atrazine adsorption kinetics of PAC: the roles of PAC pore size distribution and NOM molecular weight. *Water Res.* 37, 4863–4872.
- Li, L., Gao, N., Deng, Y., Yao, J., Zhang, K., 2012. Characterization of intracellular & extracellular algae organic matters (AOM) of *Microcystis aeruginosa* and formation of AOM-associated disinfection byproducts and odor & taste compounds. *Water Res.* 46 (4), 1233–1240.
- Li, L., Yang, S., Yu, S., Zhang, Y., 2019. Variation and removal of 2-MIB in full-scale treatment plants with source water from Lake Tai, China. *Water Res.* 162, 180–189.
- Lin, Q., Dong, F., Li, C., Cui, J., 2021. Disinfection byproducts formation from algal organic matter after ozonation or ozonation combined with activated carbon treatment with subsequent chlorination. *J. Environ. Sci.* 104, 233–241.
- Liu, M., Huang, J., Deng, Y., 2007. Adsorption behaviors of L-arginine from aqueous solutions on a spherical cellulose adsorbent containing the sulfonic group. *Bioresour. Technol.* 98, 1144–1148.
- Liu, F.F., Fan, J.L., Wang, S.G., Ma, G.H., 2013. Adsorption of natural organic matter analogues by multi-walled carbon nanotubes: comparison with powdered activated carbon. *Chem. Eng. J.* 219, 450–458.
- Liu, Y.-L., Walker, H.W., Lenhart, J.J., 2019. The effect of natural organic matter on the adsorption of microcystin-LR onto clay minerals. *Colloids Surf. A Physicochem. Eng. Asp.* 583, 123964.
- Ma, L., Peng, F., Li, H., Wang, Ch., Yang, Z., 2019. Adsorption of geosmin and 2-methylisoborneol onto granular activated carbon in water: isotherms, thermodynamics, kinetics, and influencing factors. *Water Sci. Technol.* 80 (4), 644–653.
- Marhaba, T.F., Pu, Y., Bengraïne, K., 2003. Modified dissolved organic matter fractionation technique for natural water. *J. Hazard. Mater. B* 101, 43–53.
- Matilainen, A., Lindqvist, N., Korhonen, S., Tuhkanen, T., 2002. Removal of NOM in the different stages of the water treatment process. *Environ. Int.* 28 (6), 457–465.
- Matilainen, A., Vieno, N., Tuhkanen, T., 2006. Efficiency of the activated carbon filtration in the natural organic matter removal. *Environ. Int.* 32 (3), 324–331.
- Matilainen, A., Gjessing, E.T., Lahtinen, T., Hed, L., Bhatnagar, A., Sillanpää, A., 2011. An overview of the methods used in the characterisation of natural organic matter (NOM) in relation to drinking water treatment. *Chemosphere* 83, 1431–1442.
- Matsui, Y., Yoshitaka, F., Inoue, T., Matsushita, T., 2003. Effect of natural organic matter on powdered activated carbon adsorption of trace contaminants: characteristics and mechanism of competitive adsorption. *Water Res.* 37, 4413–4424.
- Matsui, Y., Yoshida, T., Nakao, S., Knappe, D.R.U., Matsushita, T., 2012. Characteristics of competitive adsorption between 2-methylisoborneol and natural organic matter on superfine and conventionally sized powdered activated carbons. *Water Res.* 46 (15), 4741–4749.
- Matsui, Y., Nakao, S., Taniguchi, T., Matsushita, T., 2013. Geosmin and 2-methylisoborneol removal using superfine powdered activated carbon: shell adsorption and branched-pore kinetic model analysis and optimal particle size. *Water Res.* 47, 2873–2880.
- Matsui, Y., Nakao, S., Sakamoto, A., Taniguchi, T., Pan, L., Matsushita, T., Shirasaki, N., 2015. Adsorption capacities of activated carbons for geosmin and 2-methylisoborneol vary with activated carbon particle size: effect of adsorbent and adsorbate characteristics. *Water Res.* 85, 95–102.
- Matsushita, T., Matsui, Y., Sawaoka, D., Ohno, K., 2008. Simultaneous removal of cyanobacteria and earthy odor compound by a combination of activated carbon, coagulation, and ceramic microfiltration. *J. Water Supply Res. Technol. AQUA* 57 (7), 481–487.
- McMahan, R.L., Strynar, M.J., McMillan, M., DeRose, E., Lindstrom, A.B., 2016. Comparison of fipronil sources in North Carolina surface water and identification of a novel fipronil transformation product in recycled wastewater. *Sci. Total Environ.* 569–570, 880–887.
- Melin, J., Guillon, A., Enault, J., Esperanza, M., Dauchy, X., Bouchonnet, S., 2020. How to select relevant metabolites based on available data for parent molecules: case of neonicotinoids, carbamates, phenylpyrazoles and organophosphorus compounds in french water resources. *Environ. Pollut.* 265, 114992.
- Molica, R.J.R., Oliveira, E.J.A., Carvalho, P.V.V.C., Costa, A.N.S.F., Cunha, M.C.C., Melo, G.L., Azevedo, S.M.F.O., 2005. Occurrence of saxitoxin and anatoxin-a(s)-like anticholinesterase in brazilian drinking water supply. *Harmful Algae* 4, 743–753.
- Montes-Morán, M.A., Suárez, D., Menéndez, J.A., Fuente, E., 2004. On the nature of basic sites on carbon surfaces: an overview. *Carbon* 42, 1219–1225.
- Moreno-Castilla, C., 2004. Adsorption of organic molecules from aqueous solutions on carbon materials. *Carbon* 42, 83–94.
- Newcombe, G., 2006. Removal of natural organic material and algal metabolites using activated carbon. In: Newcombe, G., Dixon, D. (Eds.), *Interface Science in Drinking Water Treatment: Theory and Applications.* Elsevier Ltd., Amsterdam, pp. 133–153.
- Newcombe, G., Drikas, M., 1997. Adsorption of NOM onto activated carbon: electrostatic and non-electrostatic effects. *Carbon* 35 (9), 1239–1250.
- Newcombe, G., Drikas, M., Hayes, R., 1997. Influence of characterised natural organic material on activated carbon adsorption: II. Effect on pore volume distribution and adsorption of 2-methylisoborneol. *Water Res.* 31 (5), 1065–1073.
- Newcombe, G., Morrison, J., Hepplewhite, C., 2002a. Simultaneous adsorption of MIB and NOM onto activated carbon. I. Characterisation of the system and NOM adsorption. *Carbon* 40, 2135–2146.
- Newcombe, G., Morrison, J., Hepplewhite, C., Knappe, D.R.U., 2002b. Simultaneous adsorption of MIB and NOM onto activated carbon II. Competitive effects. *Carbon* 40, 2147–2156.
- Newcombe, G., Morrison, J., Hepplewhite, C., Knappe, D., 2002c. In the (adsorption) competition between NOM and MIB, who is the winner, and why? *Water Sci. Technol.* 2 (2), 59–67.
- Nishiwaki-Matsushima, R., Ohta, T., Nishiwaki, S., Suganuma, M., Kohyama, J., Ishikawa, T., Carmichael, W.W., Fujiki, H., 1992. Liver tumor promotion by the cyanobacterial cyclic peptide toxin microcystin-LR. *J. Cancer Res. Clin. Oncol.* 118, 420–424.
- Nissinen, T.K., Miettinen, I.T., Martikainen, P.J., Vartiainen, T., 2001. Molecular size distribution of natural organic matter in raw and drinking waters. *Chemosphere* 45 (6–7), 865–873.
- O'Connor, A.J., Hokura, A., Kisler, J.M., Shimazu, S., Stevens, G.W., Komatsu, Y., 2006. Amino acids adsorption onto mesoporous silica molecular sieves. *Sep. Purif. Technol.* 48, 197–201.
- Oba, S.N., Ighalo, J.O., Aniagor, C.O., Igwegbe, C.A., 2021. *Sci. Total Environ.* 780, 146608.
- Oh, H., Yu, M., Takizawa, S., Ohgaki, S., 2006. Evaluation of PAC behaviour and fouling formation in an integrated PAC-UF membrane for surface water treatment. *Desalination* 192, 54–62.
- Paelr, H.W., Huisman, J., 2008. Blooms like it hot. *Science* 320 (5872), 57–58.

- Papageorgiou, A., Voutsas, D., Papadakis, N., 2014. Occurrence and fate of ozonation by-products at a full-scale drinking water treatment plant. *Sci. Total Environ.* 481, 392–400.
- Park, J.-A., Jung, S.-M., Yi, I.-G., Kim, S.-B., Lee, S.-H., 2017. Adsorption of microcystin-LR on mesoporous carbon and its potential use in drinking water source. *Chemosphere* 177, 15–23.
- Park, K.-Y., Ju, Y.-J., Yun, S.-J., Kweon, J.-H., 2019. Natural organic matter removal from algal-rich water and disinfection by-products formation potential reduction by powdered activated carbon adsorption. *J. Environ. Manag.* 235, 310–318.
- Park, J.-A., Kang, J.-K., Jung, S.-M., Choi, J.-W., Lee, S.-H., Yargeau, V., Kim, S.-B., 2020. Investigating microcystin-LR adsorption mechanisms on mesoporous carbon, mesoporous silica, and their amino-functionalized form: surface chemistry, pore structure, and molecular characteristics. *Chemosphere* 247, 125811.
- Pelekani, C., Snoeyink, V.L., 1999. Competitive adsorption in natural water: role of activated carbon pore size. *Water Res.* 33 (5), 1209–1219.
- Pelekani, C., Snoeyink, V.L., 2000. Competitive adsorption between atrazine and methylene blue on activated carbon: the importance of pore size distribution. *Carbon* 38, 1423–1436.
- Pelekani, C., Snoeyink, V.L., 2001. A kinetic and equilibrium study of competitive adsorption between atrazine and Congo red dye on activated carbon: the importance of pore size distribution. *Carbon* 39, 25–37.
- Pendleton, P., Wong, S.H., Schumann, R., Levay, G., Denoyel, R., Rouquero, J., 1997. Properties of activated carbon controlling 2-methylisoborneol adsorption. *Carbon* 35 (8), 1141–1149.
- Pendleton, P., Schumann, R., Wong, S.H., 2001. Microcystin-LR adsorption by activated carbon. *J. Colloid Interface Sci.* 240 (1), 1–8.
- Peter, A., Köster, O., Schildknecht, A., von Guten, U., 2009. Occurrence of dissolved and particle-bound taste and odor compounds in Swiss lake waters. *Water Res.* 43, 2191–2200.
- Piccolo, A., 2001. The supramolecular structure of humic substances: a novel understanding of humus chemistry and implications in soil science. *Adv. Agron.* 75, 57–135.
- Pietrzak, D., Kania, J., Kmiecik, E., Malina, G., Wator, Katarzyna, 2020. Fate of selected neonicotinoid insecticides in soil-water systems: current state of the art and knowledge gaps. *Chemosphere* 255, 126981.
- Pietsch, J., Bormann, K., Schmidt, W., 2002. Relevance of intra- and extracellular cyanotoxins for drinking water treatment. *Acta Hydrochim. Hydrobiol.* 30 (1), 7–15.
- Pivokonsky, M., Klouček, O., Pivokonska, L., 2006. Evaluation of the production, composition and aluminum and iron complexation of algal organic matter. *Water Res.* 40 (16), 3045–3052.
- Pivokonsky, M., Pivokonska, L., Baumeltova, J., Bubakova, P., 2009a. The effect of cellular organic matter produced by cyanobacteria *Microcystis aeruginosa* on water purification. *J. Hydrol. Hydromech.* 57 (2), 121–129.
- Pivokonsky, M., Polasek, P., Pivokonska, L., Tomaskova, H., 2009b. Optimized reaction conditions for removal of cellular organic matter of *Microcystis aeruginosa* during the destabilization and aggregation process using ferric sulfate in water purification. *Water Environ. Res.* 81 (5), 514–522.
- Pivokonsky, M., Safarikova, J., Bubakova, P., Pivokonska, L., 2012. Coagulation of peptides and proteins produced by *Microcystis aeruginosa*: interaction mechanisms and the effect of Fe-peptide/protein complexes formation. *Water Res.* 46 (17), 5583–5590.
- Pivokonsky, M., Safarikova, J., Baresova, M., Pivokonska, L., Kopecka, I., 2014. A comparison of the character of algal extracellular versus cellular organic matter produced by cyanobacterium, diatom and green alga. *Water Res.* 51, 37–46.
- Pivokonsky, M., Naceradska, J., Brabenc, T., Novotna, K., Baresova, M., Janda, V., 2015. The impact of interactions between algal organic matter and humic substances on coagulation. *Water Res.* 84, 278–285.
- Pivokonsky, M., Naceradska, J., Kopecka, I., Baresova, M., Jefferson, B., Li, X., Henderson, R.K., 2016. The impact of algal organic matter on water treatment plant operation and water quality: a review. *Crit. Rev. Environ. Sci. Technol.* 46 (4), 291–335.
- Quian, F., Dixon, D.R., Newcombe, G., Ho, L., Dreyfus, J., 2014. The effect of pH on the release of metabolites by cyanobacteria in conventional water treatment processes. *Harmful Algae* 39, 253–258.
- Rabe, M., Verdes, D., Seeger, S., 2011. Understanding protein adsorption phenomena at solid surfaces. *Adv. Colloid Interf. Sci.* 162 (1–2), 87–106.
- Ridal, J., Brownlee, B., McKenna, G., Levac, N., 2001. Removal of taste and odour compounds by conventional granular activated carbon filtration. *Water Qual. J. Can.* 36 (1), 43–54.
- Rodríguez, E., Onstad, G.D., Kull, T.P.J., Metcalf, J.S., Acero, J.L., von Gunten, U., 2007. Oxidative elimination of cyanotoxins: comparison of ozone, chlorine, chlorine dioxide and permanganate. *Water Res.* 41 (15), 3381–3393.
- Rositano, J., Newcombe, G., Nicholson, B., Sztajnbock, P., 2001. Ozonation of NOM and algal toxins in four treated waters. *Water Res.* 35 (1), 23–32.
- Safarikova, J., Baresova, M., Pivokonsky, M., Kopecka, I., 2013. Influence of peptides and proteins produced by cyanobacterium *Microcystis aeruginosa* on the coagulation of turbid waters. *Sep. Purif. Technol.* 118, 49–57.
- Schrader, M.E., 1975. Ultrahigh-vacuum techniques in measurement of contact angles. 4. *Water on graphite (0001)*. *J. Phys. Chem.* 79 (23), 2508–2515.
- Schreiber, B., Brinkmann, T., Schmalz, V., Worch, E., 2005. Adsorption of dissolved organic matter onto activated carbon – the influence of temperature, absorption wavelength, and molecular size. *Water Res.* 39 (15), 3449–3456.
- Sebben, D., Pendleton, P., 2015a. Analysis of ionic strength effects on the adsorption of simple amino acids. *J. Colloid Interface Sci.* 443, 153–161.
- Sebben, D., Pendleton, P., 2015b. (Amino acid silica) adsorption thermodynamics: effects of temperature. *J. Chem. Thermodyn.* 87, 96–102.
- Sengül, A.B., Ersan, G., Tüfekçi, N., 2018. Removal of intra- and extracellular microcystin by submerged ultrafiltration (UF) membrane combined with coagulation/flocculation and powdered activated carbon (PAC) adsorption. *J. Hazard. Mater.* 343, 29–35.
- Seredynska-Sobecka, B., Tomaszewska, M., Janus, M., Morawski, A.W., 2006. Biological activation of carbon filters. *Water Res.* 40, 355–363.
- Shahrokhi-Shahraki, R., Benally, C., El-Din, M.G., 2021. High efficiency removal of heavy metals using tire-derived activated carbon vs commercial activated carbon: insights into the adsorption mechanisms. *Chemosphere* 264, 128455.
- Shi, H., Ding, J., Timmons, T., Adams, C., 2012. pH effects on the adsorption of saxitoxin by powdered activated carbon. *Harmful Algae* 19, 61–67.
- Shimizu, Y., Ateia, M., Yoshimura, C., 2018. Natural organic matter undergoes different molecular sieving by adsorption on activated carbon and carbon nanotubes. *Chemosphere* 203, 345–352.
- Silvério, F., Reis, M.J.D., Tronto, J., Valim, J.B., 2008. Adsorption of phenylalanine on layered double hydroxides: effect of temperature and ionic strength. *J. Mater. Sci.* 43 (2), 434–439.
- Srinivasan, R., Sorial, G.A., 2011. Treatment of taste and odor causing compounds 2-methyl isoborneol and geosmin in drinking water: a critical review. *J. Environ. Sci.* 23 (1), 1–13.
- Sugjara, N., Nishimura, O., Kani, Y., Inamori, Y., Sudo, R., 1997. Evaluation of activated carbons for removal of musty odor compounds in the presence of competitive organics. *Environ. Technol.* 18 (4), 455–459.
- Summers, R.S., Kim, S.M., Shimabuku, K., Chae, S.-H., Corwin, C.J., 2013. Granular activated carbon adsorption of MIB in the presence of dissolved organic matter. *Water Res.* 47 (10), 3507–3513.
- Sun, J., Bu, L., Shi, Z., Zhou, S., 2018. Removal of *Microcystis aeruginosa* by UV/chlorine process: inactivation mechanism and microcystins degradation. *Chem. Eng. J.* 349, 408–415.
- Takaara, T., Sano, D., Konno, H., Omura, T., 2007. Cellular proteins of *Microcystis aeruginosa* inhibiting coagulation with polyaluminum chloride. *Water Res.* 41, 1653–1658.
- Tang, L., Ma, X.Y., Wang, Y., Zhang, S., Zheng, K., Wang, X.C., Lin, Y., 2020. Removal of trace organic pollutants (pharmaceuticals and pesticides) and reduction of biological effects from secondary effluent by typical granular activated carbon. *Sci. Total Environ.* 749, 141611.
- Tentorio, A., Canova, L., 1989. Adsorption of α -amino acids on spherical TiO₂ particles. *Colloids Surf.* 39, 311–319.
- Terzyk, A.P., Rychlicki, G., Biniak, S., Lukaszewicz, J.P., 2003. New correlations between the composition of the surface layer of carbon and its physicochemical properties exposed while paracetamol is adsorbed at different temperatures and pH. *J. Colloid Interface Sci.* 257 (1), 13–30.
- Thurman, E.M., 1985. *Organic Geochemistry of Natural Waters*. Martinus Nijhoff/Dr. W. Junk Publishers, Boston, p. 497.
- Titus, E., Kalkar, A.K., Gaikar, V.G., 2003. Equilibrium studies of adsorption of amino acid on NaZSM-5 zeolite. *Colloids Surf. A Physicochem. Eng. Aspects* 233, 55–61.
- Velten, S., Knappe, D.R.U., Traber, J., Kaiser, H.-P., von Gunten, U., Boller, M., Meylan, S., 2011. Characterization of natural organic matter adsorption in granular activated carbon adsorbers. *Water Res.* 45, 3951–3959.
- Vinu, A., Hossain, K.Z., Kumar, G.S., Ariga, K., 2006. Adsorption of L-histidine over mesoporous carbon molecular sieves. *Carbon* 44, 530–536.
- Wang, H., Ho, L., Lewis, D.M., Brookes, J.D., Newcombe, G., 2007. Discriminating and assessing adsorption and biodegradation removal mechanisms during granular activated carbon filtration of microcystin toxins. *Water Res.* 41 (18), 4262–4270.
- Wang, Q., Zietzschmann, F., Yu, J., Hofman, R., An, W., Yang, M., Rietveld, L.C., 2020. Projecting competition between 2-methylisoborneol and natural organic matter in adsorption onto activated carbon from ozonated source waters. *Water Res.* 173, 115574.
- Wang, S., Huang, L., Zhang, Y., Li, L., Lu, X., 2021. A mini-review on the modeling of volatile organic compound adsorption in activated carbons: equilibrium, dynamics, and heat effects. *Chin. J. Chem. Eng.* 31, 153–163.
- Warhurst, A.M., Raggett, S.L., McConnachie, G.L., Pollard, S.J.T., Chipofya, V., Codd, G.A., 1997. Adsorption of the cyanobacterial hepatotoxin microcystin-LR by a low-cost activated carbon from the seed husks of the pan-tropical tree, *Moringa oleifera*. *Sci. Total Environ.* 207, 207–211.
- Watson, S.B., 2013. Ecotoxicity of taste and odor compounds. In: Féraud, J.F., Blaise, C. (Eds.), *Encyclopedia of Aquatic Ecotoxicology*. Springer, New York, pp. 337–352.
- Wells, M.J.M., Stretz, H.A., 2019. Supramolecular architectures of natural organic matter. *Sci. Total Environ.* 671, 1125–1133.
- WHO, 2011. *Guidelines for Drinking-water Quality*. 4th ed. World Health Organisation, Geneva, Switzerland.
- Wongcharee, S., Aravinthan, V., Erdei, L., 2020. Removal of natural organic matter and ammonia from dam water by enhanced coagulation combined with adsorption on powdered composite nano-adsorbent. *Environmental Technology & Innovation* 17, 100557.
- Xing, J., Liang, H., Xu, S., Chuah, Ch., J. X., Luo, 2019. Organic matter removal and membrane fouling mitigation during algae-rich surface water treatment by powdered activated carbon adsorption pretreatment: enhanced by UV and UV/chlorine oxidation. *Water Res.* 159, 283–293.
- Yoon, J.Y., Kim, J.H., Kim, W.-S., 1999. The relationship of interaction forces in the protein adsorption onto polymeric microspheres. *Colloids Surf. A Physicochem. Eng. Asp.* 153 (1–3), 413–419.
- Young, W.F., Horth, H., Crane, R., Ogden, T., Arnott, M., 1995. Taste and odour threshold concentrations of potential potable water contaminants. *Water Res.* 30 (2), 331–340.
- Yu, J., Yang, M., Lin, T., Guo, Z., Zhang, Y., Gu, J., Zhang, S., 2007. Effect of surface characteristics of activated carbon on the adsorption of 2-methylisoborneol (MIB) and geosmin from natural water. *Sep. Purif. Technol.* 56, 363–370.
- Zhang, K.-J., Gao, N.-Y., Deng, Y., Shui, M.-H., Tang, Y.-L., 2011a. Granular activated carbon (GAC) adsorption of two algal odorants, dimethyl trisulfide and β -cyclocitral. *Desalination* 266, 231–237.

- Zhang, Y., Tian, J., Nan, J., Gao, S., Liang, H., Wang, M., Li, G., 2011b. Effect of PAC addition on immersed ultrafiltration for the treatment of algal-rich water. *J. Hazard. Mater.* 186 (2–3), 1415–1424.
- Zhang, H., Zhu, G., Jia, X., Ding, Y., Zhang, M., Gao, Q., Hu, C., Xu, S., 2011c. Removal of microcystin-LR from drinking water using a bamboo-based charcoal adsorbent modified with chitosan. *J. Environ. Sci.* 23 (12), 1983–1988.
- Zhang, J., Northcott, K., Duke, M., Scales, P., Gray s.R., 2016. Influence of pre-treatment combinations on RO membrane fouling. *Desalination* 393, 120–126.
- Zhang, Y., Wang, X., Jia, H., Fu, B., Xu, R., Fu, Q., 2019a. Algal fouling and extracellular organic matter removal in powdered activated carbon-submerged hollow fibre ultrafiltration membrane systems. *Sci. Total Environ.* 671, 351–361.
- Zhang, Y., Jia, H., Wang, X., Ma, Ch., Xu, R., Fu, Q., Li, S., 2019b. Comparing the effects of pre-deposited and pre-mixed powdered activated carbons on algal fouling during ultrafiltration. *Algal Res.* 44, 101687.
- Zhou, H., Wu, T., Dong, X., Wang, Q., Shen, J., 2007. Adsorption mechanism of BMP-7 on hydroxyapatite (001) surfaces. *Biochem. Biophys. Res. Commun.* 361, 91–96.
- Zhou, S., Shao, Y., Gao, N., Deng, Y., Li, L., Deng, J., Tan, Ch., 2014. Characterization of algal organic matters of *Microcystis aeruginosa*: biodegradability, DBP formation and membrane fouling potential. *Water Res.* 52, 199–207.
- Zhu, S., Yin, D., Gao, N., Zhou, S., Wang, Z., Zhang, Z., 2016. Adsorption of two microcystins onto activated carbon: equilibrium, kinetic, and influential factors. *Desalin. Water Treat.* 1–9.
- Zietzschmann, F., Stützer, C., Jekel, M., 2016. Granular activated carbon adsorption of organic micro-pollutants in drinking water and treated wastewater: aligning breakthrough curves and capacities. *Water Res.* 92, 180–187.
- Zoschke, K., Engel, Ch., Börnick, H., Worch, E., 2011. Adsorption of geosmin and 2-methylisoborneol onto powdered activated carbon at non-equilibrium conditions: influence of NOM and process modelling. *Water Res.* 45, 4544–4550.

VÝSKYT A ODSTRAŇOVÁNÍ PER- A POLYFLUOROVANÝCH ORGANICKÝCH LÁTEK PŘI ÚPRAVĚ PITNÉ VODY

JOSEF DRECHSLER^a, JAROSLAV SEMERÁD^b,
KATEŘINA FIALOVÁ^c, MICHAELA
PROKOPOVÁ^c, TOMÁŠ CAJTHAML^b, MARTIN
PIVOKONSKÝ^c a VÁCLAV JANDA^a

^a Ústav technologie vody a prostředí VŠCHT Praha, Technická 5, 166 28 Praha 6, ^b Mikrobiologický ústav AV ČR, Videňská 1083, 142 20 Praha 4, ^c Ústav pro hydrodynamiku AV ČR, Pod Patankou 30/5, 166 12 Praha 6
pivo@ih.cas.cz

Došlo 3.2.21, přijato 9.2.21.

Klíčová slova: pitná voda, perfluorované organické látky, polyfluorované organické látky

Obsah

1. Úvod
2. Toxicita a výskyt
3. Limity pro PFAS v pitné vodě
4. Odstranění PFAS při úpravě vody
5. Závěr

1. Úvod

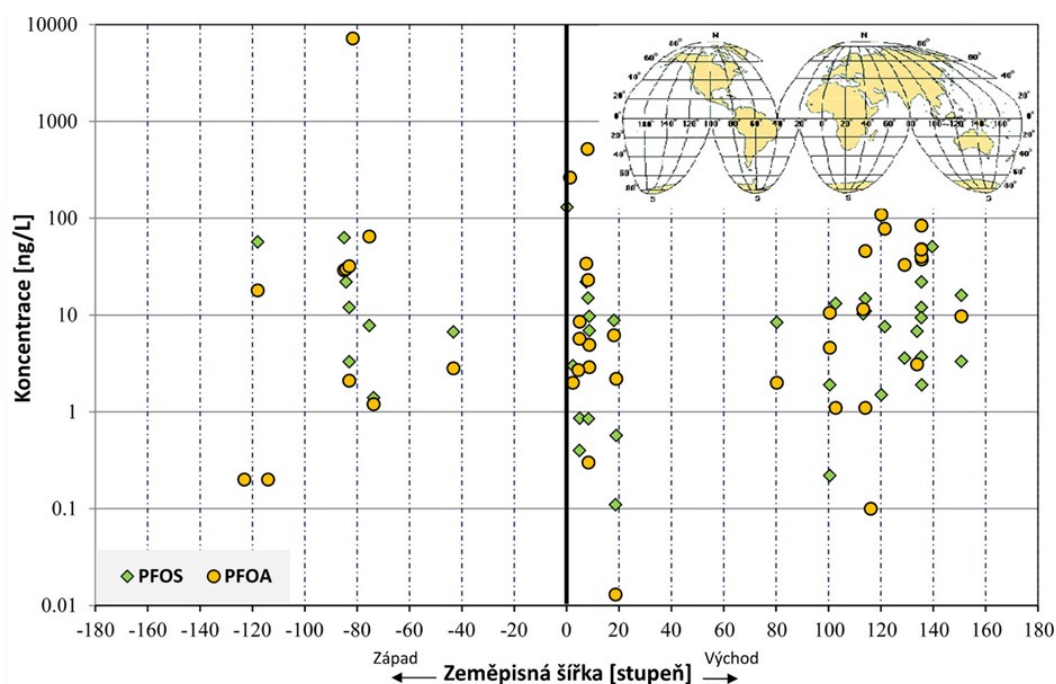
Skupina polutantů obvykle nazývaných per- a polyfluorované organické sloučeniny (per- and polyfluoroalkyl substances; PFAS) čítá v současnosti více než 4700 identifikovaných látek¹. Struktura těchto látek je tvořena perfluorovaným uhlovodíkem vytvářejícím hydrofobní část molekuly a funkční skupinou, která naopak tvoří část hydrofilní. Podle typu funkční skupiny se PFAS dají rozdělit na sulfonáty, karboxyláty, sulfonamidy, fosfonáty, akryláty, acetáty a další minoritní skupiny. Obecně jsou tyto látky v přírodě považovány za vysoce perzistentní. Za vhodných environmentálních podmínek však u některých z nich může dojít k degradaci funkční skupiny, čímž se stanou prekurzory pro tvorbu dceřiných produktů. Ty se často již dále nerozkládají a dochází k jejich kumulaci v životním prostředí. Jako příklad lze uvést degradaci perfluoroktansulfonamidu na perzistentní perfluoroktansulfonát (PFOS)².

2. Toxicita a výskyt

Ze skupiny PFAS je velká pozornost věnována perfluorovaným organickým kyselinám, především pak kyselině perfluoroktanové (PFOA) a PFOS. Vzhledem k jejich širokému používání byly tyto látky v porovnání s ostatními zástupci skupiny detekovány napříč celým životním prostředím v nejvyšších koncentracích. U zmíněných látek je také nejvíce prozkoumán mechanismus toxického účinku. Mnoho studií ukazuje hepatotoxické působení PFOS v játrech, jakožto hlavním orgánem z hlediska akumulace této a odvozených látek. Je prokázáno, že tento polutant způsobuje zvětšení jater, steatózu, hepatocelulární hyperplazii a oxidativní poškození hepatocytů^{3,4}. Tvorba reaktivních forem kyslíku během expozice různými koncentracím PFOS způsobuje pravděpodobně i neurotoxicitu, což bylo pozorováno v některých studiích⁵. Mnoho autorů popisuje u exponovaných jedinců narušení motoriky, schopnosti učení a paměti⁶⁻⁸. Rovněž byl studován potenciál této látky způsobovat zánět nervů⁵. Jedním z dalších prokázaných toxických účinků PFAS je imunotoxicita, kdy i při velmi nízkých dávkách PFOS či PFOA dochází k narušení imunitního systému organismu⁹. V nemalé míře může také PFOS způsobovat změny/poškození samčích i samičích pohlavních orgánů, a narušit tak hormonální sekreci a indukovat teratogenitu¹⁰⁻¹³. Rovněž jsou známy i endokrinně disruptivní účinky těchto látek, kdy za určitých podmínek narušují například thyroideální, estrogenní a androgenní hormonální systém^{14,15}. Mnohé další studie zabývající se toxicitou PFOS a ukazující riziko spojené s těmito látkami jsou uvedeny v přehledové studii⁸.

Kombinace rezistence PFOS a PFOA vůči degradaci, akumulace v životním prostředí a nežádoucích toxických účinků vedla k tomu, že byly obě tyto látky zahrnuty do Stockholmské úmluvy a podléhají restrikcím pro perzistentní organické polutanty¹⁶. V současnosti je také snaha nahrazovat tyto problematické zástupce PFAS jinými sloučeninami, především krátkými fluorovanými karboxylovými kyselinami a perfluorovanými ethery s nižší molekulovou hmotností. U těchto náhrad však není jejich toxicita ani mechanismus účinku doposud dostatečně prozkoumán¹⁷. Vzhledem k velmi podobné struktuře však lze předpokládat, že budou vykazovat i podobné vlastnosti, a proto by i těmto novým polutantům měla být věnována pozornost¹⁸.

Ačkoli jsou toxické účinky PFOS studovány při relativně vysokých dávkách, bioakumulační potenciál PFAS a zároveň i poslední studie¹⁹ demonstrovají riziko spojené s dlouhodobou expozicí člověka těmto látkám i ve velmi nízké koncentraci $< 1 \text{ ng l}^{-1}$. PFOS jsou nacházeny i v moči nebo vlasech dětí předškolního věku²⁰. Existuje mnoho studií z celého světa monitorujících přítomnost PFOS a PFOA v pitné vodě (obr. 1).



Obr. 1. Detekované koncentrace PFOS a PFOA v pitné vodě po celém světě (upraveno dle cit.²¹)

Z obrázku je patrné, že se koncentrace těchto látek v jednotlivých oblastech výrazně liší. V oblasti Ameriky dosahují například zjišťované koncentrace v pitné vodě^{21,22} pro PFOA až 7200 ng l^{-1} a v případě PFOS až 63 ng l^{-1} . V Evropě byly doposud nalezeny nižší hodnoty jak pro PFOA, tak pro PFOS. Kromě PFOS a PFOA byly dále v rámci některých těchto studií sledovány ve vodě i další perfluorované karboxyláty a kratší perfluorované sulfonáty. Například na území Francie byl proveden monitoring pitné vody a množství PFAS (10 látek včetně PFOS a PFOA) dosahovalo koncentrací až 199 ng l^{-1} pro surovou a 156 ng l^{-1} pro upravenou vodu²³. Autoři další studie provedli obdobný monitoring na území Německa a Španělska²⁴, kdy koncentrace PFAS (12 látek včetně PFOS a PFOA) v pitné vodě dosahovaly sumárních maximálních hodnot $21,7$, resp. $502,7 \text{ ng l}^{-1}$. Další studie rovněž popisuje úroveň kontaminace pitné vody na území Německa²⁵, kde autoři detekovali maximální koncentrace PFAS dosahující 598 ng l^{-1} . Výjimkou nejsou ani data získaná ve Francii²⁶. I výsledky dalších studií zabývajících se pitnou vodou v dalších zemích světa potvrzují rozsáhlou kontaminaci a nefunkčnost či nedostatečnou účinnost většiny standardních technologií používaných při úpravě pitné vody²¹. Komplexní studie na území ČR zatím chybí, nicméně z předběžného šetření autorů tohoto projektu na několika úpravách vody vyplývá, že koncentrace v pitné vodě v ČR dosahují hodnot do 30 ng l^{-1} v sumě 10 zástupců PFAS (PFOS 5 ng l^{-1})²⁷.

3. Limity pro PFAS v pitné vodě

S narůstajícími informacemi o PFAS, především o mechanismu jejich toxicity a rezistenci vůči degradaci, dochází k celosvětovému zavádění a zpřísnování limitů. Zákonný limit však v EU pro pitnou vodu donedávna stanoven nebyl. Rovněž v současnosti platná vyhláška č. 252/2004 Sb. ošetřující mimo jiné i požadavky na kvalitu pitné vody na území ČR tuto problematiku neřeší.

Nová Směrnice²⁸ Evropského parlamentu a Rady EU 2020/2184 již hovoří o parametru „PFAS celkové“ s limitem 500 ng l^{-1} a „sumě PFAS“ s limitem 100 ng l^{-1} . „Sumou PFAS“ se rozumí suma per- a polyfluorovaných alkylových sloučenin (především karboxylových kyselin) považovaných za znepokojivé, pokud jde o vodu určenou k lidské spotřebě. Jedná se o dílčí skupinu látek zahrnutých do „PFAS celkové“, které obsahují perfluoralkylovou skupinu se třemi a více uhlíky (tedy C_nF_{2n-} ; $n \geq 3$) nebo perfluoralkyletherovou skupinu se dvěma a více uhlíky (tedy $\text{C}_n\text{F}_{2n}\text{OC}_m\text{F}_{2m-}$; n a $m \geq 1$), především pak perfluoralkoxylové kyseliny.

4. Odstranění PFAS při úpravě vody

Souhrnná studie²¹ hodnotící efektivitu eliminace PFOS a dalších PFAS ve vodě na více než 30 úpravách pitné vody ukazuje, že konvenční postupy a technologie nejsou pro odstraňování těchto polutantů účinné. Nízké koncentrace a vysoká hydrofilita komplikují jejich efektivní odstranění koagulací/flokulací či sedimentací²⁹. Nedáv-

né studie³⁰ prováděné v malém měřítku uvádějí účinnost odstranění PFAS pomocí těchto technologií maximálně do výše 35 %. Navíc vysoká elektronegativita atomů fluoru v molekulách těchto látek způsobuje jejich rezistenci vůči oxidaci, a tedy i oxidačním procesům běžně používaným při úpravě vody³¹. Ozonizace, chlorace i chloraminace se ukázaly v procesu eliminace PFAS jako velmi neefektivní²¹. Navíc lze oxidačními procesy v surové vodě docílit degradace některých perfluorovaných prekurzorů na PFOS a PFOA, které jsou pak následně detekovány ve výsledném produktu, tedy pitné vodě. Jako potenciálně neefektivnější technologie se pro odstraňování PFAS jeví ultrafiltrace přes vysokotlaké membrány, iontová výměna a sorpce na porézních materiálech. Nanofiltrace, mikrofiltrace a reverzní osmóza či jejich kombinace ukazují v laboratorních podmínkách při tomto procesu vysokou účinnost. Avšak v rámci prováděných testů nebyla brána v úvahu přítomnost přirozených organických látek, tedy rozpuštěného organického uhlíku (dissolved organic carbon, DOC), běžně se vyskytujícího v surové vodě, který má na funkci těchto membrán zásadní vliv^{32–34}. Jelikož se většina PFAS vyskytuje v životním prostředí ve formě aniontů, jeví se jako slibná technologie pro reálné použití separace těchto látek pomocí ionexů. Laboratorní studie zabývající se testováním technologie iontové výměny pro odstraňování PFAS v průběhu úpravy vody ukazují její vysoký potenciál^{35–37}. Přítomnost dalších aniontů ve vodě však může výrazně negativně ovlivnit účinnost ionexů v reálném provozu, stejně jako přítomnost DOC.

Elektrochemické, sonochemické, plasmové nebo pokročilé oxidační technologie^{38,39} zatím nepřekročily rámec laboratorního výzkumu.

Poslední z vodárenských technologií, která má potenciál pro odstraňování PFAS z vody, je sorpce. Na úpravách pitné vody se nejběžněji používá adsorpce na aktivním uhlí. Tento typ sorbentu vykazuje v reálných podmínkách poměrně vysokou účinnost při odstraňování PFAS s větší molekulovou hmotností. Pro PFAS s kratšími řetězci je však tato technologie účinná jen velmi málo a po omezenou dobu⁴⁰. Míra sorpce s časem velmi rychle klesá a následně je nutná častá regenerace sorbentu^{41,42}. A stejně jako v případě iontové výměny je i adsorpce velmi negativně ovlivněna přítomností rozpuštěné organické hmoty, tedy přítomností DOC (cit.⁴³). Technologie adsorpce na aktivním uhlí může tedy sice do jisté míry obsah určitých PFAS snížit, avšak je nutné vzít v úvahu možnou častou regeneraci granulovaného aktivního uhlí nebo vysokých dávek práškového aktivního uhlí, a to jak v závislosti na koncentraci polutantu, tak na hodnotě DOC.

5. Závěr

Per- a polyfluorované organické látky jsou dnes prakticky všudypřítomné v životním prostředí. Jednou z cest jejich přísunu do lidského těla je pitná voda.

Z celosvětových studií je patrné, že účinnost současných technologií úpravy vody pro odstraňování PFAS je nízká. Je tedy nutný vývoj nových technologií či vhodných

sorpčních materiálů, které umožní odstraňování PFAS spolu s jinými mikropolutanty a zbytkovými organickými látkami a pomohou eliminovat rizika spojená s expozicí člověka těmto látkám v pitné vodě.

Autoři děkují za finanční podporu pro svoji práci projektu TAČR TJ04000212.

LITERATURA

1. Lim, X.: *Nature* 566, 26 (2019).
2. Buck R. C., Franklin J., Berger U., Conder J. M., Cousins I. T., de Voogt P., Jensen A. A., Kannan K., Mabury S. A., van Leeuwen S. P.: *Integr. Environ. Assess. Manage.* 7, 513 (2011).
3. Du Y., Shi X., Liu C., Yu K., Zhou B.: *Chemosphere* 74, 723 (2009).
4. Tse W. K. F., Li J. W., Tse A. C. K., Chan T. F., Hin Ho J. C. H., Wu R. S. S., Wong C. K. C., Lai K. P.: *Chemosphere* 159, 166 (2016).
5. Chen X., Nie X., Mao J., Zhang Y., Yin K., Jiang S.: *Neurotoxicology* 66, 32 (2018).
6. Onishchenko N., Fischer C., Wan Ibrahim W. N., Negri S., Spulber S., Cottica D., Ceccatelli S.: *Neurotoxicity Res.* 19, 452 (2011).
7. Johansson N., Fredriksson A., Eriksson P.: *Neurotoxicology* 29, 160 (2008).
8. Zeng Z., Song B., Xiao R., Zeng G., Gong J., Chen M., Xu P., Zhang P., Shen M., Yi H.: *Environ. Int.* 126, 598 (2019).
9. DeWitt J. C., Blossom S. J., Schaidler L. A.: *J. Exp. Sci. Environ. Epidem.* 29, 148 (2019).
10. Chen J., Das S. R., Du J. L., Corvi M. M., Bai C., Chen Y., Liu X., Zhu G., Tanguay R. L., Dong Q., Huang C.: *Environ. Toxicol. Chem.* 32, 201 (2013).
11. Yang Q., Wang W., Liu C., Wang Y., Sun K.: *Reproductive Toxicol.* 63, 142 (2016).
12. Qu J. H., Lu C. C., Xu C., Chen G., Qiu L. L., Jiang J. K., Ben S., Wang Y. B., Gu A. H., Wang X. R.: *Environ. Toxicol. Pharmacol.* 45, 150 (2016).
13. Lou Q. Q., Zhang Y. F., Zhou Z., Shi Y. L., Ge Y. N., Ren D. K., Xu H. M., Zhao Y. X., Wei W. J., Qin Z. F.: *Ecotoxicology* 22, 1133 (2013).
14. Lewis R. C., Johns L. E., Meeker J. D.: *Int. J. Environ. Res. Public Health* 12, 6098 (2015).
15. Gao Y., Li X. X., Guo L. H.: *Environ. Sci. Technol.* 47, 634 (2013).
16. Ahrens L.: *J. Environ. Monitor.* 13, 20 (2011).
17. Wang Y., Chang W. G., Wang L., Zhang Y. F., Zhang Y., Wang M., Wang Y., Li P.: *Ecotoxicol. Environ. Saf.* 182, 109402 (2019).
18. Gomis M. I., Vestergren R., Borg D., Cousins I. T.: *Environ. Int.* 113, 1 (2018).
19. Grandjean P.: *Environ. Health* 17, 62 (2018).
20. Na L., Guang-Guo Y., Huachang H., Wen-Jing D.: *Environ. Pollut.* 270, 116219 (2021).
21. Rahman M. F., Peldszus S., Anderson W. B.: *Water Res.* 50, 318 (2014).
22. Emmett E. A., Shofer F. S., Zhang H., Freeman D.,

- Desai C., Shaw L. M.: *J. Occup. Environ. Med.* **48**, 759 (2006).
23. Boiteux V., Dauchy X., Rosin C., Munoz J. F.: *Arch. Environ. Contam. Toxicol.* **63**, 1 (2012).
24. Llorca M., Farre M., Pico Y., Muller J., Knepper T. P., Barcelo D.: *Sci. Total Environ.* **431**, 139 (2012).
25. Skutlarek D., Exner M., Farber H.: *Environ. Sci. Pollut. Res.* **13**, 299 (2006).
26. Fillol C., Oleko A., Saoudi A., Zeghnoun A., Balicco A., Gane J., Rambaud L., Leblanc A., Gaudreau E., Marchan P., Le Bizec B., Bouchart V., Le Gleau F., Durand G., Denys S.: *Environ. Int.* **147**, 106340 (2021).
27. Předběžné výsledky projektu TAČR TJ04000212.
28. EU: Směrnice Evropského parlamentu a Rady EU 2020/2184 ze dne 16. prosince 2020 o jakosti vody určené k lidské spotřebě, platná od 2021.
29. Shivakoti B. R., Fujii S., Nozoe M., Tanaka S., Kunacheva C.: *Water Supply* **10**, 87 (2010).
30. Xiao F., Simcik M. F., Gulliver J. S.: *Water Res.* **47**, 49 (2013).
31. Szajdzinska-Pietek E., Gebicki J. L.: *Res. Chem. Intermed.* **26**, 897 (2000).
32. Thompson J., Eaglesham G., Reungoat J., Poussade Y., Bartkow M., Lawrence M., Mueller J. F.: *Chemosphere* **82**, 9 (2011).
33. Lipp P., Sacher F., Baldauf G.: *Desalin. Water Treat.* **13**, 226 (2010).
34. Appleman T. D., Dickenson E. R. V., Bellona C., Higgins C. P.: *J. Hazard. Mater.* **260**, 740 (2013).
35. Deng S. B., Yu Q. A., Huang J., Yu G.: *Water Res.* **44**, 5188 (2010).
36. Dixit F., Barbeau B., Mostafavi S. G., Mohseni M.: *Environ. Sci.: Water Res. Technol.* **5**, 1782 (2019).
37. Zaggia A., Conte L., Falletti L., Fant M., Chiorboli A.: *Water Res.* **91**, 137 (2016).
38. Wanninayake D. M.: *J. Environ. Manage.* **283**, 111977 (2021).
39. Seema S., Shang-Lien L., Vimal C. S., Qicheng Q., Pinki S. J.: *Taiwan Inst. Chem. Eng.* **000**, 110 (2021), v tisku. Dostupné na Science Direct.
40. Eschauzier C., Beerendonk E., Scholte-Veenendaal P., De Voogt P.: *Environ. Sci. Technol.* **46**, 1708 (2012).
41. Takagi S., Adachi F., Miyano K., Koizumi Y., Tanaka H., Watanabe I., Shisuke T., Kurunthachalam K.: *Water Res.* **45**, 3925 (2011).
42. Holzer J., Goen T., Rauchfuss K., Kraft M., Angerer J., Kleeschulte P., Wilhelm M.: *Int. J. Hyg. Environ. Health* **212**, 499 (2009).
43. Yu J., Lv L., Lan P., Zhang S. J., Pan B. C., Zhang W. M.: *J. Hazard. Mater.* **225**, 99 (2012).

J. Drechsler^a, J. Semerád^b, K. Fialová^c, M. Prokopová^c, T. Cajtham^b, M. Pivokonský^c, and V. Janda^a
 (^aDepartment of Water Technology and Environmental Engineering, University of Chemistry and Technology, Prague, ^bInstitute of Microbiology, Czech Academy of Sciences, Prague, ^cInstitute of Hydrodynamic, Czech Academy of Sciences, Prague): **Occurrence and Removal of Per- and Polyfluorinated Organic Substances during Drinking Water Treatment**

A group of pollutants denoted to as per- and polyfluoroalkyl substances (PFAS) currently comprises more than 4,700 identified substances. Their structure consists of a per- or polyfluorinated hydrocarbon chain forming the hydrophobic part of the molecule and a functional group which in turn forms a hydrophilic part. Depending on the type of functional group, PFAS can be divided into sulfonates, carboxylates, sulfonamides, phosphonates, acrylates, acetates and other minor groups. These substances are nowadays ubiquitous in the environment. In general, they are considered as highly persistent in nature. However, under suitable environmental conditions, some of them may degrade due to the presence of highly polar functional groups. The intermediates or final products of the degradation first step are less or non-polar. These are not readily (bio)degradable and can accumulate in the environment. Current technologies are not able to remove per- and polyfluorinated compounds from drinking water efficiently. It is therefore necessary to develop new technologies or efficient sorption materials that will enable the removal of both per- and polyfluorinated compounds, micropollutants and residual organic substances and thus to eliminate or at least to decrease the risk associated with human exposure to these substances in drinking water.

Keywords: drinking water, perfluorinated organic compounds, polyfluorinated organic compounds

Acknowledgements

The authors gratefully acknowledge the Technology Agency of the Czech Republic (project No. TJ04000212).

Coagulation/flocculation of per- and polyfluoroalkyl substances (PFAS) in drinking water treatment

Michaela Prokopova^{1,2}, Katerina Fialova^{1,2}, Lenka Cermakova¹, Jaroslav Semerad^{2,3}, Martin Pivokonsky¹

¹Institute of Hydrodynamics of the Czech Academy of Sciences, Pod Patankou 30/5, 166 12 Prague 6, Czech Republic,

²Institute for Environmental Studies, Faculty of Science, Charles University, Benatska 2, 128 01 Prague 2, Czech Republic,

³Institute of Microbiology, Czech Academy of Sciences, Videnska 1083, CZ-142 20, Prague 4, Czech Republic

KEY WORDS

perfluorinated organic substances, polyfluorinated organic substances, coagulation, flocculation, drinking water

INTRODUCTION

A group of pollutants denoted as per- and polyfluoroalkyl substances (PFAS), that were detected in both surface and groundwater, currently comprises more than 4,700 identified compounds (Lim, 2019). Their structure consists of a per- or polyfluorinated hydrocarbon chain forming the hydrophobic part of the molecule and a functional group that forms a hydrophilic part. Depending on the type of a functional group, PFAS can be divided into sulfonates, carboxylates, sulfonamides, phosphonates, acrylates, acetates and other minor groups. These substances are nowadays ubiquitous in the environment. In general, they are considered highly persistent in nature. However, under suitable environmental conditions, some of them may degrade due to the presence of highly polar functional groups. The intermediates or final products of the first degradation step are less or non-polar. These are not readily (bio) degradable and can accumulate in the environment. Current technologies are not able to remove PFAS from drinking water efficiently (Rahman et al., 2014). This work investigates coagulation/flocculation of selected PFAS (perfluorooctanoic acid – PFOA, perfluorooctane sulfonate – PFOS, pentafluorobenzoic acid – PFBA, perfluorobutane sulfonate – PFBS) with an aim to optimize the process for maximum PFAS removal and to describe the coagulation mechanisms.

METHODOLOGY/PROCESS

To investigate the coagulation behaviour of PFAS, laboratory jar tests were performed using a variable speed paddle stirrer (LMK 8-03, IH CAS, Czech Republic) and 2 L jars. Demineralized water (with alkalinity adjusted to 1.0 mmol L⁻¹ by 0,125 M NaHCO₃) and natural raw water (6.8 mg L⁻¹ of dissolved organic carbon (DOC); alkalinity of 0.7 mmol L⁻¹) were used for the jar tests. Experiments with demineralized water were conducted so as to understand the coagulation mechanisms during PFAS removal. Natural raw water was then used as a background to describe the coagulation of PFAS during the real drinking water treatment process. An individual PFAS was added to the water (100 µg L⁻¹ of PFOA, PFOS, PFBA or PFBS) and jar tests were performed using coagulant doses of 20, 40, and 60 mg L⁻¹ as anhydrous ferric sulphate or aluminium sulphate at the coagulation pH range of 4.5–7.5. The mixing step included 1 min at $G = 186 \text{ s}^{-1}$ and 60 min at $G = 47 \text{ s}^{-1}$. The residual concentration of PFAS, Al/Fe, and DOC (if applicable) were then measured after the separation of aggregates via centrifugation (at 3000 rpm for 20 min) by LC-MS/MS (Shimadzu Nexera 2 LC, Japan; Sciex 4500 MS, USA), ICP-OES (5110 Series, Agilent Technologies, USA), and a TOC-VCPH analyser (Shimadzu, Japan), respectively. The coagulation/flocculation of PFAS was then investigated also at larger scale at pilot plant with a continuous flow and a two-stage suspension (aggregate) separation (sedimentation and filtration). Natural raw water already comprising PFAS (namely PFOA and PFOS) was treated at the pilot plant. The coagulation conditions applied at the plant were based on the preceding laboratory jar test results. The mixing step included homogenization mixing for a few seconds at $G = 300 \text{ s}^{-1}$, and flocculation mixing for 5 min at $G = 200 \text{ s}^{-1}$ and subsequently 15 min at $G = 20 \text{ s}^{-1}$. These conditions simulate mixing in the drinking water treatment plant where the pilot plant is located. The sedimentation time was 45 min.

RESULTS/OUTCOMES

The results of the coagulation of PFAS in demineralized water showed that the coagulant dose or the pH value did not have a significant effect on their removal. The removal efficiency of individual PFAS did not exceed 9% for aluminium sulphate, resp. 12% for ferric sulphate. In the raw water matrix (Figure 1), the highest removal efficiency of individual PFAS and Al by aluminium sulphate was

achieved at pH 6.5 to 7.5, while the removal efficiency of DOC was the highest at pH 5.5. In the case of ferric sulphate, the highest efficiency of individual PFAS, Fe, and DOC was achieved at a pH of 5.0. Apparently, the removal efficiency of PFAS did not depend on their interaction with natural organic matter but rather on the appropriate aggregation conditions of the coagulant agent. During the pilot plant tests, the resulting quality parameters of treated water (PFOA, PFOS, DOC, Al/Fe) were monitored at the outlet of the mixing tank (1), at the lamellar settling tank (2), and at the outlet of the gravity filter (3). The PFAS removal efficiency in individual technological steps 1 to 3 was 6%, 12%, and 15% for PFOA and 17%, 23%, and 25% for PFOS by aluminium sulphate, respectively, and 7%, 12%, and 14% for PFOA and 18%, 33%, and 36% for PFOS by ferric sulphate.

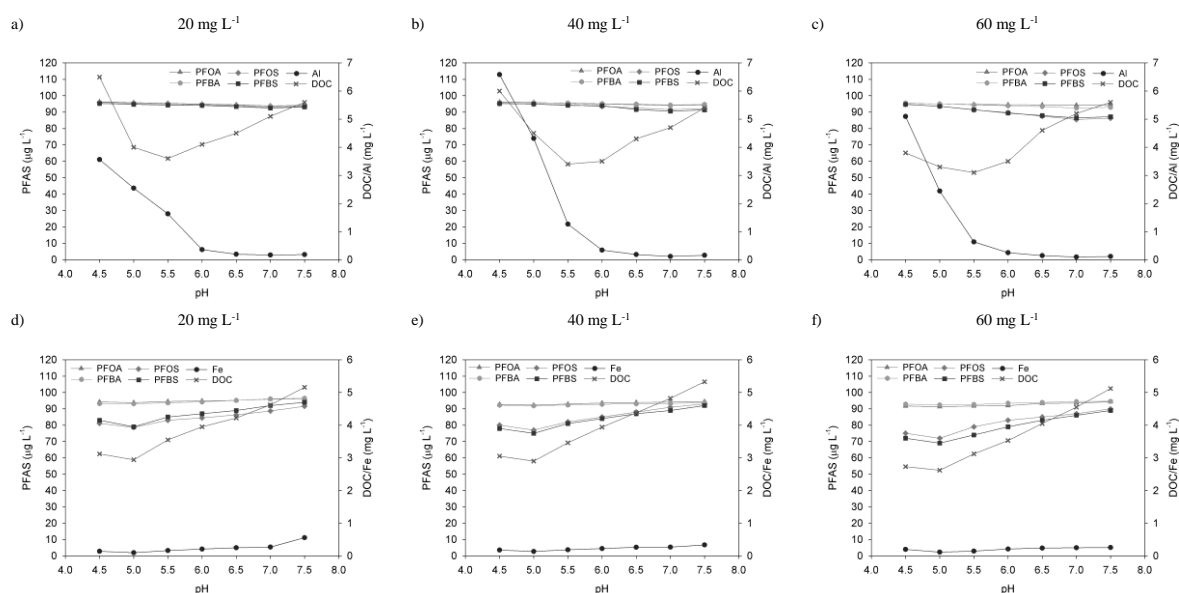


Figure 1: The residual concentrations of selected PFAS, DOC and Al/Fe at a dose of 20–60 mg L^{-1} for $\text{Al}_2(\text{SO}_4)_3$ (a–c), resp. $\text{Fe}_2(\text{SO}_4)_3$ (d–f). The initial concentration of DOC: 6.4 mg L^{-1} and PFAS: 100 $\mu\text{g L}^{-1}$.

DISCUSSION AND CONCLUSION

The results of PFAS coagulation showed that despite the investigated PFAS did not actively participate in the coagulation mechanisms they were partially removed during the suspension formation and separation by sedimentation and sand filtration with the removal efficiency of up to 15% for PFOA and up to 36% for PFOS. Thus, the removal mechanism of PFAS is anticipated to be the adsorption on aggregates comprising the coagulants and other impurities. The removal efficiency of individual PFAS is given by the nature of selected compounds – molecular weight and hydrophilicity/hydrophobicity (Pramanik et al., 2015), and the nature of the coagulating agent. During coagulation by ferric sulphate, larger and more compact aggregates are produced as compared to aluminium sulphate. These ferric aggregates have a larger surface area and weight and therefore facilitate the removal of PFAS during sedimentation and sand filtration (Jarvis et al., 2012). If coagulation/flocculation is operated under optimal conditions, it is likely that the highest possible removal efficiency of PFAS will be achieved.

REFERENCES

- Jarvis, P., Sharp, E., Pidou, M., Molinder, R., Parsons, S.A., Jefferson, B. (2012). Comparison of coagulation performance and floc properties using a novel zirconium coagulant against traditional ferric and alum coagulants. *Water Research* 46, 4179–4187.
- Lim, X. (2019). The fluorine detectives. *Nature* 566(7742), 26–29.
- Pramanik, B., Kumar Pramanik, S., Suja, F. (2015). A comparative study of coagulation, granular and powdered activated carbon for the removal of perfluorooctane sulfonate and perfluorooctanoate in drinking water treatment. *Environmental technology* 36, 1–25.
- Rahman, M. F., Peldszus, S., Anderson, W. B. (2014). Behaviour and fate of perfluoroalkyl and polyfluoroalkyl substances (PFASs) in drinking water treatment: A review. *Water Research* 50, 318–340.



Continuous long-term monitoring of leaching from microplastics into ambient water – A multi-endpoint approach

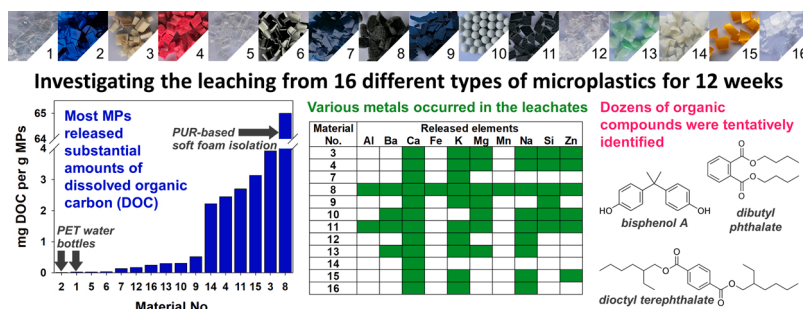
Katerina Novotna, Lenka Pivokonska, Lenka Cermakova, Michaela Prokopova, Katerina Fialova, Martin Pivokonsky*

Institute of Hydrodynamics of the Czech Academy of Sciences, Pod Patankou 30/5, 166 12 Prague 6, Czech Republic

HIGHLIGHTS

- Majority of the 16 studied types of microplastics exhibited significant DOC leaching.
- Some leachates also comprised DIC, metals (Al, Ba, Ca, Fe, K, Mg, Mn, Na, Zn), or Si.
- Amounts of leached elements depended on the duration of contact of MPs with water.
- Eighty different organic compounds were tentatively identified in the leachates.
- The leached compounds included some harmful to human health.

GRAPHICAL ABSTRACT



ARTICLE INFO

Editor: <R Teresa>

Keywords:

Additives
Dissolved inorganic carbon (DIC)
Dissolved organic carbon (DOC)
Metals
Plastics

ABSTRACT

Widespread pollution of aquatic environments by microplastics (MPs) is a serious environmental threat. Despite the knowledge of their occurrence and properties rapidly evolving, the potential leaching from MPs remains largely unexplored. In this study, 16 different types of MPs prepared from consumer products were kept in long-term contact with water, while the leachates were continuously analysed. Most of the MPs released significant amounts of dissolved organic carbon, up to approximately 65 mg per g MPs after 12 weeks of leaching, and some MPs also released dissolved inorganic carbon. Other elements identified in the leachates were Al, Ba, Ca, Fe, K, Mg, Mn, Na, Si, and Zn. Of those, Ca, K, and Na were detected most frequently, while Ca reached the highest amounts (up to almost 2.5 mg per g MPs). Additionally, 80 organic individuals were tentatively identified in the leachates, mostly esters, alcohols, and carboxylic acids. Some compounds considered harmful to human health and/or the environment were detected, e.g., bisphenol A or phthalate esters. The current results provide insight into the transfer of various compounds from MPs to ambient water, which might have consequences on the fluxes of carbon and metals, as well as of specific organic contaminants.

1. Introduction

Plastic pollution is among the most serious threats that the aquatic

environment faces. Currently, great attention is given to microplastics (MPs) – plastic debris sized less than 5 mm. Their occurrence has been revealed worldwide in oceans and seas (Andrady, 2011), rivers, lakes,

* Correspondence to: Pod Patankou 30/5, 166 12 Prague 6, Czech Republic.
E-mail address: pivo@ih.cas.cz (M. Pivokonsky).

dams (Eerkes-Medrano et al., 2015; Lu et al., 2021; Wang et al., 2022), and even in treated drinking water (Novotna et al., 2019). MPs were found not only in water bodies in proximity to industrial or densely populated areas but also in very remote locations (Andrady, 2011; Eerkes-Medrano et al., 2015; Wang et al., 2022). The reported amounts of MPs vary greatly, from a few items per m³ to several thousand MPs per litre, presumably owing to differences in MP spatial distribution as well as variations between sampling, sample processing, and analytical methods applied during MP quantification. MPs detected in water span a wide size range and have been reported to comprise various synthetic polymers, but MPs composed of polypropylene (PP), polyethylene (PE), and polyethylene terephthalate (PET) occur most often (Novotna et al., 2019; Lu et al., 2021; Wang et al., 2022). Although the omnipresence of MPs raises significant environmental concerns, their input to the environment is an ongoing issue, as it is inevitably connected to the extensive utilisation of plastic materials by human society. The global production of plastics has a long-term increasing trend, reaching 367 million tonnes in 2020 (Plastics Europe, 2021).

Most plastic materials are not meant to breakdown easily, and MPs are therefore considered persistent pollutants (Hahladakis et al., 2018). However, plastics do not always remain unaltered when exposed to the action of various physical, chemical, or biological factors, either during their utilisation or when discarded at landfills or inappropriately in the environment (Andrady, 2011; Eerkes-Medrano et al., 2015). Plastics can undergo macroscopic changes, such as surface cracking, embrittlement and fragmentation, or, at the molecular level, chain scission and depolymerization, chain stripping, etc. (Gewert et al., 2015; Hahladakis et al., 2018). These processes may result in the production of secondary MPs from larger plastic items (Andrady, 2011) or in changes in the properties of already existing MPs. For example, MPs exposed to solar irradiation exhibited changes in colour, surface morphology, or carbonyl content (Zhu et al., 2020).

While many studies have been devoted to the quantification of MPs in aquatic environments and their characterisation in terms of size, shape, polymer type, etc. (Novotna et al., 2019; Lu et al., 2021; Wang et al., 2022), the potential transformations and leaching from MPs when they are in contact with water have been less investigated. However, it has been shown that plastics might release some organic additives, including endocrine disrupting compounds such as bisphenol A (Shi et al., 2021) or toxic metals such as Pb or Sb (Capolupo et al., 2020). Additives such as plasticisers, stabilisers, slip agents, fillers, reinforcements, or flame retardants might comprise a significant proportion (10–70%) of a plastic material in terms of its weight (Hahladakis et al., 2018). In most cases, additives are not chemically bound to the plastic polymer and therefore might potentially migrate to a medium in contact with the material (Gewert et al., 2015; Hahladakis et al., 2018; Bridson et al., 2021). The results of some studies suggest that leachates from plastics might exhibit adverse effects on algae or aquatic animals (Bejgarn et al., 2015; Capolupo et al., 2020). The potential leaching of harmful compounds from MPs is therefore one of the potential threats for living organisms arising from the presence of MPs in the environment (Hahladakis et al., 2018). Additionally, MPs were proposed as a significant source of dissolved organic carbon (DOC) to the aquatic environment (Romera-Castillo et al., 2018, 2022a). However, knowledge of its leaching from MPs still needs to be broadened. The scarce studies typically cover only a few plastic materials (Lee et al., 2020a; b; Lee and Hur, 2020; Zhu et al., 2020) and/or monitor leaching for a limited time, typically on the order of several days (Ateia et al., 2020; Romera-Castillo et al., 2022a; b). Moreover, the current studies mentioning DOC release mostly do not focus on other endpoints, while leaching of multiple compounds from MPs is highly possible owing to the complex composition of plastic materials (Hahladakis et al., 2018).

In this study, aqueous leachates of MPs derived from 16 various consumer products were continuously analysed for 12 weeks. The investigated materials involved different polymers, including but not limited to those most commonly identified as MPs in the environment, i.

e., PP, PE, and PET. The specific objectives were (i) to determine the amounts of leached DOC from MPs composed of the different materials depending on the leaching time; (ii) to identify and quantify other elements potentially leaching from the MPs; and (iii) to identify specific compounds leached from MPs into ambient water. To the best of our knowledge, this is the first study that continuously investigated long-term leaching from such a wide range of real MPs with a focus on various target analytes.

2. Material and methods

2.1. Source and preparation of microplastics

Plastic products intended for MP preparation were purchased in common retail stores. Selection of the products was aimed to cover different polymers and various appearances (hardness, colour, etc.) of materials, while their composition was determined via μ -Raman spectroscopy (see Section 2.4 for methodological details). To prepare the MPs, homogenous parts of the products in terms of structure and colour were selected, and these were gently cleaned with ultrapure water (Ateia et al., 2020; Cao et al., 2022) and air-dried under clean-lab conditions (negative-pressure air conditioning system and HEPA air filters class H 13; KS BESTFIL, KS Klima-Service, Czech Republic). Then, they were cut into pieces corresponding to the size of MPs (< 5 mm), i.e., the size of the prepared MPs was approximately 3–4 mm at their largest dimension. In total, 16 different types of MPs were utilised in the experiments, and they are denoted Material Nos. 1–16 throughout the manuscript for simplicity. Their polymer composition and products of origin are listed in Table 1; additional details are provided in Table S1, Supplementary material (SM).

2.2. Setup of leaching experiments and sample collection

The prepared MPs were leached in ultrapure water for 12 weeks in total. Specifically, 4 g of MPs comprised of a single material was put into a laboratory glass bottle with a screw cap, and 200 mL of ultrapure water was added. Parallel samples with the same material were prepared to provide replicates for subsequent carbon, metal, and additive measurements. Samples were prevented from potential microbial growth by the addition of sodium azide (Cao et al., 2022); the arising concentration of Na was subtracted from the leaching results where required. The leaching experiments were performed in a laboratory at room temperature of 22 °C and natural ambient light-dark conditions, while the samples were continuously mixed at 130 rpm using a magnetic stirrer.

Table 1
A list of investigated MPs – their products of origin and identified polymers.

Material No.	Product of origin	Polymer	
1	Water bottle (transparent)	PET	polyethylene terephthalate
2	Water bottle (coloured)	PET	polyethylene terephthalate
3	Floor covering	PVC	polyvinyl chloride
4	Exercise mat	NBR	nitrile butadiene rubber (acrylonitrile and butadiene copolymer)
5	Construction board	PC	polycarbonate
6	Water hose	PE	polyethylene
7	Shopping bag	PE	polyethylene
8	Soft foam isolation	PUR	polyurethane
9	T-shirt	PET	polyethylene terephthalate
10	Airsoft balls	PS	polystyrene
11	Kitchen table mat	PVC	polyvinyl chloride
12	Bubble packing foil	PE	polyethylene
13	Box filler	PS	polystyrene
14	Isolation foam	PUR	polyurethane
15	Inflatable ball	PVC	polyvinyl chloride
16	Clothes packaging	PP	polypropylene

Blank samples (ultrapure water only or with sodium azide) were also prepared and analysed together with the MP samples.

The first sampling of the leachates for C and metal measurements was conducted immediately after MPs had been mixed with water (Day 0) and then at Days 1, 2, 3, 7, and weekly since then. Samples for the analysis of additives were collected at the end of the investigated period, i.e., after 12 weeks of leaching. Prior to any above mentioned analysis, the leachates were filtered through 0.45 μm membrane filters (Millipore, USA). Additionally, the initial and final pH values of the samples were also measured (Table S2, SM).

2.3. Carbon and metal measurements

DOC and dissolved inorganic carbon (DIC) were measured using a total organic carbon analyser (TOC-L, Shimadzu, Japan); a differential method was applied for DOC determination. Potassium hydrogen phthalate, sodium bicarbonate, and sodium carbonate (Sigma-Aldrich, USA) were used as calibration and control standards; controls were measured daily. Selected metals (Al, Ba, Ca, Fe, K, Mg, Mn, Na, Zn) and one metalloid (Si) were measured by inductively coupled plasma-optical emission spectrometry (ICP-OES, 5110 Series, Agilent Technologies, USA). The selection of the elements to be quantitatively analysed was based on preliminary leachate screening in scanning mode. A mixed metal standard and Si standard (AstaSol, Analytika, Czech Republic) were then used for calibration and controls. The blank samples without MPs always exhibited values below the method detection limits (i.e., 0.18 mg L^{-1} for DOC, 0.20 mg L^{-1} for DIC, 0.01 mg L^{-1} or lower for metals, 0.04 mg L^{-1} for Si). The results for samples with MPs are presented normalised to the weight of the MPs. The error bars depicted in the figures represent standard deviations for replicate samples.

2.4. μ -Raman spectroscopy

μ -Raman spectroscopy was used to determine the composition of the materials (MPs) utilised for the leaching experiments and, if feasible, for analysing the leachates (preceded with the leachates preconcentration via a rotary evaporator (Hei-VAP Expert, Heidolph Instruments, Germany) and subsequent evaporation of the leachates using a laboratory drying oven (ECO line, Ecocell, MMM Medcenter, Germany)). A DXR2xi μ -Raman imaging microscope system (Thermo Fisher Scientific, USA) was utilised (532 nm or 785 nm laser, laser spot size of approximately 0.5 μm , Raman shift of 50–3550 cm^{-1} , spectral resolution of 5 cm^{-1}). Collected spectra were processed by Omnic 9 software; the compound determination was based on comparing the observed spectra to libraries (FDM Raman Organics/Inorganics, HR Aldrich Raman/Raman Inorganics, Organics by Raman, RRUFF Raman Minerals, STJ Raman Polymers and Additives/Dyes and Pigments/Coatings); the match factor threshold was 0.80 or higher.

2.5. Leachate analysis by GC-MS

Gas chromatography-mass spectrometry (GC-MS) was employed for tentative identification of compounds in the 12-week leachates, preceded by solid-phase extraction (SpeExtra HLB Enviro SPE column, 60 μm , 200 $\text{mg}/3\text{ mL}$, Chromservis, Czech Republic; 100 μL initial sample volume, elution to 3 mL acetone). Tribenzylamine (1 μg) was added as an internal standard. The GC-MS analysis was then conducted using a 7000A GC/MS Triple Quad System (Agilent Technologies, USA) in electron ionisation (EI; 75 eV) mode. Capillary column DB-5MS (30 $\text{m} \times 0.25\text{ mm} \times 0.25\text{ }\mu\text{m}$; J&W, Agilent Technologies, USA) was utilised; helium served as a carrier gas at a flow rate of 1 mL min^{-1} ; samples were injected in splitless mode at 280 $^{\circ}\text{C}$; the injection volume was 2 μL ; the applied temperature programme was 50 $^{\circ}\text{C}$ for 1 min, followed by ramp to 310 $^{\circ}\text{C}$ (10 $^{\circ}\text{C min}^{-1}$), and 3 min isothermal. Scan mode was applied to identify unknown compounds based on their mass spectra. The obtained spectra were compared to the NIST/EPA/NIH Mass Spectral

Library with the help of the NIST Mass Spectral Search Programme. Semiquantitative evaluation was conducted based on the comparison of peak areas to that of the internal standard.

3. Results and discussion

3.1. Leaching of DOC

DOC release was observed from all the investigated MPs. However, while some of the materials exhibited only negligible DOC leaching under the applied conditions, certain MPs released substantial amounts of DOC (Fig. 1). The highest leaching was observed for material 8 (PUR-based soft foam isolation; Fig. 1a), i.e., approximately 65 mg DOC per g MPs after 12 weeks, corresponding to 6.5% of the MP weight. The total DOC leaching of other MPs was at least an order of magnitude lower, yet in most cases, it was still significant. Each of materials 3, 4, 11, 14, and 15 leached over 2 mg DOC per g MPs (Fig. 1b), i.e., the amount of released DOC after 12 weeks reached approximately 3.9, 2.5, 2.7, 2.2, and 3.1 mg DOC per g MPs for materials 3, 4, 11, 15, and 15, respectively. These masses of leached DOC roughly correspond to 0.2–0.4% of the MP weight. Materials 7, 9, 10, 12, 13, and 16 leached between 0.1 and 0.5 mg DOC per g MPs (Fig. 1c), corresponding to only 0.01–0.05% of the MP mass. The overall lowest DOC release (< 0.05 mg DOC per g MPs after 12 weeks; Fig. 1d) was observed for materials 1, 2, 5, and 6, i.e., for PET water bottles, PC construction board, and PE water hose.

Diverse DOC leaching among MPs prepared from different plastic products was in agreement with some previous studies (Ateia et al., 2020; Zhu et al., 2020; Lee et al., 2021). Ateia et al. (2020) conducted 3-day experiments with 17 materials soaked in distilled deionized water and reported final DOC ranging from < 0.1 to almost 4 mg DOC per g MPs . This range is roughly comparable to our results from the first days of leaching; however, Ateia et al. (2020) did not monitor further DOC evolution with time. A great diversity in DOC leaching was also observed in the seawater matrix. After 14 days, DOC release from expanded PS (EPS) and PVC was approximately 5 times higher than that from PP (Lee et al., 2021). MPs were allowed to leach in seawater for longer, i.e., 54 days, in a study by Zhu et al. (2020). They reported a final DOC release under simulated sunlight of 68.2, 39.1, and 1.1 mg per g C for post-consumer EPS, PP, and PE MPs, respectively. Despite relating DOC to the amount of C instead of the total MP weight as in the current study and using a different water matrix, the pattern of DOC leaching depending on the material (decrease in the order PS > PP > PE) observed by Zhu et al. (2020) is in agreement with our results.

The variations in DOC leaching could be related to the fact that polymer degradation pathways might vary, e.g., between polymers with a carbon-carbon backbone and those that comprise heteroatoms in the main chain or depending on the presence of unsaturated double bonds in a polymer backbone (Gewert et al., 2015, 2018). This is in line with the observations that differences in DOC leaching occurred when comparing pristine, additive-free MPs (Lee et al., 2020a; b). In addition to the polymer type, a significant impact on DOC leaching can be most likely ascribed to additives (Lee et al., 2020a). To illustrate, in the case of pure PS and PVC MPs, PS leached more DOC; however, in the case of PS and PVC MPs prepared from commercial plastic sheets (presumably comprising additives), PVC exhibited significantly higher leaching (Lee et al., 2020a). Ambiguous roles of additives in DOC leaching and in the degradation of MPs in general have been proposed in the literature (Gewert et al., 2015; Lee et al., 2020a). On the one hand, some additives are intended to improve material properties such as their durability and UV stability. On the other hand, there are also some pro-oxidant additives that enhance degradation. Additionally, additives in general are usually not chemically bound to polymers (Gewert et al., 2015; Hahladakis et al., 2018), and additives themselves were found to partially leach from plastic materials under certain circumstances (Bridson et al., 2021).

Accordingly, DOC derived from MPs might comprise various

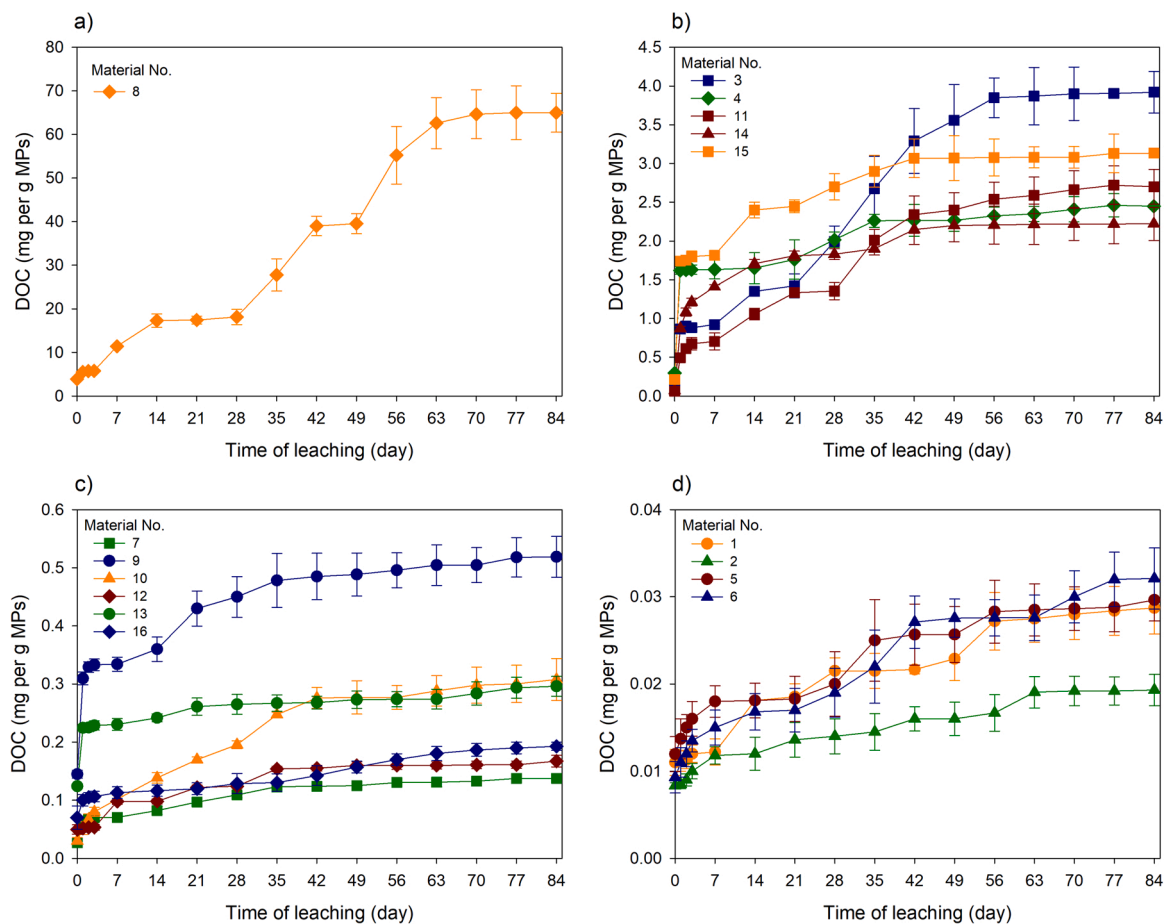


Fig. 1. Dependency of the amounts of leached DOC on the time of leaching for individual plastic materials.

additives, residual chemicals from the manufacturing process, and polymer degradation products, monomers, oligomers, or any nanosized debris passing the filter (Gewert et al., 2015, 2018; Romera-Castillo et al., 2018, 2022a; Lee et al., 2020a). Exhaustive identification of all compounds leached is challenging owing to the very complex and variable composition of plastic materials (Hahladakis et al., 2018), while knowledge of their degradation products is still limited (Gewert et al., 2015, 2018). Nevertheless, the composition of the leachates with a focus on organic compounds is further elaborated in Section 3.4.

Another unexplored aspect of DOC leaching is its dynamics. In the current study, quantifiable amounts of DOC were released into the water immediately after triggering the experiments (Day 0). This might be partially associated with their disruption during the preceding cutting process; however, a general increasing trend in the quantities of DOC with time was observed for all the MPs (Fig. 1). The leaching dynamics varied among the materials, but a substantial retardation in the DOC increase was typically apparent after a certain time of leaching (typically on the order of several weeks). This might be explained by either depletion of C content releasable as DOC under the applied conditions or by outweighing the DOC release by opposing processes, which might include DOC reverse adsorption back on the MPs, DOC release as volatile compounds (Romera-Castillo et al., 2018), and/or DOC abiotic degradation (discussed in Section S1, SM). Additionally, partial biodegradation of MP-derived dissolved organic matter (MP-DOM) is possible (Romera-Castillo et al., 2018, 2022a; b; Zhu et al., 2020), and it was also evidenced for DOM from the materials investigated herein (see Section S1, SM); however, biodegradation was not considered in the C leaching experiments since the samples were prevented from microbial growth, as described in Section 2.2.

In most previous studies, DOC was determined only after a certain

time of leaching, lacking insight into its dynamics, and/or the total leaching time was typically much shorter compared to our study (Ateia et al., 2020; Lee and Hur, 2020; Lee et al., 2021; Romera-Castillo et al., 2022a; b). An exception is a study by Zhu et al. (2020), who measured DOC continuously for 54 days; its leaching accelerated over time for postconsumer EPS and PP and pristine PE, while postconsumer PE exhibited linear leaching. Lee et al. (2020a) leached PVC and PS MPs prepared from commercial products in artificial freshwater for a shorter period (24 days) but measured DOC several times. DOC of the leachates exposed to light increased with time, while no clear trend was observed, and a similar observation was reported for pristine PE and PP leached for 14 days under comparable conditions (Lee et al., 2020b). In contrast, Romera-Castillo et al. (2018) measured instantaneous DOC leaching from virgin PE and PP MPs and then after 6 or 30 days and reported that most of DOC was released when MPs first had contact with water. The observed differences might be associated either with the variations in the overall composition of the materials, even those based on the same polymer, their history, or to different experimental conditions. For example, ageing and particularly exposure to UV light were found to significantly enhance leaching (Zhu et al., 2020; Lee et al., 2020a; b; Romera-Castillo et al., 2022a; b).

The present results support the need to consider the potential impacts of aquatic plastic pollution on the global C cycle. Based on leaching experiments with PE and PP MPs, Romera-Castillo et al. (2018) proposed that floating marine plastics might result in a release of up to 26, 600 t DOC annually. The estimation was subsequently increased to 57, 000 t DOC annually based on the leaching behaviour of other types of MPs, particularly those that underwent natural ageing (Romera-Castillo et al., 2022a). When considering the average total DOC leaching determined herein (i.e., 5 mg DOC per g MPs) and the rough estimate of

the mass of land-based plastic waste entering the ocean within the range of 4.8–12.7 million tonnes per year (Jambeck et al., 2015), the amount of annually released DOC would be between 24,000 and 63,500 t. However, much more research is necessary to provide credible estimation of the DOC input to aquatic environments arising from plastic pollution.

Despite being of different origin and composition, MP-DOM appears to exhibit some similarities to natural organic matter (NOM) in terms of physicochemical behaviour. MP-DOM derived from PVC and PS MPs was found to adsorb onto minerals (goethite, kaolinite), similar to NOM. The adsorption of MP-DOM was pH-dependent and presumably involved electrostatic interactions (Lee and Hur, 2020). Also interactions between MP-DOM and metals were suggested based on the observed binding of Cu by DOM derived from PP, PVC, and EPS (Lee et al., 2021). Such interactions might significantly impact the environmental fate and effects of MP-DOM, as well as their behaviour during water treatment processes. Additionally, similar to NOM, MP-DOM was proven to act as a precursor for the formation of hazardous disinfection byproducts (trihalomethanes and haloacetonitriles) upon chlorination that is commonly applied during drinking water treatment (Ateia et al., 2020). Accordingly, the release of nanoplastics/DOC has been pronounced as one of the major threats to drinking water production arising from the widespread occurrence of MPs (Li et al., 2020).

3.2. Leaching of DIC

Certain materials (Nos. 3, 4, 7, 9, and 11) displayed substantial release of DIC (Fig. 2); DIC leaching from the remaining materials was none or negligible. The overall highest DIC release was observed for material 11 (PVC-based kitchen table mat), which released almost 2 mg DIC per g MPs, followed by materials 3 and 4, which each released approximately 1.5 mg DIC per g MPs. The three mentioned materials shared a similar trend in DIC leaching with time (Fig. 2a), i.e., negligible immediate DIC release, substantial increase in DIC values during the first 5 weeks of leaching, and then reaching a plateau. Materials 7 and 9 each released approximately 0.1 mg DIC per g MPs and had a diverse leaching pattern with time (Fig. 2b). However, the DIC increase terminated or at least significantly slowed down during the observed time period for all the samples. Similar to DOC leaching, this may be ascribed to the depletion of C content releasable as DIC, potential adsorption of leached DIC back onto the MPs, and/or possible release of DIC as volatile compounds.

In natural waters, DIC typically consists of three main constituents – free carbon dioxide, bicarbonate and carbonate ions – while the bicarbonate ion typically completely prevails (Stumm and Morgan, 1996). The occurrence of DIC in the MP leachates might be associated with the

content of carbonates comprised as additives in the plastic materials, e.g., CaCO_3 , utilised as filler (Civancik-Uslu et al., 2018; Hahladakis et al., 2018). DIC can also be formed via photooxidation of DOC (Campeau et al., 2017). Although the relationship between irradiation and leaching was beyond the focus of the current study, the photooxidation of DOC might have occurred since the samples were exposed to ambient light, and even highly penetrating irradiation of relatively long wavelengths that could have accessed the samples (UVA and photosynthetically active radiation) is involved in the photooxidation processes (Johansson et al., 2021). The release of DIC as a consequence of respiration was not considered herein, since as already mentioned, the samples for the C leaching experiment were prevented from microbial growth.

To the best of our knowledge, the release of DIC from MPs has not been reported in any other study thus far. Therefore, the formation of DIC arising from MPs is completely unexplored, as is its potential environmental impacts. However, naturally occurring DIC is of great importance since the carbonate system significantly contributes to the buffering capacity of most natural waters, DIC species are involved in calcium-carbonate equilibrium (Stumm and Morgan, 1996), and DIC is a significant segment of biogeochemical C cycling (Campeau et al., 2017).

3.3. Leaching of metals

Preliminary screening revealed the occurrence of several metals (Al, Ba, Ca, Fe, K, Mg, Mn, Na, and Zn) and one metalloid (Si) in the leachates of one or more samples; therefore, these elements were subsequently monitored in all leachates at the same frequency as DOC. Fig. 3 provides an overview of which elements were detected in individual leachates. Material 8 (PUR-based soft foam isolation) released all the mentioned elements; in contrast, materials 1, 2, 5 and 6 (PET water bottles, PC construction board, PE water hose) were not found to release any. The remaining leachates each comprised 1–8 of the monitored compounds. Ca, K, and Na occurred most frequently (in 12, 10, and 9, respectively, out of the 16 investigated leachates), but their concentrations greatly varied. In contrast, Fe and Mn were detected in only one leachate. The dependency of the released amounts of individual elements on the time of leaching is then depicted in Fig. 4.

The overall highest leaching was observed for Ca and materials 3 (PVC-based floor covering) and 11 (PVC-based kitchen table mat), which both released up to approximately 2.3 mg Ca per g. Additionally, material 4 (NBR-based exercise mat) exhibited extraordinary Ca leaching of approximately 1.5 mg per g. For these materials, the most rapid increase in released Ca concentration was observed during the first three weeks (Fig. 4a). Ca leaching from the remaining materials (if detected) was significantly lower, not exceeding 0.2 mg per g MPs (Fig. 4b). However, Ca was found in most of the leachates. The origin of Ca is

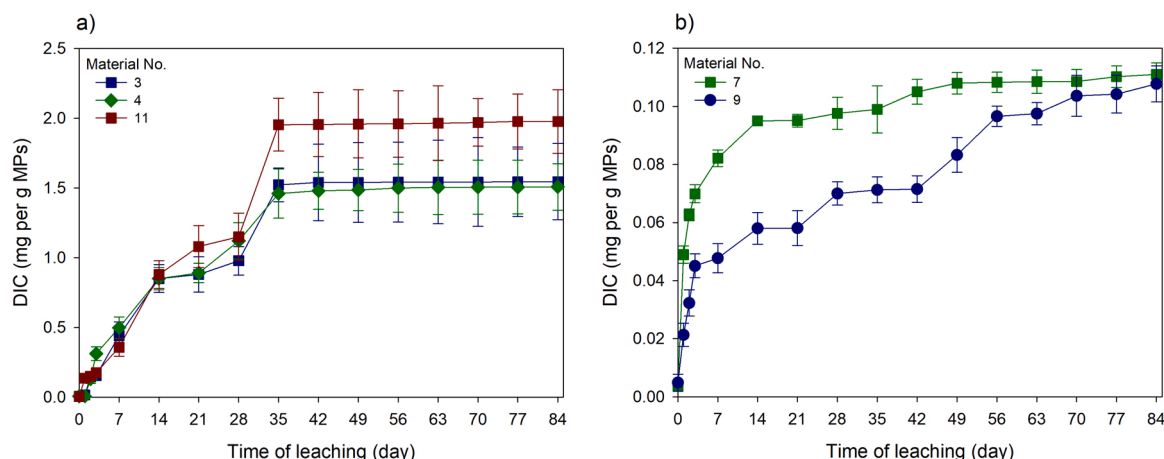


Fig. 2. Dependency of the amounts of leached DIC on the time of leaching for individual plastic materials.

Material No.	Released elements									
	Al	Ba	Ca	Fe	K	Mg	Mn	Na	Si	Zn
1										
2										
3										
4										
5										
6										
7										
8										
9										
10										
11										
12										
13										
14										
15										
16										

Fig. 3. Overview of the occurrence of different elements in the leachates of individual plastic materials; shaded fields indicate the presence of the elements in the corresponding leachates.

presumably associated with the content of inorganic fillers in the corresponding materials (Civancik-Uslu et al., 2018; Hahladakis et al., 2018). Fillers are commonly used in plastics to improve their properties and/or reduce manufacturing costs (Civancik-Uslu et al., 2018), and they may comprise up to 50% of the material weight (Hahladakis et al., 2018; Bridson et al., 2021). In general, CaCO_3 is recognised as the most commonly used inorganic filler in plastics, owing to its good availability and superior functions (Civancik-Uslu et al., 2018), and CaCO_3 was detected as a component of materials 3, 4, and 11 by μ -Raman spectroscopy (Table S1, SM). Interestingly, these materials that exhibited the highest Ca leaching also displayed the highest leaching of DIC (Section 3.2). This is in agreement with the idea of releasing CaCO_3 components from the materials, and in addition to DIC enrichment, the release of Ca species to water might contribute to altering its calcium-carbonate equilibrium (Stumm and Morgan, 1996). However, there are also other Ca-comprising fillers, e.g., CaSO_4 (Civancik-Uslu et al., 2018). To the best of our knowledge, leaching of Ca from MPs has not been reported in any previous study. However, Selbes et al. (2015) reported Ca leaching from scrap car and truck tyres, which was associated with their rubbery parts.

In general, no other elements reached as high concentrations in the leachates as Ca did. The released amounts of K, Na, Zn, and Si ranged from negligible to several tenths mg per g MPs (Fig. 4c–f). The highest amounts of both K and Na were released by material 4, and the leaching of Zn and Si was the most significant for materials 3 and 11, respectively. The remaining elements did not exceed the released amount of 0.1 mg per g MPs in any sample. To illustrate, although leaching of Mg was quite frequent among the investigated samples, the released amounts were relatively low, with the exception of material 11 (Fig. 4g). Similar to the occurrence of Ca, the other elements might also be associated with the utilisation of inorganic fillers (MgO , $\text{Mg}(\text{OH})_2$, SiO_2 , ZnO , kaolin,

mica, talc, etc.) in plastics (Civancik-Uslu et al., 2018; Hahladakis et al., 2018), while some inorganic compounds were detectable in the leached materials and/or their evaporated leachates via μ -Raman spectroscopy (Table S1 and S3, SM).

Interestingly, Ba was detected in four leachates (Fig. 4h), and the highest amount was released from material 10 (almost 0.06 mg Ba per g MPs). Increased and/or chronic exposure to Ba is considered harmful to human health, with potential associations with cardiovascular and kidney diseases and metabolic and neurological disorders; negative impacts of Ba were also observed in animals. However, Ba is widely used in the manufacturing of plastics (Kravchenko et al., 2014), e.g., in the form of BaSO_4 as a filler (Civancik-Uslu et al., 2018) or as a pigment agent (ECHA, 2022a). As BaSO_4 was identified by μ -Raman spectroscopy in material 10 (Table S1, SM) as well as in its evaporated leachate (Table S3, SM), it was most likely responsible for the occurrence of Ba. Additionally, Al was detected in the leachate of material 8 (almost 0.04 mg per g MPs) and at a lower amount in the leachate of material 11 (Fig. 4i). Al is generally recognised as toxic to humans. Its overload is most often associated with bone and neurodegenerative diseases, and Al also negatively affects plants and animals (Crisponi et al., 2013; Exley, 2013). In plastics, Al_2O_3 or $\text{Al}(\text{OH})_3$ can be utilised as fillers (Civancik-Uslu et al., 2018), the latter also with flame retardant properties (ECHA, 2022a). Finally, both Fe and Mn were found only in the leachate of material 8, while the amount of Fe was significantly higher (Fig. 4j).

To this end, the leaching of specific elements other than C from MPs has rarely been investigated. Of the metals detected in the leachates from MPs in this study, Al, Mn, Fe, or Zn leaching was previously noted for some MPs in contact with freshwater and/or seawater; however, the leaching behaviour with time was not described (Capolupo et al., 2020). In the current study, the leaching dynamics were specific for individual materials and elements (Fig. 4), but the most rapid increase in released

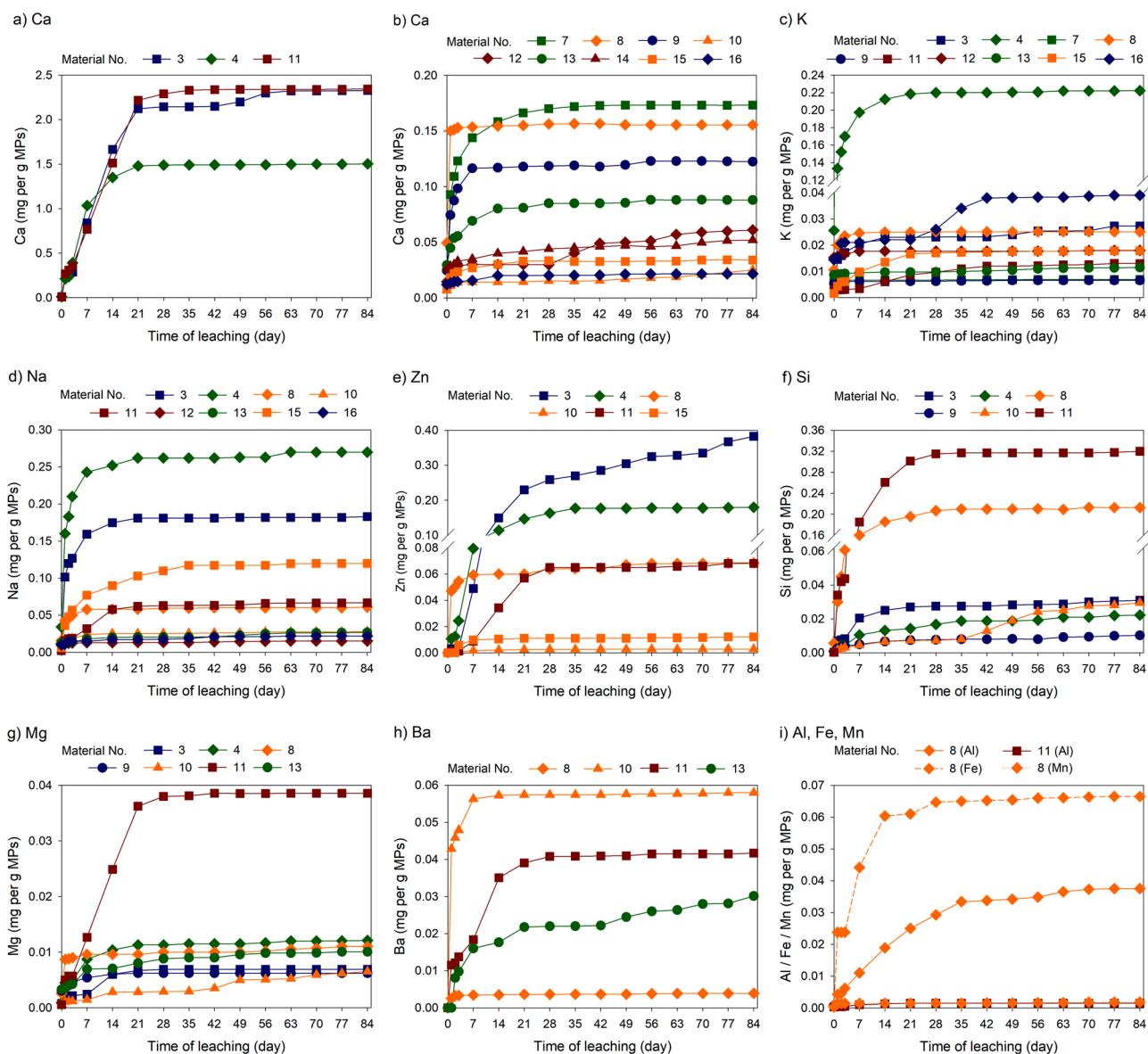


Fig. 4. Dependency of the amounts of leached elements on the time of leaching for individual plastic materials. Error bars are not depicted to maintain clarity; standard deviations were below 10%.

metal concentration was typically observed during the first weeks of leaching.

Some attention was previously given to the release of toxic metals/metalloids from plastics. An example is the release of Sb from plastic products, particularly PET beverage bottles (Shotyk and Krachler, 2007; Westerhoff et al., 2008). In some cases, Sb concentrations in water stored in PET bottles were found to increase over time at room temperature (Shotyk and Krachler, 2007), similar to the leaching patterns observed for metals in this study. Elsewhere, Sb release was observed only at higher temperatures (Westerhoff et al., 2008). Historically, highly hazardous metals/metalloids, such as As, Cd, Cr, and Pb, have also been used in plastics, and despite current restrictions on their utilisation, they might appear in old durable products or in new products as a result of plastic recycling (Turner and Filella, 2021). However, most of the metals detected in the MP leachates in this study are not considered harmful to humans or other organisms, with the exception of Al and Ba, the leached amounts of which were, however, relatively low. Additionally, both Al and Ba are naturally present in the environment and have many industrial applications (Crisponi et al., 2013; Exley, 2013; Kravchenko et al., 2014); the potential contribution of MP-related Ba or

Al to their effects in water is therefore questionable.

However, the released amounts of some other metals were quite high, and considering the amounts of MPs that presumably end up in aquatic environments on the order of several million tonnes annually (Jambeck et al., 2015), the leaching of various elements from MPs deserves attention in terms of potentially associated local environmental alterations or even global cycles of the corresponding elements.

3.4. Identification of leached compounds

Organic compounds leached out from the plastic materials were tentatively identified via GC-MS. The number of compounds distinguished in individual leachates ranged from 10 to 29, while the majority were identifiable based on the library spectra. In total, 80 chemical individuals were recognised, some of them repeatedly in multiple samples. The leachates comprised organic compounds belonging to various classes; the most frequent were esters, alcohols, and carboxylic acids.

The list of compounds detected in each leachate is provided in Table 2. Although the nature of the analysis enabled only semi-quantitative determination of the compounds, their amounts

Table 2

Compounds tentatively identified in the leachates from materials 1–16 via GC-MS. Groups A, B, and C include compounds with estimated concentrations of > 1000, 100–1000, and < 100 µg L⁻¹, respectively. Unidentifiable compounds/compounds tentatively identified with low reliability are denoted as “other”.

Material No.	Compounds tentatively identified in the leachates
1	Group C: tetradecane; 2,4-di-tert-butylphenol; p-benzoyltoluene; octadecane; 7 other (presumably includes hydrocarbons and silicones)
2	Group C: tetradecan-1-ol; tetradecane; 2,4-di-tert-butylphenol; hexadecane; bis(2-ethylhexyl) fumarate; 5 other (presumably includes hydrocarbons)
3	Group A: nonan-1-ol; nonanoic acid Group B: 2,2,4-trimethyl-1,3-pentanediol diisobutyrate; cyclohexyl acrylate; hexamethylene diacrylate; tetraethylene glycol; hexaethylene glycol; ethanol, 2-butoxy, phosphate (3:1); 5 other (presumably includes polyethylene glycols) Group C: triethylene glycol; 3 other (possibly includes 12-crown-4 and/or 12-crown-5)
4	Group A: dioctyl terephthalate Group B: 2-ethylhexan-1-ol; octanoic acid; decanoic acid; tetraethylene glycol; pentaethylene glycol; hexaethylene glycol; 5 other (presumably includes polyethylene glycols) Group C: nonanoic acid; dodecanoic acid; 1 other
5	Group C: dodecan-1-ol; 3,3'-oxybis(butan-2-ol); tetradecan-1-ol; 2,4-di-tert-butylphenol; hexadecane; diphenyl ether; bisphenol A; bis(2-ethylhexyl) fumarate; triphenylphosphine oxide; 5 other (presumably includes hydrocarbons and silicones)
6	Group C: 2,2,4-trimethyl-1,3-pentanediol diisobutyrate; tetradecan-1-ol; tetradecane; 2,4-di-tert-butylphenol; diethyl phthalate; hexadecane; benzophenone; triallyl isocyanurate; 4,6-di-tert-butyl-m-cresol; bis(2-ethylhexyl) fumarate; 8 other (presumably includes silicones and phthalates)
7	Group C: 3,3,5-trimethylcyclohexan-1-one; 3,3,5-trimethylcyclohexan-1-ol; dodecan-1-ol; octadecan-1-ol; tetradecane; 2,4-di-tert-butylphenol; dibutyl itaconate; hexadecane; octadecane; bis(2-ethylhexyl) fumarate; 4 other (presumably includes silicone)
8	Group A: bis[2-(2-butoxyethoxy)ethyl] adipate; 2 other (presumably adipates) Group B: diethylene glycol; adipic acid; 1,4-dimethoxynaphthalene; 2 other (presumably includes adipate) Group C: toluene 2,6-diisocyanate; toluene 2,4-diisocyanate; 6-tert-butyl-2-methyl-1 H-benzimidazole; 1-[4-(1-hydroxy-1-methylethyl)phenyl]ethanone; N-butylbenzenesulfonamide; 11 other (presumably includes phthalate, adipate, polyethoxylates, and fatty acid)
9	Group C: tris(1-chloro-2-propyl) phosphate; trimethylsilyl palmitate; tributyl citrate; bis(2-ethylhexyl) fumarate; bis(2-ethylhexyl) adipate; 5 other (presumably includes silicones and phthalate) Group B: 1 other
10	Group C: diethylene glycol; 2-methyl-1,3-cyclopentanediol; 1-phenylethan-1-ol; benzoic acid; toluene 2,4-diisocyanate; toluene 2,6-diisocyanate; 4-phenyl-3,4-dihydro-1(2 H)-naphthalenone; 11 other Group A: 2-ethylhexan-1-ol; 1 other Group B: ethylene glycol diacetate; p-toluenethiol; 2-butoxyethan-1-ol; 2,4,7,9-tetramethyl-5-decyn-4,7-diol; 4-tert-butylbenzoic acid; p-toluenesulfonamide; acetone p-tosylhydrazone; p-tolyl disulphide; 8 other Group C: methyl p-tolyl sulphide; (4-methylphenylthio)acetone; dioctyl terephthalate; 8 other (presumably includes glycole)
11	Group C: p-toluenethiol; 2,4-di-tert-butylphenol; dibutyl phthalate; bis(2-ethylhexyl) fumarate; 3,5-di-tert-butyl-4-hydroxyphenylpropionic acid; p-tolyl p-toluenethiosulfonate; 5 other
12	Group C: p-toluenethiol; 2-phenyl-2-propanol; benzothiazole; 2,4-di-tert-butylphenol; bis(2-ethylhexyl) fumarate; 11 other (presumably includes hydrocarbons)
13	Group A: tris(1-chloro-2-propyl) phosphate; 1 other Group B: 2 other (presumably includes phosphate and ester) Group C: phthalic acid; 8 other (presumably includes phosphates and ester)
14	Group A: 1-(2-butoxyethoxy)ethanol; dimethyl phthalate; 3 other (presumably butyl citrates) Group B: glycerol α-monoacetate; glycerine triacetate; 4-tert-butylbenzoic acid; 2 other Group C: 4-chlorobenzoic acid, 2-ethylhexyl ester; 3 other
15	Group C: ethylene glycol diacetate; 2-ethylhexan-1-ol; acetophenone; 2-ethylhexanoic acid; 1-(2-butoxyethoxy)ethanol; phthalic anhydride; glycerine triacetate; 2,4,7,9-tetramethyl-5-decyn-4,7-diol; dimethyl

Table 2 (continued)

Material No.	Compounds tentatively identified in the leachates
	phthalate; cyclodecane; 2,4-di-tert-butylphenol; diethyl phthalate; triethyl citrate; tris(1-chloro-2-propyl) phosphate; 4,6-di-tert-butyl-m-cresol; dibutyl phthalate; 2,5-di-tert-butyl-1,4-benzoquinone; acetyl tributyl citrate; 9 other

presumably varied greatly, from negligible up to several mg L⁻¹. Particularly high concentrations were estimated in the case of nonan-1-ol and nonanoic acid (leachate 3); dioctyl terephthalate (DOTP; leachate 4); bis[2-(2-butoxyethoxy)ethyl] adipate (DBEEA; leachate 8); 2-ethylhexan-1-ol (leachate 11); tris(2-chloroisopropyl)phosphate phosphate (TCPP; leachate 14); 1-(2-butoxyethoxy)ethanol and dimethyl phthalate (DMP; leachate 15). Interestingly, these leachates (Nos. 3, 4, 8, 11, 14, and 15) are those that comprised the overall highest organic content determined as DOC (Section 3.1). Additionally, considering the nature and applications of the mentioned organic compounds, their presence in the leachates of plastic materials is reasonable. Nonan-1-ol is commonly used in a variety of consumer products (or during their production), including those made of plastic materials (ECHA, 2022b). Nonanoic acid, initially of natural origin, is commonly prepared synthetically and utilised, e.g., in the production of plasticisers and stabilisers for PVC and other materials (Sahin et al., 2006). DOTP is a widely utilised plasticiser and is an alternative to phthalate plasticisers that appear harmful to human health (Demir and Ulutan, 2013; ECHA, 2022a). Additionally, some adipates, including DBEEA, serve as alternative plasticisers (ECHA, 2022a). 2-Ethylhexan-1-ol is a widely used chemical, the applications of which include the production of plasticisers (Stamatelatos et al., 2011). TCPP is extensively used as a flame retardant in plastics (Bridson et al., 2021), and DMP is a plasticiser (Cao et al., 2022). Many other of the identified compounds have applications as (i) plasticisers, e.g., acetyl tributyl citrate (Hahladakis et al., 2018), bis(2-ethylhexyl) adipate (ECHA, 2022a), dibutyl phthalate (DBP), diethyl phthalate (DEP) (Bridson et al., 2021; Cao et al., 2022; ECHA, 2022a), tributyl citrate, triethyl citrate (ECHA, 2022a), (ii) other additives, e.g., 2,4-di-tert-butylphenol – an antioxidant (Capolupo et al., 2020), or (iii) intermediates in chemical syntheses, e.g., acetophenone (Capolupo et al., 2020) or bisphenol A (BPA) (Hahladakis et al., 2018; Shi et al., 2021). The list of identified compounds also includes some that are recognised as harmful to the environment and/or human health, e.g., BPA and phthalate esters are known for their endocrine disrupting effects (Hahladakis et al., 2018; Shi et al., 2021; Cao et al., 2022).

As already mentioned, additives are usually not chemically bound to the polymer, which makes them prone to leaching under suitable circumstances (Gewert et al., 2015; Hahladakis et al., 2018). The migration of specific additives to the surrounding media has been documented before, often in the context of investigating the safety of food contact materials (Hahladakis et al., 2018; Bridson, 2021; Cao et al., 2022). However, the release of additives also deserves attention with regard to the quality of aquatic environments, which is also supported by the reported occurrence of additives such as phthalate esters, organophosphate esters, and bisphenols in natural stream waters (Schmidt et al., 2020; Bolívar-Subirats et al., 2021), including some compounds identified in the leachates herein (TCPP, DMP, DEP, DBP, BPA, benzophenone).

Some of the compounds listed in Table 2 are not recognised as typical additives. It has been suggested before that the pool of organic compounds associated with MPs should not be limited only to additives and/or adsorbed compounds but also the degradation products of the polymers should be taken into account (Biale et al., 2022). To illustrate, various carboxylic acids were identified among the main degradation products of pristine PE, PP, PS, and PET MPs artificially aged in Milli-Q water (Gewert et al., 2018) as well as PE and PP MPs in seawater, while PS provided relatively more compounds, including diverse aromatic

species (Biale et al., 2022). MPs may comprise and subsequently release also unreacted monomers, oligomers, or other compounds from the manufacturing process (Hahladakis et al., 2018).

Additionally, in the current study, analysis of the evaporated leachates was conducted via μ -Raman spectroscopy. It was successful only in the case of some leachates, typically those that provided evaporated residues visible to the naked eye (Table S3, SM). CaCO_3 was detected most often, i.e., in the leachates of materials 3, 4, 7, 9, 11, 12, and 13, which is in accordance with the results on leached Ca (Fig. 4). As discussed in Section 3.1, CaCO_3 is widely utilised as an inorganic filler for plastics (Civancik-Uslu et al., 2018; Hahladakis et al., 2018). Other inorganic compounds identified via μ -Raman spectroscopy were K_2SO_4 and BaSO_4 , and also some organic compounds, such as esters or carboxylic acid, were distinguished (Table S3, SM). Nevertheless, the results support the finding that not only organic but also inorganic leaching of MPs deserves attention.

4. Conclusions

In the current study, the long-term leaching of 16 different types of MPs derived from various consumer products was investigated. A variety of elements and specific compounds were observed to be released from MPs and enter the aqueous dissolved phase (herein defined as the fraction passing through a 0.45 μm membrane filter), while leaching was most rapid during the first weeks of MP contact with water. Organic carbon was released by all of the investigated MPs; however, the leached amounts greatly varied from negligible to up to approximately 65 mg per g MPs. Additionally, leaching of inorganic carbon was observed for some of the materials. The organic leaching might be associated either with the release of non-chemically bound additives and chemical intermediates, breakdown and degradation of the main polymer, or fragmentation of MPs to nanoplastics. Other elements (metals and metalloid) detected in one or more of the leachates were Al, Ba, Ca, Fe, K, Mg, Mn, Na, Si, and Zn. Of these, the highest and the most frequent leaching was observed in the case of Ca – up to almost 2.5 mg per g MPs. The release of the listed elements is most likely associated primarily with the content of inorganic fillers. Additionally, screening for specific organic compounds in the leachates revealed 80 chemical individuals, most frequently esters, alcohols, and carboxylic acids. The results show that some MPs deposited in aquatic environments can release significant amounts of various dissolved compounds to their surroundings, which might affect water quality at the local scale and potentially also global element cycles. However, more research is required to provide better insight into the leaching behaviour of MPs, since many factors might be influential in this regard, and MPs actually are a very wide and diverse group of environmental pollutants.

Environmental implication statement

This study explores continuous long-term leaching from microplastics (MPs) to water; 16 different types of MPs prepared from consumer products were used to resemble real MPs occurring in aquatic environments. The current results confirm MPs should be considered hazardous pollutants as (i) some MPs released toxic metals (Al, Ba) and/or harmful organic substances (bisphenol, phthalate esters, etc.) and (ii) many MPs released significant amounts of, e.g., C, Ca, K, or Na, which might affect local water quality, or potentially also global element cycles. Thorough exploration of interactions between MPs and ambient water is necessary to comprehensively assess their environmental impacts.

CRedit authorship contribution statement

Katerina Novotna: Conceptualization, Methodology, Investigation, Writing – original draft, Visualization. **Lenka Pivokonska:** Methodology, Validation, Investigation. **Lenka Cermakova:** Validation, Writing –

review & editing, Visualization. **Michaela Prokopova:** Investigation, Writing – review & editing. **Katerina Fialova:** Investigation, Writing – review & editing. **Martin Pivokonsky:** Conceptualization, Writing – review & editing, Supervision.

Declaration of Competing Interest

The authors declare that they have no known competing financial interests or personal relationships that could have appeared to influence the work reported in this paper.

Data availability

Data will be made available on request.

Acknowledgements

The authors acknowledge the institutional support of the Czech Academy of Sciences [RVO: 67985874] and thank Strategy AV21 of the Czech Academy of Sciences (VP20 – Water for life) for valuable support.

Appendix A. Supporting information

Supplementary data associated with this article can be found in the online version at doi:10.1016/j.jhazmat.2022.130424.

References

- Andrady, A.L., 2011. Microplastics in the marine environment. *Mar. Pollut. Bull.* 62, 1596–1605. <https://doi.org/10.1016/j.marpolbul.2011.05.030>.
- Atea, M., Kanan, A., Karanfil, T., 2020. Microplastics release precursors of chlorinated and brominated disinfection byproducts in water. *Chemosphere* 251, 126452. <https://doi.org/10.1016/j.chemosphere.2020.126452>.
- Bejarn, S., MacLeod, M., Bogdal, C., Breitholtz, M., 2015. Toxicity of leachate from weathering plastics: an exploratory screening study with *Nitocra spinipes*. *Chemosphere* 132, 114–119. <https://doi.org/10.1016/j.chemosphere.2015.03.010>.
- Biale, G., Mattonai, M., Corti, A., Castelvetro, V., Modugno, F., 2022. Seeping plastics: potentially harmful molecular fragments leaching out from microplastics during accelerated ageing in seawater. *Water Res.* 219, 118521 <https://doi.org/10.1016/j.watres.2022.118521>.
- Bolívar-Subirats, G., Rivetti, C., Cortina-Puig, M., Barata, C., Lacorte, S., 2021. Occurrence, toxicity and risk assessment of plastic additives in Besos river, Spain. *Chemosphere* 263, 128022. <https://doi.org/10.1016/j.chemosphere.2020.128022>.
- Bridson, J.H., Gaugler, C.G., Smith, D.A., Northcott, G.L., Gaw, S., 2021. Leaching and extraction of additives from plastic pollution to inform environmental risk: a multidisciplinary review of analytical approaches. *J. Hazard. Mater.* 414, 125571 <https://doi.org/10.1016/j.jhazmat.2021.125571>.
- Campeau, A., Wallin, M.B., Giesler, R., Löfgren, S., Mörth, C.-M., Schiff, S., Venkiteswaran, J.J., Bishop, K., 2017. Multiple sources and sinks of dissolved inorganic carbon across Swedish streams, refocusing the lens of stable C isotopes. *Sci. Rep.* 7, 9158. <https://doi.org/10.1038/s41598-017-09049-9>.
- Cao, Y., Lin, H., Zhang, K., Xu, S., Yan, M., Leung, K.M.Y., Lam, P.K.S., 2022. Microplastics: a major source of phthalate esters in aquatic environments. *J. Hazard. Mater.* 432, 128731 <https://doi.org/10.1016/j.jhazmat.2022.128731>.
- Capolupo, M., Sørensen, L., Jayasena, K.D.R., Booth, A.M., Fabbri, E., 2020. Chemical composition and ecotoxicity of plastic and car tire rubber leachates to aquatic organisms. *Water Res.* 169, 115270 <https://doi.org/10.1016/j.watres.2019.115270>.
- Civancik-Uslu, D., Ferrer, L., Puig, R., Fullana-i-Palmer, F., 2018. Are functional fillers improving environmental behavior of plastics? A review of LCA studies. *Sci. Total Environ.* 626, 927–940. <https://doi.org/10.1016/j.scitotenv.2018.01.149>.
- Crisponi, G., Fanni, D., Gerosa, C., Nemolato, S., Nurchi, V.M., Crespo-Alonso, M., Lachowicz, J.I., Faa, G., 2013. The meaning of aluminium exposure on human health and aluminium-related diseases. *Biomol. Concepts* 4 (1), 77–87. <https://doi.org/10.1515/bmc-2012-0045>.
- Demir, A.P., Ulutan, S., 2013. Migration of phthalate and non-phthalate plasticizers out of plasticized PVC films into air. *J. Appl. Polym. Sci.* 128 (3), 1948–1961. <https://doi.org/10.1002/APP.38291>.
- ECHA (European Chemicals Agency), 2022a. Information on Chemicals – Mapping exercise – Plastic additives initiative. (<https://echa.europa.eu/mapping-exercise-plastic-additives-initiative>) (Accessed on 8th August 2022).
- ECHA (European Chemical Agency), 2022b. Substance Information – Substance Infocard – Nonan-1-ol. (<https://echa.europa.eu/substance-information/-/substanceinfo/100.005.076>) (Accessed on 8th August 2022).
- Eerkes-Medrano, D., Thompson, R.C., Aldridge, D.C., 2015. Microplastics in freshwater systems: a review of the emerging threats, identification of knowledge gaps and prioritisation of research needs. *Water Res.* 75, 63–82. <https://doi.org/10.1016/j.watres.2015.02.012>.

- Exley, C., 2013. Human exposure to aluminium. *Environ. Sci.: Process. Impacts* 15, 1807–1816. <https://doi.org/10.1039/c3em00374d>.
- Gewert, B., Plassmann, M.M., MacLeod, M., 2015. Pathways for degradation of plastic polymers floating in the marine environment. *Environ. Sci.: Process. Impacts* 17, 1513–1521. <https://doi.org/10.1039/C5EM00207A>.
- Gewert, B., Plassmann, M., Sandblom, O., MacLeod, M., 2018. Identification of chain scission products released to water by plastic exposed to ultraviolet light. *Environ. Sci. Technol. Lett.* 5, 272–276. <https://doi.org/10.1021/acs.estlett.8b00119>.
- Hahladakis, J.N., Velis, C.A., Weber, R., Iacovidou, E., Purnell, P., 2018. An overview of chemical additives present in plastics: migration, release, fate and environmental impact during their use, disposal and recycling. *J. Hazard. Mater.* 344, 179–199. <https://doi.org/10.1016/j.jhazmat.2017.10.014>.
- Jambeck, J.R., Geyer, R., Wilcox, C., Siegler, T.R., Perryman, M., Andrady, A., Narayan, R., Law, K.L., 2015. Plastic waste inputs from land into the ocean. *Science* 347, 768–771. <https://doi.org/10.1126/science.1260352>.
- Johannsson, O.E., Ferreira, M.S., Smith, D.S., Wood, C.M., Val, A.L., 2021. Interplay of oxygen and light in the photo-oxidation of dissolved organic carbon. *Water Res.* 201, 117332 <https://doi.org/10.1016/j.watres.2021.117332>.
- Kravchenko, J., Darrah, T.H., Miller, R.K., Lyerly, H.K., Vengosh, A., 2014. A review of the health impacts of barium from natural and anthropogenic exposure. *Environ. Geochem. Health* 36, 797–814. <https://doi.org/10.1007/s10653-014-9622-7>.
- Lee, Y.K., Hur, J., 2020. Adsorption of microplastic-derived organic matter onto minerals. *Water Res.* 187, 116426 <https://doi.org/10.1016/j.watres.2020.116426>.
- Lee, Y.K., Murphy, K.R., Hur, J., 2020. Fluorescence signatures of dissolved organic matter leached from microplastics: polymers and additives. *Environ. Sci. Technol.* 54, 11905–11914. <https://doi.org/10.1021/acs.est.0c00942>.
- Lee, Y.K., Romera-Castillo, C., Hong, S., Hur, J., 2020. Characteristics of microplastic polymer-derived dissolved organic matter and its potential as a disinfection byproduct precursor. *Water Res.* 175, 115678 <https://doi.org/10.1016/j.watres.2020.115678>.
- Lee, Y.K., Hong, S., Hur, J., 2021. Copper-binding properties of microplastic-derived dissolved organic matter revealed by fluorescence spectroscopy and two-dimensional correlation spectroscopy. *Water Res.* 190, 116775 <https://doi.org/10.1016/j.watres.2020.116775>.
- Li, Y., Li, W., Jarvis, P., Zhou, W., Zhang, J., Chen, J., Tan, Q., Tian, Y., 2020. Occurrence, removal and potential threats associated with microplastics in drinking water sources. *J. Environ. Chem. Eng.* 8, 104527 <https://doi.org/10.1016/j.jece.2020.104527>.
- Lu, H.-C., Ziajahromi, S., Neale, P.A., Leusch, F.D.L., 2021. A systematic review of freshwater microplastics in water and sediments: recommendation for harmonisation to enhance future study comparisons. *Sci. Total Environ.* 781, 146693 <https://doi.org/10.1016/j.scitotenv.2021.146693>.
- Novotna, K., Cermakova, L., Pivokonska, L., Cajthaml, T., Pivokonsky, M., 2019. Microplastics in drinking water treatment – current knowledge and research needs. *Sci. Total Environ.* 667, 730–740. <https://doi.org/10.1016/j.scitotenv.2019.02.431>.
- Plastics Europe, 2021. *Plastics – the Facts 2021*. (<https://plasticseurope.org/wp-content/uploads/2021/12/Plastics-the-Facts-2021-web-final.pdf>) (Accessed on 1st June 2022).
- Romera-Castillo, C., Pinto, M., Langer, T.M., Álvarez-Salgado, X.A., Herndl, G.J., 2018. Dissolved organic carbon leaching from plastics stimulates microbial activity in the ocean. *Nat. Commun.* 9, 1430. <https://doi.org/10.1038/s41467-018-03798-5>.
- Romera-Castillo, C., Birnstiel, S., Álvarez-Salgado, X.A., Sebastián, M., 2022. Aged plastic leaching of dissolved organic matter is two orders of magnitude higher than virgin plastic leading to a strong uplift in marine microbial activity. *Front. Mar. Sci.* 9, 861557 <https://doi.org/10.3389/fmars.2022.861557>.
- Romera-Castillo, C., Malleco-Fornies, R., Saá-Yáñez, M., Álvarez-Salgado, X.A., 2022. Leaching and bioavailability of dissolved organic matter from petrol-based and biodegradable plastics. *Mar. Environ. Res.* 176, 105607 <https://doi.org/10.1016/j.marenvres.2022.105607>.
- Sahin, N., Kula, I., Erdogan, Y., 2006. Investigation of antimicrobial activities of nonanoic acid derivatives. *Fresenius Environ. Bull.* 15 (2), 141–143.
- Schmidt, N., Castro-Jiménez, J., Fauvelle, V., Ourgaud, M., Sempéré, R., 2020. Occurrence of organic plastic additives in surface waters of the Rhône River (France). *Environ. Pollut.* 257, 113637 <https://doi.org/10.1016/j.envpol.2019.113637>.
- Selbes, M., Yilmaz, O., Khan, A.A., Karanfil, T., 2015. Leaching of DOC, DN, and inorganic constituents from scrap tires. *Chemosphere* 139, 617–623. <https://doi.org/10.1016/j.chemosphere.2015.01.042>.
- Shi, Y., Liu, P., Wu, X., Shi, H., Huang, H., Wang, H., Gao, S., 2021. Insight into chain scission and release profiles from photodegradation of polycarbonate microplastics. *Water Res.* 195, 116980 <https://doi.org/10.1016/j.watres.2021.116980>.
- Shotky, W., Krachler, M., 2007. Contamination of bottled waters with antimony leaching from polyethylene terephthalate (PET) increases upon storage. *Environ. Sci. Technol.* 41, 1560–1563. <https://doi.org/10.1021/es061511>.
- Stamatelatos, K., Pakou, C., Lyberatos, G., 2011. Occurrence, toxicity, and biodegradation of selected emerging priority pollutants in municipal sewage sludge. In: Murray, M.-Y. (Ed.), *Comprehensive Biotechnology*, second ed., 6. Elsevier, pp. 473–484. <https://doi.org/10.1016/B978-0-08-088504-9.00496-7>.
- Stumm, W., Morgan, J.J., 1996. Dissolved carbon dioxide. *Aquatic Chemistry – Chemical Equilibria and Rates in Natural Waters*, third ed. John Wiley & Sons., pp. 148–205.
- Turner, A., Filella, M., 2021. Hazardous metal additives in plastics and their environmental impacts. *Environ. Int.* 156, 106622 <https://doi.org/10.1016/j.envint.2021.106622>.
- Wang, Y., Zhou, B., Chen, H., Yuan, R., Wang, F., 2022. Distribution, biological effects and biofilms of microplastics in freshwater systems – a review. *Chemosphere* 299, 134370. <https://doi.org/10.1016/j.chemosphere.2022.134370>.
- Westerhoff, P., Prapaipong, P., Shock, E., Hillaireau, A., 2008. Antimony leaching from polyethylene terephthalate (PET) plastic used for bottled drinking water. *Water Res.* 42, 551–556. <https://doi.org/10.1016/j.watres.2007.07.048>.
- Zhu, L., Zhao, S., Bittar, T.B., Stubbins, A., Li, D., 2020. Photochemical dissolution of buoyant microplastics to dissolved organic carbon: rates and microbial impacts. *J. Hazard. Mater.* 383, 121065 <https://doi.org/10.1016/j.jhazmat.2019.121065>.

Continuous long-term monitoring of leaching from microplastics into ambient water – a multi-endpoint approach

Katerina Novotna^a, Lenka Pivokonska^a, Lenka Cermakova^a, Michaela Prokopova^a, Katerina Fialova^a, Martin Pivokonsky^{a,*}

^aInstitute of Hydrodynamics of the Czech Academy of Sciences, Pod Patankou 30/5, 166 12 Prague 6, Czech Republic

*Corresponding author: E-mail: pivo@ih.cas.cz (Martin Pivokonsky); Tel: +420 233 109 022; Address: Pod Patankou 30/5, 166 12 Prague 6, Czech Republic

This supplementary material contains following tables, figures, and sections:

Table S1. Detailed information on the investigated MPs – their products of origin, appearance, and compounds identified via μ -Raman spectroscopy.









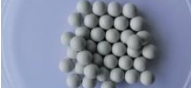



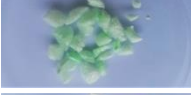



Table S2. Initial pH of the test solution before MP addition and final pH values of the leachates (Day 85).

Section S1. Biodegradability of MP-DOM

Fig. S1. (Bio)degradation of MP-DOM expressed as DOC decrease with time in individual leachates of different materials.

Table S3. Visual appearance of the leachates and compounds identified therein via μ -Raman spectroscopy.

Table S1. Detailed information on the investigated MPs – their products of origin, appearance, and compounds identified via μ -Raman spectroscopy.

Material No.	Product of origin	MPs before leaching	Main polymer	Other identified compounds
1	Water bottle		PET	-
2	Water bottle		PET	-
3	Floor covering		PVC	Calcium carbonate; zinc carbonate
4	Exercise mat		NBR	Aluminum potassium sulfate dodecahydrate; calcium carbonate; dioctyl terephthalate; potassium hydrogen carbonate; FD&C red No. 40 powder
5	Construction board		PC	-
6	Water hose		PE	-
7	Shopping bag		PE	Pigment blue 15
8	Soft foam isolation		PUR	Dibutyl adipate; methyl valerate
9	T-shirt		PET	Pigment blue 29
10	Airsoft balls		PS	Barium sulfate
11	Kitchen table mat		PVC	Calcium carbonate; dioctyl terephthalate; magnesium carbonate hydroxide pentahydrate; 2-amino-4-(4-chlorophenyl)thiazole
12	Bubble packing foil		PE	-
13	Box filler		PS	-
14	Isolation foam		PUR	Phorone
15	Inflatable ball		PVC	Pigment yellow 83
16	Clothes packaging		PP	-

PET – polyethylene terephthalate; PVC – polyvinyl chloride; NBR – nitrile butadiene rubber (acrylonitrile and butadiene copolymer); PC – polycarbonate; PE – polyethylene; PUR – polyurethane; PS – polystyrene; PP – polypropylene

Table S2. Initial pH of the test solution before MP addition and final pH values of the leachates (Day 85).

Initial pH	
Sample	pH (-)
Test solution	6.2 ± 0.2
Final pH	
Material No.	pH (-)
1	6.4 ± 0.3
2	6.5 ± 0.3
3	7.1 ± 0.2
4	7.0 ± 0.3
5	8.1 ± 0.4
6	8.0 ± 0.2
7	7.4 ± 0.2
8	4.3 ± 0.1
9	6.3 ± 0.2
10	5.8 ± 0.2
11	7.1 ± 0.1
12	7.8 ± 0.3
13	7.5 ± 0.1
14	6.7 ± 0.2
15	6.0 ± 0.2
16	6.5 ± 0.3
Blank	6.3 ± 0.2

S1. Biodegradability of MP-DOM

Methodology

For the determination of biodegradability, the DOC die-away test was adopted (OECD, 1992). It was conducted for MP leachates that exceeded a certain DOC concentration, sufficient for biodegradability assessment. Samples for biodegradation were collected after 7 days of leaching and filtered through 0.45 μm membrane filters (Millipore, USA). The leachates were mixed with ultrapure water and mineral medium so that the final volume was 500 mL, the DOC concentration was approximately 10 mg L^{-1} , and the mineral medium comprised half the volume. Samples for biodegradability were inoculated with a surface water-derived inoculum, while abiotic controls were preserved with sodium azide instead. The samples were kept at a constant temperature of 22 $^{\circ}\text{C}$ in the dark, while aeration and continuous shaking were assured. Control samples comprising sodium acetate were also prepared and analysed. The initial DOC concentration in each flask was recorded, and samples for DOC measurement were then collected at Days 1, 2, 3, 7, and weekly since then. The test was terminated when the DOC concentrations remained stable, i.e., after 8 weeks.

Results and discussion

The biodegradability of the leachates was examined for the materials that exhibited the most rapid DOC release during the first week of leaching, i.e., materials 3, 4, 8, 11, 14, and 15. The rate of gradual DOC degradation for the 7-day leachates of the individual materials is depicted in Fig. S1. In addition to the biodegradation experiments, the results of abiotic controls are also depicted since a noticeable decrease in DOC without the contribution of inoculum addition was observed for all the leachates. However, the total DOC decrease was mostly higher in the biodegradation experiments than in the abiotic controls, indicating the contribution of microorganisms to MP-DOM degradation. The most degradable leachates were those from materials 8 and 15, which exhibited 84% and 78% DOC decreases, respectively, in the biodegradation experiments and coincidentally 55% DOC decreases in the abiotic controls. In the leachates of materials 3 and 11, 50% and 43% decreases in DOC, respectively, occurred in the biodegradation experiments, and these values were 43% and 24% in the abiotic controls. The leachates of materials 4 and 11 were the least biodegradable. In both cases, the DOC decrease in abiotic controls approached the values obtained in the biodegradation experiments, which reached only approximately 30%.

In general, biodegradation of plastics is anticipated to be preceded by abiotic degradation, starting with macroscopic changes such as surface cracking or embrittlement, and continued by changes at the molecular level such as chain scission and depolymerization, resulting in the formation of low molecular weight products accessible to microorganisms (Andrady, 2011; Gewert et al., 2015). In this case, the investigated leachates were already the products of the degradation of MPs, thus represented a suitable substrate for potential biodegradation. The current results imply that at least part of MP-DOM can be utilised by microorganisms that facilitate mineralisation of the compounds. However, as already mentioned, a considerable DOC decrease was also observed in those samples intended as abiotic controls. In theory, abiotic mineralisation of organic compounds is possible, driven, e.g., via photochemical pathways (Brandt et al., 2009; Fang et al., 2017). Although the current experiments were conducted under dark conditions, it is possible that reactive oxidation species (ROS) preformed during the leaching phase under light conditions might have been involved in the triggering of abiotic mineralisation of MP-DOM. Previously, organic materials, including different types of DOM, were found to induce the formation of ROS under light, which was proposed to play an important role in contaminant transformation in aquatic environments (Fang et al., 2017). However, more detailed and focused research is required to provide better insight into the bio/degradability of MP-DOM.

To the best of our knowledge, this is the first study that examined the biodegradation of MP-DOM in a simulated freshwater environment. However, partial biodegradation of MP-DOM was also reported in other studies, in which seawater conditions were simulated. The degradability determined based on the DOC decrease ranged between approximately 20–80% (Romera-Castillo et al., 2018, 2022a,b; Zhu et al., 2020). Biodegradability was proposed to depend on the leached material (Zhu et al., 2020), its history, such as prior exposure to UV irradiation, and the DOC concentration (Romera-Castillo et al., 2022a,b). Considering the conditions applied in the current study, the composition of the leached material (MPs) was presumably the key factor affecting the subsequent DOM degradability.

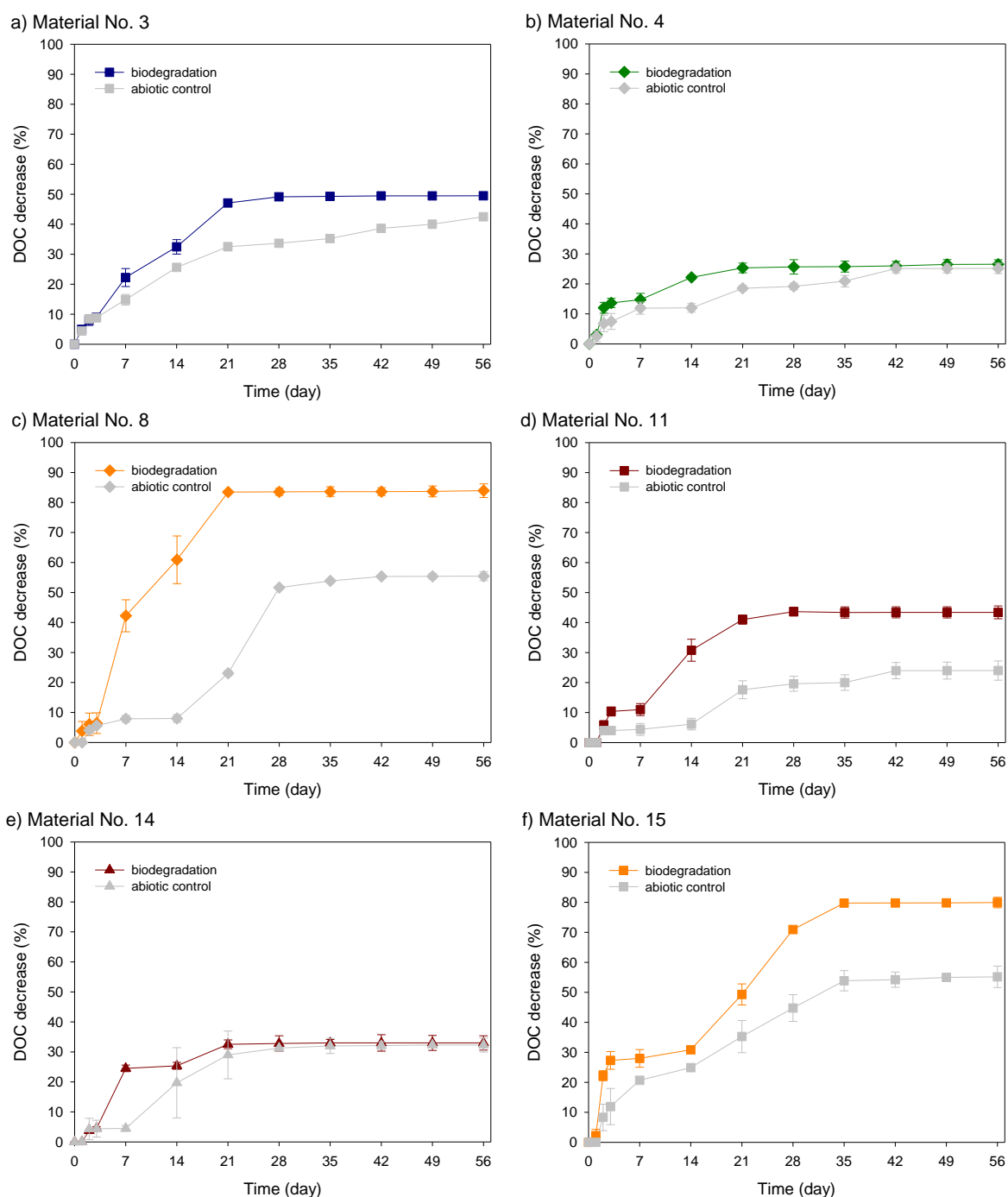







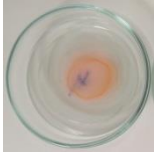





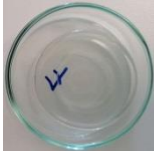



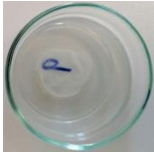
















Fig. S1. (Bio)degradation of MP-DOM expressed as DOC decrease with time in individual leachates of different materials.

Table S3. Visual appearance of the leachates and compounds identified therein via μ -Raman spectroscopy.

Material No.	Product of origin (constituting polymer)	Pre-concentrated liquid leachates and their residuals after evaporation		Identified compounds
1	Water bottle (PET)			-
2	Water bottle (PET)			-
3	Floor covering (PVC)			Calcium carbonate; diisooctyl azelate; isopentyl benzoate
4	Exercise mat (NBR)			Calcium carbonate; FD&C red No. 40 powder
5	Construction board (PC)			-
6	Water hose (PE)			-
7	Shopping bag (PE)			Calcium carbonate
8	Soft foam isolation (PUR)			Adipic acid
9	T-shirt (PET)			Calcium carbonate; poly(ethylene adipate)

10	Airsoft balls (PS)			Barium sulfate
11	Kitchen table mat (PVC)			Calcium carbonate
12	Bubble packing foil (PE)			Calcium carbonate; poly(ethylene adipate); potassium sulfate
13	Box filler (PS)			Calcium carbonate
14	Isolation foam (PUR)			Ethylene glycol diacetate
15	Inflatable ball (PVC)			Diisooctyl azelate; poly(vinyl stearate)
16	Clothes packaging (PP)			Dibutyl adipate; paraffin wax

References:

- Andrady, A.L., 2011. Microplastics in the marine environment. *Marine Pollution Bulletin* 62, 1596–1605. <https://doi.org/10.1016/j.marpolbul.2011.05.030>
- Brandt, L.A., Bohnet, C., King, J.Y., 2009. Photochemically induced carbon dioxide production as a mechanism for carbon loss from plant litter in arid ecosystems. *Journal of Geophysical Research* 114, GO2004. <https://doi.org/10.1029/2008JG000772>
- Gewert, B., Plassmann, M.M., MacLeod, M., 2015. Pathways for degradation of plastic polymers floating in the marine environment. *Environmental Science: Processes & Impacts* 17, 1513–1521. <https://doi.org/10.1039/C5EM00207A>
- Fang, G., Liu, C., Wang, Y., Dionysiou, D.D., Zhou, D., 2017. Photogeneration of reactive oxygen species from biochar suspension for diethyl phthalate degradation. *Applied Catalysis B: Environmental* 214, 34–45. <http://dx.doi.org/10.1016/j.apcatb.2017.05.036>
- OECD, 1992. OECD GUIDELINE FOR TESTING OF CHEMICALS – Ready Biodegradability. Available at: <https://www.oecd.org/chemicalsafety/risk-assessment/1948209.pdf>
- Romera-Castillo, C., Pinto, M., Langer, T.M., Álvarez-Salgado, X.A., Herndl, G.J., 2018. Dissolved organic carbon leaching from plastics stimulates microbial activity in the ocean. *Nature Communications* 9, 1430. <https://doi.org/10.1038/s41467-018-03798-5>
- Romera-Castillo, C., Birnstiel, S., Álvarez-Salgado, X.A., Sebastián, M., 2022a. Aged Plastic Leaching of Dissolved Organic Matter Is Two Orders of Magnitude Higher Than Virgin Plastic Leading to a Strong Uplift in Marine Microbial Activity. *Frontiers in Marine Science* 9, 861557. <https://doi.org/10.3389/fmars.2022.861557>
- Romera-Castillo, C., Mallenco-Fornies, R., Saá-Yáñez, M., Álvarez-Salgado, X.A., 2022b. Leaching and bioavailability of dissolved organic matter from petrol-based and biodegradable plastics. *Marine Environmental Research* 176, 105607. <https://doi.org/10.1016/j.marenvres.2022.105607>
- Zhu, L., Zhao, S., Bittar, T.B., Stubbins, A., Li, D., 2020. Photochemical dissolution of buoyant microplastics to dissolved organic carbon: Rates and microbial impacts. *Journal of Hazardous Materials* 383, 121065. <https://doi.org/10.1016/j.jhazmat.2019.121065>